

**On the human radiation exposure as derived
from the analysis of natural and man-made
radionuclides
in soils**

**Vom Fachbereich
Physik
der Universität
Hannover**

zur Erlangung des Grades

**Doktor der Naturwissenschaften
Dr. rer. nat.
genehmigte Dissertation**

von

**(M.Sc. Phys.)
*Shaban Ramadan Mohamed Harb***

**geboren am 10.01.1966
in Qena, Ägypten**

2004

Referent: Prof. Dr. Rolf Michel
Korreferent: PD. Dr. Ingo Leya
Tag der Promotion: 11.02.2004

Content

| | |
|-------------------------------------------------------------------------------------------------------------------------------------------------|-----------|
| Content | I |
| List of Tables | IV |
| List of Figures | VII |
| Summary | X |
| Zusammenfassung | XII |
| Acknowledgements | XIII |
| 1 Introduction | 1 |
| 1.1 Radioactivity in the environment | 1 |
| 1.1.1 Natural Radionuclides in the environment | 1 |
| 1.1.1.1 Cosmogenic radionuclides | 2 |
| ➤ Tritium (^3H) | 3 |
| ➤ Beryllium-7, 10 | 3 |
| ➤ Carbon-14 | 3 |
| ➤ Krypton | 4 |
| 1.1.1.2 Terrestrials sources of radiation | 5 |
| 1.1.1.2.1 Potassium-40 | 5 |
| 1.1.1.2.2 Rubidium-87 | 6 |
| 1.1.1.2.3 Uranium-238 series | 6 |
| ➤ Uranium-238 subseries (^{238}U , ^{234}Th , $^{234\text{m}}\text{Pa}$, ^{234}U) | 7 |
| ➤ Radium-226 | 8 |
| ➤ Radon-222 and its short-lived products (^{218}Po , ^{214}Pb , ^{214}Bi , ^{214}Po) | 8 |
| ➤ Long-lived decay products of Radon-222 (^{210}Pb , ^{210}Bi , ^{210}Po) | 10 |
| 1.1.1.2.4 Thorium-232 series | 10 |
| ➤ Thorium-232 | 11 |
| ➤ Radium-228 subseries (^{228}Ra , ^{228}Ac , ^{228}Th , ^{224}Ra) | 11 |
| ➤ Randon-220 and its decay products (^{215}Po , ^{212}Pb , ^{212}Bi , ^{212}Po , ^{208}Tl) | 12 |
| 1.1.1.2.5 The actinium series | 12 |
| 1.1.1.2.6 The neptunium series | 13 |
| 1.1.1.2.7 Decay Relationships Series | 13 |
| 1.1.2 Man-made Radionuclides in the environment | 20 |
| 1.1.2.1 Strontium-90 | 21 |
| 1.1.2.2 Iodine-131 | 22 |
| 1.1.2.3 Cesium-134 and 137 | 22 |
| 1.2 The human radiation exposure | 23 |
| 1.2.1 External exposure | 25 |
| 1.2.2 Internal exposures | 27 |
| 1.2.2.1 Ingestion | 27 |
| 1.2.2.2 Inhalation | 28 |
| 1.2.3 Mean values and variability of the natural radiation exposure | 28 |
| 2 Experimental | 32 |
| 2.1 Soil sampling | 32 |
| 2.1.1 The trench method | 32 |
| 2.1.2 Template method | 32 |
| 2.1.3 The bore core method | 34 |
| 2.2 Sample preparation | 35 |
| 2.3 Experimental methods, measurements and evaluations | 36 |
| 2.3.1 Gamma spectrometry | 36 |
| 2.3.2 HPGe detector | 40 |
| 2.3.3 Gamma spectrometry System (HPGe) | 41 |

| | | |
|---------|-------------------------------------------------------------------------------------------------------------------------------------------------------------------------|-----|
| 2.3.4 | Energy calibration | 42 |
| 2.4 | Calibration and efficiency determination of detectors for different measuring geometries and sample containers..... | 43 |
| 2.4.1 | Preparation of reference standard solution (Calibration source QCY48)..... | 44 |
| 2.4.2 | Preparation of standard soil sample procedure | 45 |
| 2.4.3 | Efficiency calibration | 45 |
| 2.4.4 | Analytical efficiency expressions..... | 45 |
| 2.5 | Natural Background | 58 |
| 2.6 | Calculation of elemental concentrations | 60 |
| 2.7 | Experimental uncertainties..... | 62 |
| 2.8 | Quality assurance including Ringversuch..... | 67 |
| 2.9 | Characteristic limits..... | 69 |
| 3 | Analysis of radionuclides in soils..... | 72 |
| 3.1 | Concentration of artificial radionuclides in depth profile and surface..... | 72 |
| 3.1.1 | ¹³⁷ Cs concentration in depth profile soil samples from Lower Saxony, North Germany..... | 73 |
| 3.1.1.1 | ¹³⁷ Cs deposition densities in soil samples from Lower Saxony, North Germany... | 79 |
| 3.1.1.2 | Activity concentration of ¹³⁷ Cs and ⁴⁰ K [Bq kg ⁻¹] in surface soil samples from different sites in Lower Saxony, North Germany..... | 81 |
| 3.1.2 | ¹³⁷ Cs in depth profile soil samples from Lippe, North Rhine-Westphalia, Germany..... | 83 |
| 3.1.2.1 | ¹³⁷ Cs deposition densities in soil samples from Lippe, (North Rhine-Westphalia), Germany..... | 83 |
| 3.1.2.2 | Activity concentration of ¹³⁷ Cs and ⁴⁰ K [Bq kg ⁻¹] in surface soil samples from Lippe (North Rhine-Westphalia, NRW), Germany..... | 84 |
| 3.1.3 | ¹³⁷ Cs concentrations in depth profile soil samples from Ukraine..... | 85 |
| 3.1.3.1 | Highly contaminated (Zone II)..... | 87 |
| 3.1.3.2 | Medium contaminated (ZoneIII)..... | 89 |
| 3.1.3.3 | Not contaminated | 90 |
| 3.1.3.4 | ¹³⁷ Cs and ¹³⁴ Cs deposition densities [Bq m ⁻²] in soil taken from different sites in Ukraine..... | 91 |
| 3.2 | Concentration of natural radionuclides in depth profile and surface soil samples.... | 93 |
| 3.2.1 | Natural radionuclides in soil samples from Lower Saxony, North Germany..... | 93 |
| 3.2.1.1 | Natural radionuclides in depth profiles soil samples from Lower Saxony, North Germany..... | 93 |
| 3.2.1.2 | Natural radionuclides in surface soil from Lower Saxony, North Germany..... | 97 |
| 3.2.2 | Natural radionuclides in soil samples from Lippe, North Rhine-Westphalia, Germany..... | 98 |
| 3.2.2.1 | Natural radionuclides in depth profiles soil from Lippe, (North Rhine-Westphalia), Germany..... | 98 |
| 3.2.2.2 | Natural radionuclides in surface soil samples from Lippe, (North Rhine-Westphalia), Germany..... | 100 |
| 3.2.3 | Natural radionuclides in depth profiles from Ukraine | 102 |
| 3.3 | Elemental correlation, equilibrium and disequilibrium for natural radionuclides in depth profile and surface soil samples..... | 105 |
| 3.3.1 | Elemental correlation for natural radionuclides in depth profile and surface soil samples from Lower Saxony, North Germany..... | 105 |
| 3.3.1.1 | Depth profiles soil samples from Lower Saxony, North Germany..... | 105 |
| 3.3.1.2 | Surface soil samples From Lower Saxony, North Germany..... | 111 |

| | | |
|---------|-----------------------------------------------------------------------------------------------------------------------------------------------------------------------------------------|------------|
| 3.3.2 | Elemental correlation, equilibrium and disequilibrium for natural radionuclides in surface soil samples form Lippe, (North Rhine-Westphalia), Germany..... | 114 |
| 3.3.2.1 | Depth profiles form Lippe, (North Rhine-Westphalia), Germany..... | 114 |
| 3.3.2.2 | Surface soil from Lippe, (North Rhine-Westphalia), Germany..... | 115 |
| 3.3.3 | Elemental correlation. equilibrium and disequilibrium for natural radionuclides in soil samples form depth profiles from Ukraine..... | 118 |
| 4 | Modeling of ambient dose rates from radionuclide concentrations in soil.... | 121 |
| 4.1 | External gamma-dose rate of ^{137}Cs in soil | 121 |
| 4.1.1 | External gamma-dose rate of ^{137}Cs in soil from Loser Saxony, North Germany. .. | 121 |
| 4.1.2 | External gamma-dose rate of ^{137}Cs in soil from Lippe, North Rhine-Westphalia, Germany..... | 122 |
| 4.1.3 | External gamma-dose rate of ^{137}Cs in soil from Ukraine (Chernobyl)..... | 123 |
| 4.2 | Ambient dose rates from natural radionuclides in soil at height of 1 m above ground in investigation sites..... | 125 |
| 4.2.1 | Ambient dose rate in air from gamma-radiation 1 m above the ground surface in Lower Saxony, Germany..... | 125 |
| 4.2.2 | Ambient dose rates at Lippe, North Rhine-Westphalia, Germany..... | 129 |
| 4.2.3 | ^{226}Ra , ^{232}Th and ^{40}K concentrations in soil samples and calculated values of the external Gamma dose rates in n Sv h^{-1} at Ukraine..... | 132 |
| 4.3 | External gamma dose rate of natural and artificial radionuclides in North Germany..... | 133 |
| 5 | Internal and external gamma radiation exposure from soil..... | 135 |
| 5.1 | Realistic Modeling of transfer of radionuclides from soils to man..... | 135 |
| 5.1.1 | External gamma radiation exposure from soil | 136 |
| 5.1.2 | Internal gamma radiation exposure from inhalation dust..... | 137 |
| 5.1.3 | Internal gamma radiation exposure from ingestion direct soil..... | 138 |
| 5.2 | External exposure from radionuclides in soil from Lower Saxony, Lippe (Germany) and Ukraine..... | 138 |
| 5.3 | Internal exposure from inhalation of radionuclides in soil (dust) from Lower Saxony, Lippe, (NRW), (Germany) and Ukraine..... | 141 |
| 5.3.1 | Internal exposure from direct ingestion of radionuclides in soil from Lower Saxony, Lippe, NRW, (Germany) and Ukraine..... | 145 |
| 5.4 | Comparesion between external and internal exposure from radionuclides in soil from different locations: Lower Saxony, Lippe (Germany) and Ukraine..... | 149 |
| 6 | Appendices | 152 |
| 6.1 | Appendix A | 152 |
| 6.2 | Appendix B | 157 |
| 7 | References | 185 |

List of Tables

| | | |
|--------------|---------------------------------------------------------------------------------------------------------------------------------------------------------------------------------------------------------------------------------------------------------------------------------------------------------------------|----|
| Table 1-1: | Estimated annual effective dose equivalents from natural sources in normal background areas, worldwide [UNS88]. | 30 |
| Table 2-1: | Crystal characteristics and detection performance of coaxial detector manufactured. | 36 |
| Table 2-2: | Radionuclides used for efficiency calibration QCY40. | 44 |
| Table 2-3: | Radionuclides used for efficiency calibration QCY48. | 45 |
| Table 2-4: | Radionuclides used for efficiency calibration. | 46 |
| Table 2-5: | Radionuclides used for efficiency calibration of 1119 g soil in marinelli beaker for detector 1: | 48 |
| Table 2-6: | Results of the EFFIC for the calculate of the efficiency for a 1100 g soil sample in marinelli beaker measured by a HPGe detector 1 (Be window). | 51 |
| Table 2-7: | Count efficiency variation with masses of soil in marinelli beaker for ^{210}Pb 46.54 keV gamma-ray line. | 51 |
| Table 2-8: | Count efficiency variation with masses of soil in marinelli beaker for ^{210}Pb 46.54 keV gamma-ray line. | 52 |
| Table 2-9: | Variation of efficiency-energy curves with heights of soil in marinelli beaker for a constant density. | 53 |
| Table 2-10: | Efficiency-energy values for different height of soil in Bottle 1000 ml detector 2. | 53 |
| Table 2-11: | Efficiency for different height of soil in Marinelli beaker for detector 2 (Karl). | 55 |
| Table 2-12: | Efficiency of soil in marinelli beaker with different masses in the same volume for HPGe detector (1). | 55 |
| Table 2-13: | Efficiency of soil in marinelli beaker with different masses in the same volume for HPGe detector 1. | 56 |
| Table 2-14: | Efficiency of soil in marinelli beaker with different masses in the same volume for HPGe detector (2). | 57 |
| Table 2-15: | Radionuclides which were measured in soil sample and also be found only natural radionuclides in background [Sch98]. | 62 |
| Table 2-16 : | The values of radionuclides (Bq kg^{-1}) in soil sample (ST-27/1998 Ringversuch) by PTB and present work at ZSR. | 69 |
| Table 3-1: | Activity concentration of ^{137}Cs [Bq kg^{-1}] in different geometry and activity concentration of layers [Bq m^{-2}] in profile samples from Klein Lobke (field), North Germany. The numbers in parentheses give the fraction of ^{137}Cs observed in the layer. | 73 |
| Table 3-2: | Activity concentration of ^{137}Cs [Bq kg^{-1}] in different geometry and activity concentration of layers [Bq m^{-2}] in profile samples from Twenge (field), Lower Saxony, North Germany. The numbers in parentheses give the fraction of ^{137}Cs observed in the layer. | 74 |
| Table 3-3: | Data of the specimen place "acre Twenge". | 75 |
| Table 3-4: | Activity concentration of ^{137}Cs [Bq kg^{-1}] in different geometry and activity concentration of layers [Bq m^{-2}] in profile samples from Eilenriede (Forest), North Germany. The numbers in parentheses give the fraction of ^{137}Cs observed in the layer. | 76 |
| Table 3-5: | Data of the specimen place "forest Eilenriede". | 77 |

| | | |
|-------------|------------------------------------------------------------------------------------------------------------------------------------------------------------------------------------------------------------------------------------------------------------------------------------------------|-----|
| Table 3-6: | Activity concentration of ^{137}Cs [Bq kg^{-1}] in different geometry and activity concentration of layers [Bq m^{-2}] in profile samples from Neßmerpolder (meadow), North Germany | 78 |
| Table 3-7: | ^{137}Cs deposition densities [Bq m^{-2}] in soil were taken from different sites in Lower Saxony, Germany..... | 80 |
| Table 3-8: | Activity concentration of ^{137}Cs and ^{40}K [Bq kg^{-1}] in soil were collected from Lower Saxony, North Germany..... | 81 |
| Table 3-9: | Activity concentration of ^{137}Cs [Bq kg^{-1}] in different geometry and activity concentration of layers [Bq m^{-2}] in profile samples Lippe (North Rhine-Westphalia), Germany..... | 83 |
| Table 3-10: | ^{137}Cs deposition densities [Bq m^{-2}] in soil were taken from different sites in Lippe, | 83 |
| Table 3-11: | Activity concentration of ^{137}Cs and ^{40}K [Bq kg^{-1}] in soil were collected from Lippe | 84 |
| Table 3-12: | Characteristic of soil from zone II, Ukraine. | 86 |
| Table 3-13: | Activity concentration [Bq kg^{-1}] and deposition densities [Bq m^{-2}] of ^{137}Cs in depth profile soil samples from Nosdrischtsche II, Ukraine..... | 87 |
| Table 3-14: | Activity concentration [Bq kg^{-1}] and deposition densities [Bq m^{-2}] of ^{137}Cs in depth profile soil samples from Chirstinovka meadow, Ukraine..... | 88 |
| Table 3-15: | Activity concentration [Bq kg^{-1}] and deposition densities [Bq m^{-2}] of ^{137}Cs in depth profile soil samples from Tschigiri 1, Ukraine..... | 89 |
| Table 3-16: | Activity concentration [Bq kg^{-1}] and deposition densities [Bq m^{-2}] of ^{137}Cs in depth profile soil samples from Oserjanka1, Ukraine..... | 90 |
| Table 3-17: | ^{137}Cs and ^{134}Cs deposition densities [Bq m^{-2}] in soil were taken from different sites in Ukraine..... | 92 |
| Table 3-18: | Activity concentration [Bq kg^{-1}] of ^{238}U , ^{226}Ra , ^{210}Pb , ^{235}U , ^{40}K , ^{228}Ra , ^{228}Th , and ^{232}Th in soil profile samples collected from Ricklingen (meadow), North Germany..... | 94 |
| Table 3-19: | Activity concentration of ^{238}U , ^{226}Ra , ^{210}Pb , ^{235}U , ^{40}K , ^{228}Ra , ^{228}Th , and ^{232}Th [Bq kg^{-1}] in soil profile samples collected from Eilenrede (forest), North Germany. . | 95 |
| Table 3-20: | Activity concentration of ^{238}U , ^{226}Ra , ^{210}Pb , ^{235}U , ^{40}K , ^{228}Ra , ^{228}Th , and ^{232}Th , [Bq kg^{-1}] in soil profile samples collected from Twenge, North Germany..... | 96 |
| Table 3-21: | Activity concentration of ^{238}U , ^{226}Ra , ^{210}Pb , ^{235}U , ^{228}Ra , ^{228}Th , and ^{232}Th , [Bq kg^{-1}] in soil were collected from Lower Saxony, North Germany. | 97 |
| Table 3-22: | Bp 4 -14 Activity concentration of ^{238}U , ^{226}Ra , ^{210}Pb , ^{235}U , ^{40}K , ^{228}Ra , ^{228}Th , and ^{232}Th [Bq kg^{-1}] in soil collected from Lippe, North Rhine-Westphalia, Germany. | 99 |
| Table 3-23: | Activity concentration of ^{238}U , ^{226}Ra , ^{210}Pb , ^{235}U , ^{228}Ra , ^{228}Th , and ^{232}Th [Bq kg^{-1}] in soil collected from Lippe (North Rhine-Westphalia), Germany..... | 100 |
| Table 3-24: | Activity concentration of ^{238}U , ^{226}Ra , ^{210}Pb , ^{235}U , ^{40}K , ^{228}Ra , ^{228}Th , and ^{232}Th [Bq kg^{-1}] in soil collected from Tschigiri 2, Ukraine..... | 102 |
| Table 3-25: | Activity concentration of ^{238}U , ^{226}Ra , ^{210}Pb , ^{235}U , ^{40}K , ^{228}Ra , ^{228}Th , and ^{232}Th [Bq kg^{-1}] in soil collected from Oserjanka1, Ukraine..... | 103 |
| Table 3-26: | Natural radionuclide content in soil from UNSEARA 2000 [UNS00]. | 104 |
| Table 3-27: | Elemental correlation between natural radionuclides in soil samples from Lower Klein Lobke, Saxony, North Germany..... | 105 |
| Table 3-28: | Elemental correlation between natural radionuclides in soil samples from Ricklingen, Lower Saxony, North Germany..... | 107 |
| Table 3-29: | Elemental correlation between natural radionuclides in soil samples from Twenge, Lower Saxony, North Germany. | 109 |

| | | |
|--------------|------------------------------------------------------------------------------------------------------------------------------------------------------------------------------------------------------------------|-----|
| Table 3-30: | Elemental correlation between natural radionuclides in soil samples from Lower Saxony, North Germany..... | 111 |
| Table 3-31: | Elemental correlation between natural radionuclides in soil samples from Lippe, (North Rhine-Westphalia), Germany..... | 114 |
| Table 3-32: | Elemental correlation between natural radionuclides in soil samples from Lippe, (North Rhine-Westphalia), Germany..... | 115 |
| Table 3-33: | Elemental correlation between natural radionuclides in soil samples from Chirstinovka meadow, Ukraine..... | 118 |
| Table 3-34: | Elemental correlation between natural radionuclides in soil samples from schigiri2, Ukraine..... | 120 |
| Table 3-35: | Elemental correlation between natural radionuclides in soil samples from Oserjanka1, Ukraine..... | 120 |
| Table 4-1: | External gamma-dose rate of ^{137}Cs in n Sv h^{-1} and densities deposition of ^{137}Cs in different sites in Lower Saxony, North Germany..... | 121 |
| Table 4-2: | External gamma-dose rate of ^{137}Cs in n Sv h^{-1} and densities deposition of ^{137}Cs in different sites in Lippe, North Rhine-Westphalia, Germany..... | 122 |
| Table 4-3: | External gamma-dose rate of ^{137}Cs in n Sv h^{-1} and densities deposition of ^{137}Cs in different sites in Ukraine..... | 123 |
| Table 4-4: | Absorbed dose rate in air from gamma-radiation 1 m above the ground surface in Lower Saxony, Germany..... | 125 |
| Table 4-5: | Calculated absorbed dose rate in air from gamma-radiation 1 m above the ground surface in Lower Saxony..... | 127 |
| Table 4-6: | ^{226}Ra , ^{232}Th and ^{40}K concentrations in soil samples and measured and calculated values of the external Gamma dose rates in n Sv h^{-1} at Lippe, NRW, Germany..... | 129 |
| Table 4 - 7: | Absorbed dose rate in air from gamma-radiation 1 m above the ground surface in Ukraine..... | 132 |
| Table 4 - 8: | External gamma dose rates in n Sv h^{-1} for two sites in Germany..... | 133 |
| Table 5-1: | External exposure (in m Sv) from U-series and Th-series in soil from Lower Saxony, North Germany..... | 139 |
| Table 5-2: | External exposure (in m Sv) from U-series and Th-series in soil from Lippe, NRW, Germany..... | 139 |
| Table 5-3: | Ages and external exposure(in m Sv) from U-series and Th-series in soil from Ukraine..... | 140 |
| Table 5-4: | Relation between internal exposure (in $\mu\text{ Sv}$) from inhalation of natural radionuclides in soil (dust) from Lower Saxony (Germany) and age group..... | 141 |
| Table 5-5: | Relation between internal exposure (in $\mu\text{ Sv}$) from inhalation of natural radionuclides in soil (dust) from Lippe, (Germany) and age group..... | 143 |
| Table 5-6: | Relation between internal exposure (in $\mu\text{ Sv}$) from inhalation of natural radionuclides in soil (dust) from Ukraine and age group..... | 144 |
| Table 5- 7: | Annual effective dose from inhalation of uranium and thorium series radionuclides [UNS00]...... | 145 |
| Table 5- 8: | Internal exposure from direct ingestion of radionuclides in soil from Lower Saxony, (Germany) and age group..... | 146 |
| Table 5-9: | Internal exposure from direct ingestion of radionuclides in soil from Lippe, NRW, (Germany) and age group..... | 147 |

| | |
|----------------------------------------------------------------------------------------------------------------------|-----|
| Table 5-10: Internal exposure from direct ingestion of radionuclides in soil from Ukraine and age group..... | 148 |
| Table 5-11: Annual intake and effective dose from ingestion of uranium and thorium series radionuclides [UNS00]..... | 149 |

List of Figures

| | |
|----------------------------------------------------------------------------------------------------------------------------------------------------------------------------------|----|
| Fig. 1-1: Decay scheme for krypton-85 [Led77]..... | 4 |
| Fig. 1-2: Decay scheme of ^{40}K [Led77]..... | 5 |
| Fig. 1-3: A schematic diagram of the uranium series [CRW02]..... | 7 |
| Fig. 1-4: A schematic diagram of the Thorium series [CRW02]..... | 11 |
| Fig. 1-5 : A schematic diagram of U-235 radioactive decay series (actinium) [CRW02]..... | 13 |
| Fig. 1-6: Secular equilibrium..... | 14 |
| Fig. 1-7: Transient Equilibrium..... | 16 |
| Fig. 1-8: No equilibrium..... | 17 |
| Fig. 1-9: The site of the Chernobyl nuclear power station [UNS00]..... | 21 |
| Fig. 1-10: decay scheme of Cs-137 [NCR87]..... | 22 |
| Fig. 1-11: Shows some of the possible pathways of contamination to humans [Can02]..... | 24 |
| Fig. 1-12: Absorber dose rates in air from terrestrial gamma radiation ranked according to levels outdoors [UNS93]..... | 30 |
| Fig. 2-1: Map of locations of soil depth profile samples from north Ukraine [IAE91]..... | 33 |
| Fig. 2-2: Template method. By this method soil samples from Ukraine was taken..... | 33 |
| Fig. 2-3: Locations of soil sampling sites from Lippe, North Rhine-West phalia,Germany..... | 35 |
| Fig. 2-4: Locations of soil sampling site from Lower Saxony, Germany..... | 35 |
| Fig. 2-5: Schematics of semiconductor types of HPGe p or n type at the top, Cross sections perpendicular to the cylindrical axis of the crystal are shown at bottom [Kno00]..... | 38 |
| Fig. 2-6: Beryllium window at the face of the detector [Ortic]..... | 40 |
| Fig. 2-7: Block diagram of a typical gamma ray spectrometry system..... | 42 |
| Fig. 2-8: Gamma-ray spectrum of an energy calibration source..... | 43 |
| Fig. 2-9: Full energy peak efficiency as a function of gamma ray energy for a typical HPGe detector 1 for 1200 g soil in marinelli beaker..... | 47 |
| Fig. 2-10: Gamma-ray spectrum of the standard efficiency calibration for 1119 g soil in marinelli beaker of HPGe detector for 4 hours is the time of counts..... | 48 |
| Fig. 2-11: Full energy peak efficiency as a function of gamma ray energy for a typical HPGe detector 1 for 1200 g soil sample in marinelli beaker by using Gnuplot program..... | 49 |
| Fig. 2-12: Efficiency-Energy relation by using gray fit for 1100 g soil in marinelli beaker by using HPGe detector 1 (Be window)..... | 49 |
| Fig. 2-13: Variation of the efficiency versus mass of soil with gamma-ray energy 46.54 keV (Pb-210) in a marinelli beaker..... | 52 |
| Fig. 2-14: Count efficiency variation with masses of soil in marinelli beaker for ^{210}Pb 46.54 keV gamma-ray line..... | 52 |
| Fig. 2-15: Variation of efficiency-energy curves with heights of soil in marinelli beaker for a constant density..... | 53 |
| Fig. 2-16: Variation of efficiency-energy curves with heights of soil in Bottle 1000 ml for a constant density..... | 54 |
| Fig. 2-17: Variation of efficiency-energy curves with heights of soil in Marinelli beaker for detector 2..... | 55 |
| Fig. 2-18: Efficiency Variation of efficiency curves with heights of soil in marinelli beaker in the same volume for HPGe detector (1)..... | 56 |

| | |
|------------------------------------------------------------------------------------------------------------------------------------------------------------------------|-----|
| Fig. 2-19: Efficiency Variation of efficiency curves with heights of soil in marinelli beaker in the same volume for HPGe detector (1)..... | 57 |
| Fig. 2-20: Efficiency for different masses of soil in Bottle 250ml HPGe detector (2)..... | 58 |
| Fig. 2-21: A low-background shield configuration for a germanium detector [Kno00]..... | 59 |
| Fig. 2-22: The background spectrum recorded for germanium detector using the shield shown on Fig.2-21 for a counting time of 72 hours. | 60 |
| Fig.2-23: Comparison between radionuclides (Bq kg ⁻¹) in soil sample (ST-27/1998 Ringversuch) by PTB and present work at ZSR..... | 68 |
| Fig. 3-1: Depth distribution of ¹³⁷ Cs [Bq kg ⁻¹] in soil profile from Klein Lobke, North Germany..... | 74 |
| Fig. 3-2: Depth distribution of ¹³⁷ Cs [Bq kg ⁻¹] in soil profile from Twenge, (field) North Germany..... | 75 |
| Fig. 3-3: Depth distribution of ¹³⁷ Cs [Bq kg ⁻¹] in soil profile from Eilenrede, Lower Saxony, North Germany..... | 77 |
| Fig. 3-4: Depth distribution of ¹³⁷ Cs [Bq kg ⁻¹] in soil profile from Neßmerpolder, (meadow), North Germany..... | 79 |
| Fig. 3-5: ¹³⁷ Cs deposition densities [kBq m ⁻²] in soil taken from sites in Lower Saxony, North Germany..... | 80 |
| Fig. 3-6: Correlation between ¹³⁷ Cs and ⁴⁰ K in soil samples from Lower Saxony, North Germany..... | 82 |
| Fig. 3-7: The linear correlation between ¹³⁷ Cs and ⁴⁰ K concentrations in surface soil samples from Lippe, North Rhine-Westphalia, Germany..... | 86 |
| Fig. 3-8: Depth distribution of ¹³⁴ , ¹³⁷ Cs [Bq kg ⁻¹] in soil profile from Nosdrischtsche II, Ukraine..... | 88 |
| Fig. 3-9: Depth distribution of ¹³⁷ , ¹³⁴ Cs [Bq kg ⁻¹] in soil profile from Chiristinovka meadow, Ukraine..... | 89 |
| Fig. 3-10: Depth distribution of ¹³⁷ , ¹³⁴ Cs [Bq kg ⁻¹] in soil profile from Tschigiri 1, Ukraine... .. | 90 |
| Fig. 3-11: Depth distribution of ¹³⁷ Cs [Bq kg ⁻¹] in soil profile from Oserjanka 1, Ukraine. | 91 |
| Fig. 3-12: ¹³⁷ Cs and ¹³⁴ Cs deposition densities [kBq m ⁻²] in soil were taken from different sites in Ukraine..... | 93 |
| Fig. 3-13: Variation of Natural radionuclides with depth in depth profile soil from Ricklingen, Lower Saxony, North Germany. | 94 |
| Fig. 3-14: Variation of Natural radionuclides with depth in depth profile soil from Eilenriede, Lower Saxony, North Germany. | 96 |
| Fig. 3-15: Variation of natural radionuclides with depth in depth profile soil from Twenge, Lower Saxony, North Germany. | 97 |
| Fig. 3-16: Variation of natural radionuclides with depth in depth profile soil from Lippe (North Rhine-Westphalia), Germany..... | 99 |
| Fig. 3-17: Variation of natural radionuclides with depth in depth profile soil from Tschigiri 2, Ukraine..... | 103 |
| Fig. 3-18: Variation of natural radionuclides with depth in depth profile soil from Oserjanke1, Ukraine..... | 104 |
| Fig. 3-19: Elemental correlation between natural radionuclides in soil samples from Klein Lobke, Lower Saxony, North Germany..... | 106 |
| Fig. 3-20: Elemental correlation between natural radionuclides in soil samples from Ricklingen, Lower Saxony, North Germany. | 108 |
| Fig. 3-21: Elemental correlation between natural radionuclides in soil samples from Twenge, Lower Saxony, North Germany. | 110 |
| Fig. 3-22: Elemental correlation between natural radionuclides in soil samples from different sites in Lower Saxony, North Germany..... | 113 |

| | |
|----------------------------------------------------------------------------------------------------------------------------------------------------------------------------------------|-----|
| Fig. 3-23: Elemental correlation between natural radionuclides in soil samples from Lippe, (North Rhine-Westphalia), Germany. | 117 |
| Fig. 3-24: Elemental correlation between natural radionuclides in soil samples from Chirstinovka meadow, Ukraine. | 119 |
| Fig. 4-1: External gamma-dose rate (n Sv h ⁻¹) of ¹³⁷ Cs from Chernobyl-derived and past atmosphere in different locations in Lower Saxony, North Germany. | 122 |
| Fig. 4-2: Correlation between results of measurements and calculations dose rates in different sites in Ukraine. | 124 |
| Fig. 4-3: Calculated external gamma-dose rate (n Sv h ⁻¹) of ¹³⁷ Cs from Chernobyl-fellout in different locations in Ukraine. | 124 |
| Fig. 4-4: Calculated dose rates from natural radionuclides in soil samples from different locations in Lower Saxony, North Germany. | 126 |
| Fig. 4-5: Correlation between results of measurements and calculations dose rates at Lippe, NRW, Germany. | 131 |
| Fig. 4-6: Dose rate from natural radionuclides in soil samples from different sites in Ukraine | 133 |
| Fig. 4-7: The total external gamma dose rate in different sites, (a) Lippe (b) Lower Saxony | 134 |
| Fig. 5-1: Relation between different ages and external exposure from natural radionuclides in soil from Lower Saxony, North Germany. | 139 |
| Fig. 5-2: Relation between different ages and external exposure from natural radionuclides in soil from Lippe, NRW, Germany. | 140 |
| Fig. 5-3: Relation between different ages and external exposure from natural radionuclides in soil from Ukraine. | 141 |
| Fig. 5-4: Relation between different ages internal exposure (in μ Sv) from inhalation of natural radionuclides in soil (dust) from Lower Saxony, Germany. | 142 |
| Fig. 5-5: Relation between different ages internal exposure (in μ Sv) from inhalation of natural radionuclides in soil (dust) from Lippe, (Germany). | 143 |
| Fig. 5-6: Relation between different ages internal exposure (in μ Sv) from inhalation of natural radionuclides in soil (dust) from Ukraine. | 144 |
| Fig. 5-7: Internal exposure from direct ingestion of radionuclides in soil from Lower Saxony, (Germany) and age group. | 146 |
| Fig. 5-8: Internal exposure from direct ingestion of radionuclides in soil from Lippe, (Germany) and age group. | 147 |
| Fig. 5-9: Internal exposure from direct ingestion of radionuclides in soil from Ukraine. | 148 |
| Fig. 5-10: Annual external gamma radiation exposure (m Sv) from radionuclides in soil from Lower Saxony, Lippe, (Germany) and Ukraine. | 150 |
| Fig. 5-11: Annual internal gamma radiation exposure (μ Sv) from inhalation of radionuclides in soil from Lower Saxony, Lippe, (Germany) and Ukraine. | 150 |
| Fig. 5-12: Annual internal gamma radiation exposure (μ Sv) from direct ingestion of soil (dust) from Lower Saxony, Lippe (Germany), and Ukraine. | 151 |

Summary

Radioactivity can be found in almost every environmental medium, when sensitive detection methods were used. Measurement of environmental radioactivity is necessary for radiation protection purposes, but can also be useful to reveal transport processes in the environment. In this Thesis, were perform gamma-spectroscopy of calibration sources and of a soil sample which were collected. The soil samples were collected from 8 depth profile and surface soil from different locations in the Lower Saxony, Lippe (NRW) Germany and 22 depth profiles from Ukraine.

Collected soil samples from investigated sites and preparation these samples then measured these samples by using gamma spectrometry (HPGe).

This part of the thesis summaries the results obtained from monitoring radioactivity in the environment 1999-2003 in three chapters: analysis of radionuclides in soil, modeling of ambient dose rates from radionuclide concentrations in soil and internal and external gamma radiation exposure from soil

1. Analysis of radionuclides in soil

It is important to distinguish between radioactive contamination on the site and the 'background' level of radioactivity, which arises from natural radioactivity in the soils and from levels of man-made radionuclides originating from sources unrelated to the site (for example, atmospheric fallout from the Chernobyl accident).

Background levels of radioactivity will vary (i) from site to site and (ii) spatially within a site. The principal factor that controls the background level of natural radionuclides at a site is the level of radioactivity in the rock from which the soil was derived. Natural series radionuclides can also be concentrated in different parts of the soil column and weathering profile, typically associated with iron oxides, clay minerals and organic material. Therefore, it is to be expected that background levels of naturally occurring radionuclides in the rocks and soils will vary with depth.

Artificial radionuclides in the soil such as $^{137}, ^{134}\text{Cs}$. ^{137}Cs reaches values of up to 2.835 kBq m^{-2} in soil in Barum, and 7.324 kBq m^{-2} in Klein Lobke, Lowe Saxony, Germany and three different contaminated locations in Ukraine, the ^{137}Cs and ^{134}Cs deposition densities in high site are 5003 and 2729 k Bq m^{-2} , medium contaminated 795 and 558 kBq m^{-2} and not contaminated is 7.9 kBq m^{-2} for Nosdritsche2, Wornowo 4 and Oserjnaka 1, respectively. The natural decay series of uranium and thorium, the mean activities of ^{238}U , ^{226}Ra , ^{210}Pb , ^{235}U , ^{228}Ra , ^{228}Th , ^{232}Th and ^{40}K were 28.9, 27.9, 48.1, 1.3, 27.9, 27.3, 27.6 and 508 Bq kg^{-1} , respectively for surface soil from Lower Saxony and from Lippe NRW, Germany the range activities of ^{238}U , ^{226}Ra , ^{210}Pb , ^{235}U , ^{228}Ra , ^{228}Th , ^{232}Th and ^{40}K were 8-36.7, 13-572, 30-372, 0.37-1.8, 11-159, 10-149, 10-154 and 320 Bq kg^{-1} respectively.

The results of this study into the anomalous $^{226}\text{Ra}/^{238}\text{U}$ disequilibrium ($^{226}\text{Ra}/^{238}\text{U}$ of 0.96 - 35.427) in surface soil samples from Lippe. The high $^{226}\text{Ra}/^{238}\text{U}$ ratio is due to loss of ^{238}U relative to ^{226}Ra via oxidation and mobilisation of ^{238}U in the upper layers of the soil and subsequent loss in solution. At the lower Saxony, depths of the soil profile and surface soil, ^{238}U and ^{226}Ra are essentially in equilibrium (mean ration in Klein Lobke is 1.01 and surface soil is 1.06).

Calculation of the specific activity for ^{238}U , ^{235}U , ^{226}Ra , ^{210}Pb , ^{232}Th , ^{228}Th , ^{228}Ra , ^{40}K , ^{137}Cs , ^{134}Cs and these ratios $^{226}\text{Ra}/^{238}\text{U}$, $^{232}\text{Th}/^{238}\text{U}$, $^{210}\text{Pb}/^{226}\text{R}$, $^{40}\text{K}/^{238}\text{U}$, $^{40}\text{K}/^{232}\text{Th}$, $^{228}\text{Ra}/^{228}\text{Th}$, $^{134}\text{Cs}/^{137}\text{Cs}$ for depth profiles from different investigation areas.

2. Modeling of ambient dose rates from radionuclide concentrations in soil

The external dose from ^{137}Cs deposition densities in soil was calculated for detector at 1 m from a surface in a semi-infinite volume, and an soil depth profile. The external dose from ^{137}Cs ranged from 5.74 to 20.6 n Sv h⁻¹ and 0.002 to 6.0904 μ Sv h⁻¹ for lower Saxony, Germany and Ukraine, respectively.

Ambient dose rates from natural gamma ray calculated from a height of 1 m above the ground surface calculated from the activity concentrations of the radionuclides measured ^{238}U , ^{232}Th and ^{40}K . The mean dose rate at Lower Saxony 38.7 ± 2.5 n Sv h⁻¹, Lippe, NRW 126 ± 12.6 n Sv h⁻¹, and for Ukraine is 41.3 n Sv h⁻¹, and measurement of ambient dose rate for all investigation site

3. Internal and external gamma radiation exposure from soil

The man-made and natural radiation dose in the environment are of much concern recently. Some of the developed countries have made detailed assessment. The recent world average was assessed by the United Nations Scientific Committee on the Effects of Atomic Radiation UNS88□ the population dose may differ from different locations and living styles. The world average of natural radiation is around 2.4 mSv a⁻¹, but the maximum may be higher than 100 mSv a⁻¹. The world average of medical exposure is around 0.3 move a⁻¹, but in some developed countries it may be as high as 2.2 mSv a⁻¹ which is 7 times higher than the average (UNS93).

Hence, it is necessary to assess the population dose so as to support the radiation protection policy.

The radiation doses are calculated using the models and dose factors contained in the Bundesamt fuer Stralenschutz (BfS99), International Commission on Radiation Units and measurements (ICR94) and International Commission on Radiological Protection (ICR90)

Calculation of annual total external inhalation exposure from gamma radiation in Lower Saxony are the total annual external ingestion of direct soil exposure from gamma radiation are summaries in this table for all locations and for group ages.

Keyword

Soil samples, natural, artificial radionuclides, ambient dose rate, internal and external exposure

Zusammenfassung

In dieser Arbeit wurden gammaspektrometrische Untersuchungen mit Reinstgermaniumdetektoren (HPGe) an Quellen zur Kalibrierung und gesammelten Bodenproben vorgenommen. Bei den Bodenproben handelt es sich um acht Tiefenprofile und Oberflächenproben von verschiedenen Orten in Niedersachsen und Lippe (Nordrhein-Westfalen) sowie 22 Tiefenprofile aus der Ukraine.

Dieser Teil der Arbeit fasst die Ergebnisse aus der Überwachung von Radioaktivität in der Umwelt von 1999 bis 2003 in drei Kapiteln zusammen: Analyse von Radionukliden in Böden, Modellierung der externen Dosisleistung aufgrund von Radionuklidkonzentrationen in Böden, sowie interne und externe Exposition durch Gammastrahlung aus Böden.

4. Analyse von Radionukliden in Böden

Bei den untersuchten künstlichen Radionukliden handelt es sich um ^{134}Cs und ^{137}Cs . ^{137}Cs erreicht Depositionsdichten in Böden von bis zu $2,835 \text{ kBq}\cdot\text{m}^{-2}$ in Barum und $7,324 \text{ kBq}\cdot\text{m}^{-2}$ in Klein Lobke (Niedersachsen). Die ^{137}Cs - bzw. ^{134}Cs -Depositionsdichten betragen 5003 bzw. $2729 \text{ kBq}\cdot\text{m}^{-2}$ in der hochkontaminierten Zone (Probennahmestelle: Nosdritsche), 795 bzw. $558 \text{ kBq}\cdot\text{m}^{-2}$ in der mittelkontaminierten Zone (Wornoewo) und $7,9 \text{ kBq}\cdot\text{m}^{-2}$ in der nichtkontaminierten Zone (Oserjanka).

Für die Nuklide ^{238}U , ^{226}Ra , ^{210}Pb , ^{235}U , ^{228}Ra , ^{228}Th , ^{232}Th aus den natürlichen Zerfallsreihen von Uran und Thorium sowie ^{40}K betragen die mittleren spezifischen Aktivitäten in Oberflächenproben aus Niedersachsen und Lippe 28,9; 27,9; 48,1; 1,3; 27,9; 27,3; 27,6 bzw. $508 \text{ Bq}\cdot\text{kg}^{-1}$.

Diese Arbeit zeigte ein anormales Verhältnis von ^{226}Ra zu ^{238}U von 0,96 - 35,43 in Oberflächenproben aus Lippe. In den niedersächsischen Tiefenprofilen und Oberflächenproben befinden sich diese beiden Nuklide im wesentlichen im Gleichgewicht (der Mittelwert für $^{226}\text{Ra}/^{238}\text{U}$ beträgt 1,01 für Klein Lobke).

5. Modellierung der externen Dosisleistung aufgrund von Radionuklidkonzentrationen in Böden

Die externe Dosisleistung durch ^{137}Cs reicht von $5,74$ bis $20,6 \text{ nSv}\cdot\text{h}^{-1}$ für Niedersachsen und $0,002$ bis $6,090 \text{ }\mu\text{Sv}\cdot\text{h}^{-1}$ für die Ukraine.

Externe Dosisleistungen in 1 m Höhe über der Oberfläche durch natürliche Gammastrahlung aus Böden wurden aus den gemessenen spezifischen Aktivitäten von ^{238}U , ^{232}Th und ^{40}K berechnet. Die mittlere Dosisleistung beträgt $38,7 \pm 2,5 \text{ nSv}\cdot\text{h}^{-1}$ für Niedersachsen, $126 \pm 12,6 \text{ nSv}\cdot\text{h}^{-1}$ für Lippe und $41,3 \text{ nSv}\cdot\text{h}^{-1}$ für die Ukraine.

6. Interne und externe Exposition durch Gammastrahlung aus Böden

Die Strahlungsdosen wurden mit Hilfe von Modellen und Dosisfaktoren aus [Bfs99], [ICR94] und [ICR90] berechnet.

Schlafworte

Bodenproben, natürlichen, künstlichen Radionukliden, Ortosisleistung, Interne und externe Exposition

Acknowledgements

All gratitude is due to Almighty ALLAH who guided and aided me to bring- forth to light this thesis

The research described in this thesis was performed at the Center for radiation protection and radioecology (ZSR), Hannover University, Germany, under the supervision of Prof. Dr. R. Michel. I am grateful to have an opportunity to thank the many people who have contributed to this work. First, I would like to thank my thesis advisor, Prof. Dr. R. Michel for suggesting the present point of study, the support and encouragement he has provided over the last five years, continuous help during the progress of work and his critical reading of the manuscript, correcting the grammar, improving the text and giving helpful comments.

Also thanks to Dr. Bunnenberg for her encouragement, kindness and nobility, and Ms. Bunnenberg for her sympathy.

I would like to thank also Dr. M. Taeschner for repairing all defects of my computer during this study. A special word of gratitude is due to Dr. D. Jakob for his great helps and efforts during the collecting and preparation of soil samples and reading and corrected of my Ph.D. Thesis.

I also want to thank Mr. Jan W. Valburch for his help, friendship, scientific and fruitful discussions and the work we shared together will always remain memorable. Many thanks are rendered to the help, efforts and experience of Mr. R. Sachse for making computer programme for calculation external dose rate of ^{137}Cs and also help me to learn how did I make standard sources.

I would like to thank Dr. W. Botsch for his help me at the beginning of my work at ZSR. Special thanks are due to the members of the ZSR for their efforts for the many facilities provided during this study. My greatest thanks to my beloved home country Egypt and to the Egyptian Government who through a Ph.D. fellowship grant enabled me to perform the present study. Without this fellowship, this work would never have been possible.

All thanks are due to my parents (father and mother) my for their patience and their pray for me during my stay in Germany. "My Lord, have mercy on them, for they have raised me from infancy".

Finally, I can't forget my wife (Amany) and her good cooking. Many thanks for her encouragement, support, understanding, during our residence in Hannover, and children (Amal and Ahmed) for leaved their always all the time.

Hannover in
24.10.03



S. Harb

1 Introduction

1.1 Radioactivity in the environment

It is important to identify the concentrations of radioactive isotopes in soil because it constitutes a path for radioactivity to humans, plants and animals, and is an indicator of radioactive accumulation in the environment. Soil includes submarine, sediment and river-bed soil, but here it includes only soil from cultivated land. Detection and quantification of environmental radiations and radioactivity may be performed for a number of reasons. The basic purpose may be a desire to satisfy basic scientific curiosity and gain knowledge and an improved understanding of the world. A second reason may be to assess the impact of human activities involving radioactivity and radiation on the environment, a process which may require differentiation of natural and anthropogenic sources of radioactivity and lead to assessment of dose from environmental sources.

Differentiation between naturally occurring and artificially introduced radioactivity implies some sort of isotopic analysis technique, as well as knowledge of what was present prior to the introduction of man-made sources. Environmental dose assessment is a sequential procedure that begins with the characterization of the radionuclides or radiation sources. This logical first step is followed by determination of the radionuclide distributions and quantification in the environment, and the detection of external radiations incident on man and the uptake and accumulation of radioactivity by man. Once these data have been determined, they serve as the basis for the calculation of dose incurred from environmental sources. Any environmental surveillance program involving dose assessment must thus be designed to consider all of the factors that may result in or modify doses to people [Kat84].

Practically all natural material contains radioactive nuclides, though usually in such low concentration that they can be detected only by very sensitive analysis. This is true for water (rain water, rivers, lakes, sea), rocks and soil, and all living matter, as well as for structures based on natural raw materials [Cho95].

1.1.1 Natural Radionuclides in the environment

The radionuclides in our environment can be divided into:

- Natural radionuclides which formed from cosmic radiation, those that are part of the natural decay chains being with thorium uranium, and potassium (K-40).
- Radionuclides from modern techniques the sources of which can be categorized as anthropogenic (Man - made).

Natural sources of radiation are cosmic radiation and terrestrial radiation arising from the decay of naturally occurring radioactive substances. One hundred years of industrialization has produced and redistributed increasing amounts of radioactive matter. Industrialization releases additional radiation through mining (especially uranium), coal combustion, cement production, street construction and other human activities.

Radioactive elements defined by the number of protons in their nuclei are differentiated from their isotopes. An isotope is formed by the penetration of sub-atomic particles such as neutrons into the nucleus, resulting in a new, usually unstable, nucleus. These natural radionuclides are background loads, distributed over great areas. They enter the human body through foodstuffs, drinking water and air.

There are two sources of natural background radiation: the interaction of cosmic radiation with various atoms in the atmosphere and a fixed geochemical quantity of naturally occurring radionuclides in the earth's crust. Atmospheric processes include the bombardment of stable nuclei by cosmic rays, other radioactive particles and atomic particles, as well as collisions between selected stable nuclei. Some terrestrial radionuclides decay to gaseous elements (e.g., radon), which reach the earth's surface through diffusion through soil layers and can then enter the atmosphere. The cosmogenic production of radionuclides and release to the atmosphere of radionuclides from crustal processes occur at rates that are balanced by the decay of the radionuclides produced and released. The natural production of atmospheric radionuclides is essentially a steady-state process, provided the cosmic ray flux and the concentration of target atoms remain constant.

Radionuclides ultimately decay to stable (non-radioactive) nuclides. Further, the decay of radioactive crustal material continuously decreases the natural radioactive content of terrestrial materials. This assures that, over geological time (millions of years), the total inventory of natural background radionuclides declines globally and systematically.

Assessing the natural background of a radionuclide is often a difficult task, and some of the estimates include scientific and political controversies. Although the natural background level should either remain constant or decrease, sometimes a situation arises of an apparent increase in natural background levels reported for a radionuclide, usually explained by either various environmental processes that transport or translocate radionuclides from one region to another (e.g., climatic processes, oceanic movements, geophysical upheaval) or that past monitoring of background levels of a given radionuclide was not sufficient by today's standards to quantify the sources of a radionuclide. Once in the environment, contributions from various natural sources (in disturbed and undisturbed states relative to the natural occurrence) and artificial sources were subject to the various mixing processes that incorporate the radionuclide into the ambient observed radiation. This observed ambient radiation is sometimes equate to natural background, although it actually represents some unknown summation of contributions from natural and artificial sources.

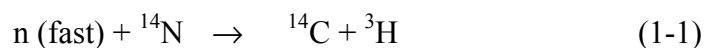
1.1.1.1 Cosmogenic radionuclides

The interaction of cosmic radiation with the earth's atmosphere produces many radionuclides. At high altitudes, hydrogen atom nuclei (protons) are 95% of the available targets subject to cosmic ray bombardment. Other atmospheric targets include ions and nuclei of helium, argon, krypton, oxygen, and nitrogen and the carbon atoms in carbondioxide and carbonmonoxide. Many cosmogenically produced radionuclides have short half-lives and so they do not affect the inventory of natural radionuclides. These nuclides are produced at constant rates and brought to the earth surface by rain water. Though they are formed in extremely low concentrations, the global inventory is by no means small. Equilibrium is assumed to be established between the production rate and the mean residence time of these radionuclides in terrestrial reservoirs (the atmosphere, the sea, lakes, soil, plants, etc) leading to constant specific radioactivities of the elements in each reservoir. If a reservoir is closed from the environment, its specific radioactivity decreases. This can be used to determine exposure times of meteorites to cosmic radiation and the constancy of the cosmic radiation field, using ^{81}Kr , dating marine sediments (using ^{10}Be , ^{26}Al), groundwater (^{36}Cl), glacial ice (^{10}Be), dead biological materials (^{14}C). The shorter-lived cosmogenic radionuclides have been used as natural tracers for atmospheric mixing and precipitation processes (e.g. ^{36}Cl or ^{38}S) [Cho95].

➤ Tritium (^3H)

Although tritium is produced in the atmosphere, it is more difficult to determine its natural background, because environmental measurements of tritium began after the onset of nuclear weapons testing. UNSCEAR [UNS82] reviewed data that suggested that the natural concentration of tritium in lakes, rivers, and potable waters was $0.2\text{--}1.0\text{ Bq l}^{-1}$ ($5\text{--}25\text{ pCi l}^{-1}$) prior to the advent of weapons testing. Most cosmogenically formed tritium deposits in oceans. The small fraction that goes to the great lakes can be estimated by comparing the size of the great lakes with that of the oceans.

Much larger amounts are formed in the atmosphere through nuclear reactions; e.g., between fast neutrons and nitrogen atoms



Tritium is also a product in the nuclear energy cycle, some of which is released to the atmosphere and some to the hydrosphere.

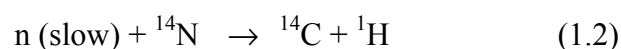
➤ Beryllium-7, 10

Two radioactive beryllium radionuclides, ^7Be (half-life: 53.6 days) and ^{10}Be (half-life: 2.6 million years), are produced cosmogenically, mainly in the stratosphere. Exchanges between atmospheric compartments produce a slow build-up of these isotopes in the troposphere. On the average, the tropospheric concentration of the longer-lived cosmogenic radionuclides increase during the spring at mid-latitudes because of a spring maximum in the rate of downward transport in the stratosphere and upper troposphere that occur in the region of the tropopause gap. The seasonal variations at high and low latitudes will be somewhat different from those at mid-latitudes, because of the increased distance from the mid-latitude source region [You81].

According to [NCR75] Beryllium deposited in wet and dry fallout goes mainly to sediments and terrestrial soils. Land surfaces accumulate 71% of ^7Be , and aquatic surfaces receive 28%. Deep ocean sediments receive 71% of the ^{10}Be , and terrestrial areas receive 28%. The differences in the inventories for the two isotopes reflect the differences in their half-lives: the longer lasting ^{10}Be reaches terrestrial and aquatic repositories before it has decayed significantly.

➤ Carbon-14

Carbon-14 has always been present on the earth. It is produced by cosmic ray interactions in the atmosphere. This nuclide is a pure beta-emitter, with a half-life of 5730 years, a maximum energy of 185 keV and an average energy of 49.47 keV [NCR78]. Carbon-14 is produced by the action of cosmic ray neutrons on nitrogen atoms, both in the stratosphere and in the upper troposphere, [UNS77] has estimated the natural production rate to be about 10^{15} Bq per year, a value which has been derived from assessments of the natural ^{14}C inventory.



This reaction occurs with a yield of approximately 22000 atoms ^{14}C formed per s and m^2 of the earth's surface; the global annual production is $\sim 1\text{ PBq}$, and global inventory $\sim 8500\text{ PBq}$

(corresponding to ~75 tons). Of this amount -140 PBq remain in the atmosphere while the rest is incorporated in terrestrial material. Probably more is known about the natural background of ^{14}C Than any other cosmogenically produced radionuclide, ^{14}C is produced by neutron bombardment of ^{14}N in the atmosphere. The variations in the atmospheric content of ^{14}C are caused by changes in the cosmic ray flux. The neutron bombardment of ^{14}N also follows airborne detonation of nuclear weapons.

UNSCEAR [UNS77] noted that "the fossil records of ^{14}C in tree rings, lake and ocean sediments suggest that the natural ^{14}C levels have remained relatively unchanged for many thousands of years the long-term fluctuation over a period of 10,000 years is attributed to a cyclical change of the dipole strength of the earth's magnetic field, which results in a cyclical change of the cosmic ray flux, which in turn changes the ^{14}C production rate." UNSCEAR thus implied that the normal geochemical ratio value of $^{14}\text{C}/^{12}\text{C}$ has been constant since primordial times despite different estimates for the natural production rate of radiocarbon, ranging from a low of $1.8 \text{ atoms}\cdot\text{cm}^{-2}\cdot\text{s}^{-1}$ to a high of $2.5 \text{ atoms}\cdot\text{cm}^{-2}\cdot\text{s}^{-1}$. UNSCEAR cited as a value, $2.28 \text{ atoms}\cdot\text{cm}^{-2}\cdot\text{s}^{-1}$, although some geochemists have long used the upper value of $2.5 \text{ atoms}\cdot\text{cm}^{-2}\cdot\text{s}^{-1}$ in calculations of a radiocarbon inventory.

➤ Krypton

Krypton is element number 36 in the periodic table. It belongs, to the group of inert gases together with helium, neon, argon, xenon and radon. The naturally occurring stable krypton isotopes and their atom percentage abundances are: ^{78}Kr (0.35%), ^{80}Kr (2.27%), ^{82}Kr (11.56%), ^{83}Kr (11.55%), ^{84}Kr (56.9%), ^{86}Kr (17.37%).

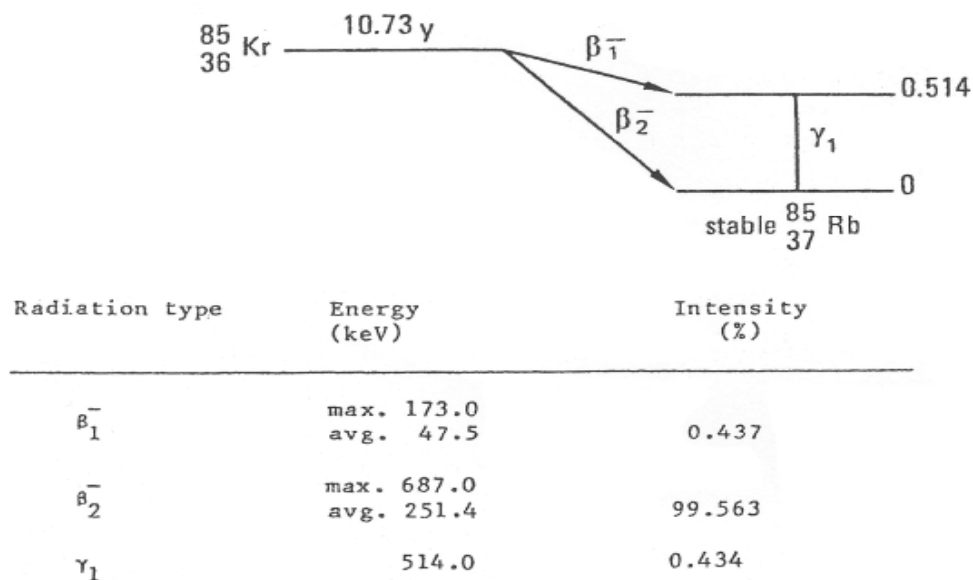


Fig. 1-1: Decay scheme for krypton-85 [Led77]

The radioactive isotopes of krypton include mass numbers of 74-77, 79, 79m, 81, 81m, 85, 85 m, 87-95 and 97. Some of these occur naturally in low trace amounts as a result of cosmic ray induced reactions with stable krypton isotopes and by spontaneous fission of natural uranium. The radioactive isotope ^{85}Kr is produced in nuclear fission. With a half-life of 10.7 years, it can become widely dispersed in the atmosphere following release. The decay scheme of ^{85}Kr is presented in Figure (1-1) Two beta particles and a single gamma photon are emitted,

along with several low-energy conversion electrons and x rays. Krypton-85 is produced by cosmic ray interactions in the atmosphere, in nuclear power reactors, and nuclear explosions.

The main release source is the dissolution step in the reprocessing of nuclear fuel. Krypton-85 is present in small amounts in the environment as a result of spontaneous fission of natural uranium and interactions of cosmic ray neutrons with atmospheric ^{84}Kr . The steady state environmental inventories of ^{85}Kr from these sources have been calculated: $7.4 \cdot 10^{10}$ Bq in the upper 3 m of the total land and water surface due to spontaneous fission of natural uranium, $3.7 \cdot 10^{11}$ Bq in the atmosphere from cosmic ray production and $3.7 \cdot 10^5$ Bq in the oceans from the atmospheric source [Die72]. Another source of ^{85}Kr associated with nuclear weapons is in the production of plutonium in military reactors.

1.1.1.2 Terrestrials sources of radiation

If the half-life of a radionuclide found in geological strata approximates the estimated age of the earth, then the radionuclide is primordial; it was presumably present from the time of the earth's beginning. Inventories of primordial radionuclides are essential parts of the natural background level of radioactivity in the environment.

Two classes of radionuclides occur naturally in geological strata: those in the decay series of thorium and uranium and those which do not originate from decay series. Uranium and thorium are natural radioactive elements in various minerals and ores as well as trace contaminants in coal and phosphate-bearing rocks. The non-decay series radionuclides include the well-known ^{40}K (potassium-40) and ^{87}Rb (rubidium-87); radioactive forms of vanadium, cadmium, platinum, cerium, and other rare earth (lanthanide) elements; and one isotope of bismuth.

1.1.1.2.1 Potassium-40

Potassium-40 is a primordial radioisotope of potassium that is quite possibly the most important radionuclide of terrestrial origin, at least from a biological standpoint. Potassium, a member of the highly reactive Group 1A alkali metal family, has three isotopes with mass numbers 39, 40, and 41; only ^{40}K is radioactive and has a half-life of $1.3 \cdot 10^9$ years. As potassium is essential to life, ^{40}K is found in all living and formerly living things.

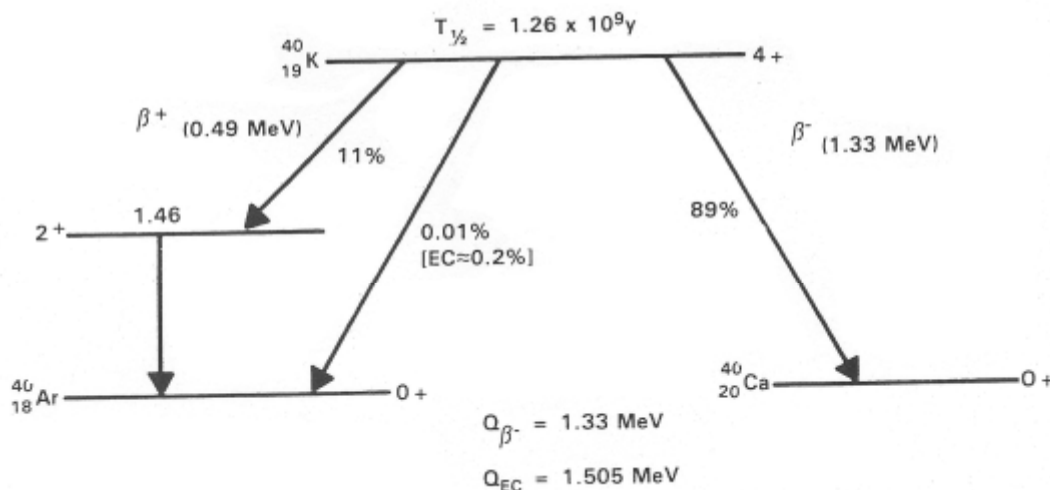


Fig. 1-2: Decay scheme of ^{40}K [Led77]

The isotopic abundance of ^{40}K is small, only 0.012% of naturally occurring potassium, which gives a specific activity of 855 pCi g^{-1} (31.6 Bq g^{-1}) of natural potassium. The decay scheme for ^{40}K is shown in Fig. (1-2) ^{40}K , with a half-life of 1.26×10^9 years, undergoes decay to stable ^{40}Ca 89% of the time, emitting a $1.314 \text{ MeV}_{\text{max}}$ beta particle in the process. With the exception of a tiny fraction of decays ($1 \times 10^{-3} \%$) by electron capture (EC), ^{40}K undergoes decay by positron emission the remaining 11 % of the time, emitting a characteristic photon with energy of 1.460 MeV. This photon is highly useful for identification and quantification of ^{40}K by gamma spectrometry, and makes an excellent calibration point because of the presence of potassium in essentially all environmental samples [Kat84].

1.1.1.2.2 Rubidium-87

Of the two rubidium isotopes found in nature, ^{85}Rb and ^{87}Rb , only the latter is radioactive, with a half-life of 4.8×10^{10} years. Rubidium-87 is a pure β^- -emitter, and it is present in elemental rubidium in the amount of 27.8%, which endows this element with a specific activity of $0.02 \text{ }\mu\text{Ci g}^{-1}$ (0.74 kBq g^{-1}). The rubidium content of all but highly humic soils is about 0.01%. The ^{87}Rb content of ocean water has been reported to be 2.8 pCi l^{-1} (104 Bq m^{-3}), with marine fish and invertebrates ranging from 0.008 to 0.08 pCi g^{-1} (0.3 to 3 Bq kg^{-1} wet weight) [Eis97]. It is estimated [NCR87] that the whole-body dose from ^{87}Rb is 0.3 mrem y^{-1} ($3 \text{ }\mu\text{Sv y}^{-1}$) on average.

1.1.1.2.3 Uranium-238 series

Uranium, element number 92, is the most massive of the naturally-occurring elements (sp. gr. $18.8 \text{ gm}\cdot\text{cm}^{-3}$). It is the fourth element in the actinide series which is analogous to the lanthanide series of rare earth elements structurally and geochemically. Uranium appears to be concentrated in the upper lithosphere, particularly in silicic igneous rocks and in late magmatic fluids. Uranium does not occur as a native element, nor does it form sulfides, tellurides, or arsenides. It behaves geochemically as a strongly oxyphile element.

The three naturally occurring isotopes of uranium have atomic weights of 234, 235 and 238. Uranium-234 is one of the intermediate progeny in the uranium-238 $[4n + 2]$ decay series (Fig. 1-3). It has a half-life of 2.5×10^5 years, and decays by alpha-decay to yield thorium-230. Uranium-234 makes up a very small fraction (approximately 0.0055%) of natural uranium, and is important only as a critical intermediate nuclide in the generation of radon-222 by the breakdown of uranium-238.

Uranium-235 makes up approximately 0.7% of natural uranium. This isotope has a half-life of 7.1×10^8 years, and is one of the "primordial" nuclides in the earth's crust. Uranium-235 will undergo fission with slow neutrons and because it can sustain a chain fission reaction with the release of large amounts of energy, it is important as a nuclear fuel. Uranium-235 yields radon-219 as an intermediate daughter in the $[4n+3]$ decay series (Fig.1-5). Uranium-238 is by far the most abundant uranium isotope, and makes up more than 99.2% of natural uranium. Uranium-238 has a very long half-life (4.5×10^9 years), and like uranium-235 is among the "primordial" nuclides of the crust. The $[4n+2]$ radioactive decay series headed by uranium-238 yields the most important and longest-lived radon isotope, radon-222 [Maj90].

According to [Iva92], the uranium series is the longest known series. It begins with the heaviest naturally occurring nuclide, ^{238}U , and passes a second time through Z as a consequence

transitions. The continuous beta spectrum accompanying this decay has the high end-point energy of 2290 keV. The isomer $^{234}\text{Pa}^*$ has an extremely complex beta, gamma and conversion-electron spectrum.

The fourth member of the uranium ($4n + 2$) decay series is ^{234}U ($t_{1/2} = 2.48 \times 10^5$ a). It is a beta-stable alpha-emitter. The energy of the first group is 4.768 MeV (72 per cent), and of the second group is 4.717 MeV (28 per cent). An additional group with an energy of 4.6 MeV (0.3 per cent) has been observed and gamma-ray groups of 53 and 118 keV have been measured. The observations are summarized in the decay scheme of Fig. 1.8. As can be seen from Fig. 1.8, the immediate daughter resulting from the alpha decay of ^{234}U is ^{230}Th . This nuclide is another alpha-emitter with a half-life of 7.52×10^4 a. At least four alpha groups have been identified with energies and intensities as follows: 4.682 MeV (76 per cent), 4.615 MeV (24 per cent), 4.476 MeV (0.12 per cent), and 4.437 MeV (0.03 per cent). Numerous gamma rays have been observed [Iva92].

➤ Radium-226

Radium is a divalent alkaline-earth metal (Group IIA of the Periodic Table). It shares the chemical properties of beryllium, magnesium, calcium and strontium, and exhibits very strong geochemical coherence with barium. Radium is produced by the radioactive decay of uranium and thorium, and it occurs primarily in rocks bearing those elements, most notably the sialic (alkaline) igneous rocks, pegmatites, and certain hydrothermal veins. Like the other elements in the group, radium forms a wide range of minerals, most of which have more familiar calcium, magnesium or barium analogues; the radium-bearing minerals are usually characterized by high melting points and very low solubility in water. Radium commonly replaces the other alkaline-earth metals diadochically, substituting for calcium, magnesium and barium in common carbonate, sulfate and phosphate minerals. There are four naturally-occurring radium isotopes, three of which have relatively short half-lives (radium-223, 11.4 days; radium-224, 3.6 days; radium-228, 5.75 years). The fourth and most abundant isotope, radium-226, has a half-life of 1.620 years, long enough to allow significant concentrations of radium to persist in geologically recent deposits without a supporting concentration of uranium or thorium. It is an alpha-emitter with four known alpha groups: 4.781 MeV (94 per cent), 4.598 MeV (5.1 per cent), 4.340 MeV (7×10^{-3} per cent) and 4.191 MeV (1×10^{-3} per cent). Several gammas are observed in the energy region between 186 and 610 keV. Thus, the radium concentration in certain post-Pleistocene marine deposits and in some modern marine organisms is greater than the amount in equilibrium with the coexisting uranium.

Except for some recent deposits, the distribution of radium is determined by the occurrence of uranium or thorium, modified somewhat by the chemical properties of radium itself. In Pleistocene and older rocks, the element is invariably found in association (and usually in radioactive equilibrium) with its parent nuclides [Maj90].

➤ Radon-222 and its short-lived products (^{218}Po , ^{214}Pb , ^{214}Bi , ^{214}Po)

Radon, element number 86, is the heaviest of the noble gases. Both odorless and colorless, it is produced by the radioactive decay of several isotopes of radium, which, in turn, are among the daughter nuclides found in uranium- and thorium-bearing rocks of the earth's crust. Chemically, radon shares the properties of other elements of the noble gas group. Radon has the highest boiling point (-62°C) and the highest freezing point (-71°C) of the noble gases. It is the most soluble of the noble gases in water and is very soluble in organic liquids including crude

petroleum. In near-surface environments it occurs most commonly as a component of soil gases, in solution in ground- or surface-water or in solution in petroleum and associated oil field brines. Ordinarily the gas diffuses to the earth's surface where it is quickly dispersed in the atmosphere. Its concentration in dry air at the surface is on the order of 0.27 Bq l^{-1} (10^{-10} ppb by weight), and diminishes in abundance rapidly with altitude as a result of the combined effects of dilution and radioactive decay.

There are three naturally occurring isotopes of radon; all are intermediate progeny in decay series starting with uranium or thorium and ending in stable isotopes of lead (Figs 1-3, 1- 4, 1-5) Radon-219 (historically "actinon"), is produced by alpha decay of radium-223, in the uranium-235 ("actinium" or $[4n+3]$) decay series (Fig. 1-5). Because of its very short half-life (3.96 seconds) and the relatively small natural abundance of uranium-235 (0.7% of naturally occurring uranium), radon-219 is of minor environmental significance, and may be neglected.

Radon-220 (historically "thoron"), with a half-life of 56 seconds, is the daughter of radium-224 in the thorium-232 ($[4n]$) decay series (Fig. 1- 4). Although the half-life of radon-220 is short, thorium is more abundant in nature than uranium-238, and thorium-232 is the only naturally occurring isotope. Radon-220 may therefore make up a significant fraction of natural radon in some environments.

By far the most important isotope is radon-222. Its half-life of 3.82 days, although short by geological standards, is sufficiently long relative the rates of soil gas diffusion, atmospheric convection or ground-water flow to allow wide dispersal of the gas even in the absence of its radium-226 parent. It is an intermediate daughter in the $[4n + 2]$ uranium decay series headed by the most abundant naturally occurring uranium isotope, uranium-238 (Fig.1-3). Together, its relatively long half-life and the abundance of its parent nuclide ensure that radon-222 and its progeny will be the dominant contributors to environmental radon contamination. With a maximum half-life of less than four days, appreciable concentrations of radon can exist only where continuously replenished by the decay of its radium progenitors. In the absence of radium-226, for example, less than 0.5 % of the original concentration of radon-222 will remain after thirty-one days. The shorter-lived isotopes would vanish in less than an hour. Therefore, the natural occurrence of radon will be determined primarily by the distribution of radium in the rocks, soil and fluids of the earth's crust; the distribution of radium being controlled, in turn, by the natural occurrence of its progenitors, uranium and thorium. The mobility imparted to radon gas by its physical state, by its solubility, and by its chemical stability, however, implies that under certain circumstances the gas may migrate from the immediate area of its formation, and accumulate at a substantial distance from its radium source. This fact introduces a significant uncertainty into regional "radon potential" surveys based on the distribution of uranium, thorium or radium [Maj90].

Radon in soil gas is mainly derived in situ by the decay of radium contained in or on the solid particles of the soil. Where this occurs, the radon concentration in the soil gas will be directly related to the local abundance of radium, although it will be affected by soil porosity and permeability, by soil mineralogy, soil moisture, and by the emanation coefficient. However, because the half-life of radon-222 may be long relative to the rate of movement of soil constituents under certain conditions, the gas may become separated from its parent nuclide by diffusion or convective flow in the gas phase, or by transport in aqueous solution in moving ground- or surface-water. If the soil gas concentration is not ephemeral, it must be sustained by a

continuous transfer of radon from the source area to the site of accumulation. The transfer may take place along faults or fractures, or through caverns in bedrock, through high permeability (and high porosity) zones in soil or bedrock, or in flowing surface or sub-surface water. In many such cases, the path of radon migration can be identified and the isolated soil gas concentration linked to a radium source.

Isolated high radon levels may also occur in wells and springs supplied by aquifers rich in radium. Because the dissolved gases will be released where subjected to pressure reduction, turbulence or heating, domestic use of such radon-charged water can contribute to indoor radon pollution, although most investigators regard this as a relatively minor source of contamination except under unusual circumstances [Naz88].

The immediate daughter of ^{226}Ra is ^{222}Rn ($t_{1/2} = 3.825$ d). Radon-222 also emits only alpha particles: the predominant group of 5.486 MeV (approximately 100 per cent) and a much weaker one of 4.983 MeV ($\sim 8 \times 10^{-2}$ per cent).

The next series of decay products, ^{218}Po , ^{214}Pb , ^{214}Bi , ^{214}Po and ^{210}Tl , are quite short-lived and rapidly come to transient equilibrium with radon. This group is a mixture of alpha- and beta-emitters as illustrated in Fig 1-3. The atmospheric release of radionuclides from geological strata is a multistage process: formation of a radionuclide of a gaseous element, diffusion of the radionuclide through soils to the soil surface (soil-atmosphere interface), and release to the atmosphere. The most important gaseous radionuclide is the noble gas radon, ^{222}Rn , and its long-lived progeny ^{210}Pb and ^{210}Po . Radon gas has a half-life of 3.8 days. Once radon reaches the atmosphere, it dissipates quickly while continuing its radioactive decay. Its decay products are solids and aerosol-forming radionuclides, which can deposit on soil or water, but inventories of radon per se are not important for contamination of the water.

➤ Long-lived decay products of Radon-222 (^{210}Pb , ^{210}Bi , ^{210}Po)

The last group of radionuclides belonging to the U-series is headed by ^{210}Pb ($t_{1/2} = 22$ y) and the series ends with the stable end-product ^{206}Pb . Suffice it to add that the isotopic abundance of the stable end-product, ^{206}Pb , when compared to other lead isotopes, had considerable historical importance in the understanding of natural radioactivity and continues to have great significance for dating of minerals [Iva92].

1.1.1.2.4 Thorium-232 series

The thorium series includes alpha- and beta-emitting radionuclides with mass numbers which are multiples of 4, that is $A = 4n$. The longest-lived member of the $4n$ series is ^{232}Th ($t_{1/2} = 1.39 \times 10^{10}$ a). Its half-life is about three times longer than the currently estimated age of the earth, permitting it and its decay products to occur in nature. The immediate parent of ^{232}Th is the alpha-emitter ^{236}U , but its half-life is only 2.4×10^7 y, and it is, therefore, no longer found in nature. Along with ^{236}U a number of heavy nuclei having $A = 4n$ have been produced artificially in a variety of nuclear reactions and they all join the series above ^{232}Th . The second of the three naturally occurring series of radioactive elements is the thorium ($4n$) decay series. The series originates with ^{232}Th and terminates with the stable nuclide ^{208}Pb . The thorium series is illustrated in Fig. 1-4.

The alpha spectrum of ^{228}Th ($t_{1/2} = 1.913$ a) consists of five energy groups: 5.421 MeV (71 per cent), 5.338 MeV (28 per cent), 5.208 MeV (0.4 per cent), 5.173 MeV (0.2 per cent), and 5.137 MeV (0.03 per cent).

The immediate daughter of ^{228}Th is ^{224}Ra ($t_{1/2} = 3.64$ d). It is an alpha-emitter with two prominent alpha-particle groups: 5.684 MeV (94 per cent) and 5.447 MeV (5.1 per cent). There are three others of very low intensity: 5.159, 5.049 and 5.032 MeV. The second of the two main groups (5.447 MeV) is of particular importance in the analysis of alpha-spectra containing ^{228}Th groups because it appears hidden under the ^{228}Th alpha peak [Iva92].

➤ Randon-220 and its decay products (^{215}Po , ^{212}Pb , ^{212}Bi , ^{212}Po , ^{208}Tl)

The remaining members of the (4n) series are all very short-lived, the longest half-life being that of ^{212}Pb , 10.64 h. The complexity of the beta-decay of ^{212}Pb , ^{212}Bi and ^{208}Tl may be noted. Additional features of interest are the long-range alpha particles originating from the excited levels of ^{212}Po , the prominent gamma ray with the high energy of 2.615 MeV which occurs in 100 per cent of the disintegrations of ^{208}Tl , and the branching decay of ^{212}Bi . The stable end-product of the 4n decay series is ^{208}Pb [Iva92].

1.1.1.2.5 The actinium series

The actinium series begins in nature with its longest-lived nuclide ^{235}U , and ends with the stable lead isotope, ^{207}Pb . The actinium (4n + 3) series is summarized in Fig 1.5. The primary nuclide from which all the other nuclides in this series are derived is ^{235}U . It is conceivable that higher-mass nuclides in the actinium series like ^{239}Pu , ^{234}Cm , ^{234}Am , ^{247}Bk , etc., were also present when the elements were first formed, but of all the nuclides of the (4n + 3) type above lead, only ^{235}U ($t_{1/2} = 7.13 \times 10^8$ a) is sufficiently long-lived to have persisted throughout geologic time. Any sample of natural uranium, no matter what its source, contains ^{235}U in a constant amount relative to ^{238}U , namely 0.72 atom per cent (a notable exception are the samples from a fossil, natural ^{235}U fission reactor site at Oklo, Gabon). Thus, 1 mg of pure natural uranium emits exactly 1501 alpha particles per minute. Of these, 733.6 are emitted by ^{238}U , an equal number by ^{234}U in equilibrium with ^{238}U , and 33.7 by ^{235}U .

Uranium-235 is an alpha-emitter with a complex alpha spectrum and a correspondingly complex gamma spectrum. About ten alpha groups have been observed, all in the energy region between 4.1 and 4.6 MeV. Of these, the two most prominent groups have energies of 4.391 MeV (57 per cent) and 4.361 MeV (18 per cent).

The immediate decay product of ^{235}U is ^{231}Th ($t_{1/2} = 26.64$ h). Thorium-231 is a beta-emitter with a complicated decay scheme. The most energetic beta group has an end-point energy of 300 keV and the total decay energy is 383 keV.

The next nuclide in the actinium decay chain is ^{231}Pa ($t_{1/2} = 3.43 \times 10^4$ a). It is also an alpha-emitter and the longest-lived of the protactinium isotopes. The alpha spectrum of ^{231}Pa is complex with the highest-intensity alpha-group energies of 5.05 MeV (11 per cent), 5.016 MeV (up to 20 per cent), 4.999 MeV (25.4 per cent), 4.938 MeV (22.8 per cent), and 4.724 MeV (8.4 per cent). Its daughter is ^{227}Ac ($t_{1/2} = 22$ a). Actinium-227 is a beta-emitter with an end-point energy of about 45 keV (98.8 per cent). Alpha-decay branching occurs with only 1.2 per cent intensity. The most prominent alpha-group energies are 4.949 MeV (48.7 per cent), 4.937 MeV (36.1 per cent), 4.866 MeV (6.9 per cent), and 4.849 MeV (5.5 per cent) [Iva92].

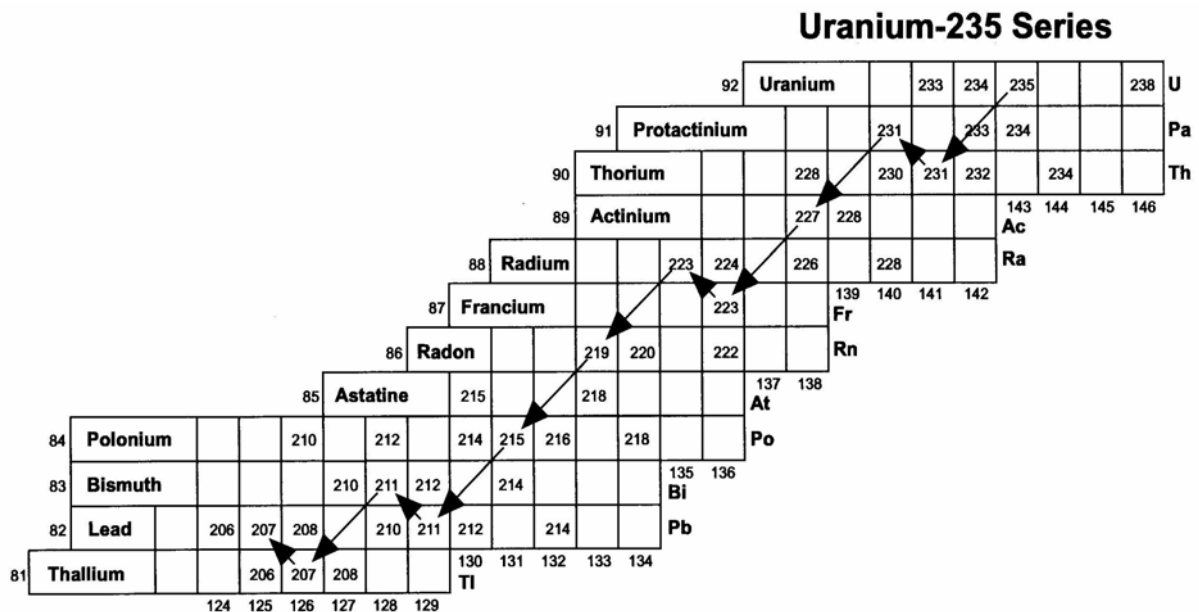


Fig. 1-5 : A schematic diagram of U-235 radioactive decay series (actinium) [CRW02].

1.1.1.2.6 The neptunium series

A fourth long radioactive decay series, the neptunium series, is composed of nuclides having mass numbers which divided by 4 have a remainder of 1 (the $4n + 1$ series). The name comes from the longest lived $A = 4n + 1$ nuclide heavier than Bi, ^{237}Np , which is considered as the parent species, it a half-life of 2.14×10^6 a. The end product of the neptunium series is ^{209}Bi , which is the only stable isotope of bismuth. Seven alpha and beta decays are required in the sequence from the parent ^{237}Np to ^{209}Bi . An important nuclide in the neptunium decay series is the uranium isotope ^{233}U , which has a half-life of 1.59×10^5 a, is fissionable by slow neutrons [Cho95].

1.1.1.2.7 Decay Relationships Series

The radioactivity decay or activity-time relationship of any radionuclide can be relatively easily derived and treated in many references ([Kat84], [Cho95], [Iva92]) The activity, A , or number of atoms decaying in a time period can also be written as N/t , in which N is the number of atoms decaying and t is the period of time. This is, of course, simply the rate of decay. If there are initially N atoms, the initial rate of decay will be N/t , but inasmuch as the radioactive atoms are constantly being removed from the system by decay, the rate of decay, or the number of atoms decaying in a unit time interval, continually becomes smaller. This change in the decay rate can be expressed in differential notation as $-dN/dt$, being negative as it is decreasing with time, and is mathematically equal to the number of atoms, N , times the probability of an atom undergoing decay in a time interval, which is represented by λ as shown in equation 1-3

$$-dN/dt = \lambda N \quad (1-3)$$

This equation can be rearranged

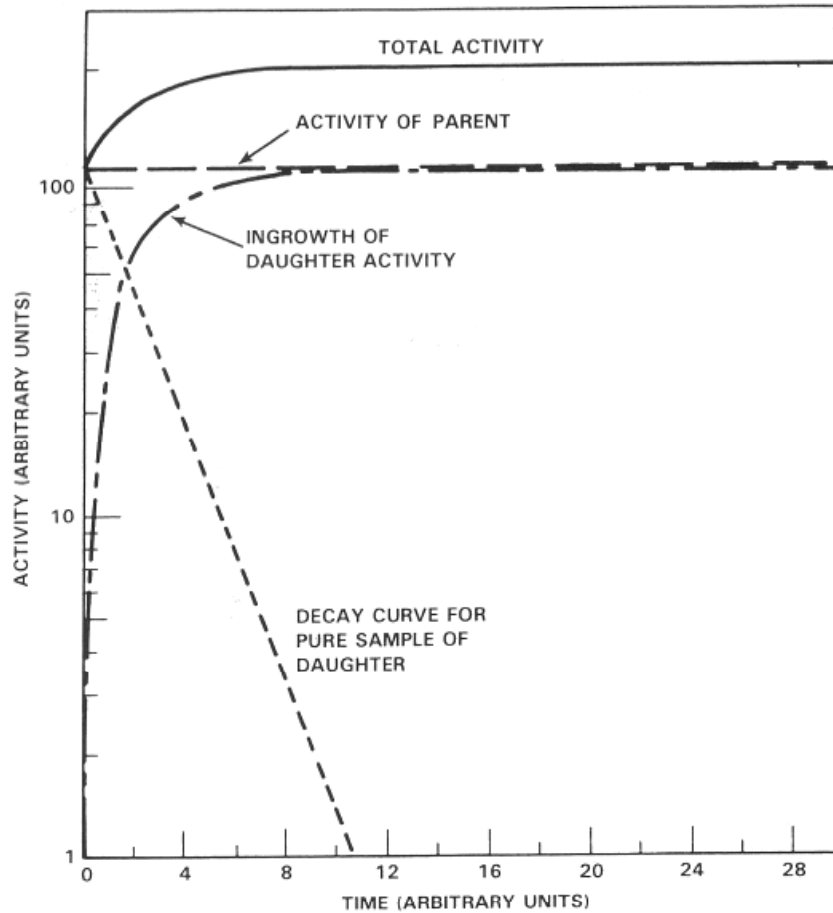


Fig. 1-6: Secular equilibrium

$$\frac{dN}{N} = -\lambda dt$$

and both sides integrated with respect to time from zero to infinity

$$\int_0^{\infty} \frac{dN}{N} = \int_0^{\infty} -\lambda dt$$

and the terms rearranged to give

$$\ln \left(\frac{N}{N_0} \right) = -\lambda t \quad (1-4)$$

The final form, equation 1-4, is known as the fundamental decay law; in this equation, N is the number of radioactive atoms remaining at any time t , N_0 is the original number of atoms (i.e., the number of atoms at zero time), and λ is the decay constant for the particular radionuclide, expressed in units of reciprocal time.

The form of the fundamental decay law given in equation 1-4 is applicable with either activity, A , or number of atoms, N , since one is a constant multiple of the other ($A = \lambda N$) and applies only in the case of radioactive parent decaying to a stable daughter. The activity relationships among members of a chain may be very complex, and are related to the decay constants of the individual members of the series. If only a two member radioactive chain is

considered that is, a chain with a radioactive parent giving rise to a radioactive daughter, three possibilities can be seen to exist:

- 1) the half-life of the parent can be greater than that of the daughter (in which case the decay constant of the parent is smaller than that of the daughter).
- 2) the half-life of the parent and daughter are equal (or nearly so).
- 3) the half-life of the parent is less than that of the daughter. With these in mind, the concept of radioactive equilibrium between radioactive parent and daughter can be examined.

There are basically three conditions of equilibrium between a radioactive parent and radioactive daughter: secular, transient, and no equilibrium. In the first case, secular equilibrium (Fig. 1-6), the half-life of the parent is very much greater than that of the daughter, and, given an initially pure parent, the activity of the daughter will gradually increase or grow in until it is exactly equal to that of the parent, or

$$\lambda_1 N_1 = \lambda_2 N_2 \quad (1-5)$$

In which the subscript 1 refers to the parent and the subscript 2 to the daughter. At equilibrium, then, the total activity is twice what was originally present from the initially pure parent; reduction in activity of the parent may be neglected inasmuch as its half-life is so much longer than that of the daughter. Essentially what happens at equilibrium is that every time the parent decays to produce a daughter atom, a daughter atom also decays. Thus, the decay of the mixture of parent and daughter follows the decay curve of the parent. Note that although the activities of parent and daughter are equal, the numbers of atoms present are not, because of the higher specific activity of the daughter, and are related to the ratios of their decay constants as shown in equation 1-6 below, which is simply a rearrangement of the terms in equation 1-5.

$$\frac{N_1}{N_2} = \frac{\lambda_2}{\lambda_1} \quad (1-6)$$

The relationship of parent to daughter activity can be expressed by equation 1-7

$$N_2 = \frac{\lambda_1 N_1}{\lambda_2} (1 - e^{-\lambda_2 t}) \quad (1-7)$$

N in which N_1 and N_2 refer to the number of atoms of parent and daughter, respectively, present at any time t , λ_1 and λ_2 are the respective decay constants. The term in parentheses is simply a build up term, and represents the fraction of equilibrium achieved; as $\lambda_2 \rightarrow \infty$ $e^{-\lambda_2 t} \rightarrow 0$ and therefore

$$\lambda_1 N_1 = \lambda_2 N_2$$

For practical purposes, 100% equilibrium is reached after about 7 daughter half-lives, assuming an initially pure parent at zero time. There are many examples of potential secular equilibrium in nature a good example is given by the first two members of the 4n chain, ^{232}Th with a half-life of 1.4×10^{10} years, and its daughter ^{226}Ra , with a half-life of only 6.7 years. If one were to start with an initially pure sample containing 1 Bq (1 disintegration per second) of ^{232}Th , about 50 years later, the activity from the thorium would not have changed, since 50 years is small relative to its half-life, but there would then be a comparable activity from the ^{226}Ra daughter.

The condition of transient equilibrium occurs when the half life of the parent is greater (but not manyfold so) than that of the daughter. In this situation, illustrated graphically in Fig. 1-7, the parent undergoes measurable decay while the buildup of the daughter is occurring. As is the case with secular equilibrium, the decay of the combined mixture of parent and daughter follows the decay of the parent after equilibrium is reached. However, because the half-lives of the two are not widely different, the combined activity from the parent and daughter never reach a value of twice the initial activity of the initially pure parent. Mathematically, the general equation for the number of daughter atoms is expressed by equation (1-8)

$$N_2 = \frac{\lambda_1}{\lambda_2 - \lambda_1} N_{01} e^{-\lambda_1 t} \quad (1-8)$$

and, since

$$N_1 = N_{01} e^{-\lambda_1 t}$$

by substitution and rearrangement, equation 1-8 reduces to:

$$\frac{N_1}{N_2} = \frac{\lambda_2 - \lambda_1}{\lambda_1}$$

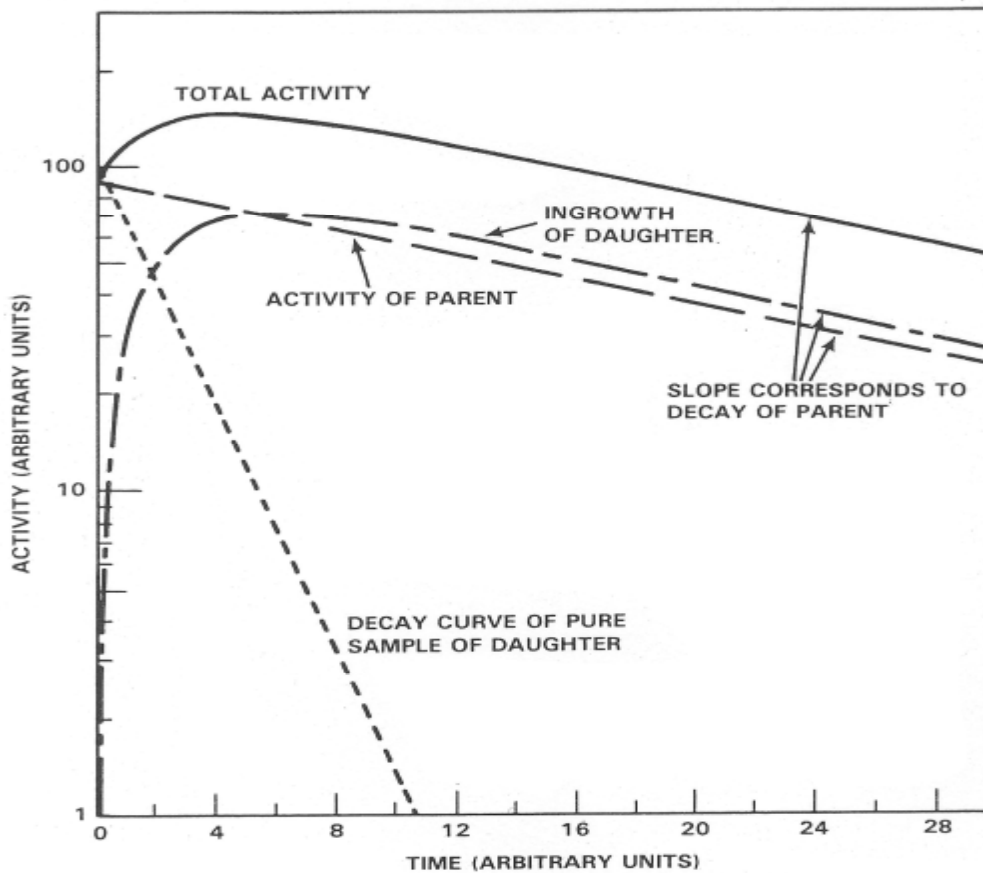


Fig. 1-7: Transient Equilibrium

The condition of no equilibrium occurs when the parent is shorter lived than the daughter, and is graphically illustrated in Fig. 1-8. The limiting case for no equilibrium is the situation where a radioactive parent decays to a stable daughter; in this case the number of daughter atoms will increase exponentially with time, and will be exactly equal to the number of parent atoms that have decayed. Both the transient and no equilibrium cases are sometimes analyzed in terms of t_m , the time required for the daughter to reach maximum activity when growing in from an initially pure quantity of the parent. The value of t_m can be readily calculated from the general case by differentiating equation 1-8 and setting the differential equal to zero when $t = t_m$, to yield:

$$\frac{\lambda_1}{\lambda_2} = e^{(\lambda_2 - \lambda_1)t_m}$$

which can then be solved for t_m :

$$t_m = \frac{\ln \lambda_2 - \ln \lambda_1}{\lambda_2 - \lambda_1}$$

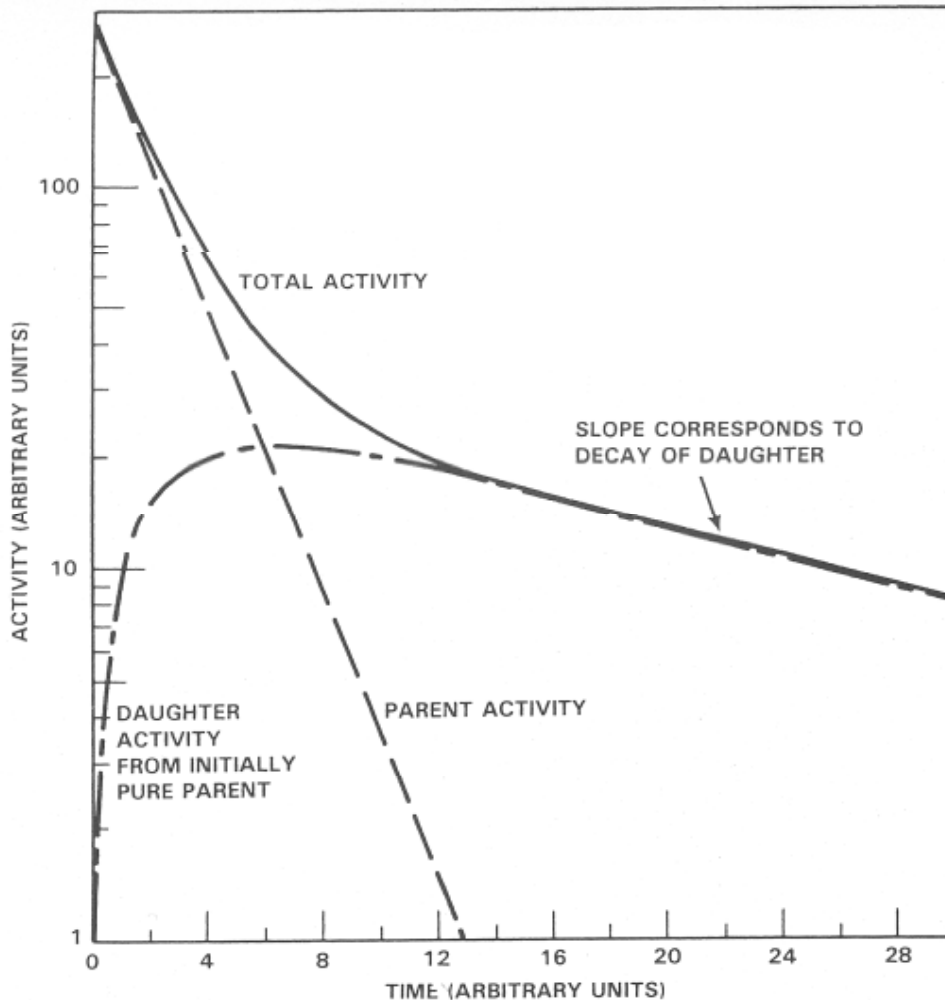


Fig. 1-8: No equilibrium

The growth of a radioactive daughter from a radioactive parent can be described mathematically by recalling that the activity of the parent can be expressed by the simple differential equation

$$-dN/dt = \lambda N_1$$

and that the daughter thus grows in at that same rate. However, since the daughter is also radioactive, it undergoes decay itself, which is described by the term $-\lambda_2 N_2$. Thus, the rate of decay of the daughter is expressed by equation 1-9

$$\frac{dN_2}{dt} = \lambda_1 N_1 - \lambda_2 N_2 \quad (1-9)$$

Assuming an initially pure parent with N atoms at zero time, the number of atoms of the parent at any time t can be calculated by equation 1-10:

$$N_1 = N_{01} e^{-\lambda_1 t} \quad (1-10)$$

which is simply a restatement of the fundamental decay law. Combining equations 1-9 and 1-10 and rearranging terms gives:

$$\frac{dN_2}{dt} + \lambda_2 N_2 - \lambda_1 N_{01} e^{-\lambda_1 t} = 0 \quad (1-11)$$

which is a first order differential equation and can be solved by assuming a solution of the form.

$$N_2 = uv \quad (1-12)$$

in which u and v are functions of t .

Differentiating equation 1-12 and substituting in equation 1-11 gives

$$u \frac{dv}{dt} + v \frac{du}{dt} + \lambda_2 uv - \lambda_1 N_{01} e^{-\lambda_1 t} = 0$$

which can be rearranged to yield

$$u \left(\frac{dv}{dt} + \lambda_2 v \right) + v \frac{du}{dt} - \lambda_1 N_{01} e^{-\lambda_1 t} = 0 \quad (1-13)$$

If the function v is selected such that the term in parentheses in equation 1-13 is 0,

then

$$\frac{dv}{dt} + \lambda_2 v = 0$$

which upon integration gives

$$v = e^{-\lambda_2 t} \quad (1-14)$$

Equation 1-12 can be substituted in equation 1-11 to yield a differential equation in terms of u , which can then be solved for u as shown

$$e^{-\lambda_2 t} \frac{du}{dt} - \lambda_1 N_{01} e^{-\lambda_1 t} = 0$$

rearranging

$$du = \lambda_1 N_{01} e^{(\lambda_2 - \lambda_1)t} dt$$

and integrating to give

$$u = \frac{\lambda_1}{\lambda_2 - \lambda_1} N_{01} e^{(\lambda_2 - \lambda_1)t} + C$$

which by substitution for N_2 yields.

$$N_2 = uv = \frac{\lambda_1}{\lambda_2 - \lambda_1} N_{01} e^{-\lambda_1 t} + C e^{-\lambda_2 t} \quad (1-15)$$

Equation 1-15 can be resolved by evaluating the constant C at zero time, when $N_{02} = N_2$

$$C = N_{02} - \frac{\lambda_1}{\lambda_2 - \lambda_1} N_{01} \quad (1-16)$$

(Equation 1-16) and then substituting equation 1-16 in equation 1-15 to obtain equation 1-17:

$$N_2 = \frac{\lambda_1}{\lambda_2 - \lambda_1} N_{01} (e^{-\lambda_1 t} - e^{-\lambda_2 t}) + N_{02} e^{-\lambda_2 t} \quad (1-17)$$

The result is the general equation for ingrowth of a radioactive daughter from a radioactive parent, as shown by equation 1-17. Inspection of the right hand side of equation 1-17 reveals the ingrowth of the daughter represented by the first group of terms, followed by the decay of these atoms, and finally a term which gives the contribution from any daughter atoms that were present initially. If the parent was initially pure this last term will be zero. The equations for the special cases of transient and secular equilibrium presented above are derivable from the general equation 1-17.

The above equations apply only to a two member chain, but may be extended to a chain or series of any length. The result is a very complex series of equations which is generally solved today with the aid of a computer. These are known as the Bateman equations, named after H. Bateman who first put forth the solution to this system of equations in 1910 for the special case of an initially pure parent (Bateman 1910). The general Bateman solution for n successive decays is shown below:

$$N_n(t) = C_1 e^{-\lambda_1 t} + C_2 e^{-\lambda_2 t} + \dots + C_n e^{-\lambda_n t} \quad (1-18)$$

in which

$$C_1 = \frac{\lambda_1 \lambda_2 \lambda_3 \dots \lambda_{n-1}}{(\lambda_2 - \lambda_1)(\lambda_3 - \lambda_1) \dots (\lambda_n - \lambda_1)} N_{01}$$

and

$$C_2 = \frac{\lambda_1 \lambda_2 \lambda_3 \dots \lambda_{n-1}}{(\lambda_1 - \lambda_2)(\lambda_3 - \lambda_2) \dots (\lambda_n - \lambda_2)} N_{01}$$

$$\vdots$$

$$C_n = \frac{\lambda_1 \lambda_2 \lambda_3 \dots \lambda_{n-1}}{(\lambda_1 - \lambda_n)(\lambda_2 - \lambda_n) \dots (\lambda_{n-1} - \lambda_n)} N_{01}$$

1.1.2 Man-made Radionuclides in the environment

Nuclear technologies over the past 50 years have introduced significant quantities of artificial radionuclides into the global environment. Historically, the greatest part of this radioactivity has come from atmospheric nuclear weapons tests conducted prior to the 1963 Limited Test Ban Treaty, although tests were carried out since then by non-signatory nations. Fallout from the tests has been distributed globally, with the maximum occurring in the North Temperate Zone, which encompasses the Great Lakes Basin. From 1963 to 1996, many weapons tests were carried out underground. Radioactive material occasionally vented to the atmosphere from these tests, but the impact on global fallout was minimal [UNS93].

Anthropogenic sources refer to those that are mainly human in origin: military, industrial, educational, recreational, medical, or somehow reflecting a human use, intervention, or process. The two main anthropogenic sources are the fallout of military weapons testing and the generation of electrical power at nuclear power plants. Medical, commercial, and other sources are many in number, but their emissions are individually very small, raising the possibility that the sources may, in the aggregate, be a major contributor to the anthropogenic inputs of radioactivity to the Basin. Of the many radionuclides produced by nuclear detonations, ^3H , ^{14}C , ^{90}Sr , and ^{137}Cs have received the greatest attention in environmental monitoring programs. They have been measured in air, water, soil, and food products. Other important radionuclides include ^{95}Zr , ^{95}Nb , ^{106}Ru , ^{131}I , ^{144}Ce , $^{239,240}\text{Pu}$, ^{241}Pu , and ^{241}Am .

On 26 April 1986 at 01: 23 hours local time an accident occurred at the fourth unit of the Chernobyl nuclear power Station. The accident destroyed the reactor core and part of the building in which the core was housed. The radioactive materials released were carried away in the form of gases and dust particles by air currents. In this manner, they were widely dispersed over the territory of the Soviet Union, over many other (mostly European) countries and, in trace amounts, throughout the northern hemisphere. The Chernobyl nuclear power Station is located in the Ukraine (Fig. 1-9).

The Chernobyl accident involved the largest short-term release from a single source of radioactive materials to the atmosphere ever recorded. Of the materials released from the reactor core, four elements have dominated the short-term and long-term radiological Situation in the affected areas of the USSR: iodine (primarily ^{131}I), cesium (^{134}Cs , ^{137}Cs), Strontium (primarily ^{90}Sr) and plutonium (^{239}Pu , ^{240}Pu). In addition, highly radioactive fuel fragments (hot particles) were released. The destroyed reactor released a very large amount of radioactive material into the environment 10^{19} Bq. Although the discharge included many radioactive chemical elements, just two of them-iodine (in the short term) and cesium (in the long term)-were particularly significant from a radiological point of view.



Fig. 1-9: The site of the Chernobyl nuclear power station [UNS00].

About 10^{18} Bq of iodine-131 were released in the accident. Iodine is mainly absorbed by a person's thyroid gland after inhalation or after consumption of contaminated foodstuffs such as milk products; its short-range beta particles irradiate the gland from the inside. Uptake of iodine by the thyroid is relatively easy to prevent, for example by banning consumption of contaminated food for a few weeks until the iodine-131 decays sufficiently or by administering small amounts of non-radioactive iodine prophylactically to block the thyroid gland.

About 10^{17} Bq of radioactive cesium's were released, and precipitated over a vast area. Exposure to cesium is difficult to prevent. Once it is deposited in the soil, its long-range gamma rays can expose anybody in the area. To clean the surfaces is difficult and, if the concentration of cesium is high, often the only feasible countermeasure is to evacuate the inhabitants. Cesium in the soil can also be transferred into agricultural products and grazing animals [Val00].

1.1.2.1 Strontium-90

Strontium is element number 38 in the periodic table; it is an alkaline earth element and is therefore similar to calcium, barium and radium. It follows calcium through the food chains from environment to man, but some degree of discrimination exists against strontium. Both strontium and calcium are retained in the body largely in bone.

Large amounts of ^{90}Sr were released in nuclear tests and dispersed throughout the world. Strontium-90 is also produced in the nuclear fuel cycle, but only small amounts are released to the environment. Strontium-90 in the environment is efficiently transferred to human diet. The absorption of ^{90}Sr by the body is relatively high and it has a long biological retention time. Because of the correspondence in behavior of strontium and calcium in the environment and in man, it has been the practice to express measurement results in diet and bone as quotients of ^{90}Sr to Ca concentrations. Discrimination is reflected as ratios of strontium to calcium quotients in samples to those in precursor samples in the transfer chain. Expressing results in terms of the strontium to calcium quotients has the practical advantage that for many environmental

transfer processes, such as absorption into the body, secretion into milk and deposition in bone, the ratios remain relatively constant and predictable. However, since the average levels of calcium in diet and man are nearly constant, assessments of ^{90}Sr can also be made on the basis of amounts per unit mass or volume of material [IPC83].

1.1.2.2 Iodine-131

There are at least 25 iodine isotopes with mass numbers ranging from 117 to 141. All except ^{127}I are radioactive, omitting the very short-lived ^{140}I and ^{141}I thirteen isotopes are produced by fission. From the point of view of environmental contamination and resulting doses to man, the most important isotopes of iodine are ^{131}I and ^{129}I . They are the only radioactive isotopes of iodine produced by fission with half-lives longer than one day, Iodine-131 is a beta-emitter with a half-life of 8.06 days and a maximum beta energy of 0.81 MeV emitting also gamma rays of 0.36 and 0.64 MeV and other energies, Iodine-129 has a very long half-life ($1.57 \cdot 10^7$ a) it is a beta-emitter (maximum energy; 0.15 MeV) with an accompanying gamma ray of 0.09 MeV in 8% of the disintegrations [Dil75]. The two isotopes are mainly found in the environment as a result of nuclear explosions and releases from nuclear reactors and fuel reprocessing plants. ^{129}I and ^{131}I are the environment as a result of spontaneous fission uranium. In view of its very long half-life, ^{29}I has accumulated in the earth's crust and also in the ocean waters from where it is available to disperse in the whole biosphere.

1.1.2.3 Cesium-134 and 137

Cesium is element number 55 in the periodic table. It is an alkali metal like potassium, and it resembles potassium metabolically. Whereas potassium is an essential element for man, there is no evidence that cesium is also an essential trace element. In fact, stable cesium, ^{133}Cs , is fairly rare in the biosphere and in geological occurrence. Average occurrence in the earth's crust is $3 \mu\text{g g}^{-1}$. In specific rock types the estimated average concentration is $1 \mu\text{g g}^{-1}$ in basalts and $5 \mu\text{g g}^{-1}$ in granite. The K/Cs ratio in basalts is 7500 [Tay65].

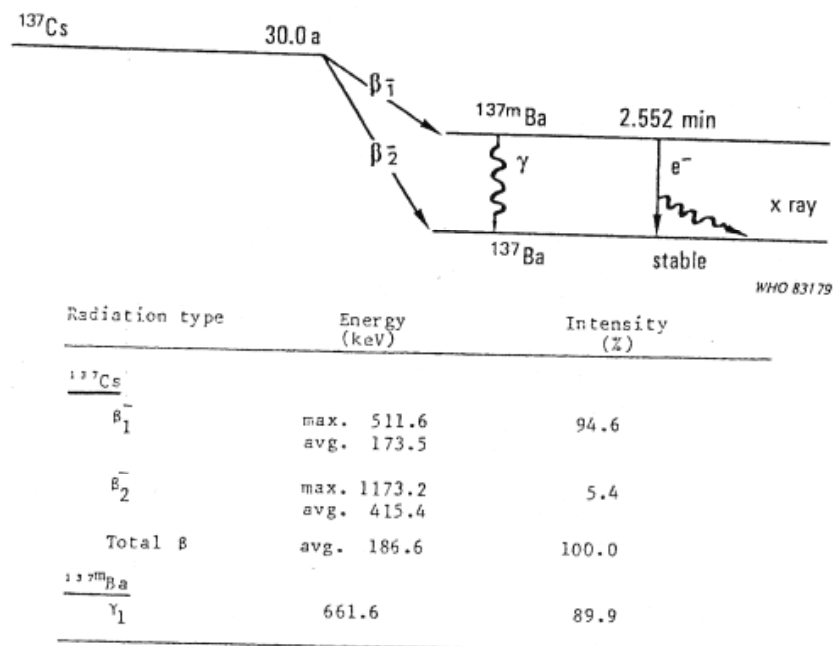


Fig. 1-10: decay scheme of Cs-137 [NCR87].

The radioactive isotope ^{137}Cs is produced in nuclear fission and is one of the more significant fission products. The fission yield is relatively high, about 6 atoms per 100 fissions, independent of the type of fission in uranium or plutonium. It has a radioactive half-life of 30.17 y and its beta decay is accompanied by a gamma ray of moderate energy. Fig. (1-10) shows the decay scheme and lists the primary transition energies.

^{137}Cs levels in the body in terms of the $^{137}\text{Cs}/\text{K}$ quotient is that age and sex differences are minimized and the values correlate more closely to ^{137}Cs concentrations per unit of lean body mass, which seems to be a more important parameter for dosimetric purposes than the whole body mass. It is expected, however, that assessments, in the future will be presented independently for ^{137}Cs without so much reliance on the stable congener element [Gus69]. A great deal of information has accumulated on ^{137}Cs in the environment, particularly the measurements of fallout ^{137}Cs in air, deposition, diet and man.

Cesium is generally rather strongly fixed in soil. Downward migration and availability to plants is thereby reduced. In mineral soils the movement of ^{137}Cs is appreciably less than that of ^{90}Sr . Three to four years after deposition on the soil surface, the median depth to which it has penetrated is usually less than 2 cm [Fre66]. Its mobility may be somewhat greater in organic soils. Much smaller amounts of ^{137}Cs than of ^{90}Sr are leached out of the soil to enter rivers and lakes. It has been reported that in clay minerals the important factor in fixation of cesium is the ability of certain layered silicates such as micas, vermiculites and illites to adsorb or fix trace quantities of cesium [Tam60].

Cesium ions are trapped in the interlayer regions of vermiculite or at the frayed edges of illites and micas. Cesium is thus more strongly retained in soils containing predominantly micaceous minerals. Soils which do not contain large quantities of micaceous minerals, such as tropical soils, peat soils, and podzolic soils, exhibit less retention and allow greater uptake of cesium by plants. Caesium-137 may be transferred to plants by direct deposition onto plant surfaces or by root uptake from accumulated deposits in soil. In general, direct foliar absorption is the predominant mode of plant contamination when the deposition rate is relatively high. Root uptake is low except in those cases mentioned above, when soil conditions allow low fixation of cesium.

1.2 The human radiation exposure

Since the primary consideration in environmental measurement is the assessment and prevention of possible health effects on humans, it is important to understand how radioactive materials can move from a release point to possible ingestion. Radioactive materials can be released into air or directly into water or soil. When released in the air, they can travel some distance, depending upon such factors as wind speed and direction and altitude of the release.

The products of airborne releases can be transported to humans by a variety of paths. First, direct ingestion by inhalation is possible. Secondly, the materials will eventually deposit themselves on the ground, where they will find their way into plant and animal life and thereby, into the food chain. Third, deposition of airborne contaminants into water can reach humans either by similarly, direct soil and water depositions find their way into the food chain via both plant and direct ingestion or via the food chain via both plant and animal life Fig. (1-11).

Rain water runoff can carry soil into rivers and streams, thereby transporting any soil contamination to water. Additionally, radioactive materials can leach into porous soils.

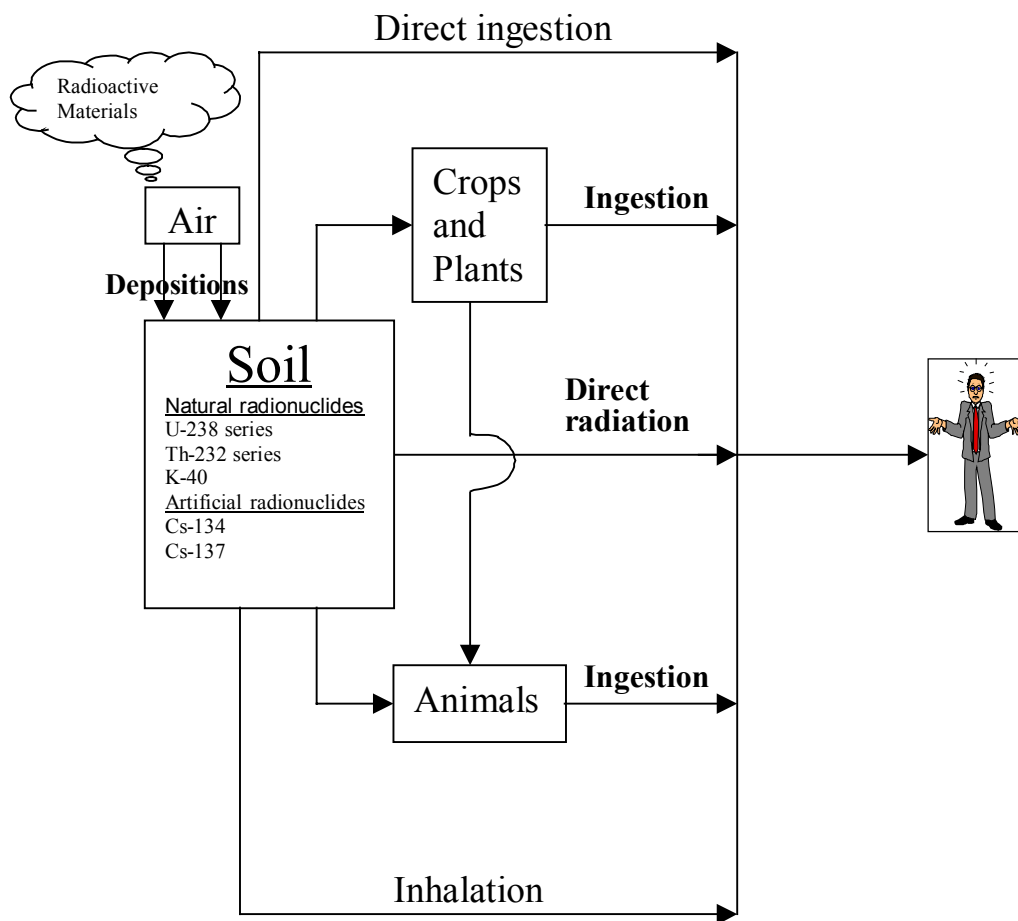


Fig. 1-11: shows some of the possible pathways of contamination to humans [Can02].

All living organisms are continually exposed to ionizing radiation, which has always existed naturally. The sources of that exposure are cosmic rays that come from outer space and from the surface of the sun, terrestrial radionuclides that occur in the earth's crust, in building materials and in air, water and foods and in the human body itself. Some of the exposures are fairly constant and uniform for all individuals everywhere, for example, the dose from ingestion of potassium-40 in foods. Other exposures vary widely depending on location. Cosmic rays, for example, are more intense at higher altitudes, and concentrations of uranium and thorium in soils are elevated in localized areas. Exposures can also vary as a result of human activities and practices. In particular, the building materials of houses and the design and ventilation systems strongly influence indoor levels of the radioactive gas radon and its decay products, which contribute significantly to doses through inhalation [UNS01].

Naturally occurring radioactive materials (NORM) and natural radiation in the environment provide the major source of human radiation exposure. For this reason, natural radiation is frequently used as a basis of comparison for various man-made sources of ionizing radiation. In addition, numerous epidemiological studies have attempted to relate health effects to exposures from elevated natural radiation as well as to exposures from medical uses; weapons test fallout and nuclear power generation [NCR94].

Natural radiation and artificial sources are classified into two categories:

- (a) External sources of extraterrestrial origin, i.e., cosmic radiation, and radiation of terrestrial origin and from Chernobyl reactor accident, i.e., the radioactive nuclides present in the crust of the earth, in building materials and in air;
- (b) Internal sources, comprising the naturally occurring radionuclides that are taken into the human body. In this investigation, calculated as the following:
 1. External gamma radiation exposure from soil
 2. Internal gamma radiation exposure from inhalation dust and,
 3. Internal gamma radiation exposure from ingestion direct soil (dust) , for these nuclides like ^{226}Ra , ^{210}Pb , ^{238}U , and ^{232}Th for all investigated sites form soil.

In the calculations of the activity in the source regions of the body following intakes at the specified ages, continuous changes with age in the transfer rates governing distribution and retention are obtained by linear interpolation according to age. This also applies to the transfer of activity from the gastrointestinal tract. For application to other ages and to protracted intakes, the ICRP Task Group considered that doses can be estimated by applying the age-specific dose coefficients to the age ranges given below [ICP96]:

| | |
|--------|------------------------|
| 3 m: | from 0 to 1 y of age |
| 1 y: | from 1 y to 2 y |
| 5 y: | more than 2 y to 5 y |
| 10 y: | more than 7 y to 12 y |
| 15 y: | more than 12 y to 17 y |
| Adult: | more than 17 y |

The decay of naturally occurring radionuclides in soil produces a gamma-beta radiation field in soil that also crosses the soil air interface to produce exposures to humans. The dose to individuals from external exposure will depend on a number of factors including the type and energy of the emitted radiations, the concentrations of radionuclides in the soil, the time spent outdoors, and the shielding by buildings. However, as the materials of which most buildings are built also contain radionuclides, the shielding by buildings of the outdoor radiation field is often more than offset by the presence of additional radionuclides in the building materials. The values of most of these parameters will vary with projected land use. This section discusses models for estimating the external $H_{Ext,a}$ and the key parameters used in these models [BfS99]. The values used to calculate the external and internal exposure radiation doses are discussed, and use scenarios for selected nuclides likely to be found in environmental contamination scenarios, these nuclides like ^{226}Ra , ^{210}Pb , ^{238}U , ^{232}Th [UNS00].

1.2.1 External exposure

External exposure from radionuclides naturally present in the environment or released from man-made practices or events is usually an important component of the exposure of human populations. These exposures derive primarily from gamma radiation arising from the decay of these radionuclides at locations outside the human body [UNS00].

External radiation comes from two sources of approximately equal magnitude, the cosmic radiation from outer space and terrestrial gamma radiation from radionuclides in the environment, mainly the earth. The external radiation field consists of energetic penetrating radiations and may be considered, as a first approximation, to irradiate the whole body

uniformly. In the case of cosmic radiation, the charged particles, primarily protons from extra-terrestrial sources that are incident on the earth's atmosphere, have sufficiently high energies to generate secondary particles. These are mostly high-energy muons and electrons, commonly referred to as the ionizing component, and a smaller number of neutrons. These neutrons are strongly absorbed in the atmosphere, so they are not important at sea level, but are significant at higher altitudes. There is some shielding by housing and, to account for this, indoor exposures from cosmic radiation are assumed in [NCR93] to be 80 percent of outdoor exposures.

The three contributors to the terrestrial gamma radiation field are ^{40}K , and the members of the thorium and the uranium series. Most of the gamma radiation comes from the top 20 cm of soil, with a small contribution from airborne radon decay products. The absorbed dose in air is converted to dose equivalent in the whole body using a factor of 0.7 to allow for self-shielding [UNS82]. It appears that the amount of indoor exposure from radionuclides in the environment is close to that outdoors, due to a balance between shielding by housing materials and the geometry of exposure from radionuclides in the walls when the individual is within a structure [NCR87].

For the case of exposure by radionuclides within the body, where measurement of dose equivalent is difficult, it is necessary to calculate the annual dose equivalents. For all cases except radon decay products in the lung, this calculation is based on measured concentrations of radionuclides, *e.g.*, ^{40}K , in the specific organs of interest. For radon decay products, it is necessary to use atmospheric characteristics and a lung deposition model to convert concentrations in air to tissue doses.

The primordial radionuclides considered include the series isotopes of U, Th, Ra, Rn, Po, Bi, and Pb of the ^{238}U and ^{232}Th series, plus ^{40}K , ^{85}Rb , and the only cosmogenic nuclide of importance, ^{14}C . These enter the body by ingestion of food, milk, and water or by inhalation. The isotopes follow the normal chemical metabolism of the element and the long-lived radionuclides are usually maintained at an equilibrium concentration or increase slowly with age. The shorter-lived radionuclides disappear by decay, but concentrations in the body are continually renewed by fresh intake [NCR93].

The average cosmic-ray annual dose equivalent is about 0.26 mSv (26 mrem) at sea level. This essentially doubles with each 2,000 m increase in altitude in the lower atmosphere. Latitude, solar cycle variations and other factors modify these exposures by about ten percent. In the United States, cities such as Denver (at 1,600 meters) have an annual external exposure from cosmic radiation of 0.5 mSv (50 mrem) [NCR87].

The NCRP Report on natural background [NCR75] noted that air travel at an altitude of 12 km (39,000 feet) gave an enhanced cosmic-ray exposure of $5\mu\text{Sv h}^{-1}$ (0.5 mrem h^{-1}).

External exposures outdoors arise from terrestrial radionuclides present at trace levels in all soils. The specific levels are related to the types of rock from which the soils originate. Higher radiation levels are associated with igneous rocks, such as granite, and lower levels with sedimentary rocks. There are exceptions, however, as some shales and phosphate rocks have relatively high content of radionuclides. There have been many surveys to determine the background levels of radionuclides in soils, which can in turn be related to the absorbed dose rates in air. The latter can easily be measured directly, and these results provide an even more extensive evaluation of the background exposure levels in different countries. All of these spectrometric measurements indicate that the three components of the external radiation field, namely from the gamma-emitting radionuclides in the ^{238}U and ^{232}Th series and ^{40}K , make

approximately equal contributions to the externally incident gamma radiation dose to individuals in typical situations both outdoors and indoors. The radionuclides in the uranium and thorium decay chains cannot be assumed to be in radioactive equilibrium. The isotopes ^{238}U and ^{234}U are in approximate equilibrium, as they are separated by two much shorter-lived nuclides, ^{234}Th and ^{234}Pa . The decay process itself may, however, allow some dissociation of the decay radionuclide from the source material, facilitating subsequent environmental transfer. Thus, ^{234}U may be somewhat deficient relative to ^{238}U in soils and enhanced in rivers and the sea. The radionuclide ^{226}Ra in this chain may have slightly different concentrations than ^{238}U , because separation may occur between its parent ^{230}Th and uranium and because radium has greater mobility in the environment. The decay products of ^{226}Ra include the gaseous element radon, which diffuses out of the soil, reducing the exposure rate from the ^{238}U series. The radon radionuclide in this series, ^{222}Rn , has a half-life of only a few days, but it has two longer-lived decay products, ^{210}Pb and ^{210}Po , which are important in dose evaluations. For the ^{232}Th series, similar considerations apply. The radionuclide ^{228}Ra has a sufficiently long half-life that may allow some separation from its parent, ^{232}Th . The gaseous element of the chain, ^{220}Rn , has a very short half-life and no long-lived decay products [UNS00].

One of the principal dose pathways resulting from contaminated surface soil is external exposure from radiation emitted from the radionuclides present in the surface soil [NCR99]. Many radionuclides occur naturally in terrestrial soils derived from them. Upon decay, these radionuclides produce an external radiation field to which all human beings are exposed. In terms of dose, the principal primordial radionuclides are ^{232}Th , and ^{238}U . Both ^{232}Th and ^{238}U head series of radionuclides that produce significant human exposures. The two series are discussed fully and also in Figs. (1-3, 1-4) [UNS00].

1.2.2 Internal exposures

Internal exposures arise from the intake of terrestrial radionuclides by inhalation and ingestion. Doses by inhalation result from the presence in air of dust particles containing radionuclides of the ^{238}U and ^{232}Th decay chains. The dominant component of inhalation exposure is the short-lived decay products of radon. Doses by ingestion are mainly due to ^{40}K and to the ^{238}U and ^{232}Th series radionuclides present in foods and drinking water. The dose rate from ^{40}K can be determined directly and accurately from external measurements of its concentration in the body. The analysis of the content of uranium- and thorium-series radionuclides in the body requires more difficult chemical analyses of tissues, and fewer data are available. The analysis of the radionuclide contents of foods and water, along with bioassay data and knowledge of the metabolic behavior of the radionuclides, provides an alternative basis for dose estimation. The samples are more readily obtained, and they can reflect widely different locations. With these data, dose estimates for children as well as adults can be derived.

1.2.2.1 Ingestion

Ingestion intake of natural radionuclides depends on the consumption rates of food and water and on the radionuclide concentrations. Concentrations of naturally occurring radionuclides in foods vary widely because of the differing background levels, climate, and agricultural conditions that prevail. There are also differences in the types of local foods that may be included in the categories such as vegetables, fruits, or fish. In the [UNS93] Report, reference values were selected for the concentrations of uranium- and thorium-series radionuclides in foods. Obviously, these values must be derived from the most widely available and representative data possible. It is difficult to select reference values from the wide ranges of concentrations reported for uranium- and thorium-series radionuclides in foods.

If contaminated land is used for the production of food for either human or animal ingestion, the ingestion of this food or of the by-products (meat, milk) from animals eating forage grown on the contaminated land may result in a radiation exposure [NCR99].

Ingestion exposure occurs when radionuclides in the environment enter food chains. This component and that of external exposure are usually the significant and continuing sources of exposure following releases of radionuclides to the environment.

Ingestion exposures have been evaluated by UNSCEAR for natural radionuclides present in the environment and for several cases of radionuclide release to the environment, including atmospheric testing, releases from nuclear fuel cycle installations and the Chernobyl accident. For the most part, annual average values have been considered with the aim of evaluating committed exposures. This is adequate for longer-term or continuous releases. Short-term releases at particular times, such as was the case for the Chernobyl accident, require taking into account some seasonal variations.

1.2.2.2 Inhalation

Another potential pathway for human doses from contaminated sites is inhalation of airborne radionuclides on suspended contaminated soil. Unlike external exposure, which contributes only to the annual dose in the year exposed, inhaled radionuclides can result in a dose in subsequent years as well, depending on how long the radionuclide remains in the body. The potential exposure from this pathway depends on a number of factors including the average activity of the airborne resuspended soil, the length of time exposed either inside or outdoors, the particle size distribution of the suspended soil, the nuclide and its chemical form, and the age and breathing rate of the person exposed. The resuspension pathway is generally not a significant contributor to long-term exposure for most sites and/or nuclides. However, it is potentially important for dusty sites where the nuclide remains in the surface soil and for nuclides which are insoluble and thus are likely to remain in the lung for long periods of time after inhalation. For alpha-emitting nuclides such as plutonium, which do not emit any high-energy penetrating radiation and are not readily absorbed from the GI tract, the external radiation and ingestion pathway doses are usually minimal [NCR99].

Inhalation intake of natural radionuclides other than radon and its decay products makes only a minor contribution to internal exposure. The uranium- and thorium-series radionuclides are present in air because of resuspended soil particles; the decay products of radon are present because of radon gas in air. A dust concentration of $50 \mu\text{g m}^{-3}$ is generally assumed [UNS82]. With ^{238}U and ^{232}Th concentrations in the soil of $25\text{-}50 \text{ Bq kg}^{-1}$, the concentrations in air would be expected to be $1\text{-}2 \mu\text{Bq m}^{-3}$, and this is generally what is observed. In the [UNS93], representative values of the concentrations of terrestrial radionuclides in air were selected. As the database has changed very little, most of these values are still considered valid. The highest concentration is for ^{210}Pb . The concentrations of the other radionuclides are lower by factors of 10, 500, or 1,000.

1.2.3 Mean values and variability of the natural radiation exposure

The quantity effective dose equivalent, used in Table (1-1) [UNS88] to summarize the contributions of natural sources to the radiation exposure of human populations living in areas of normal radiation background. The mean annual effective dose equivalent is estimated to be 2.4 m Sv. This refers to exposures of adults in the populations. Some of the contributions to the total exposure to natural radiation background are quite constant in space and time and practically

independent of human practices and activities. This is true for doses from ingestion of ^{40}K , which is homeostatically controlled, and for doses from inhalation and ingestion of cosmogenic radionuclides, as such radioactive materials are to a first approximation homogeneously distributed over the surface of the globe. At the other end of the spectrum are exposures that depend strongly on human activities and practices and present a wide variability. Doses from indoor inhalation of radon and thoron decay products are typical: building design and practices, as well as the choice of building materials and of ventilation systems, influence indoor levels, thus implying a variation with time of the doses from radon as the techniques and practices evolve. Variability from one dwelling to another also stems from the wide range of radon entry rates from soil, which are to a large extent still unpredictable. In between those extreme types of exposures are several other types:

- (a) External doses from cosmic rays which, though affected by human practices and quite predictable, cannot be controlled except by moving to an area with a lower dose level;
- (b) Doses from inhalation and ingestion of long-lived nuclides of the ^{238}U and ^{232}Th decay series, which represent a small contribution to the total dose from natural sources and which are relatively constant in space;
- (c) Doses from external irradiation by terrestrial sources, which are also significantly altered by human activities and practices, especially through indoor exposure. Such doses, however, are, as a rule, smaller than those from inhalation of radon decay products and much less variable.

Annual effective dose equivalents from internal exposure to primordial radionuclides have been reassessed slightly downwards for the ^{238}U and ^{210}Pb series, as well as for the decay products of ^{220}Rn , whereas those for the short-lived decay products of ^{222}Rn have been increased by about $300\ \mu\text{Sv}$ on the basis of more comprehensive results of nation-wide indoor surveys. The net effect of these corrections is a 20% increase in the estimate of the overall annual effective dose equivalent from natural sources of radiation.

According to UNSCEAR [UNS93], the exposure to gamma rays from natural radionuclides occurs outdoors and indoors. Surveys by direct measurements of dose rates have been conducted during the last few decades in many countries. They are illustrated in Fig. 1-12. For the doses outdoors three fifths of the population of the world is represented. National averages range from 24 to 160 nGy h. In the open, much human exposure occurs over paved surfaces, but some also occurs over soil; it is determined by the activity per unit mass of the principal radionuclides in the superficial layer.

Table 1- 1: Estimated annual effective dose equivalents from natural sources in normal background areas, worldwide [UNS88].

(Estimates from the UNSCEAR 1982 Report are given in parentheses)

| Source | Annual Effective Dose Equivalent μSv | | | | | |
|-----------------------------|-------------------------------------------------|-------|----------|--------|-------|--------|
| | External | | Internal | | Total | |
| Cosmic rays | 300 | (280) | | | 300 | (280) |
| Ionizing Component | 55 | (21) | | | 55 | (21) |
| Neutron Component | | | 15 | (15) | 15 | (15) |
| Cosmogenic Radionuclides | | | | | | |
| Primordial Radionuclides | | | | | | |
| K-40 | | | 180 | (180) | | |
| Rb-87 | 150 | (120) | 6 | (6) | 300 | (300) |
| U-238 series : | | | | | 6 | (6) |
| U-238 \rightarrow U-234 | | | 5 | (10) | | |
| Th-230 | | | 7 | (7) | | |
| Ra-226 | | | 7 | (7) | | |
| Rn-222 \rightarrow Po-214 | 100 | (90) | 1100 | (800) | 1300 | (1044) |
| Pb-210 \rightarrow Po-210 | | | 120 | (130) | | |
| Th-232 series: | | | | | | |
| Th-232 | | | 3 | (3) | | |
| Ra-228 \rightarrow Ra-224 | 160 | (140) | 13 | (13) | 340 | (330) |
| Rn-220 \rightarrow Tl-208 | | | 160 | (170) | | |
| Total(Rounded) | 800 | (650) | 1600 | (1340) | 2400 | (2000) |

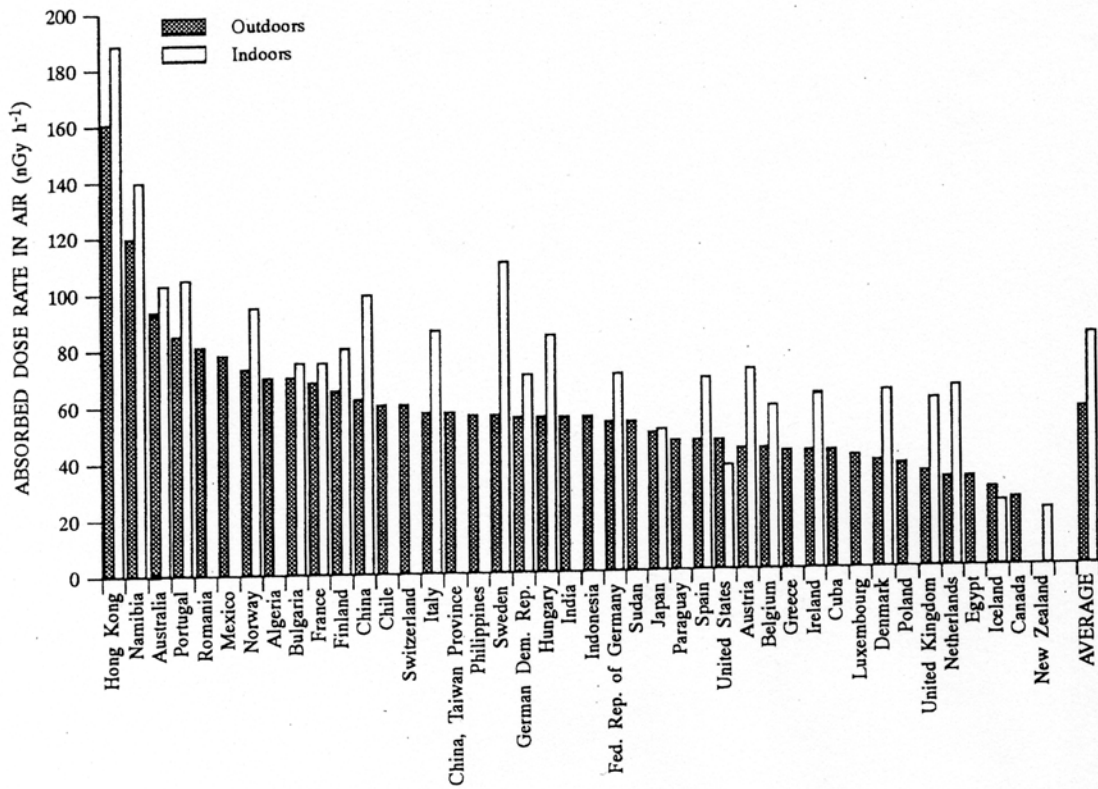


Fig. 1-12: Absorber dose rates in air from terrestrial gamma radiation ranked according to levels outdoors [UNS93].

The radionuclides released from the Chernobyl reactor that caused exposure of individuals are mainly iodine-131, caesium-134 and caesium-137. Iodine-131 has a short radioactive half-life (eight days), but it can be transferred to humans relatively rapidly from the air and through milk and leafy vegetables. Iodine becomes localized in the thyroid gland. For reasons related to the intake of those foods by infants and children, as well as the size of their thyroid glands and their metabolism, the radiation doses are usually higher for them than for adults.

The isotopes of caesium have relatively longer half-lives caesium-134 has a half-life of 2 years while that of caesium-137 is 30 years). These radionuclides cause longer term exposures through the ingestion pathway and through external exposure from their deposition on the ground. Many other radionuclides were associated with the accident, which have also been considered in the exposure assessments.

Average doses to those persons most affected by the accident were about 100 mSv for 240,000 recovery operation workers with for 1986 to 87.30 mSv for 116,000 evacuated persons and 10 mSv during the first decade after the accident to those who continued to reside in contaminated areas. Maximum values of the dose may be an order of magnitude higher. Outside Belarus, the Russian Federation and Ukraine, other European countries were affected by the accident. Doses there were at most 1 mSv in the first year after the accident with progressively decreasing doses in subsequent years. The dose over a lifetime was estimated to be 2-5 times the first-year dose. These doses are comparable to an annual dose from natural background radiation and are, therefore, of little radiological significance [UNS00].

2 Experimental

2.1 Soil sampling

In 1995, soil samples were taken from different locations from these zones (Zone II, III and IV (see Fig. 2-1) in Ukraine by means of the template method as displayed in Fig. 2-2. On September 1999, soil samples were taken from 7 sampling locations from Lower Saxony, Germany by the trench method. Further sampling was done from Lippe embankments, North Rhine-West phalia, Germany (Fig.2-3) on July, August, September and November 2000. On May, July, August, and September 2001 were taken some samples from Lower Saxony by means of the bore core method and one soil depth profile at a location (map Fig. 2-4) and the description of these locations of soil depth profiles and soil samples are in details in tables A-1, A-2, A-3, A-4, A-5. Soil can be sampled by three main methods to take soil samples can be identified:

2.1.1 The trench method

The trench method ([Isa97], [Chi97]) is used to determine the depth of penetration of a radionuclide or contaminant or to establish a detailed depth profile. The most suitable area for taking soil profiles is one where there are no rocks and stones, and very few pebbles. The procedure works well in sandy loam, loam or loamy sand types of soil, the depth profile samples are taken so that the weight and depth of the material collected can be directly related to the area. If the vegetation represents a seasonal growth, it should be clipped to 2.5-5 cm over a measured area. Usually the sod (Humus soil) can be cut out in blocks making it easy appropriate size for ease of access immediately adjacent to the clipped area, placing the dirt where to replace after sampling. The face of the trench is smoothed from side to side with a flat blade shovel, making it perpendicular to the surface.

In this method to take soil samples from different depth in which a trench is dug to a depth of about one to two meters or more. The samples are then taken horizontally from the walls of the trench. The main advantage of this method is the possibility of taking samples at a precisely defined depth.

2.1.2 Template method

The usual application of this method is to scrape or shovel off layer after layer of soil within a chosen area as in figure 2-2, which could be defined by some sort of rigid frame, in some cases pressed down into the soil to a certain depth ([Pap88], [Sim89], [Bon93] [Ant95] [Chi97]). The size of the area usually varies between a quarter of a square meter up to one square meter. The advantage of this method is that a reproducible area is sampled but there is also a possibility that the particular area chosen for measurement is not representative for the measurement site. It may contain an unrepresentatively high or low amount of ^{137}Cs compared with other areas in the close vicinity, mine just one particular site is sampled. Soil sampling with this method is also very time consuming and results in a large amount of soil, from which aliquots are usually taken. In addition there is a tendency for the sampled area to decrease with increasing depth (when no frame is used, for this reason we used frame 20 cm²). The method could under certain conditions be suitable for determining the vertical distribution of radionuclides at a well defined location. In this method the soil and rocks are removed with chisels and scoops down to the desired depth. The rocks are included and weighed with the sample. The large rocks can be discarded after removing loose dirt.

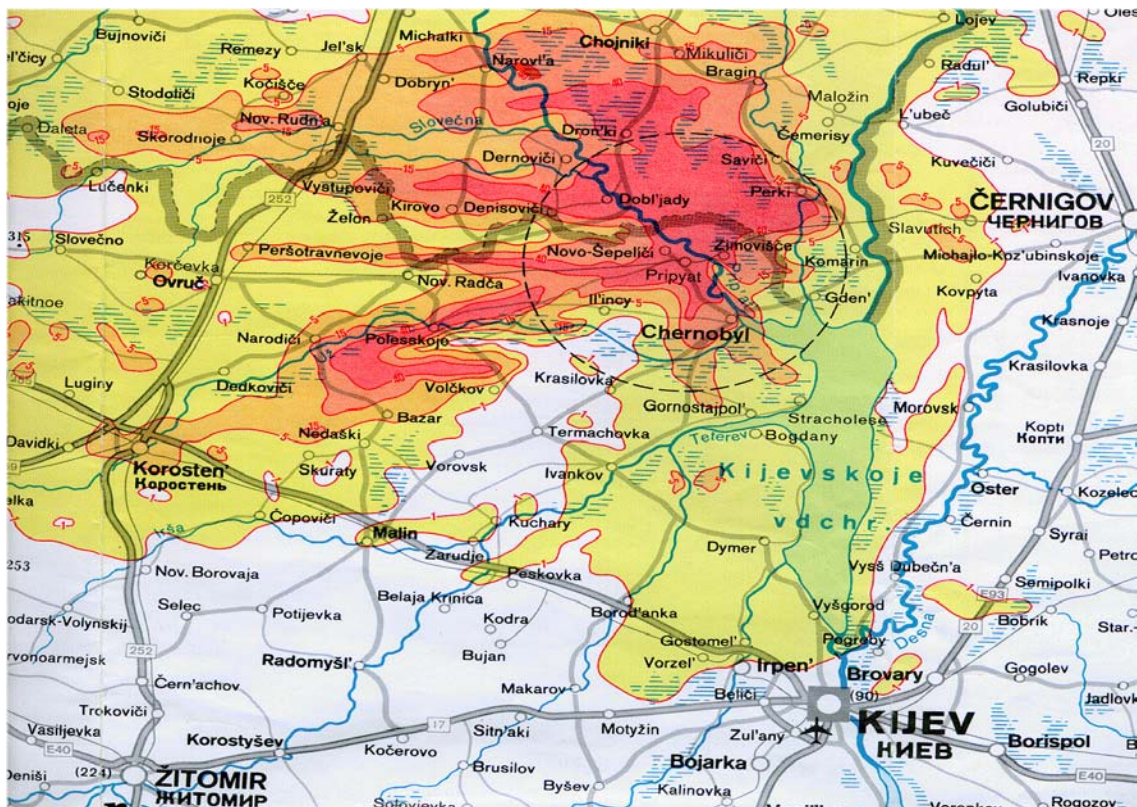


Fig. 2-1: Map of locations of soil depth profile samples from north Ukraine [IAE91]

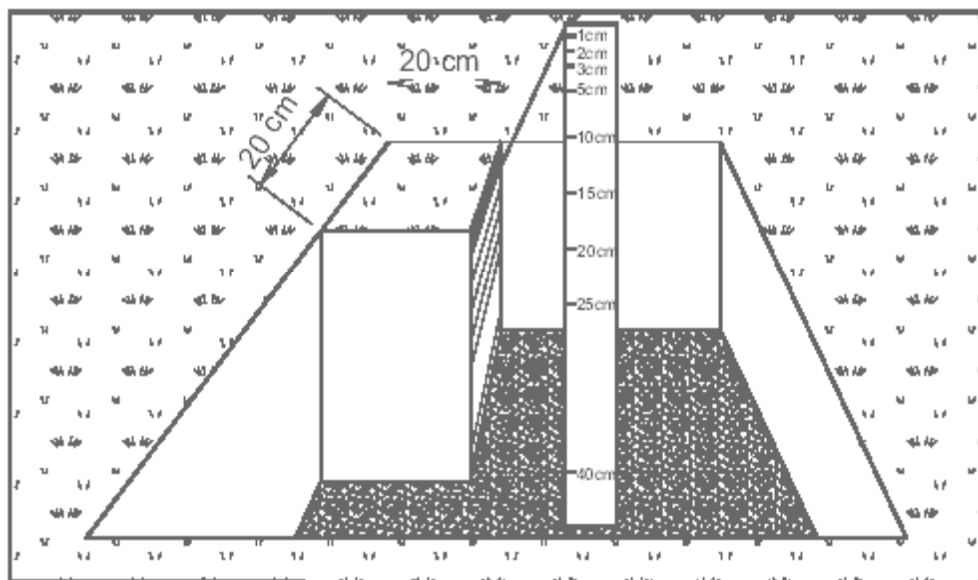


Fig. 2-2: Template method. By this method soil samples from Ukraine was taken.

The remaining smaller rocks are crushed as part of the sample. The soil adjacent to the exterior of the eara is removed to the depth of the eara. The confined volume of soil is then transferred to a plastic bag using an appropriate tool. Depth profile may be drawn using this method by repeating the steps for each subsequent depth to be sampled.

2.1.3 The bore core method

The third method of examining the activity concentration in the soil over an area is to take samples in the form of bore cores arranged in different geometries, or at random, over the area of interest ([Isa97]; [Arn89]; [Mil90]; [Bla95]; [Ros96]). If the purpose of the sampling is to determine the depth distribution of radionuclides the bore cores could then be divided into horizontal sections and analyzed. If several samples are taken over a sampling site and analyzed separately, this method gives a good estimate of both the horizontal as well as the vertical distribution of the activity concentration at the measuring site.

The analysis of the soil samples could be very time-consuming if the number of bore cores is large and the cores in addition are divided into several different layers. The number of samples could be reduced if the soil at a given depth from different cores is mixed and analyzed together as general samples [Chi97]. Although this certainly will shorten the time of analysis, most of the information about the horizontal distribution will be lost. An average vertical distribution can, however, still be determined. This method is particularly suitable for studying the transfer of radionuclides from soil to plants.

One obvious problem with the core method is the risk for cross contamination and compression of the soil. The cross contamination occurs when soil from upper, more contaminated, layers are pressed down to greater depths by the bore. Compression of the soil could be expected when the soil is pressed out of the bore.

Core samplers are tubes that are usually made of carbon steel or stainless steel. They can be fitted with either a core tip or an auger tip. Undisturbed samples are taken by pushing the sampler with a core tip into the material to be sampled. Pushing can be done by hand or using a slide hammer. Samples taken by pushing the tool are suitable for geotechnical analyses that require undisturbed samples. Liners can be used in the sampler to retain and seal the sample from contact with air.

Core samplers with core tips can typically be advanced to about 30 cm in unconsolidated materials. Core samplers may, however, be pushed into undisturbed material at the bottom of holes that have been drilled using another method. The presence of cobbles or gravel will generally preclude significant penetration, and core samplers are sometimes difficult to push in heavy clays. Extraction of core can be difficult, but the use of liners and split-core designs alleviate this problem.

The sampler with an auger tip can be used to make a hole or to take disturbed samples. The auger tip is usually advanced by hand using a cross handle to turn the auger bit. Samples taken this way are physically disturbed.

Sample retention is a problem for noncohesive materials such as sludge. Sludge samplers are essentially core samplers with core and auger bits that have been fitted with valves that are designed to retain samples from noncohesive materials. Although they are used primarily for very shallow sampling, some designs allow sampling up to about 30 cm depths. Liners can also be used with sludge samplers [EM97].

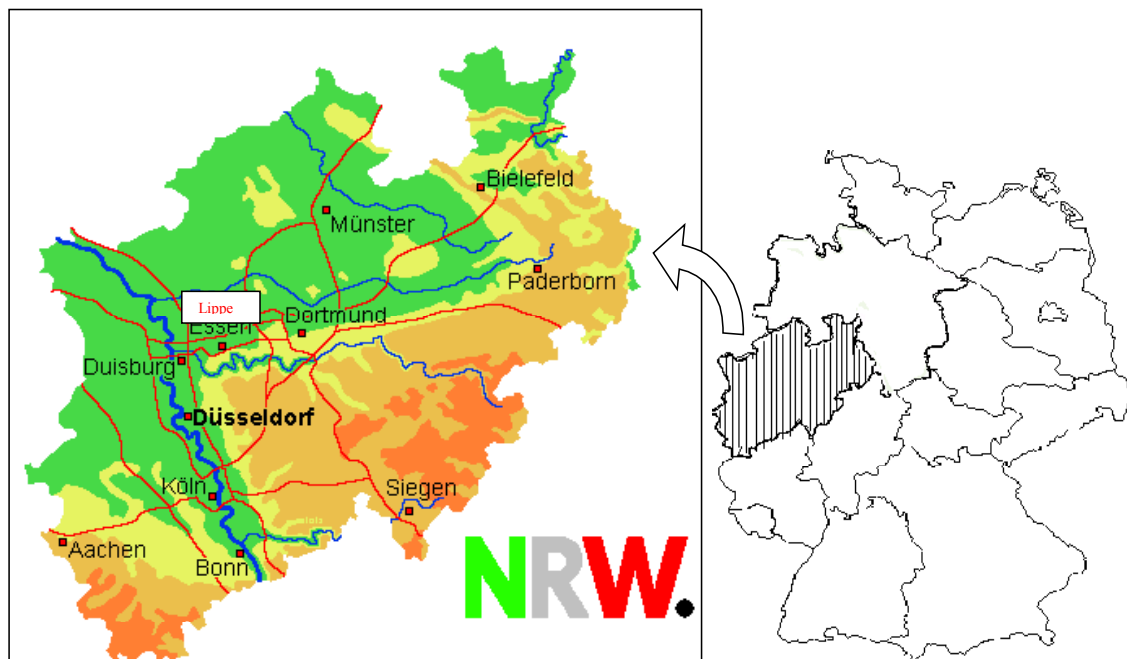


Fig. 2-3: Locations of soil sampling sites from Lippe, North Rhine-Westphalia, Germany.

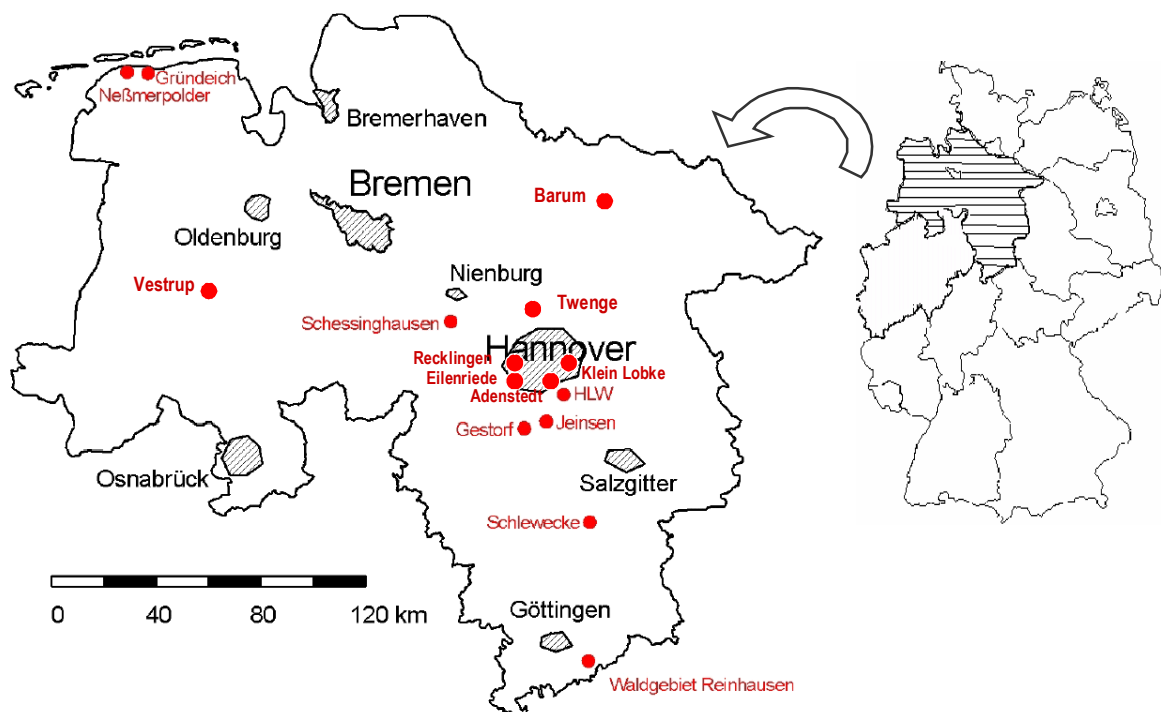


Fig. 2-4: Locations of soil sampling site from Lower Saxony, Germany

2.2 Sample preparation

The soil was taken to the laboratory from a collection spot wrapped in plastic bags. The soil may be crushed to reduce the size of stones, sieved to remove sample content above a

desired size, blended to obtain a more homogenous distribution of particle sizes, or milled to reduce the particle size of the soil. If the sample was sieved or split in the field or a small sample was taken, the preparation process may be eliminated. For some purposes, it is possible to remove large nonporous stones and not grind them to size, but they must be weighed separately and an appropriate allowance made. As a general rule, each soil sample was individually dried under laboratory temperature and also we used oven at 50 °C at least 2 days. The dry soil was ground, pulverized, homogenized and sieved to pass through 2 mm mesh ([NCR76], [Chi97]). The meshed soil samples were transferred to Marinelli beakers (1000 ml capacity) or a bottle (1000 ml and 250 ml capacity) for gamma activity analysis. Each soil sample were weighed and carefully sealed for 4 weeks to reach secular equilibrium between ^{226}Ra and its daughters.

2.3 Experimental methods, measurements and evaluations

One of the most valuable techniques for low-level radioactivity measurements is gamma-ray spectrometry. The various systems, consisting of scintillation and, or, semiconductor detectors coupled to multichannel analyzers, provide for rapid simultaneous measurement of many radionuclides in the same sample. The fundamental characteristics of semiconductor detectors 1 and 2 which used in this work are described in Table 2-1.

Table 2- 1: Crystal characteristics and detection performance of coaxial detector manufactured

| Characteristics | Detector 1 (Benno) | Detector 2 (Karl) |
|---------------------------------------------------|----------------------|-------------------|
| Model No. | GMX-30200-P (n-type) | IGC 54 (p-type) |
| Cryostat Conifiration | PopTop | --- |
| Preamplifier Model | 237N | --- |
| Crystal Diameter | 59.9 mm | 65 mm |
| Crystal Length | 53.5 mm | 74 mm |
| EnCap to Crystal | 4 mm | --- |
| Absorbing Layers (Beryllium) | 0.5 mm | --- |
| Inactive Germanium | 0.3 um | 0.9 mm |
| High Voltage Bias | - 2500 V dc | + 4000 V dc |
| Resolution (FWHM) at 1.33 MeV, ^{60}Co | 1.84 keV | 2.00 |
| Peak-to-Compton ratio | 58.2 | 70.2 : 1 |
| Relative Efficiency at 1.33 MeV, ^{60}Co | 33.1% | 55.8 % |
| Peak Shape (FWTM/FWHM), ^{60}Co | 1,85 | 3.82 |
| Peak Shape (FWFM/FWHM), ^{60}Co | 4,44 | --- |
| Resolution (FWHM) at 122 keV, ^{57}Co | --- | 0.92 |
| Resolution (FWHM) at 5.3 keV, ^{55}Fe | 792 | --- |
| Amplifier time constant | 6 us | 4 us |

2.3.1 Gamma spectrometry

The development of radiation detectors fabricated from single crystals of semiconducting material has revolutionized the detection of X rays and gamma rays. These devices, which are now available in reasonably large volumes, have the advantage of the high detection efficiency for gamma radiation afforded by NaI(Tl) scintillation detectors, but exhibit superior energy resolution. Pulse-amplitude analyzing systems employing detectors fabricated from single

crystals of silicon and germanium are extensively utilized for elemental and radionuclidic analysis.

When used as a detector of gamma rays, the interaction of a gamma ray in the detector produces a primary excited electron that, in turn, excites a cascade of secondary electrons in the process of dissipating its energy within the detector volume. In this manner, the energy of the primary electron is expended in the production of electron-hole pairs which are then collected. The number of electrons collected will be proportional to the energy of the primary electron, and hence related to the energy of the detected photon.

Semiconductor crystals that are free from impurities or structural defects (which can act as traps for secondary electrons) can be used directly for the fabrication of detectors. During the early period of development of these detectors, sufficiently pure material was not available and it was necessary to compensate for the impurities by drifting lithium ions through the detector material at elevated temperature. As the mobility of lithium ions within the crystal lattice is not negligible at room temperature, such detectors must be maintained at cryogenic temperatures throughout their lifetime. Due to difficulties in obtaining semiconductor material with sufficient purity, it has not been possible to achieve complete collection of charge at depths exceeding 1.5 to 2 cm. In these devices the lithium is drifted from the outer surface of the crystal, leaving a p-type core. This type of structure provides a large sensitive volume and has been widely used in the fabrication of Ge(Li) detectors for gamma-ray spectrometry. Active volumes in excess of 150 cm³ can be obtained. Geometries employed in the fabrication of coaxial Ge detectors are illustrated in Fig. 2-5.

Single crystals of germanium are now produced with sufficient purity to make high-quality detectors without lithium drifting to compensate for residual acceptors [Peh77]. Planar detectors with areas of 20 cm² and volumes of 30 cm³ and coaxial detectors with volumes greater than 150 cm³ are now available. Such detectors, which are sometimes termed "intrinsic" but more properly "high-purity" (HPGe), have many advantages. As lithium-ion mobility is not a problem they need not be kept cold at all times. They can be assembled at room temperature, warmed up deliberately or accidentally without damage, shipped without liquid nitrogen and, if necessary, annealed by the user to repair radiation damage.

It should be emphasized that HPGe as well as Ge(Li) detectors must be operated near liquid-nitrogen temperatures to eliminate thermally generated electrons from the conduction band. With the cryostat at 77 K, the balance between the thermal conductivity of the detector mount and thermal radiation from the vacuum enclosure holds the detector between 80 and 85 K. In systems employing a cooled-FET preamplifier, the input-stage FET (field-effect transistor) is mounted on the cryostat to keep its temperature in the range 100 to 140 K.

The operating characteristics of Ge(Li) and HPGe detectors are similar and "Ge detector" can mean either type. Detector-grade HPGe is not quite "intrinsic"; the very low residual concentration of acceptors or donors ($>10^{-10}$ cm⁻³ or $<10^{-12}$ Ge atoms) leaves it slightly p-type or n-type. The use of n-type HPGe (with a thin p-type outer contact) instead of the more usual p-type HPGe makes possible detectors sensitive to low-energy x-rays down to 3 keV [Rau79]. As is indicated in Fig. 2-5, the electrode configuration of the n-type HPGe is the reverse of that for the closed-end p-type HPGe detector; a core is removed and the thick (≈ 300 μ m) lithium n-contact is diffused on the inner surface. The outer p-type contact forming the p-n junction is made by ion-implantation of a boron layer only 0.3 μ m thick. Thus the inactive surface layer is

eliminated and the low-energy detection limit is determined principally by the cryostat vacuum enclosure which can be fitted with a thin beryllium window.

A useful bonus with the reversed-electrode geometry in coaxial detectors is a greatly reduced sensitivity to radiation damage, particularly from fast neutrons, an important consideration in accelerator-target rooms. This comes about because the principal damaging effect of radiation is the production of holes traps. With the reversed electrodes the holes are collected at the outside contact and in cylindrical geometry more material is closer to the outside so most holes have a shorter distance to travel and a smaller chance of being trapped. Also, compared with a p-type detector, for a given bias voltage the space-charge distribution results in a higher field in the outer regions which further reduces trapping [Rau79]. As a result of these two effects coaxial n-type HPGe detectors can sustain a greater than 30-fold more radiation damage than p-type detectors before their performance is significantly degraded [Peh79].

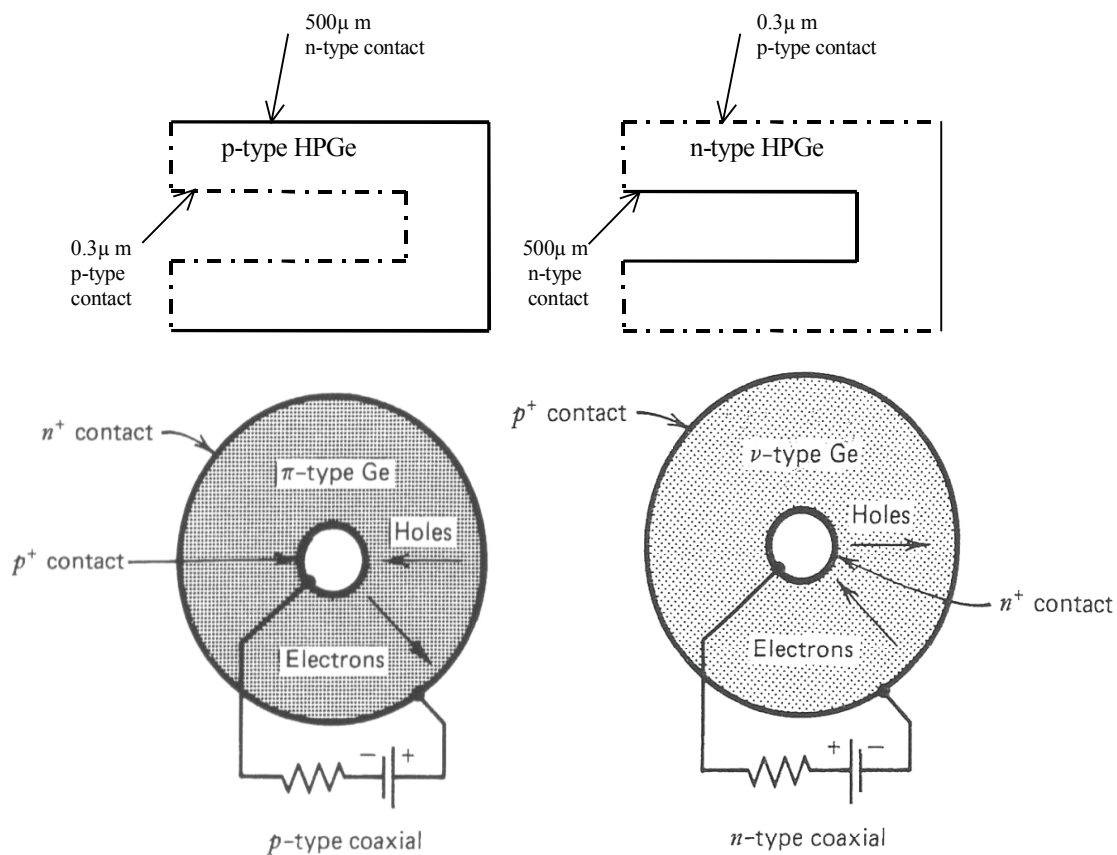


Fig. 2-5: Schematics of semiconductor types of HPGe p or n type at the top, Cross sections perpendicular to the cylindrical axis of the crystal are shown at bottom [Kno00].

The necessity of cooling Ge detectors limits their use where space or liquid nitrogen supply are a problem, e.g., around nuclear reactors, in industry, in space and in nuclear medicine. Needs in these fields have motivated several research groups to develop semiconductor γ -ray detectors which can be operated from room temperature to $\approx 50^\circ\text{C}$. The operating temperature of a semiconductor detector is limited by the requirement that negligible numbers of thermally excited electrons cross the band gap, E_g , from the valence to conduction bands. In practice, for room-temperature operation this means $E_g > 1 \text{ eV}$, preferably in the range ≈ 1.4 to 2.4 eV ($E_g = 1.12 \text{ eV}$ for Si and 0.68 eV for Ge).

The most promising semiconductors at room temperature nuclear-radiation detectors are HgI₂ ($E_g = 2.13$ eV) and CdTe ($E_g = 1.47$ eV), with GaAs ($E_g = 1.43$ eV) running a not-too-close third, but gaining. To-date, however, defects due to residual impurities and small departures from stoichiometry have prevented good charge collection and limited spectroscopy-grade HgI₂ and CdTe detectors to volumes of ≈ 100 mm³ as compared to the ≈ 100 cm³ available in Ge. These small detectors by reason of their high atomic numbers, compared with Ge, have very high detection efficiencies per unit volume, particularly for x rays. They have found many applications where small size is a virtue rather than a drawback, especially as medical probes, x-ray detectors and personal radiation monitors ("chirpers") [Zan78].

The detection of radiation is based on the interactions of the various types of ionizing radiations with matter. The differences between the interactions and the penetrating abilities of the various radiations are very relevant to radiation detection and measurement.

The energy lost by ionizing radiation in semiconductor detectors ultimately results in the creation of electron-hole pairs. Details of the processes through which incoming radiation creates electron-hole pairs are not well known, but the average energy e necessary to create an electron-hole pair in a given semiconductor at a given temperature is independent of the type and the energy of the ionizing radiation. The values of E are: 3.62 eV in silicon at room temperature; 3.72 eV in silicon at 80 K, and 2.95 eV in germanium at 80 K. Since the forbidden band gap value is 1.115 eV for silicon at room temperature and is 0.73 eV for germanium at 80 K, it is clear that not all the energy of the ionizing radiation is spent in breaking covalent bonds. Some of it is-ultimately released to the lattice in the form of phonons.

The importance of these interactions for detectors is in how they relate to incident gamma ray energy deposited in the crystal. An ideal detector converts all of the energy of the gamma ray into an electric pulse that is directly proportional to the gamma ray energy, i.e.: linear. For gamma rays the Compton scattering often results in only a fraction of the energy being deposited because the gamma ray can scatter and then escape from the crystal without further interaction. The full-energy peak can be produced by a photoelectric absorption, or one or more Compton scattering followed by photoelectric absorption, if pair production occurs, the positron slows down in the material and then annihilates, producing two 511 keV gamma rays. Each of these may escape from the detector totally, or leave part of their energy by Compton scattering. If one or both totally escapes, the deposited energy is the full energy minus 511, or 1022 keV, leading to designation of these peaks as "single escape" and "double escape" peaks.

The constant value of E for different types of radiation and for different energies contributes to the versatility and flexibility of semiconductor detectors for use in nuclear spectroscopy. The low value of e compared with the average energy necessary to create an electron-ion pair in a gas (typically 15 to 30 eV) results in the superior spectroscopic performance of semiconductor detectors.

If all of the energy lost by ionizing radiation in a semiconductor were spent breaking covalent bonds in the detector's sensitive volume, no fluctuations would occur in the number of electron-hole pairs produced by ionizing radiation of a given energy. At the other extreme, if that energy entering the semiconductor detector that is partitioned between breaking covalent bonds and lattice vibrations or phonon production were completely uncorrelated, Poisson statistics would apply. The variance in the number of electron-hole pairs n would then be $\langle n \rangle^2 = n$ [Val00].

2.3.2 HPGe detector

A modern Ge detector is a suitably shaped cylinder of highly purified germanium; it is rather hard to imagine that on 10^{10} atoms of germanium we have only one atom of an impurity. The modern metallurgical methods, zone refining, allow us to obtain such extreme purity of material. There are very few laboratories where germanium can be refined to this purity, and a single crystal can be grown; there are only three that produce such crystal for commercial uses. And even these three have difficulties in producing really big crystals [Val00].

After a good vacuum has been created in the cryostat, and the detector has been cooled by placing the assembly in liquid nitrogen, the characteristics of the detectors are measured. If the detector shows the resolution of 1.68 keV, it will obtain a high price tag. With the resolution of 2.2 keV, it will cost only half as much. And if it has resolution of 3 keV, it will be thrown away.

The "classical" coaxial Ge detector is made of p-type germanium, and is used for spectroscopy of gamma rays. It covers the energy range from 100 keV to several MeV. On the low energy side, its efficiency is limited by the fact that low energy gamma rays cannot penetrate the wall of the cryostat. High energy gamma rays might not be detected because they just pass the volume of the detector without the creating a signal that would reflect all the energy of the ray.

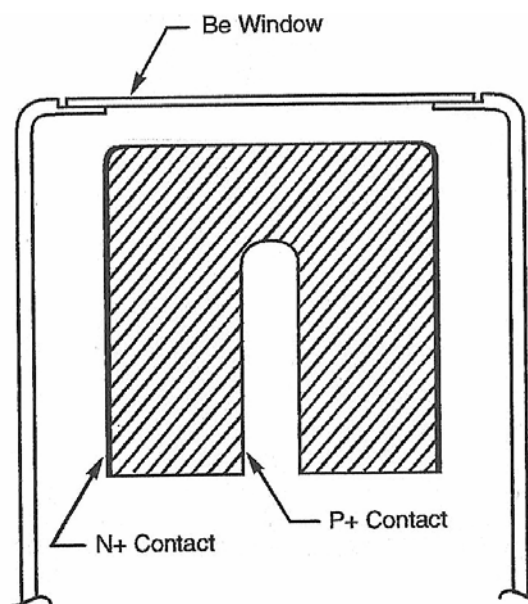


Fig. 2-6: Beryllium window at the face of the detector [Ortic]

If the detector crystal is made of n-type germanium, the outer electrode can be made rather thin. Include a thin aluminum or a beryllium window at the face of the detector, so that low energy electromagnetic radiation will be able to enter the volume of the detector, and in the investigation used HPGe detector to measure low energy 46.54 keV for Pb-210. Instead of a cylindrically shaped detector, one can take only a slice of the mono-crystal [Val00].

This will make a planar Ge detector. With a beryllium entrance window Fig. 2-6, it can be used for X-rays. The last addition to the world of Ge detectors is the Low Energy Germanium

detector. If made by Canberra, it will be called LEGE. It is excellent for low energy gamma-rays; its energy range extends from 10 to 300 keV.

High-purity detection systems having a very low background are suitable tools for the direct measurement of low-level radioactivity in environmental samples. The background features of the detection system are of considerable importance because they have to be known for one to obtain an estimate of the detection limit and of the minimum detectable activity [Cur68]. The natural radioactivity background originates from the uranium and the thorium series from ^{40}K and from cosmic rays. Natural radioactivity is found in most materials, and it is necessary to shield the detector using carefully selected materials of high density.

The conventional coaxial germanium detector is often referred to as Pure Ge, HPGe, Intrinsic Ge, or Hyperpure Ge. Regardless of the superlative used, the detector is basically a cylinder of germanium with an n-type contact on the outer surface, and a p-type contact on the surface of an axial well (Figure 2.5).

Germanium detectors are semiconductor diodes having a P-I-N structure in which the Intrinsic (I) region is sensitive to ionizing radiation, particularly X rays and gamma rays. Under reverse bias, an electric field extends across the intrinsic or depleted region. When photons interact with the material within the depleted volume of a detector, charge carriers (holes and electrons) are produced and are swept by the electric field to the P and N electrodes. This charge, which is in proportion to the energy deposited in the detector by the incoming photon, is converted into a voltage pulse by an integral charge-sensitive preamplifier.

Because germanium has a relatively low band gap, these detectors must be cooled in order to reduce the thermal generation of charge carriers (thus reverse leakage current) to an acceptable level. Otherwise, leakage current induced noise destroys the energy resolution of the detector. Liquid nitrogen, which has a temperature of 77 °K, is the common cooling medium for such detectors. The detector is mounted in a vacuum chamber which is attached to or inserted into a LN's Dewar. The sensitive detector surfaces are thus protected from moisture and other contaminants [Val00].

2.3.3 Gamma spectrometry System (HPGe)

- A vertical high purity germanium (HPGe). The detector should have an efficiency of 18-20%. Generally, the efficiency of germanium detectors is specified as the photopeak efficiency relative to that of a standard 7.62 cm × 7.62 cm cylindrical NaI(Tl) scintillation crystal and is normally based on the measurement of the 1.33 MeV gamma ray photopeak of a ^{60}Co source with a source detector spacing of 25 cm used in both measurement systems. The resolution of the detector - which is normally specified for germanium detectors as the full width (in keV) at half maximum (FWHM) of the full energy peak of the 1.33 MeV peak of ^{60}Co is 33.1% in Table 2-1. A preamplifier is necessary. This is normally an integral part of the detector unit and is located very near the detector in order to take advantage of the cooling which is necessary for the operation of the detector and which aids the preamplifier to operate with low noise.
- A bias high voltage power supply is required to supply high voltage to the detector through the preamplifier. A of 2500 V dc is adequate for the operation of germanium detectors.
- A linear amplifier to process the output signals from the preamplifier is required.
- A detector shield will be needed with a cavity adequate to accommodate samples and constructed of either lead or steel with some type of graded liner to degrade x-rays. Lead

shields have a much lower backscatter effect than steel shields. The back scatter effect also decreases as the internal dimensions of the shield increase. Typically, lead shields have walls 10 cm thick lined inside with graded absorbers of cadmium and copper (~0.4 mm).

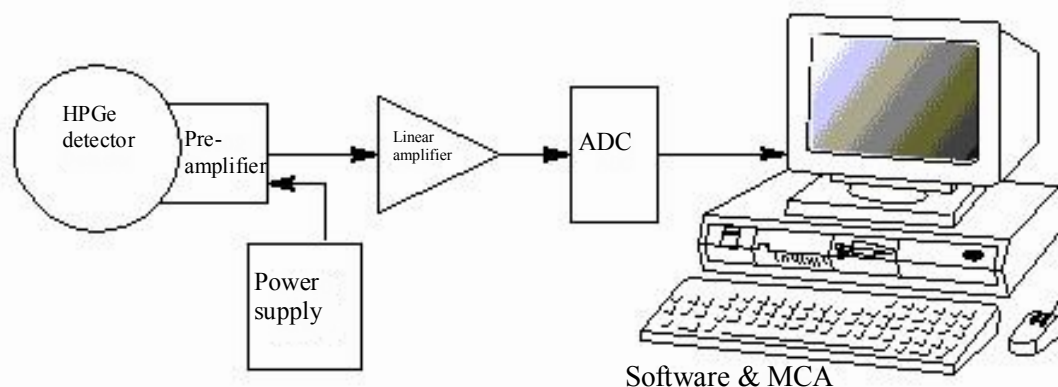


Fig. 2-7: Block diagram of a typical gamma ray spectrometry system.

- A multichannel analyzer (MCA) with a 4096 channels should be connected to a keyboard and display screen for input and output of data and interaction with a computer. Several kits are available for the conversion of personal computers (PCs) into MCAs. Basically there are three types of conversion kits. One type makes use of a board with analog-to-digital converter (ADC) that simply clips in the PC; a second type uses a clip-in board with an external ADC; and the third type uses a multichannel buffer (MCB) connected to the PC. All of these PC-based MCA systems are relatively inexpensive and very suitable for use in germanium and sodium iodide gamma ray spectrometry.
- A rapid data storage and recovery system is needed. It can consist of magnetic tape, hard disc, floppy disc, or a combination of these media. This system can be used for programming, short term storage of data, and archiving data.
- Software for system operation and data reduction is usually supplied with the MCA system. Software packages with varying features and capabilities are available for MCAs based on PCs .

2.3.4 Energy calibration

All nuclear instrumentation is calibrated with standard sources. The equipment is usually checked daily with secondary counting standards to ensure proper operation. Samples are periodically analyzed in duplicate or with the addition of known amounts of a radionuclide to check precision and accuracy. When a nuclide was not detected, the result is given as "less than" (<) the detection limit by the analytical method used [Gol95].

An essential requirement for the measurement of gamma emitters is the exact identity of photopeaks present in a spectrum produced by the detector system. The procedure for identifying the radionuclides within a spectrum relies upon methods which match the energies of the principal gamma rays observed in the spectrum to the energies of gamma rays emitted by known radionuclides. This procedure can be performed either by manual inspection or by computer

analysis. In either case, one must have an accurate energy calibration for the germanium detector system so that correct energies may be assigned to the centroid of each full energy peak (FEP) in a sample spectrum. The energy calibration of a germanium detector system is made by measuring two standard sources of known radionuclides with well-defined energies within the energy range of interest, usually 60 keV to 2000 keV. The use of the lower energy photons emitted by ^{241}Am may indicate changes in the intercept and the higher energy photons emitted (1464 keV) by ^{40}K in Potassium sulphate (K_2SO_4) the Fig. 2-7 shows that. It is also recommended that the gain of the system be adjusted to 0.5 keV/channel. Once these adjustments are made, the gain of the system should remain fixed. The energy calibration source should be counted long enough to produce well defined photopeaks. The channel number that corresponds to the centroid of each FEP on the MCA should be recorded and plotted on logarithmic graph paper on the X-axis versus the gamma ray energy on the Y-axis. A log curve will result in the plot of these data if the system is operating properly. The slope and intercept of the energy calibration line should be determined by least squares calculations. Computerized systems are usually equipped to perform their slope and intercept calculations automatically during the calibration routine. The system should be checked each day of operation for the stability of the slope and intercept by the measurement and plot of at least two different gamma energies.

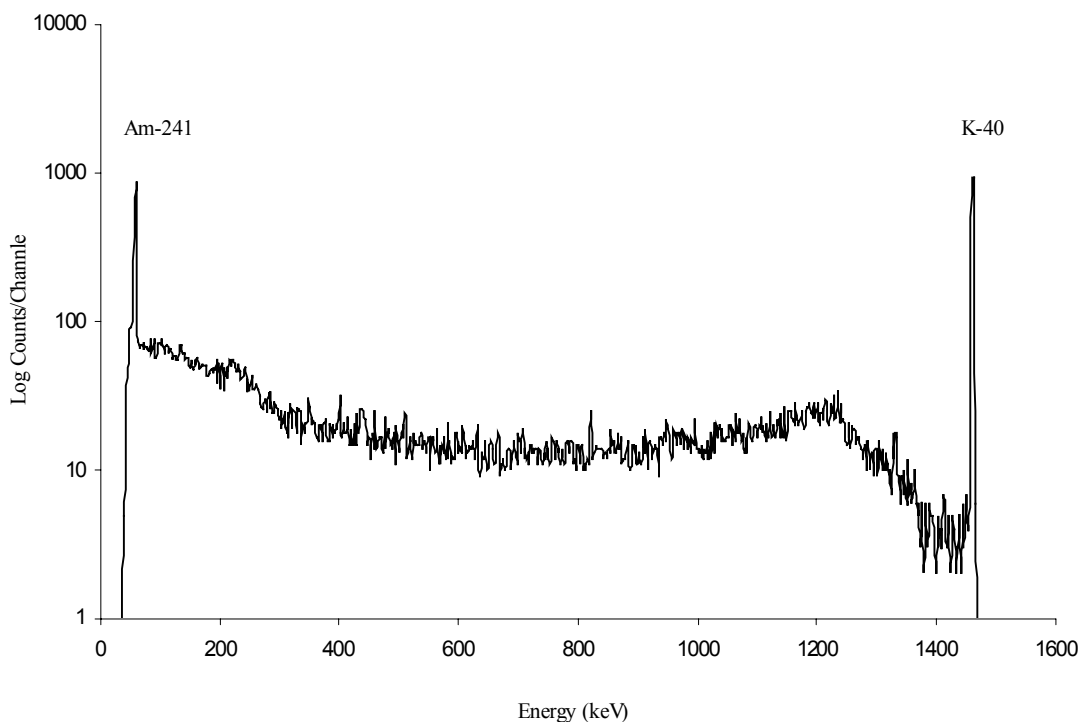


Fig. 2-8: Gamma-ray spectrum of an energy calibration source.

2.4 Calibration and efficiency determination of detectors for different measuring geometries and sample containers

Samples should be counted only in the types of container used to acquire the counting efficiencies. The density, volume and height of the sample in the container must be the same as that of the standards used for calibration. Any change of these factors will require additional calibrations to match the characteristics of the sample.

In this work, obtained different efficiencies with different mass, soil in different geometry (1-l marinelli beaker and different bottle: 1-l and 250 ml) with different height and density and also different detectors so used different calibration efficiency for all these cases.

2.4.1 Preparation of reference standard solution (Calibration source QCY48)

This mixed radionuclide gamma-ray reference standard consists of a solution in 4 ml Hcl of the ten radioelements listed in the table (2-2). Dilution of the radionuclide standard solution means a process of dispensing a known amount of the master solution (in g) to a 250 cm³ polyethylene bottle that contain solution (i.e. of distilled water with 4 m Hcl. The bottle is then shaken slowly and carefully to homogenize the solution. Appropriate radionuclides must be selected for use as standards in efficiency calibration. Solutions of certified mixed radionuclides with reasonably long half-lives are available from several reputable suppliers (PTB). Accurate absolute gamma ray emission rates should be stated in the certificates supplied with the standards.

If radionuclides, such as ¹³⁹Ce, ⁸⁸Y, ²⁰³Hg or ⁸⁵Sr, that decay by cascade transitions and produce multilined spectra, are used in the efficiency calibration, great care must be taken to correct for the counting losses created by coincidence summing effects. Radionuclides that are used for determinations of efficiency can be classified into two groups: those radionuclides with only a few prominent gamma rays, and those with many prominent gamma rays. The radionuclides (QCY48) listed in Table (2 - 3) belong to the first group and have been used extensively for efficiency calibrations. By the proper selection and combination of these radionuclides, an efficiency curve can be determined over the energy range of interest (usually 60 keV to 1836 keV).

By the same method we prepared a second group of radionuclides (QCY40) listed in Table (2-2) energy range of interest (usually 46.54 keV to 122.1 keV).

By the proper selection and combination of these radionuclides with soil sample, an efficiency curve can be determined over the energy range of interest (usually 46.54 keV to 1836 keV). The energy range must be adequately covered by calibration points so that interpolation between the points is accurate.

Table 2- 2: Radionuclides used for efficiency calibration QCY40

| Nuclides | Energy (keV) | Gamma/g*s | Uncertainty (%) | Half-life time (d) |
|----------|--------------|-----------|-----------------|--------------------|
| Pb-210 | 46.54 | 439 | 2 | 8145 |
| Am-241 | 59.54 | 734 | 2 | 158047 |
| Cd-109 | 88.03 | 380 | 2 | 462.6 |
| Co-57 | 122.1 | 897 | 2 | 271.4 |

Table 2- 3: Radionuclides used for efficiency calibration QCY48

| Nuclides | Energy (keV) | Gamma/g*s | Uncertainty (%) | Half-life time (d) |
|----------|--------------|-----------|-----------------|--------------------|
| Am-241 | 59.54 | 1114 | 2.6 | 158047 |
| Cd-109 | 88.03 | 642 | 6.2 | 462.6 |
| Co-57 | 122.1 | 580 | 1.5 | 271.4 |
| Ce-139 | 165.9 | 679 | 1.4 | 137.64 |
| Hg-203 | 279.2 | 1916 | 1.4 | 46.6 |
| Zn-113 | 391.7 | 2059 | 3.2 | 115.09 |
| Sr-85 | 514 | 3871 | 2.5 | 64.84 |
| Cs-137 | 661.7 | 2445 | 2 | 10958 |
| Y-88 | 898 | 6316 | 1.6 | 106.6 |
| Co-60 | 1173 | 3346 | 1.5 | 1924.9 |
| Co-60 | 1333 | 3351 | 1.5 | 1924.9 |
| Y-88 | 1836 | 6676 | 1.4 | 106.61 |

2.4.2 Preparation of standard soil sample procedure

In order to make a standard soil sample, one selects a soil of the same density which has been measured before. Then a well defined amount of the standard solution of radionuclides is added. In our case 1 ml, each, of the diluted standards QCY40 and QCY48 multi-isotopic solution. Then, it was heated to 90 °C until the mixture had evaporated to near dryness. Complete the drying in an air oven at 80 °C.

Fill a marinelli beaker with the chosen powdered matrix material e.g. soil / sediment. Ensure that the powder has settled by regular tapping. For routine, reproducible sample analyses, the containers used for counting must be selected taking into account both the quantity of sample material available and the sensitivity acquired by the geometry of the sample in the container. Some examples of sample containers are, marinelli beakers, and cylindrical plastic containers, different volume 250 ml and 1000 ml) with screw caps (bottles). In general, the dimensions of the container should be well suited to the dimensions of the detector and lead housing, e.g. not too tall or too thin.

2.4.3 Efficiency calibration

An accurate efficiency calibration of the system is necessary to quantify radionuclides present in a sample. It is essential that this calibration be performed with great care because the accuracy of all quantitative results will depend on it. It is also essential that all system settings and adjustments be made prior to determining the efficiencies and be maintained until a new calibration is undertaken. Small changes in the settings of the system components may have slight but direct effects on counting efficiency.

2.4.4 Analytical efficiency expressions

Data reduction and efficiency calibration of the spectra obtained from the analysis of various background samples on detectors 1 and 2 were utilized to create distinct background files. For any calibration standard analyzed on a given detector, the corresponding background file was used to subtract contributions of background peaks from the sample peaks. The net full-

energy-peak area was calculated using the efficiency calibration procedure for each background-subtracted peak in the standard spectrum which corresponds to a calibrated gamma-ray emission.

The absolute detector efficiency at that energy was then calculated by dividing the net count rate in the full-energy peak by the decay corrected gamma-ray-emission rate of the standard source. After the absolute detection efficiency was determined for each calibration peak, a weighted least-squares fit was made to a polynomial expression of log of efficiency vs log of energy. Efficiency curves were constructed from these full-energy-peak efficiencies [Wil92].

$$\epsilon_{\text{abs}} = \frac{\text{number of pulses recorded (cps experimental)}}{\text{number of radiation quanta emitted by source (cps theoretical)}} \quad (2-1)$$

$$\epsilon_{\text{abs}} = \left[\left(\frac{NoS_2}{ToC_{s_2}} \right) - \left(\frac{Ns_1}{ToC_{s_1}} \right) - \left(\frac{CoB}{ToC_b} \right) \right] / (G_s) \exp(-\ln 2 \cdot t / t_{1/2}) \quad (2-2)$$

Where

- NoS_2 count in a standard soil sample
 ToC_{s_2} time in a counting of standard soil sample (4 hours or more)
 Ns_1 count of soil sample before added standard solution
 ToC_{s_1} time of counting of soil sample before added standard solution (18 hours)
 CoB count of background
 ToC_b time of counting of background (72 hours).
 G_s counting of gamma ray of used standard solution
 t the time of decay
 $t_{1/2}$ half-life time of radionuclide

we used eq. (2-2) for all energy of radionuclides in Table 2-4:

Table 2- 4: Radionuclides used for efficiency calibration

| Nuclide | Energy (keV) | ϵ % | $u_{\text{rel}}(\epsilon)$ |
|---------|--------------|--------------|----------------------------|
| Pb-210 | 46.54 | 1.862 | 0.114 |
| Am-241 | 59.54 | 4.230 | 0.047 |
| Cd-109 | 88.03 | 4.912 | 0.083 |
| Co-57 | 122.1 | 5.086 | 0.038 |
| Ce-139 | 165.9 | 4.470 | 0.020 |
| Hg- 203 | 279.2 | 3.151 | 0.018 |
| Sn-113 | 391.7 | 2.280 | 0.042 |
| Sr- 85 | 514 | 1.877 | 0.026 |
| Cs-137 | 661.7 | 1.425 | 0.022 |
| Y-88 | 898 | 1.050 | 0.017 |
| Co-60 | 1173 | 0.848 | 0.018 |
| Co-60 | 1333 | 0.764 | 0.017 |
| Y-88 | 1786.5 | 0.576 | 0.015 |

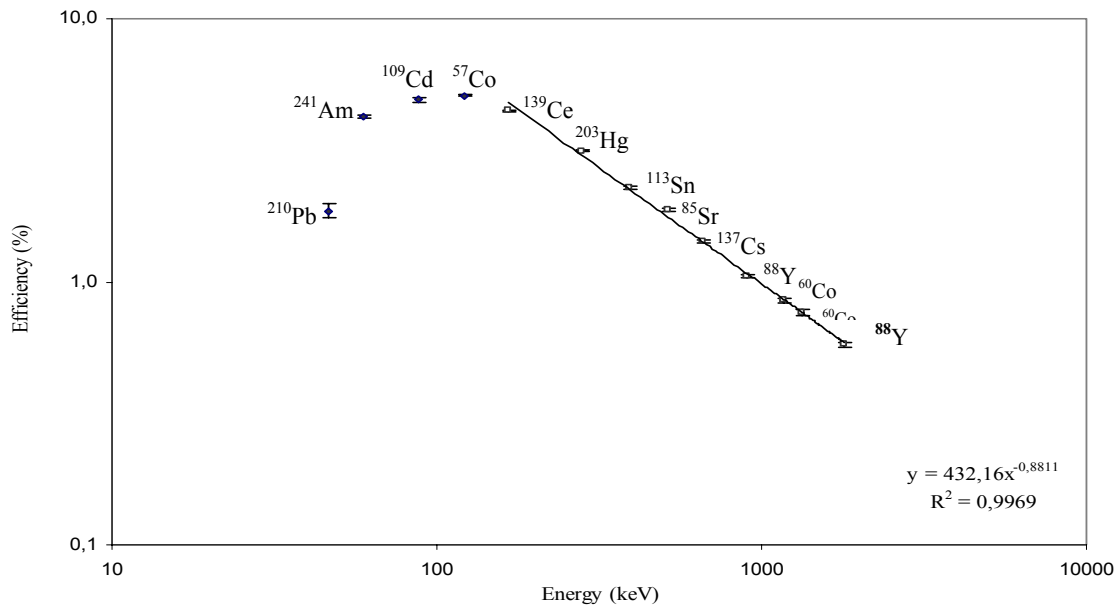


Fig. 2-9: Full energy peak efficiency as a function of gamma ray energy for a typical HPGe detector 1 for 1200 g soil in marinelli beaker.

From the measurement of calibration sources, experimental efficiencies are calculated. The experimental efficiency at energy E for a given set of measuring conditions can be computed by:

$$\varepsilon_{\text{abs}} = A \times E^B \quad (2-3)$$

Where E is the energy and A, B are parameters from the Fig 2-9 are $A = 4.3216$ and $B = -0.8811$ for 1200 g standard soil in marinelli beaker on detector 1, and we used the eq 2-3 to determine relation between efficiency and energies higher than 165 keV and then used it to determine specific activities for all radionuclides in soil samples under investigation see table 2-14, the relation between efficiency and energies less than 165 keV for curve in Fig. 2-9 we used another treatment to obtain a relation between efficiency and energy and then used it to determine specific activities for nuclides less than 165 keV, these treatment by Gray fit.

Once a sufficient number of data are acquired experimentally in the energy region of interest, a means of representing the efficiency as a function of energy should be chosen. Gray fitting procedures are used to fit the efficiency data to an analytical expression. A generally accepted and simple expression for efficiency (\mathcal{E}) is as follows [Gra85], [Deb88]:

$$\mathcal{E}(E) = \frac{I}{E} \cdot \sum_{i=0}^8 a_i \left(\ln \frac{E}{E_0} \right)^{i-1} \quad (2-4)$$

where E represents energy in MeV. This expression is adequate for determining efficiency of gamma energies from 46.54 keV to 1836 keV. A typical efficiency curve for a germanium detector is given. We can take one sample and measure it by the same last method and get the results in Table 2-4 and also by using fitting program with Gnuplot. So we get fitting parameters and also Fig.2-9 shows full energy peak efficiency as a function of gamma ray energy for a typical HPGe detector for 1119 g soil sample in marinelli beaker by using Gnuplot program see appendix A.

Table 2- 5: Radionuclides used for efficiency calibration of 1119 g soil in marinelli beaker for detector 1:

| Nuclide | Energy (keV) | ϵ % | $u_{rel}(\epsilon)$ |
|---------|--------------|--------------|---------------------|
| Pb-210 | 46.54 | 2.0333 | 0.1041 |
| Am-241 | 59.54 | 4.3055 | 0.0467 |
| Cd-109 | 88.03 | 5.0042 | 0.0830 |
| Co-57 | 122.1 | 5.0109 | 0.0377 |
| Ce-139 | 165.9 | 4.4649 | 0.0200 |
| Hg -203 | 279.2 | 3.1001 | 0.0174 |
| Sn-113 | 391.7 | 2.2465 | 0.0420 |
| Sr -85 | 514 | 1.9449 | 0.0260 |
| Cs-137 | 661.7 | 1.4301 | 0.0221 |
| Y-88 | 898 | 1.0580 | 0.0173 |
| Co-60 | 1173 | 0.8518 | 0.0174 |
| Co-60 | 1333 | 0.7769 | 0.0177 |
| Y-88 | 1836 | 0.5866 | 0.0151 |

We get these parameters (see appendix A) from Gunplot program and we used these parameter to get the efficiency for energy of ^{210}Pb (46.54 keV) and also for all energy below 165 keV by using Microsoft Excel.

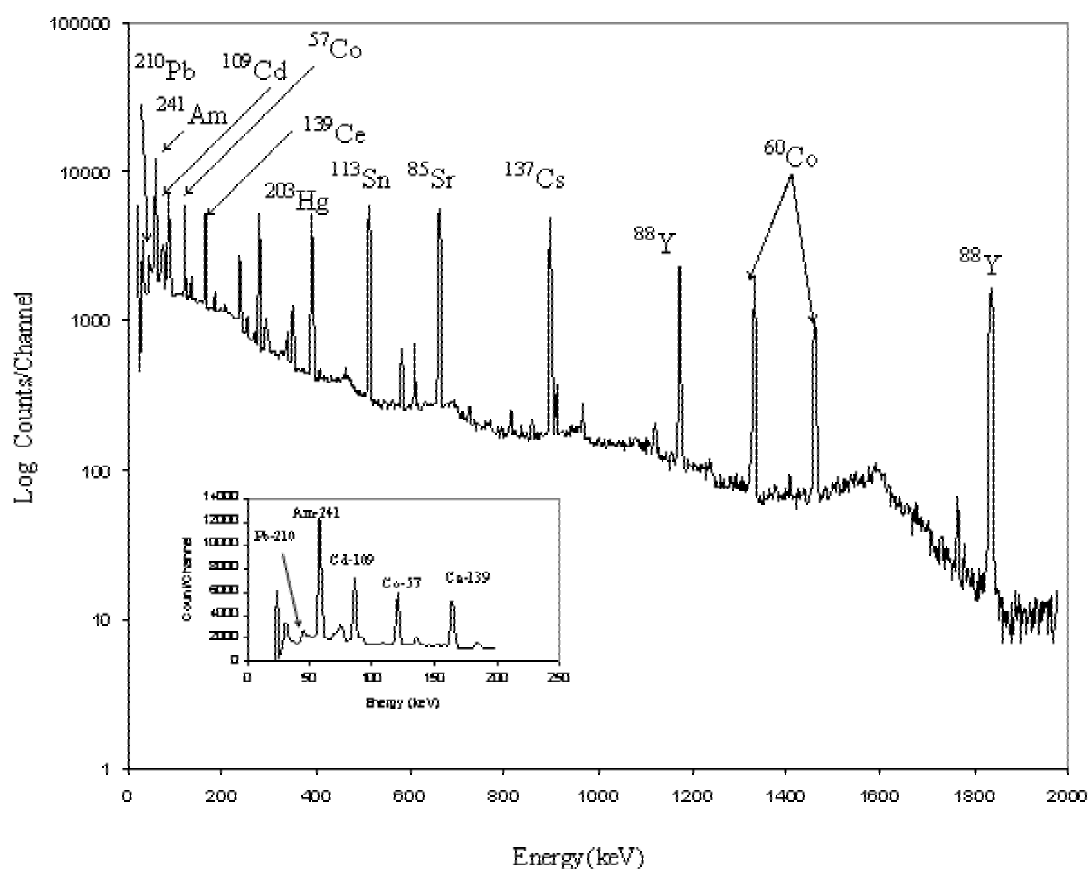


Fig. 2-10: Gamma-ray spectrum of the standard efficiency calibration for 1119 g soil in marinelli beaker of HPGe detector for 4 hours is the time of counts.

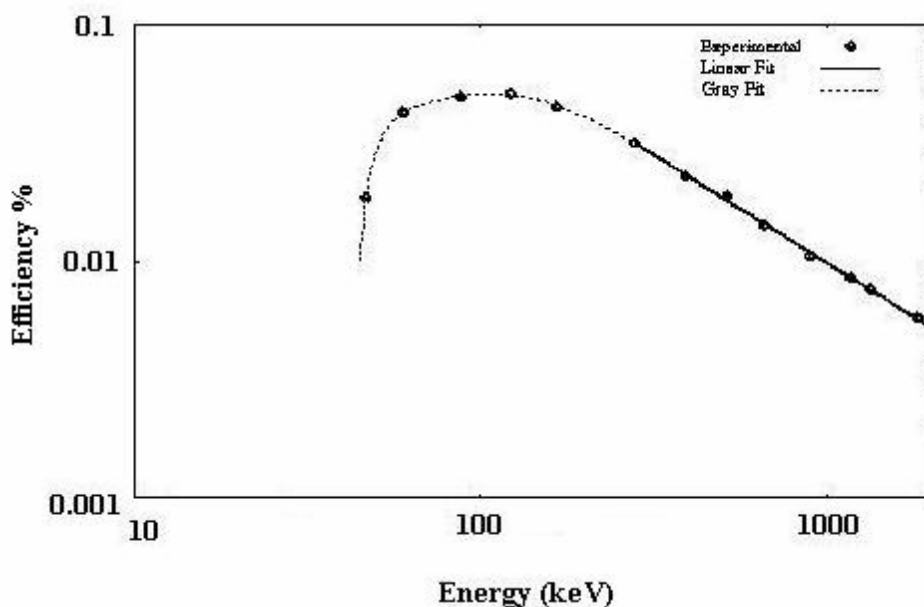


Fig. 2-11: Full energy peak efficiency as a function of gamma ray energy for a typical HPGe detector 1 for 1200 g soil sample in marinelli beaker by using Gnuplot program.

In this work, we used also another computer program EFFIC for Gray function and we get the result in Table 2-5 and Fig. 2-12 shows the efficiency for 1100 g soil in marinelli beaker on detector 1.

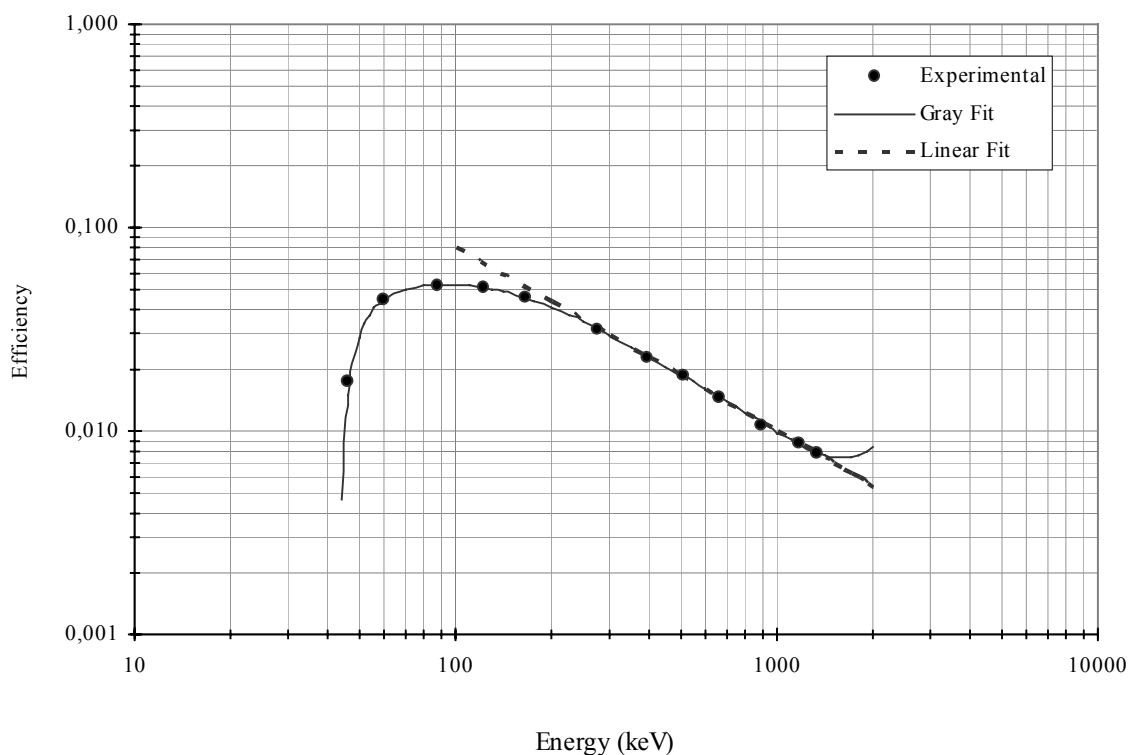


Fig. 2-12: Efficiency-Energy relation by using gray fit for 1100 g soil in marinelli beaker by using HPGe detector 1 (Be window).

In this work we have calibrated a HPGe detector for efficiency over the [46.54 -1836 keV] energy range for the measurement of environmental samples in different arrangements. The wider the range in energy, the larger the number of radionuclides whose concentration can be determined. To measure the main natural γ -ray emitters, the efficiency should be known at least from 46.54 keV (^{210}Pb) to 1460.83 keV (^{40}K). The detection of several artificial radionuclides that are radiologically important (e.g. ^{137}Cs) and a more accurate determination of the activity of some naturally occurring radionuclides demands the extension of the energy range up to 2000 keV.

The most accurate efficiency determinations for a HPGe-crystal γ -ray spectrometer are based on experimental measurements, where one has no need to make approximations. The direct measurement of different calibration sources containing isolated γ -ray emitters within the energy range of interest, and their subsequent fitting to a parametric function, yields the best results. However, when the energy interval is broad, it requires a large number of primary standards, implying a high financial cost, a long counting time and much work in preparing samples. Moreover, the risk of committing uncontrolled errors increases. An economical alternative is the calculation of the efficiency values by Monte Carlo Simulations (MCS). However, the lack of precise information about detector characteristics and matrix composition magnifies the errors on the low-energy efficiency values. Methods based on MCS provide accurate results to within 3%, rising to more than 5% at energies below 100 keV, for complex matrices in extended sources [Kar02], [Vid02], [Daz01], [Vid01].

Measurements of standard sources with the different geometries are needed: the first geometry is bottle (250 ml and 1000 ml) other is marinelli beaker geometry both with different heights and different density. The efficiencies obtained are subsequently employed in developing a parametric function. The outcome of the method is an analytical function relating the efficiencies in the two geometries mentioned above taking into account the differences in the geometrical and matrix effects.

For the soil samples, the values found for the detection efficiency were in tables 2-7, 2-8. Starting from these values, an analysis of how the detection efficiency varies with sample mass was accomplished. Using the measurements efficiencies for the whole mass range, from 800 g to 1200 g and 1100 g to 1444 g. So, for the mentioned work, there is the variation in the counting efficiency due to the sample mass from 800 to 1200 g and 1100 g to 1444 g for that energy was evident. In fact, there is a dependence of efficiency on the sample mass for the soil samples [Wil92] it was possible to construct Fig. 2-13, and 2-14, which shows the data adjustment of this work for the ^{210}Pb gamma-ray line. Analyzing the counting efficiency variation for the measured mass. In Fig. 2-13, it can be noticed that for the ^{210}Pb (46.54 keV), the illustration, the variation in the efficiency is significant. For the efficiency is obtains energy. In this work, the interval from 800 to 1200 g and 1100g to 1444 g was studied and a clear dependence was found. Based on the straight-line equation of Fig. 2-13 is ($\epsilon = - 0.0032 * m + 6.4424$) and in Fig. 2-14 is ($\epsilon = - 0.001 * m + 3.1651$) it was possible to determine the efficiency for each sample mass used for the activity calculation of ^{210}Pb (46.54 keV).

Table 2- 6: Results of the EFFIC for the calculate of the efficiency for a 1100 g soil sample in marinelli beaker measured by a HPGe detector 1 (Be window).

| Energy (keV) | Efficiency (Experimental) | Energy (keV) | Efficiency (Gray) | Energy (keV) | Efficiency (Gray) | Energy (keV) | Efficiency (Linear) |
|--------------|---------------------------|--------------|-------------------|--------------|-------------------|--------------|---------------------|
| 46.5 | 0.0175 | 44 | 0.00459 | 350 | 0.0259 | 100 | 0.0804 |
| 59.5 | 0.0439 | 46 | 0.0151 | 400 | 0.0231 | 200 | 0.0429 |
| 88 | 0.0523 | 48 | 0.0231 | 450 | 0.0208 | 300 | 0.0298 |
| 122 | 0.0511 | 50 | 0.0291 | 500 | 0.019 | 400 | 0.023 |
| 166 | 0.0449 | 52 | 0.0337 | 550 | 0.0174 | 500 | 0.0188 |
| 276 | 0.0319 | 54 | 0.0373 | 600 | 0.0161 | 600 | 0.0159 |
| 392 | 0.0231 | 56 | 0.0402 | 650 | 0.0149 | 700 | 0.0138 |
| 514 | 0.0187 | 58 | 0.0424 | 700 | 0.0139 | 800 | 0.0123 |
| 662 | 0.0148 | 60 | 0.0442 | 750 | 0.0131 | 900 | 0.011 |
| 898 | 0.0108 | 70 | 0.0494 | 800 | 0.0123 | 1000 | 0.01 |
| 1170 | 0.00866 | 80 | 0.0516 | 850 | 0.0116 | 1100 | 0.0092 |
| 1330 | 0.00777 | 90 | 0.0524 | 900 | 0.0109 | 1200 | 0.0085 |
| | | 100 | 0.0525 | 950 | 0.0104 | 1300 | 0.00791 |
| | | 110 | 0.052 | 1000 | 0.00988 | 1400 | 0.0074 |
| | | 120 | 0.0512 | 1100 | 0.00904 | 1500 | 0.00695 |
| | | 130 | 0.0501 | 1200 | 0.0084 | 1600 | 0.00656 |
| | | 140 | 0.0488 | 1300 | 0.00793 | 1700 | 0.00621 |
| | | 150 | 0.0474 | 1400 | 0.00762 | 1800 | 0.00589 |
| | | 175 | 0.0438 | 1500 | 0.00745 | 1900 | 0.00561 |
| | | 200 | 0.0403 | 1600 | 0.00741 | 2000 | 0.00536 |
| | | 225 | 0.0371 | 1700 | 0.00749 | | |
| | | 250 | 0.0343 | 1800 | 0.00768 | | |
| | | 275 | 0.0317 | 1900 | 0.00797 | | |
| | | 300 | 0.0295 | 2000 | 0.00835 | | |

Table 2- 7: Count efficiency variation with masses of soil in marinelli beaker for ^{210}Pb 46.54 keV gamma-ray line.

| mass g | ϵ % | $u_{\text{rel}}(\epsilon)$ |
|-----------|--------------|----------------------------|
| 835.7 | 3.76 | 0.03 |
| 1020 | 3.08 | 0.03 |
| 1100 | 2.92 | 0.04 |
| 1200 | 2.56 | 0.04 |

Figs. 2-15, 2-16, and 2-17 and tables 2-9, 2-10, and 2-11 respectively show the variation of three efficiency-energy curves with heights (for a constant density), for calibration sources of soil in Bottle (1000 ml capacity) and marinelli beaker for detector 2, and marinelli beaker for detector 1. Therefore, the uncertainty should be taken into account to estimate the efficiency-energy curves. It can be seen in all the figures that the efficiencies decrease when the height is increased, as expected.

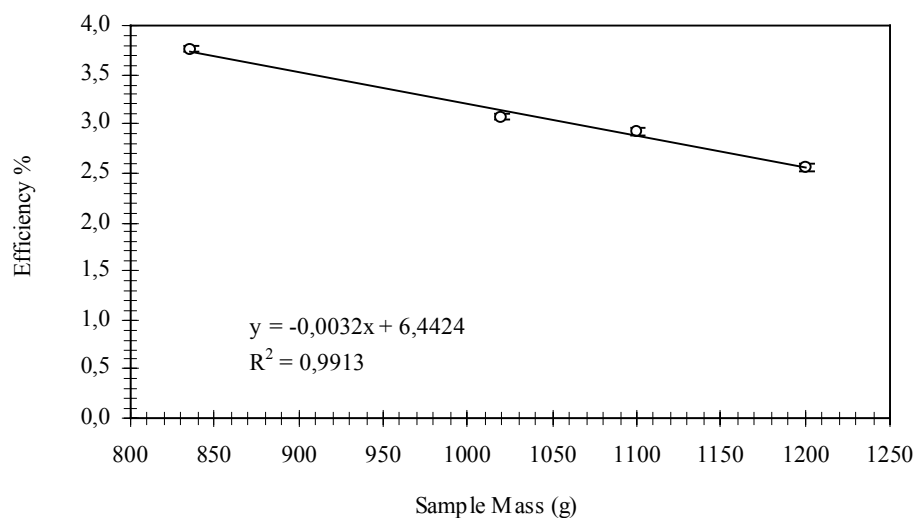


Fig. 2-13: Variation of the efficiency versus mass of soil with gamma-ray energy 46.54 keV (Pb-210) in a marinelli beaker.

Table 2- 8: Count efficiency variation with masses of soil in marinelli beaker for ^{210}Pb 46.54 keV gamma-ray line.

| mass (g) | ϵ % | $u_{rel}(\epsilon)$ |
|----------|--------------|---------------------|
| 1119 | 2.033 | 0.104 |
| 1200 | 1.862 | 0.114 |
| 1444 | 1.669 | 0.121 |

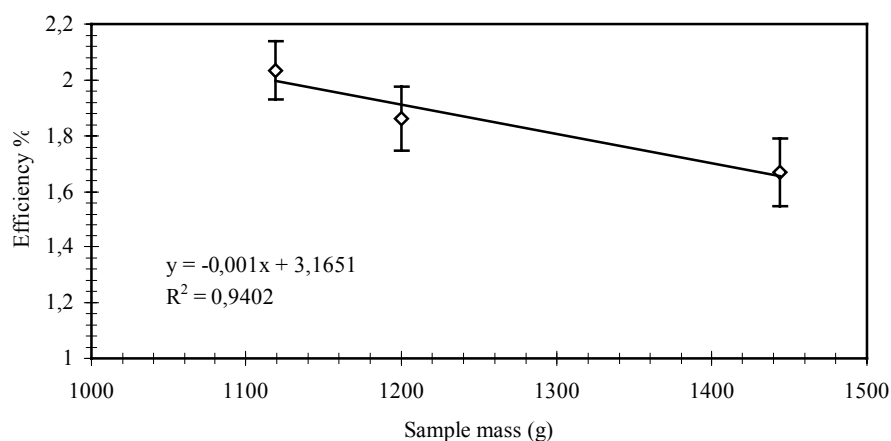


Fig. 2-14: Count efficiency variation with masses of soil in marinelli beaker for ^{210}Pb 46.54 keV gamma-ray line.

Measurements of radionuclides from environmental samples (soil) by gamma-ray spectrometry requires a correction for. The correction can be simplified or avoided by the direct calibration of spectrometers with certified mixed gamma-ray standard matrices with a composition close to that of environmental samples to be assayed [San94].

In this work used the soil samples from the same site which the same composition to avoid self-attenuation of gamma-ray specially for low gamma ray energy like Pb-210.

Table 2- 9: Variation of efficiency-energy curves with heights of soil in marinelli beaker for a constant density.

| Nuclide | Height Energy (keV) | 10 cm | | 9 cm | | 8 cm | | 7 cm | |
|---------|---------------------------|--------------|---------------------|--------------|---------------------|--------------|---------------------|--------------|---------------------|
| | | ϵ % | $u_{rel}(\epsilon)$ | ϵ % | $u_{rel}(\epsilon)$ | ϵ % | $u_{rel}(\epsilon)$ | ϵ % | $u_{rel}(\epsilon)$ |
| Pb-210 | 46.54 | 1.618 | 0.040 | 1.911 | 0.075 | 1.735 | 0.044 | 1.568 | 0.091 |
| Am-241 | 59.54 | 3.747 | 0.046 | 3.948 | 0.046 | 3.834 | 0.046 | 3.549 | 0.047 |
| Cd-109 | 88.03 | 4.478 | 0.082 | 5.947 | 0.083 | 4.626 | 0.082 | 4.286 | 0.083 |
| Co-57 | 122.1 | 4.421 | 0.036 | 4.572 | 0.038 | 4.584 | 0.036 | 4.354 | 0.039 |
| Ce-139 | 165.9 | 4.029 | 0.023 | 4.069 | 0.040 | 4.146 | 0.024 | 4.106 | 0.046 |
| Sn-113 | 391.7 | 1.902 | 0.044 | 1.338 | 0.021 | 2.021 | 0.044 | - | - |
| Cs-137 | 661.7 | 1.297 | 0.020 | 1.009 | 0.026 | 1.286 | 0.020 | 1.239 | 0.022 |
| Y-88 | 898 | 0.957 | 0.019 | 0.781 | 0.017 | 0.952 | 0.020 | 0.886 | 0.030 |
| Co-60 | 1173 | 0.771 | 0.015 | 0.696 | 0.017 | 0.767 | 0.016 | 0.742 | 0.018 |
| Co-60 | 1333 | 0.693 | 0.015 | - | - | 0.699 | 0.016 | 0.670 | 0.018 |
| Y-88 | 1836 | 0.558 | 0.016 | 0.574 | 0.017 | 0.551 | 0.017 | 0.493 | 0.028 |

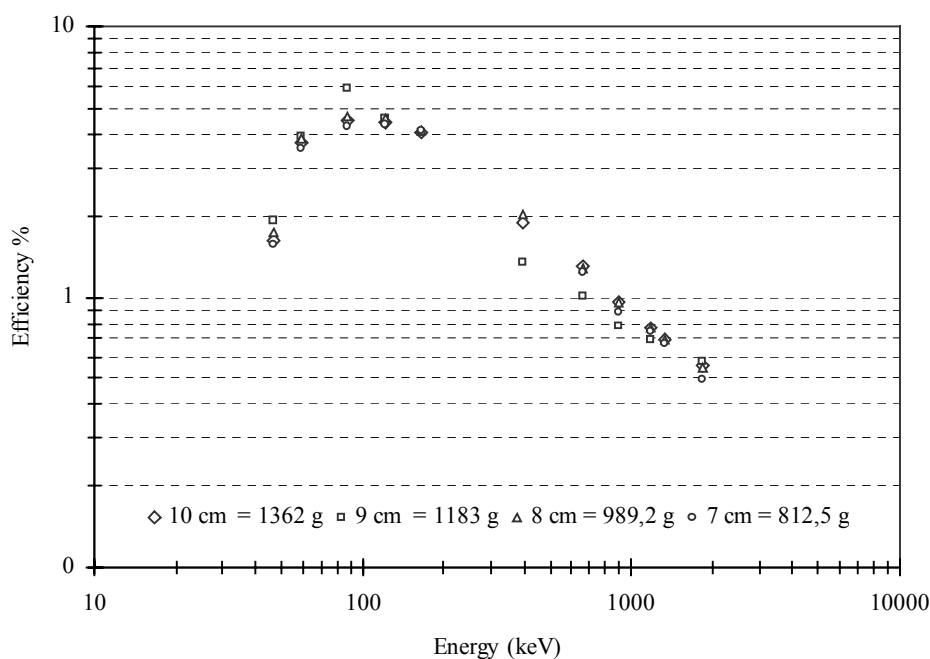


Fig. 2-15: Variation of efficiency-energy curves with heights of soil in marinelli beaker for a constant density.

Table 2- 10: Efficiency-energy values for different height of soil in Bottle 1000 ml detector 2

| Nuclide | Energy [keV] | 14 cm | | 10 cm | | 5 cm | | 4 cm | |
|---------|------------------|--------------|---------------------|--------------|---------------------|--------------|---------------------|--------------|---------------------|
| | | ϵ % | $u_{rel}(\epsilon)$ | ϵ % | $u_{rel}(\epsilon)$ | ϵ % | $u_{rel}(\epsilon)$ | ϵ % | $u_{rel}(\epsilon)$ |
| Am-241 | 59.54 | 0.388 | 0.008 | 0.208 | 0.005 | 0.197 | 0.005 | 0.180 | 0.004 |
| Cd-109 | 88.03 | 0.703 | 0.009 | 0.710 | 0.012 | 0.605 | 0.011 | 0.598 | 0.011 |
| Co-57 | 122.1 | 0.832 | 0.010 | 0.822 | 0.017 | 0.729 | 0.015 | 0.702 | 0.015 |
| Ce-139 | 165.1 | 0.982 | 0.025 | 0.879 | 0.039 | 0.848 | 0.036 | 0.869 | 0.034 |
| Zn-113 | 391.7 | 0.591 | 0.014 | 0.590 | 0.019 | 0.528 | 0.016 | 0.476 | 0.016 |
| Cs-137 | 661.6 | 0.451 | 0.005 | 0.443 | 0.005 | 0.378 | 0.004 | 0.354 | 0.004 |
| Y-88 | 898 | 0.364 | 0.006 | 0.356 | 0.007 | 0.287 | 0.006 | 0.266 | 0.006 |
| Co-60 | 1173 | 0.315 | 0.002 | 0.301 | 0.002 | 0.246 | 0.002 | 0.222 | 0.001 |
| Co-60 | 1333 | 0.290 | 0.002 | 0.276 | 0.002 | 0.224 | 0.001 | 0.203 | 0.001 |
| Y-88 | 1836 | 0.242 | 0.004 | 0.234 | 0.004 | 0.186 | 0.004 | 0.167 | 0.003 |

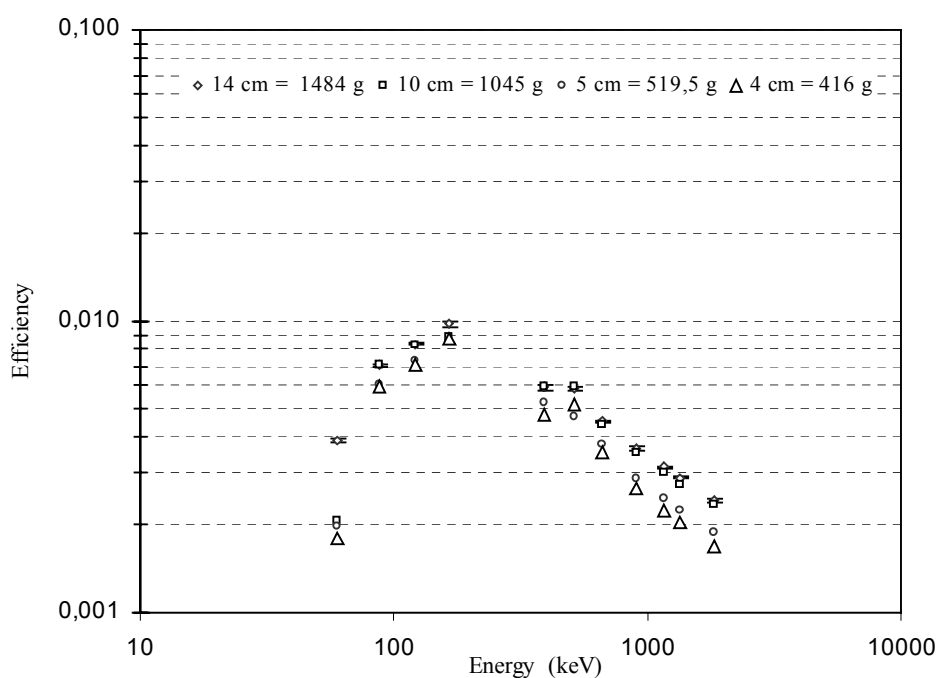


Fig. 2-16: Variation of efficiency-energy curves with heights of soil in Bottle 1000 ml for a constant density

Figs. 2-18, 2-19, and 2-20 and Tables 2-12, 2-13 and 2-14 present the variation of these efficiency curves with respect to varying mass of analyzed matrices for detectors 1 and 2, respectively. As expected, for any given detector, the gamma-ray-detection efficiency decreases with increasing media mass. The effect of mass on photon attenuation is more pronounced for gamma rays within the 46.54- to 165-keV region; although, the perturbation due to varying media mass is also observed for gamma rays with higher energies (even 1836 keV or greater). It is interesting to note that the detection efficiencies of equal-size detectors 1 and 2 are fairly similar, despite the advantageous features of detector 2, such as lesser external absorption in the Be window of the detector cryostat and ultra-thin ion-implanted contacts in the detector. Evidently, due to bulkiness of sample size, the self-absorption of photons within the sample media over shadows the benefits due to these features. Table 2-12 and Fig. 2-17 displays the detection efficiency for prominent gamma rays associated with some commonly analyzed radionuclides in different mass for detector 1.

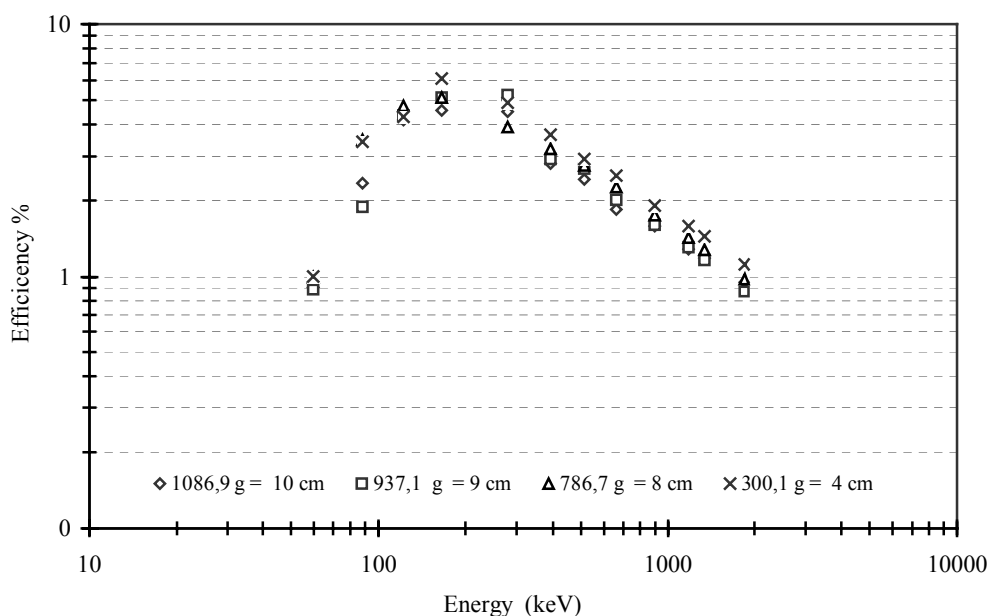


Fig. 2-17: Variation of efficiency-energy curves with heights of soil in Marinelli beaker for detector 2.

Table 2- 11: Efficiency for different height of soil in Marinelli beaker for detector 2 (Karl)

| Nuclide | Energy (keV) | 10 cm | | 9 cm | | 8 cm | | 4 cm | |
|---------|--------------|--------------|---------------------|--------------|---------------------|--------------|---------------------|--------------|---------------------|
| | | ϵ % | $u_{rel}(\epsilon)$ | ϵ % | $u_{rel}(\epsilon)$ | ϵ % | $u_{rel}(\epsilon)$ | ϵ % | $u_{rel}(\epsilon)$ |
| Am-241 | 59.54 | 0.907 | 0.047 | 0.887 | 0.052 | 1.000 | 0.047 | 1.005 | 0.047 |
| Cd-109 | 88.03 | 2.347 | 0.084 | 1.889 | 0.097 | 3.495 | 0.083 | 3.426 | 0.083 |
| Co-57 | 122.1 | 4.170 | 0.036 | 4.346 | 0.040 | 4.754 | 0.036 | 4.295 | 0.037 |
| Ce-139 | 165.9 | 4.548 | 0.021 | 5.122 | 0.035 | 5.106 | 0.020 | 6.085 | 0.019 |
| Hg -203 | 279.2 | 4.512 | 0.051 | 5.253 | 0.101 | 3.918 | 0.067 | 4.884 | 0.045 |
| Sn-113 | 391.7 | 2.810 | 0.042 | 2.929 | 0.045 | 3.209 | 0.042 | 3.660 | 0.042 |
| Sr-85 | 514 | 2.436 | 0.028 | 2.689 | 0.039 | 2.760 | 0.027 | 2.934 | 0.029 |
| Cs-137 | 661.7 | 1.852 | 0.020 | 2.021 | 0.022 | 2.261 | 0.020 | 2.517 | 0.021 |
| Y-88 | 898 | 1.585 | 0.017 | 1.606 | 0.020 | 1.753 | 0.017 | 1.913 | 0.017 |
| Co-60 | 1173 | 1.291 | 0.015 | 1.308 | 0.017 | 1.434 | 0.015 | 1.588 | 0.016 |
| Co-60 | 1333 | 1.190 | 0.015 | 1.168 | 0.017 | 1.282 | 0.015 | 1.444 | 0.016 |
| Y-88 | 1836 | 0.954 | 0.014 | 0.872 | 0.020 | 0.978 | 0.014 | 1.117 | 0.015 |

Table 2- 12: Efficiency of soil in marinelli beaker with different masses in the same volume for HPGE detector (1).

| Nuclide | Energy (keV) | 833 g | | 1078 g | | 1295 g | | 1362.7 g | |
|---------|--------------|--------------|---------------------|--------------|---------------------|--------------|---------------------|--------------|---------------------|
| | | ϵ % | $u_{rel}(\epsilon)$ | ϵ % | $u_{rel}(\epsilon)$ | ϵ % | $u_{rel}(\epsilon)$ | ϵ % | $u_{rel}(\epsilon)$ |
| Pb-210 | 46.54 | 2.458 | 0.064 | 2.377 | 0.060 | 1.932 | 0.069 | 1.618 | 0.040 |
| Am-241 | 59.54 | 4.026 | 0.046 | 3.801 | 0.046 | 3.899 | 0.046 | 3.747 | 0.046 |
| Cd-109 | 88.03 | 4.771 | 0.084 | 4.424 | 0.083 | 4.387 | 0.083 | 4.478 | 0.082 |
| Co-57 | 122.1 | 4.790 | 0.039 | 4.644 | 0.039 | 4.522 | 0.038 | 4.421 | 0.036 |
| Ce-139 | 165.9 | 4.264 | 0.053 | 4.233 | 0.048 | 4.458 | 0.038 | 4.029 | 0.023 |
| Sn-113 | 391.7 | 2.129 | 0.058 | 2.046 | 0.053 | 2.070 | 0.051 | 1.902 | 0.044 |
| Cs-137 | 661.7 | 1.356 | 0.021 | 1.356 | 0.021 | 1.377 | 0.021 | 1.297 | 0.020 |
| Y-88 | 898 | 1.036 | 0.029 | 0.961 | 0.029 | 1.003 | 0.027 | 0.957 | 0.019 |
| Co-60 | 1173 | 0.797 | 0.017 | 0.789 | 0.017 | 0.766 | 0.017 | 0.771 | 0.015 |
| Co-60 | 1333 | 0.726 | 0.017 | 0.688 | 0.017 | 0.698 | 0.017 | 0.693 | 0.015 |
| Y-88 | 1836 | 0.653 | 0.025 | 0.579 | 0.025 | 0.547 | 0.025 | 0.558 | 0.016 |

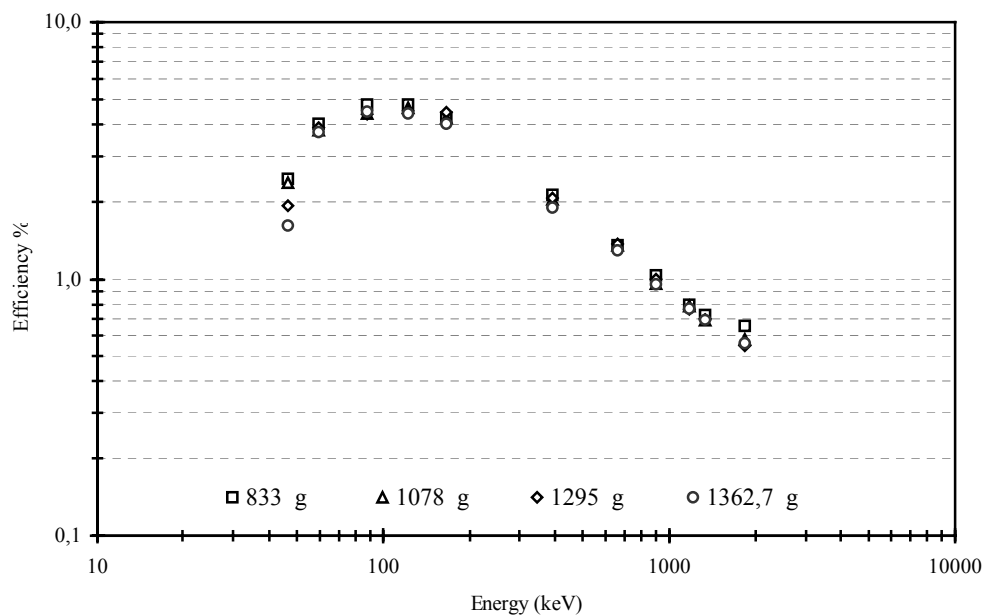


Fig. 2-18: Efficiency Variation of efficiency curves with heights of soil in marinelli beaker in the same volume for HPGe detector (1).

Table 2- 13: Efficiency of soil in marinelli beaker with different masses in the same volume for HPGe detector 1.

| Nuclide | Energy (keV) | 1119 g | | 1200 g | | 1444 g | |
|---------|--------------|--------------|---------------------|--------------|---------------------|--------------|---------------------|
| | | ϵ % | $u_{rel}(\epsilon)$ | ϵ % | $u_{rel}(\epsilon)$ | ϵ % | $u_{rel}(\epsilon)$ |
| Pb-210 | 46.54 | 2.033 | 0.104 | 1.862 | 0.114 | 1.669 | 0.121 |
| Am-241 | 59.54 | 4.306 | 0.047 | 4.230 | 0.047 | 3.872 | 0.047 |
| Cd-109 | 88.03 | 5.004 | 0.083 | 4.912 | 0.083 | 4.572 | 0.083 |
| Co-57 | 122.1 | 5.011 | 0.038 | 5.086 | 0.038 | 4.810 | 0.038 |
| Ce-139 | 165.9 | 4.465 | 0.020 | 4.470 | 0.020 | 4.033 | 0.022 |
| Hg-203 | 279.2 | 3.100 | 0.017 | 3.151 | 0.018 | 2.931 | 0.018 |
| Sn-113 | 391.7 | 2.247 | 0.042 | 2.280 | 0.042 | 2.107 | 0.042 |
| Sr-85 | 514 | 1.945 | 0.026 | 1.877 | 0.026 | 1.797 | 0.026 |
| Cs-137 | 661.7 | 1.430 | 0.022 | 1.425 | 0.022 | 1.356 | 0.022 |
| Y-88 | 898 | 1.058 | 0.017 | 1.050 | 0.017 | 1.002 | 0.017 |
| Co-60 | 1173 | 0.852 | 0.017 | 0.848 | 0.018 | 0.789 | 0.018 |
| Co-60 | 1333 | 0.777 | 0.018 | 0.764 | 0.017 | 0.681 | 0.018 |
| Y-88 | 1836 | 0.587 | 0.015 | 0.576 | 0.015 | 0.552 | 0.015 |

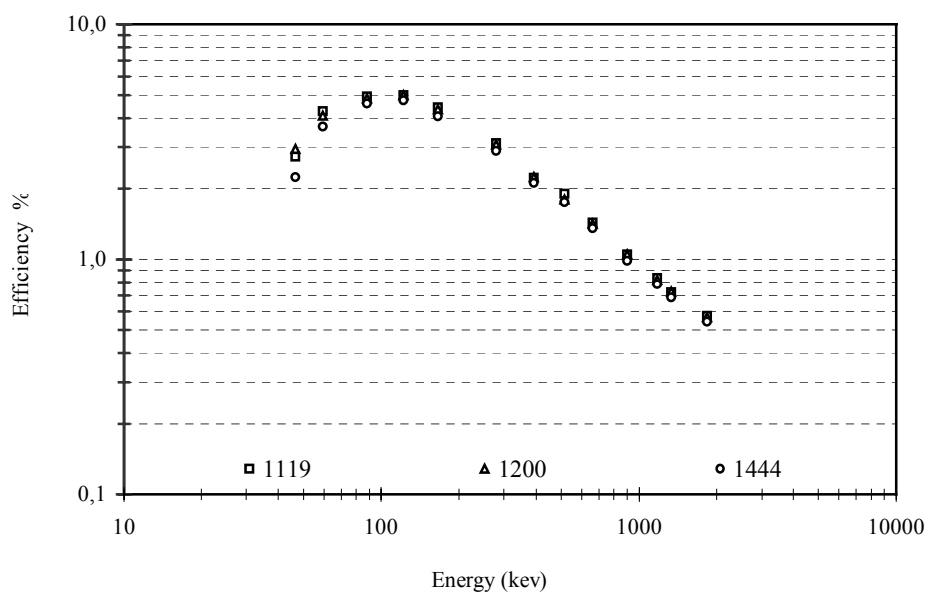


Fig. 2-19: Efficiency Variation of efficiency curves with heights of soil in marinelli beaker in the same volume for HPGe detector (1).

Table 2- 14: Efficiency of soil in marinelli beaker with different masses in the same volume for HPGe detector (2).

| Nuclide | Energy (keV) | 211 g | | 261 g | | 305 g | |
|---------|--------------|--------------|---------------------|--------------|---------------------|--------------|---------------------|
| | | ϵ % | $u_{rel}(\epsilon)$ | ϵ % | $u_{rel}(\epsilon)$ | ϵ % | $u_{rel}(\epsilon)$ |
| Am-241 | 59.54 | 0.949 | 0.052 | 0.640 | 0.056 | 0.812 | 0.053 |
| Cd-109 | 88.03 | 2.986 | 0.086 | 2.513 | 0.088 | 1.709 | 0.093 |
| Co-57 | 122.1 | 4.158 | 0.041 | 3.139 | 0.043 | 3.410 | 0.043 |
| Ce-139 | 165.9 | 3.751 | 0.054 | 3.668 | 0.051 | 3.308 | 0.055 |
| Sn-113 | 391.7 | 2.463 | 0.050 | 1.999 | 0.052 | 1.886 | 0.053 |
| Sr- 85 | 514 | 2.043 | 0.060 | 1.985 | 0.061 | 1.271 | 0.102 |
| Cs-137 | 661.7 | 1.641 | 0.023 | 1.421 | 0.022 | 1.199 | 0.024 |
| Y-88 | 898 | 1.270 | 0.027 | 1.038 | 0.027 | 1.038 | 0.030 |
| Co-60 | 1173 | 0.951 | 0.019 | 0.854 | 0.018 | 0.838 | 0.020 |
| Co-60 | 1333 | 0.965 | 0.019 | 0.720 | 0.019 | 0.797 | 0.020 |
| Y-88 | 1836 | 0.788 | 0.027 | 0.516 | 0.028 | 0.688 | 0.028 |

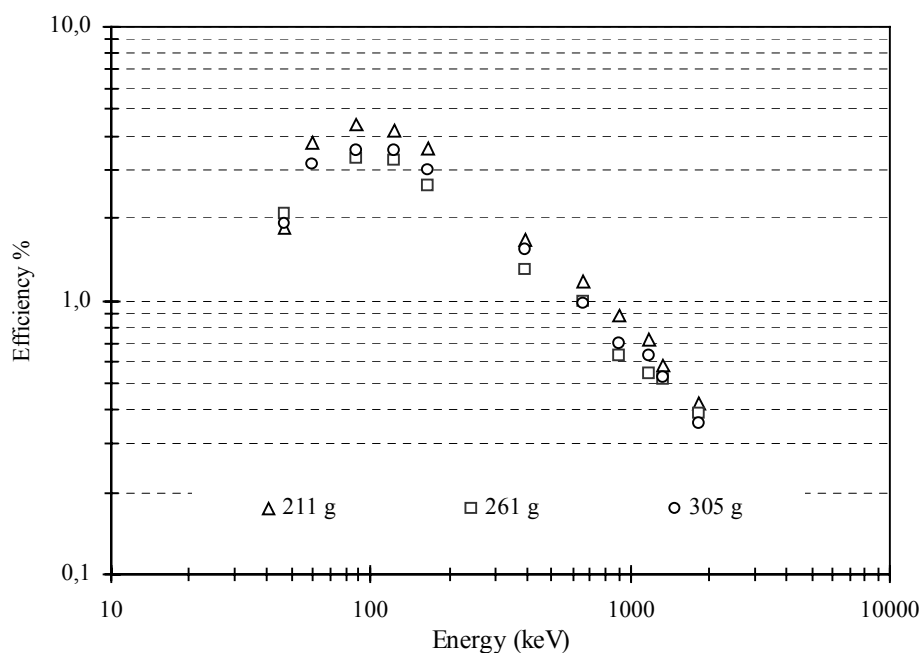


Fig. 2-20: Efficiency for different masses of soil in Bottle 250ml HPGe detector (2).

2.5 Natural Background

The background of the system has a very significant influence on the detection limit and accuracy of the measurement of low levels of activity. The counting system must have a background as low as is attainable with a minimum of spectral lines originating from natural radionuclides which may be present in the system components and the surrounding environment, i.e. the walls, floor, etc. of the counting facility.

Background measurements should be taken as frequently as is practicable and for counting times as long as possible (in this work, the measuring time was 72 hours) in order to obtain good counting statistics. A good practice is to record the background measurements on a control chart with statistically fixed limits. This provides a means both of checking the stability of the electronics of the system and of checking for contamination of the detector and/or shield. Should the background exceed the control limits, an immediate and thorough investigation should be made and appropriate steps taken to maintain a minimum background.

Great care should be taken to prevent any contamination of the detector, because the decontamination process is difficult, tedious, and time consuming. The detector should always be covered with a thin polyethylene film (foil) held in place over the detector by either Scotch tape or a rubber band [IAE89].

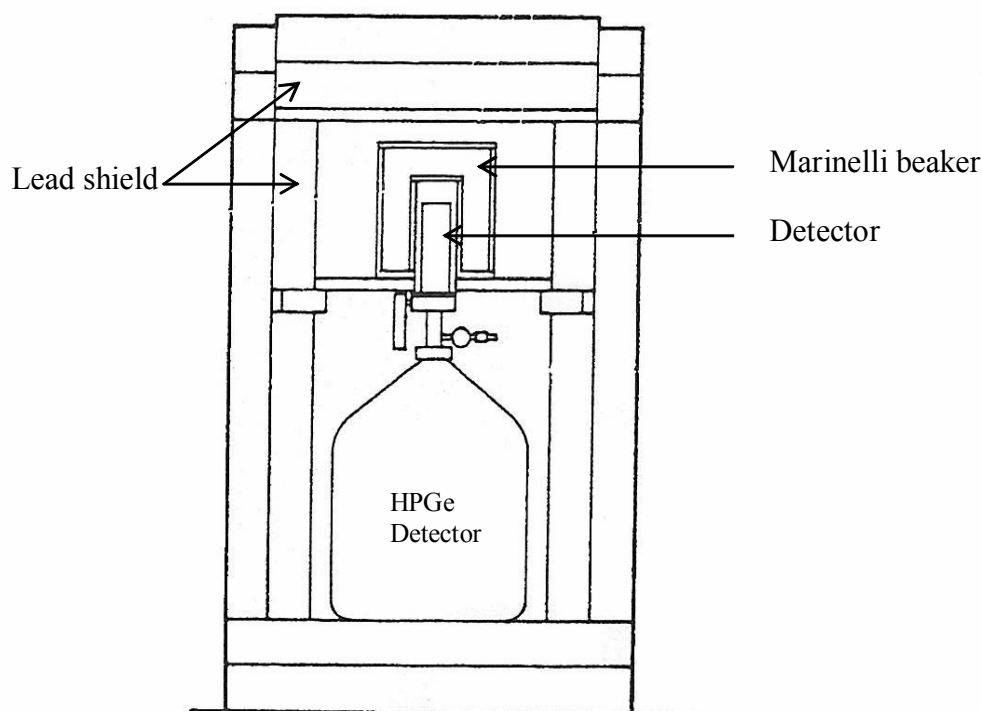


Fig. 2-21: A low-background shield configuration for a germanium detector [Kno00].

The radioactivity of ordinary construction materials is, in large part, due to low concentrations of naturally radioactive elements often contained as an impurity. The most important components are potassium, thorium, uranium, and radium.

Radiations emitted are a beta particle with 1.314 MeV endpoint energy (89% yield), a gamma ray of 1.460 MeV energy (11%), and characteristic Ar X-rays following the electron capture. The high-energy gamma rays often lead to a recognizable peak in the background spectra from gamma-ray detectors, because potassium is a widespread component in concrete and other building materials. Thorium, uranium, and radium are all members of long decay chains involving daughter products that emit a mixed spectrum of alpha, beta, and gamma rays. In the terrestrial gamma-ray spectrum shown in Fig. 2-22, the following daughter activities can be identified: in the thorium series, ^{228}Ac , ^{224}Ra , ^{212}Pb , and ^{208}Tl ; in the uranium series, ^{226}Ra , ^{214}Pb , and ^{214}Bi . The long-lived natural activities of ^{238}U and ^{40}K are also evident.

A measurable amount of background can originate with radioactivity carried by the ambient air, either in the form of trace amounts of radioactive gases or dust particles. Radon (^{222}Rn) and thoron (^{220}Rn) are short-lived radioactive gases that originate as daughter products in the decay chains of the uranium and thorium present either in the soil or construction materials of the laboratory. A significant component of detector background arises from the secondary radiations produced by cosmic-ray interactions in the earth's atmosphere. The primary cosmic radiation, which can be either of galactic or solar origin, is made up of charged particles and heavy ions with extremely high kinetic energies. In low-level counting experiments, it is therefore prudent to carry out a background determination near the time of the actual measurement itself. Background counts both before and after the measurement will help detect any changes in the background level [Kno00].

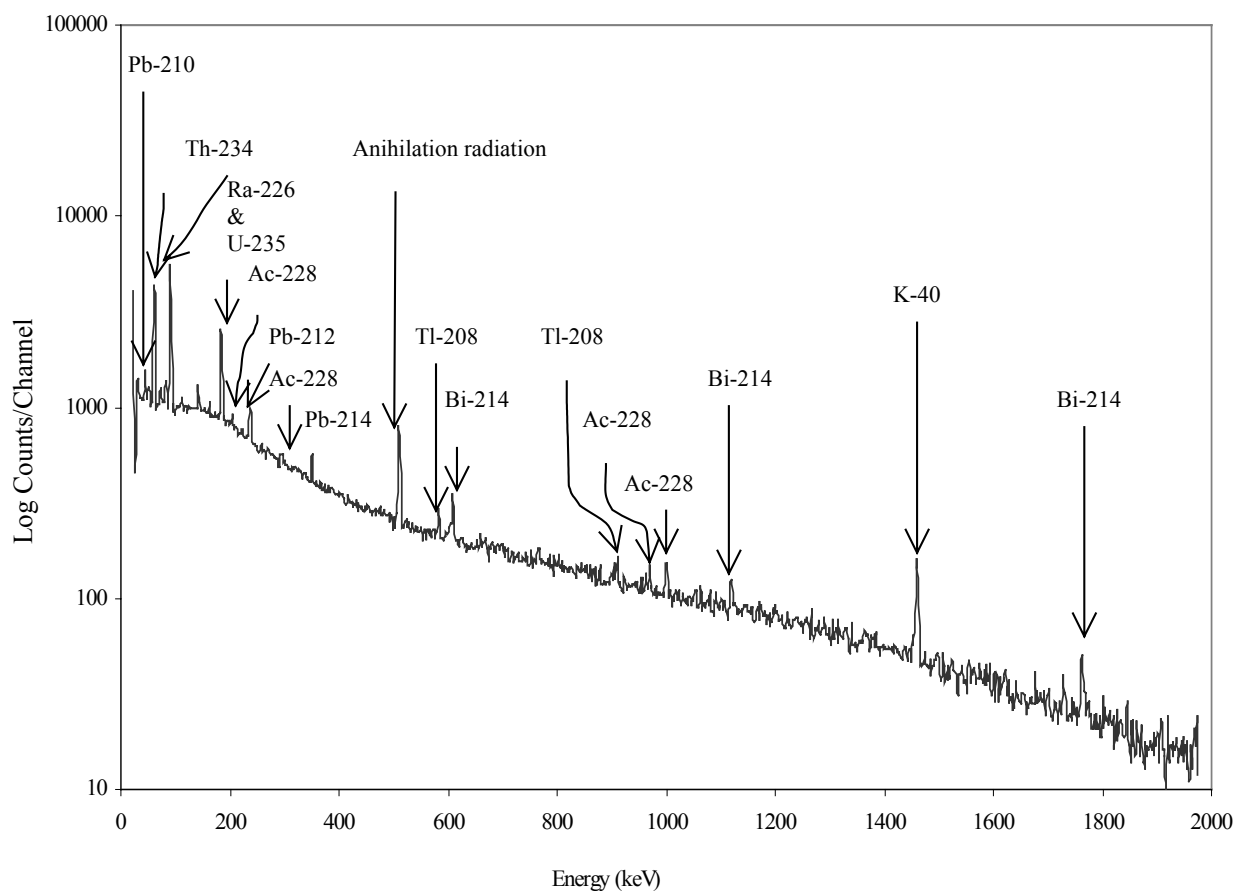


Fig. 2-22: The background spectrum recorded for germanium detector using the shield shown on Fig.2-21 for a counting time of 72 hours.

2.6 Calculation of elemental concentrations

High resolution gamma-ray spectrometry is a convenient method for measuring the activity of radioactive nuclei emitting gamma-rays. In laboratory conditions a sample is placed close to the sensitive volume of the detector and the gamma-ray spectrum is measured. In the spectrum all the photons that interact with the material within the sensitive volume of the detector are registered. Since radioactive atoms emit a discrete spectrum of photons, peaks in the spectrum occur at these photon energies due to interactions leading to full absorption of the photon energy within the sensitive volume. Only quantities describing the intensity of peaks in the spectra are the subject of this work.

After the measurement has been completed (18 hours counting time), the peak areas in the spectrum are calculated and corrected for counting losses. The corrected peak areas are proportional to the number of radioactive atoms that have decayed in the sample during the time of the measurement. Neglecting the probability for coincident detection of two or more gamma-rays, the factor of proportionality is given by the product of two probabilities: the probability that during the decay a gamma-ray with energy E is emitted and the probability that this gamma-ray is registered in the spectrum in the full-energy peak.

Following the spectrum analysis, count rates for each detected photopeak and activity per mass unit (radiological concentration) for each of the detected nuclides are calculated. The specific activity (in Bq kg⁻¹), A_{Ei} , of a nuclide i and for a peak at energy E , is given by:

$$A_{Ei} = \frac{NP}{t_c \times I_\gamma(E_\gamma) \times \varepsilon(E_\gamma) \times M} \quad (2-5)$$

where NP is the number of counts in a given peak area corrected for background peaks of a peak at energy E , $\varepsilon(E_\gamma)$ the detection efficiency at energy E , t is the counting lifetime, $I_\gamma(E_\gamma)$ the number of gammas per disintegration of this nuclide for a transition at energy E , and M the mass in kg of the measured sample. If there is more than one peak in the energy analysis range for a nuclide, then an attempt to average the peak activities is made. The result is then the weighted average nuclide activity. Based on the measured γ -ray photopeaks, emitted by specific radionuclides in the ²³²Th and ²³⁸U decay series and in ⁴⁰K, their radiological concentrations in samples collected were determined. Calculations relied on establishment of secular equilibrium in the samples, due to the much smaller lifetime of daughter radionuclides in the decay series of ²³²Th and ²³⁸U. More specifically, the ²³²Th concentration was determined from the average concentrations of ²¹²Pb and ²²⁸Ac in the samples, and that of ²³⁸U was determined from the average concentrations of the ²¹⁴Pb and ²¹⁴Bi decay products. Thus, an accurate measurement of ²³²Th and ²³⁸U radiological concentrations was made, whereas a true measurement of ⁴⁰K concentration was achieved.

The ²³⁸U activity concentration was calculated from the mean value of 5 gamma transitions obtained from the photo peaks of ²³⁴Th (63.28 keV; 92.37 keV) ²¹⁴Pb (295.22 keV, 351.93 keV) and ²¹⁴Bi (609.31 keV ; 1120 keV; 1765 keV), ²¹⁰Pb (46.54 keV).

Each tabulated value for the ²³²Th series concentration was an average of six values obtained from the photo peaks of the ²¹²Pb (238.63 keV), ²²⁸Ac (209.25 keV 338.32 keV, 911.2 keV, 968.97 keV) and ²⁰⁸Tl (583.19 keV, 86.56 keV). The 1461 keV gamma of ⁴⁰K was used to determine the concentration of ⁴⁰K in different samples. ¹³⁷Cs (661.6 keV) ¹³⁴Cs (569.33 keV 604.72 keV, 795.86 keV) all radionuclides describe in Table 2-15.

Table 2- 15: Radionuclides which were measured in soil sample and also be found only natural radionuclides in background [Sch98].

| Nuclide to be determined | Nuclide measured | Energy in keV | Probability in % | Half-life time |
|--------------------------|------------------|---------------|------------------|---------------------------|
| U-238 | Th-234 | 63.28 | 4.1 | 2.445 × 10 ⁵ a |
| | Th-234 | 92.37 | 2.42 | |
| | Th-234 | 92.79 | 2.39 | |
| | Pa-234m | 766.37 | 0.316 | 1.17 m |
| Pa-234m | 1001.03 | 0.839 | | |
| Ra-226 | Ra-226 | 186.1 | 3.51 | 1600 a |
| | Pb-214 | 295.22 | 18.15 | 26.8 m |
| | | 351.93 | 35.1 | |
| | Bi-214 | 609.31 | 44.6 | 19.9 m |
| | | 1120.29 | 14.7 | |
| | | 1764.49 | 15.1 | |
| Pb-210 | Pb-210 | 46.54 | 4.25 | 22.3 a |
| Ra-228 | Ac-228 | 209.25 | 3.89 | 6.13 h |
| | Ac-228 | 338.32 | 11.27 | |
| | Ac-228 | 911.2 | 25.8 | |
| | Ac-228 | 968.97 | 15.8 | |
| Th-228 | Ra-224 | 240.99 | 4.1 | 3.66 d |
| | Pb-212 | 238.63 | 43.3 | 10.64 h |
| | | 300.09 | 3.28 | |
| | Tl-208 | 277.36 | 2.27 | 3.07 m |
| | | 583.19 | 30.4 | |
| | | 860.56 | 4.47 | |
| | | 2614.53 | 35.64 | |
| K-40 | K-40 | 1460.83 | 10.67 | 1.28 × 10 ⁹ a |
| Cs-137 | Cs-137 | 661.6 | 85.21 | 30 a |
| Cs-134 | Cs-134 | 569.33 | 15.39 | 2.062 a |
| | | 604.72 | 97.63 | |
| | | 795.86 | 85.4 | |

2.7 Experimental uncertainties

In order to comply with the ISO 17025 standard [ISO99] testing laboratories are obliged to estimate the uncertainty of their measurement results. The uncertainty budget used in laboratories engaged in gamma-ray spectrometric measurements usually includes uncertainties from counting statistics, nuclear decay data, the counting efficiency calibration, corrections for counting losses and sample quantity. The uncertainties of the sample properties do not enter the budget explicitly but via the uncertainty of the counting efficiency calibration and uncertainty of the specific activity for radionuclides in soil samples. Namely, the efficiency calibration curves are measured with calibrated samples which resemble the unknown samples as closely as possible. It is supposed that the uncertainties of the efficiency calibration curve introduced in the process of preparation of the calibration sample resemble the uncertainties in the process of the preparation of unknown samples. If this assumption not valid or if the efficiency calibration curves are calculated using a detector model, the uncertainties of the sample properties must explicitly enter the uncertainty budget. Frequently, the samples are prepared as homogeneous cylinders by pressing or pouring the sample material into cylindrical vial which, during counting,

is placed near the detector, coaxially along its symmetry axis. Such counting geometry can be described by the sample properties of sample radius, thickness, density and composition. It has been shown by Korun 2001 [Kor01] [NIST98], [ISO95], [mic99] the case of interest is where the quantity Y being measured, called the measured, is not measured directly, but is determined from N other quantities X_1, X_2, \dots, X_N through a functional relation f , often called the measurement equation:

$$Y=f(X_1, X_2, \dots, X_N) \quad (2- 6)$$

Included among the quantities X_i are corrections (or correction factors), as well as quantities that take into account other sources of variability, such as different observers, instruments, samples, laboratories, and times. Thus, the function f of equation (2.6) should express not simply a physical law but a measurement process, and in particular, it should contain all quantities that can contribute a significant uncertainty to the measurement result.

An estimate of the measurand or output quantity Y , denoted by y , is obtained from equation (2-2) using input estimates x_1, x_2, \dots, x_N for the values of the N input quantities X_1, X_2, \dots, X_N . Thus, the output estimate y , which is the result of the measurement, is given by

$$Y=f(x_1, x_2, \dots, x_N) \quad (2- 7)$$

In general, components of uncertainty may be categorized according to the method used to evaluate them.

Standard uncertainty: Type A :

An uncertainty component obtained by a Type A evaluation is represented by a statistically estimated standard deviation s_i , equal to the positive square root of the statistically estimated variance s_i^2 , and the associated number of degrees of freedom ν_i . For such a component the standard uncertainty is $u_i = s_i$.

Standard uncertainty: Type B

In a similar manner, an uncertainty component obtained by a Type B evaluation is represented by a quantity u_j , which may be considered an approximation to the corresponding standard deviation; it is equal to the positive square root of u_j^2 , which may be considered an approximation to the corresponding variance and which is obtained from an assumed probability distribution based on all the available information. Since the quantity u_j^2 is treated like a variance and u_j like a standard deviation, for such a component the standard uncertainty is simply u_j .

A Type A evaluation of standard uncertainty may be based on any valid statistical method for treating data. Examples are calculating the standard deviation of the mean of a series of independent observations; using the method of least squares to fit a curve to data in order to estimate the parameters of the curve and their standard deviations; and carrying out an analysis of variance in order to identify and quantify random effects in certain kinds of measurements.

Mean and standard deviation

As an example of a Type A evaluation, consider an input quantity X_i whose value is estimated from n independent observations $X_{i, k}$ of X_i obtained under the same conditions of measurement. In this case the input estimate x_i is usually the sample mean

$$x_i = \bar{X}_i = \frac{1}{n} \sum_{k=1}^n X_{i,k} \quad (2-8)$$

and the standard uncertainty $u(x_i)$ to be associated with x_i is the estimated standard deviation of the mean

$$u(x_i) = s(\bar{X}_i) \quad (2-9)$$

$$u(x_i) = \left(\frac{1}{n(n-1)} \sum \left(X_{i,k} - \bar{X}_i \right)^2 \right)^{1/2} \quad (2-10)$$

The Type B evaluation of standard uncertainty is the evaluation of the uncertainty associated with an estimate x_i of an input quantity X_i by means other than the statistical analysis of a series of observations. The standard uncertainty $u(x_i)$ is evaluated by scientific judgment based on all available information on the possible variability of X_i . Values belonging to this category may be derived from previous measurement data; experience with or general knowledge of the behavior and properties of relevant materials and instruments; manufacturer's specifications; data provided in calibration and other certificates; uncertainties assigned to reference data taken from handbooks.

Calculation of combined standard uncertainty:

If the input quantities X_i are not correlated, the combined standard uncertainties $u(y_k)$ associated with y_k are calculated by the law of uncertainty propagation as the positive square root of the combined variance $u^2(y_k)$:

$$u^2(y_k) = \sum_{i=1}^n \left(\frac{\partial G_k}{\partial x_i} \right)^2 \cdot u^2(x_i); \quad (k = 1, \dots, n) \quad (2-11)$$

If the input quantities X_i are not independent but correlated the combined standard uncertainty $u(y_k)$ has to be calculated according using covariances. If the partial derivatives are not explicitly available, they can be numerically sufficiently approximated by using the standard uncertainty $u(x_i)$ as increment of x_i :

$$\frac{\partial G_k}{\partial x_i} \approx \frac{i}{u(x_i)} \cdot (G_k(x_1, \dots, x_i + u(x_i)/2, \dots, x_m) - G_k(x_1, \dots, x_i - u(x_i)/2, \dots, x_m)) \quad (2-12)$$

The standard uncertainties for specific concentration generally have to be evaluated according to the ISO Guide well in accordance with guidelines of other international bodies. In the ISO Guide, uncertainties are evaluated either by statistical methods, (type A) or by, other means, (type B), i.e., by methods of conventional statistics or Bayesian statistics. Type A uncertainties can be evaluated from repeated or counting measurements, while Type B uncertainties cannot. They are for instance uncertainties given in certificates of standard

reference materials or of calibration radiation sources which are used in the evaluation of a measurement. The evident contradiction in using different types of statistics in the definitions of the two types of uncertainties was recently overcome by the establishment of a Bayesian theory of measurement uncertainty. In this theory, uncertainties are consistently determined. They quantitatively express the actual state of incomplete knowledge of the quantities involved.

The combined standard uncertainty of the measurement result y , designated by $u_c(y)$ and taken to represent the estimated standard deviation of the result, is the positive square root of the estimated variance $u_c^2(y)$ obtained from.

Used here a somewhat simplified model of the evaluation in order to keep equations short:

$$A(E_\gamma) = \frac{R_n}{I_\gamma(E_\gamma) \cdot \varepsilon(E_\gamma) \cdot M} \quad (2-13)$$

$$= \frac{NP}{t_c \cdot I_\gamma(E_\gamma) \cdot \varepsilon(E_\gamma) \cdot M} \quad (2-14)$$

| | |
|-------------------------|------------------------------------------|
| $A(E_\gamma)$ | specific activity in Bq kg ⁻¹ |
| R_n | count under full energy peak for sample |
| t_c | counting time in second |
| $I_\gamma(E_\gamma)$ | intensity of gamma |
| $\varepsilon(E_\gamma)$ | efficiency |
| M | sample mass in kg |
| NP | net count |

The combined standard uncertainty $u^2(A_s)$ associated with A_s is calculated by:

$$\begin{aligned} u^2(A_s) &= \left(\frac{I}{t_c \cdot I_\gamma(E_\gamma) \cdot \varepsilon(E_\gamma) \cdot M} \right)^2 \cdot u^2(NP) + \left(\frac{NP}{t_c^2 \cdot I_\gamma(E_\gamma) \cdot \varepsilon(E_\gamma) \cdot M} \right)^2 \cdot u^2(t_c) \\ &+ \left(\frac{NP}{t_c \cdot I_\gamma^2(E_\gamma) \cdot \varepsilon(E_\gamma) \cdot M} \right)^2 \cdot u^2(I_\gamma(E_\gamma)) + \left(\frac{NP}{t_c \cdot I_\gamma(E_\gamma) \cdot \varepsilon^2(E_\gamma) \cdot M} \right)^2 \cdot u^2(\varepsilon(E_\gamma)) \\ &+ \left(\frac{NP}{t_c \cdot I_\gamma(E_\gamma) \cdot \varepsilon(E_\gamma) \cdot M^2} \right)^2 \cdot u^2(M) \quad (2-15) \end{aligned}$$

$$u^2(A_s) = \left(\frac{NP}{t_c \cdot I_\gamma(E_\gamma) \cdot \varepsilon(E_\gamma) \cdot M} \right)^2 \cdot \frac{u^2(NP)}{(NP)^2} + \left(\frac{NP}{t_c \cdot I_\gamma(E_\gamma) \cdot \varepsilon(E_\gamma) \cdot M} \right)^2 \cdot \frac{u^2(t_c)}{t_c^2}$$

$$\begin{aligned}
& + \left(\frac{NP}{t_c \cdot I_\gamma(E_\gamma) \cdot \varepsilon(E_\gamma) \cdot M} \right)^2 \cdot \frac{u^2(I_\gamma(E_\gamma))}{I_\gamma^2(E_\gamma)} + \left(\frac{NP}{t_c \cdot I_\gamma(E_\gamma) \cdot \varepsilon(E_\gamma) \cdot M} \right)^2 \cdot \frac{u^2 \varepsilon(E_\gamma)}{(\varepsilon(E_\gamma))^2} \\
& + \left(\frac{NP}{t_c \cdot I_\gamma(E_\gamma) \cdot \varepsilon(E_\gamma) \cdot M} \right)^2 \cdot \frac{u^2}{M^2}
\end{aligned} \tag{2-16}$$

$$u^2(A_s) = \left(\frac{NP}{t_c \cdot I_\gamma(E_\gamma) \cdot \varepsilon(E_\gamma) \cdot M} \right)^2 \left\{ \frac{u^2(NP)}{(NP)^2} + \frac{u^2(t_c)}{(t_c)^2} + \frac{u^2 I_\gamma(E_\gamma)}{I_\gamma^2(E_\gamma)} + \frac{u^2 \varepsilon(E_\gamma)}{\varepsilon^2(E_\gamma)} + \frac{u^2(M)}{M^2} \right\} \tag{2-17}$$

We can get the relative uncertainties of input value.

$$\frac{u^2(A_s)}{A_s^2} = \frac{u^2(NP)}{(NP)^2} + \frac{u^2(t_c)}{(t_c)^2} + \frac{u^2 I_\gamma(E_\gamma)}{I_\gamma^2(E_\gamma)} + \frac{u^2 \varepsilon(E_\gamma)}{\varepsilon^2(E_\gamma)} + \frac{u^2(M)}{M^2} \tag{2-18}$$

Where

$$\frac{u(NP)}{(NP)} \text{ from spectra evaluation}$$

$$NP = NP + N_0 - N_0$$

where the NP is net peak and N_0 is counting of background

$$\begin{aligned}
u^2(NP) &= u^2(NP + N_0) + u^2(N_0) \\
&= u^2(NP) + u^2(N_0) + u^2(N_0) \\
&= u^2(NP) + 2 u^2(N_0)
\end{aligned}$$

Where $u^2(NP)$ is called variance and $u(NP)$ is the standard uncertainty

$$\frac{u(t_c)}{(t_c)} < 10^{-6} \text{ neglected}$$

$$\frac{u I_\gamma(E_\gamma)}{I_\gamma(E_\gamma)} \text{ from table of intensity of gamma ray [Fir96]}$$

$$\frac{u \varepsilon(E_\gamma)}{\varepsilon(E_\gamma)} = 2.5 \%$$

$$\frac{u(M)}{M} = 1-2 \%$$

we can used equation 2.18 to get the standard uncertainties for activity of soil samples or any environmental samples

2.8 Quality assurance including Ringversuch

Radioactivities in these natural samples are usually low and difficult to measure. The slightly increased activities in these samples from radioactive discharges are usually inseparable from natural variations, and it is essential to have a good quality control system for each radioanalytical laboratories to provide accurate results on these samples. Standards such as PTB [Sch98] has been used as general guidelines for laboratories to obtain reliable results in performing trace analysis. However, quality assurance is still an on-going challenge to analytical laboratories because both technical competence and quality management must be satisfied to generate accurate results Fig. 2-23 and Table 2 -16.

Quality assurance and quality control are essential components of environmental radioactivity measurements. Quality is integrated into sample preservation, field data and sample collection, sample transportation, and sample analysis.

Quality assurance, an integral part of environmental monitoring, requires systematic control of the processes involved in sampling the environment and in analyzing the samples. These procedures specify sampling protocol, sampling devices, and containers and preservatives to be used. Chain-of-custody procedures (used with all samples) are documented, and samples are controlled and protected from the point of collection to the generation of analytical results. Data generated from field sampling can be greatly influenced by the methods used to collect and transport the samples. A quality assurance program provides the procedures for proper sample collection so that the samples represent the conditions that exist in the environment at the time of sampling. The quality assurance program mandates compliance with written sampling procedures, use of clean sampling devices and containers, use of approved sample preservation techniques, and collection of field blanks, trip blanks, and duplicate samples. Chain-of-custody procedures are strictly followed to maintain sample integrity. In order to maintain sample integrity, samples are delivered to the laboratory as soon as practicable after collection.

Quality assurance to determine radionuclides in food and environmental samples ensures that the quality of data obtained is maintained at an adequate confidence level and is objectively evaluated. Quality assurance includes quality control, which involves all those actions by which the adequacy of equipment, instruments and procedures are assessed against established requirements. For the purpose of quality assurance, the following items must be ensured- (1) equipment and instruments function correctly, (2) procedures are correctly established and implemented, (3) analysis are correctly performed, (4) errors are limited (5) records are correctly and promptly maintained, (6) the required accuracy of measurements is maintained and (7) systematic errors do not arise.

In general, the design of a quality assurance program should take the following factors into account:

- a. quality of equipment and instruments,
- b. training and experience of personnel,
- c. verification of procedures by the routine analysis of control samples and the use of standard methods for analysis,
- d. frequency of calibration and maintenance of equipment and instruments (variability in the measuring system is an important aspect of this),
- e. the need for traceability of the results of determinations to a national standard.

It is important to have each item of the quality assurance program established. Intercomparison is also necessary to generally evaluate the quality assurance of the

determinations. By this process, it is possible for data to be compared between laboratories or within a laboratory at different times.

The concept of "quality control" should be discussed in general comparison with that of the concept of "quality assurance." The basic concept of quality assurance is that quality should be assured comprehensively and wholly from the beginning to the end of a fixed volume of successive procedures. It assures that whole data acquired by using the fixed volume come to have a significant result to meet intended objectives. On the other hand, quality control is related only to definite and practical control of respective procedures, and is limited to only some portions of those procedures.

The scope of quality assurance is extended from one laboratory, to a group of laboratories in a region, then on to those in a country, and then to international groups of laboratories. The wider the scope of subjects to be assured the more effective the quality assurance. A smaller scope can be utilized as part of a larger one this means that more effects are found in scopes of quality assurance in ascending order from a single laboratory to a region, a country, a continent, and to the whole world.

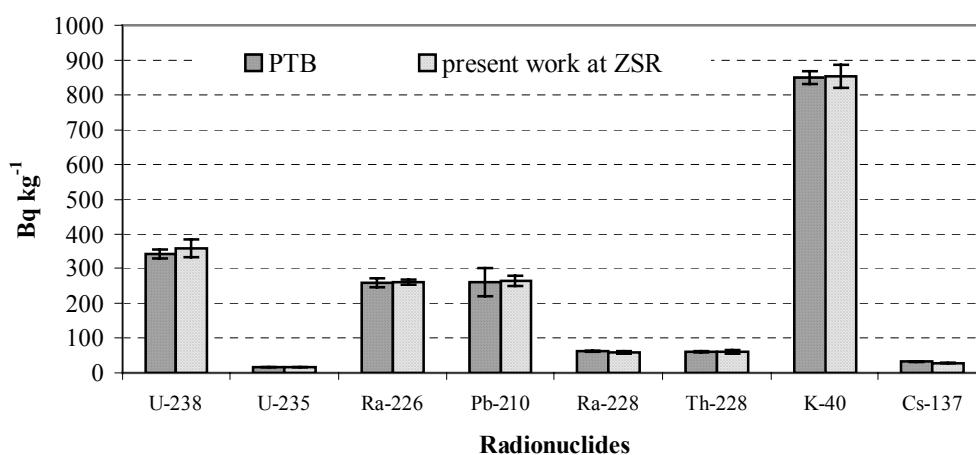


Fig. 2-23 : Comparison between radionuclides (Bq kg⁻¹) in soil sample (ST-27/1998 Ringversuch) measured by PTB and present work at ZSR

Table 2- 16 : The values of radionuclides (Bq kg^{-1}) in soil sample (ST-27/1998 Ringversuch) by PTB and present work at ZSR

| Radionuclide | PTB Bq kg^{-1} | present work Bq kg^{-1} |
|--------------|----------------------------|-------------------------------------|
| U-238 | 340 ± 13 | 357.9 ± 25.8 |
| U-235 | 16.3 ± 0.7 | 16.5 ± 0.03 |
| Ra-226 | 258 ± 13 | 260.5 ± 7.5 |
| Pb-210 | 260 ± 40 | 264 ± 14 |
| Ra-228 | 62.4 ± 2.1 | 59.12 ± 3.5 |
| Th-228 | 60.6 ± 1.8 | 59.7 ± 5.4 |
| K-40 | 850 ± 19 | 853 ± 3.3 |
| Cs-137 | 32.5 ± 1.2 | 28.2 ± 1.0 |

2.9 Characteristic limits

Errors in radioactivity measurements are attributable to (a) the random nature of radioactive decay, (b) lack of instrument sensitivity or stability, (c) inaccuracies in the calibration radionuclide standards and the calibration procedures, (d) uncertainties in the decay properties of the radionuclides, and (e) other errors such as those due to variations in source positioning or geometry. Because of the stability of many modern instruments, the errors resulting from their used are essentially those associated with the random nature of the decay process itself. Such errors can be estimated with the relatively simple statistical treatment, but estimation of total error requires many repeated measurements and consideration of possible sources of systematic errors, such as may be due to c, d, and e.

Most counting instruments are calibrated by reference to standard sources having known error limits, which must be incorporated into the overall error. Refinements in knowledge of the radionuclide decay schemes may involve significant changes in the branching fractions and emission energies and change the uncertainties in the amounts of radionuclides determined. Errors associated with these latter uncertainties are usually, but not always, small.

Detection limit requirements for analytical procedures and measurements are not easily determined. Although limiting doses and concentrations recommended by advisory groups indicate such limits, regulatory bodies and public concern are now requiring operation below these standards. These techniques require large samples, high efficiency detectors, low background shielding, and long counting times. At such low counting rates, counting statistics become extremely important.

Without a detailed mathematical foundation of Bayesian characteristic limits, which may be found elsewhere, we can now define the characteristic limits for a non-negative measurand Y which is a concentration of an element or an activity of a radionuclide in a sample. The true value η is zero if the element or the radionuclide is not present. Let y be the estimate of the true value η of the measurand Y with the associated standard uncertainty $u(y)$. The decision threshold and the detection limit are defined on the basis of statistical test testing the null hypothesis $H_0: \eta = 0$ against the alternative hypothesis $H_1: \eta > 0$.

A decision quantity Y has to be attributed to the measurand which being a random variable is likewise an estimator of the measurand. It is postulated that the expectation $E(Y)$ of the

decision quantity Y is equal to the true value of the measured. A value y of the estimator Y derived from measurements is an estimate of the measurand. As a result of the measurement, y and its standard uncertainty $u(y)$ are derived according to the ISO Guide [ISO93] as a complete results of the measurement. Y and $u(y)$ have to be derived by evaluation of measured quantities and of other information by way of a mathematical model which takes into account all relevant quantities. Generally, it will not be explicitly made use of the fact that the measured is non-negative. Therefore, y may become negative, in particular, if the true value of the measured is close to zero.

For the determination of the decision threshold and the detection limit, the standard uncertainty of the decision quantity has to be calculated if possible as a function $\tilde{u}(\eta)$ of the true value η of the measurand.

Then, the decision threshold y^* is a characteristic limit which when exceeded by a result y of a measurement one decides that the element or radionuclide is present in the sample. If $y = y^*$ the null hypothesis, $H_0: \eta = 0$, cannot be rejected and one decides that the element or radionuclide is not found in this sample. If this decision rule is observed, a wrong acceptance of the alternative hypothesis, $H_1: \eta > 0$, occurs with the probability α which is the probability of the error of the first kind of the statistical test used. The decision threshold is given by

$$y^* = k_{1-\alpha} \cdot \tilde{u}(0) \quad (2-19)$$

with $k_{1-\alpha}$ being the $(1-\alpha)$ quantile of the standardized normal distribution. $\tilde{u}(0)$ is the uncertainty associated with the measurand if its true value equals zero. If the approximation $\tilde{u}(\eta=0) = u(y)$ is sufficient, one gets

$$y^* = k_{1-\alpha} \cdot u(y) \quad (2-20)$$

The detection limit η^* is the smallest true value of the measurand detectable with the measuring method. It is sufficiently larger than the decision threshold that the probability of an error of second kind is equal to β . The detection limit is given by

$$\eta^* = y^* + k_{1-\beta} \cdot \tilde{u}(\eta^*) \quad (2-21)$$

with $k_{1-\beta}$ being $(1-\beta)$ -quantile of the standardized normal distribution. $\tilde{u}(\eta^*)$ is the uncertainty associated with the measurand if its true value equals the detection limit η^* . Equation (14) is an implicit one. The detection limit can be calculated from it by iteration using for example the starting approximation $\eta^* = 2 \cdot y^*$

For the numerical calculation of the decision threshold and the detection limit the function $\tilde{u}(\eta)$ is needed which gives the standard uncertainty of the decision quantity as function of the (true) value η of the measurand. This function generally has to be determined in the course of the evaluation of the measurement according to the ISO Guide. Often this function is only slowly increasing. Therefore it is justified in many cases to use the approximation $\tilde{u}(\eta) = u(y)$. If the approximation $\tilde{u}(\eta) = u(y)$ is sufficient for all true values η , then $\eta^* = (k_{1-\alpha} + k_{1-\beta}) \cdot u(y)$ is valid. This applies in particular if the primary estimate y of the measurand is not much larger than its standard uncertainty $u(y)$. Frequently, the value of y is calculated as the difference (net effect) of two quantities of approximately equal size with x_1 being the gross effect and x_0 being

the background or blank effect, both obtained from independent measurements. In this case of $y = x_1 \cdot x_0$ one gets $\tilde{u}^2(\eta) = u^2(x_1) + u^2(x_0)$ with the standard uncertainties $u(x_1)$ and $u(x_0)$ of x_1 and x_0 , respectively. From this, one obtains $\tilde{u}^2(0) = 2 \cdot u^2(x_0)$. If only $\tilde{u}^2(0)$ and $u(y)$ are known, the approximation by linear interpolation according to Eq. (15) is often sufficient for $y > 0$:

$$\tilde{u}^2(\eta) = \tilde{u}^2(0) \cdot (1 - \eta/y) + u^2(y) \cdot \eta/y \quad (2-22)$$

In many practical cases $\tilde{u}^2(\eta)$ is a slowly increasing linear function of η . This justifies the approximations above, in particular, the linear interpolation of $\tilde{u}^2(\eta)$ instead of $\tilde{u}(\eta)$, itself.

With the interpolation formula according to Eq. (2.22) one gets the approximation

$$\eta = a + \sqrt{a^2 + (k_{1-\beta}^2 - k_{1-\alpha}^2) \cdot \tilde{u}^2(0)} \quad (2-23)$$

with

$$a = k_{1-\alpha} \cdot u(0) + \frac{1}{2} (k_{1-\beta}^2 / y) \cdot (u^2(y) \cdot \tilde{u}^2(0))$$

For $\alpha = \beta$ one receives $\eta^* = 2a$

The confidence interval includes for a result y of a measurement which exceeds the decision threshold y^* the true value of the measurand with a probability $1 - \gamma$. It is enclosed by the lower and upper limit of the confidence interval, respectively η_l and η_u , according to

$$\eta_l = y - k_p \cdot u(y) \quad \text{with} \quad p = \omega \cdot (1 - \gamma/2) \quad (2-24)$$

$$\eta_u = y - k_q \cdot u(y) \quad \text{with} \quad q = 1 - \omega \cdot \gamma/2 \quad (2-25)$$

$$\omega = \frac{1}{\sqrt{2\pi}} \int_{-\infty}^{y/u(y)} \exp(-z^2/2) dz = \Phi(y/u(y)) \quad (2-26)$$

Values of the function $\Phi(t)$, which is the distribution function of the standardized normal distribution, as well as the quantiles k_p of the standardized normal distribution are tabulated. The confidence limits are not symmetrical around the values y .

But, for $y \gg u(y)$ the well known formula

$$\eta_{l,u} = y \pm k_{1-\gamma/2} \cdot u(y) \quad (2-27)$$

is valid as an approximation. Equation (2-27) is applicable if $y > \approx 2 \cdot k_{1-\gamma/2} \cdot u(y)$.

3 Analysis of radionuclides in soils

The main purpose of the present work is to quantify the concentration values of natural radionuclides ^{238}U , ^{226}Ra , ^{210}Pb , ^{235}U , ^{40}K , ^{228}Ra , ^{228}Th , and ^{232}Th and artificial radionuclides ^{137}Cs and ^{134}Cs (deposition densities), and their activity ratio (element correlation, radioactive equilibrium and disequilibrium) in different depths profiles and surface soil samples obtained from Germany (Lower Saxony and North Rhine-Westphalia) and Ukraine (see Figs 2-1, 2-3, and 2-4) which were studied by the laboratory HPGe-spectrometry at ZSR. To calculate specific activity was used eq. (2-5) for all radionuclides in table (2-15) in chapter 2.

The specific activity (in Bq kg^{-1}), $A_{E_{\gamma_i}}$ of a radionuclide i and for a peak at energy E_{γ} , is given by:

$$A_{E_{\gamma_i}} = \frac{NP}{t_c \cdot I_{\gamma}(E_{\gamma}) \cdot \varepsilon(E_{\gamma}) \cdot M} \quad (3 - 1)$$

where NP is the number of counts in a given peak area corrected for background peaks of a peak at energy E_{γ} , $\varepsilon(E_{\gamma})$ the detection efficiency at energy E_{γ} , t is the counting lifetime, $I_{\gamma}(E_{\gamma})$ the number of gammas per disintegration of this nuclide for a transition at energy E , and M the mass in kg of the measured sample.

3.1 Concentration of artificial radionuclides in depth profile and surface

After the Chernobyl accident in 1986 and in some subsequent years the regional distribution of the Chernobyl contamination was estimated by ^{134}Cs and ^{137}Cs in soils of the northern hemisphere. Since ^{137}Cs remained the only important gamma-emitter, the in-situ HPGe spectrometer could be used as a simpler and more efficient instrument to measure the initial regional distribution of the Chernobyl deposition in investigation locations like Germany and Ukraine. To describe the vertical distribution of ^{137}Cs one has to know the total inventory. The total ^{137}Cs areal activity (Bq m^{-2}) of a sampling point was calculated as follows:

$$^{137}\text{Cs}_{\text{aa}} = \sum_{i=1}^z C_i \cdot \text{BD}_i \cdot \text{DI}_i \cdot (100)^2 \quad (3 - 2)$$

with $^{137}\text{Cs}_{\text{aa}}$ = total ^{137}Cs areal activity (Bq m^{-2}) for all depths, I = sampling depth, z = maximum number of sample depths with detectable ^{137}Cs , C_i = activity concentration per unit mass (Bq kg^{-1}) for depth i , BD_i = bulk density (g cm^{-3}) for depth I , DI_i = depth increment (1, 2, 5, ...cm) for sample i ,

According to eq. (3-2) ^{137}Cs the calculate areal activity is strongly affected by changes of soil bulk density (BD), and it is important to decrease this effect. Because BD increased significantly with the age of the pasture, due to soil compaction by trampling and erosion [Gar95], total ^{137}Cs areal activity was corrected by a factor derived from the differences in soil bulk density.

$$A_{(0)} = A_{(t)} e^{0.693 \cdot t / T_{1/2}} \quad (3 - 3)$$

$$A_{\text{Chernobyl}} = A_{\text{measured}} e^{0.693 \cdot t / 30.2} \quad (3 - 4)$$

$A_{(0)}$ is the activity of radionuclide at $t = 0$ (Chernobyl accident 26.04.1986), $A_{(t)}$ is the activity of radionuclide after time t , t is the time between Chernobyl accident and measuring time, $T_{1/2}$ is the half live time of radionuclide ($^{137}\text{Cs} = 30.2 \text{ a}$).

The results were decay corrected to the date Chernobyl accident (26.04.1986). All uncertainties are named and uncertainties according to [Iso95] and if the results measured were below the decision threshold they are named “nd” in the all tables and were measured these samples for 7 days and we did not find ^{137}Cs in all depth profile samples under 50 cm and all of the detected ^{137}Cs occurred within the top 50 cm at all depth profiles under investigation. All results of specific activities are expressed on the dry weight bases in Bq kg^{-1} . The areal concentrations of ^{137}Cs calculated for each sampling sites are reported in Bq m^{-2} .

This work presents the results of a study of the concentration of ^{137}Cs in the depth profile and surface soil samples from different sites, Germany (Lower Saxony and Lippe, NRW) and Ukraine (See Figs 2-1, 2-2, 2-3).

3.1.1 ^{137}Cs concentration in depth profile soil samples from Lower Saxony, North Germany.

The results of specific activities of ^{137}Cs in different geometries (bottles 1-l and Marinelli beaker) and activities of layers for the soil profiles from 8 depth profiles soil from different sites in Lower Saxony, North Germany are given in Tables 3-1 to 3-4, and Tables B-1 to B-4 and Figs. 3-1 to 3 - 4 in appendix B show the concentration vertical profiles of ^{137}Cs in a soil profile. The depth distribution of ^{137}Cs for field sites (Klein Lobke, and Twenge in Lower Saxony) shown in Figs 3-1 and 3-2. The physical and chemical characteristics of the soils were analysed according to [Tho03] and are summarized in Tables 3-3 and 3-5 and Tables B-1 to B-7 in appendix B. The assessment of the values obtained was done according to the German taxonomy.

Table 3 - 1: Activity concentration of ^{137}Cs [Bq kg^{-1}] in different geometry and activity concentration of layers [Bq m^{-2}] in profile samples from Klein Lobke (field), North Germany. The numbers in parentheses give the fraction of ^{137}Cs observed in the layer.

| Depth [cm] | Dry density [g cm^{-3}] | Activity concentration (Bottle) | Marinelli Beaker | | |
|------------|------------------------------------|---------------------------------|------------------------|-------------------|---------------------|
| | | | Activity concentration | Activity of layer | |
| | | | | 01.09.1999 | 26.04.1986 |
| 0-15 | 1.28 | 13 ± 0.5 | 12 ± 0.4 | 2277 ± 4 | 3089 ± 5 (31 %) |
| 15-30 | 1.25 | 13 ± 0.5 | 12 ± 0.4 | 2209 ± 4 | 2996 ± 5 (30 %) |
| 30-40 | 1.18 | 13 ± 0.5 | 11 ± 0.4 | 1304 ± 2 | 1769 ± 3 (18 %) |
| 40-50 | 1.25 | 13 ± 0.5 | 11 ± 0.4 | 1398 ± 3 | 1896 ± 3 (19 %) |
| 50-70 | 1.48 | 0.5 ± 0.1 | 1.4 ± 0.1 | 136 ± 6 | 184 ± 8 (2 %) |
| 70-90 | 1.27 | nd | nd | nd | nd |
| 90-105 | 1.36 | nd | nd | nd | nd |
| 105-130 | 1.24 | nd | nd | nd | nd |
| 130-150 | 1.27 | nd | nd | nd | nd |
| 150-200 | 1.29 | nd | nd | nd | nd |
| 200-250 | 1.35 | nd | nd | nd | nd |

The ^{137}Cs activity concentration value (Table 3-1) at the surface are $13 \pm 0.5 \text{ Bq kg}^{-1}$ in bottle and $12 \pm 0.4 \text{ Bq kg}^{-1}$ in marinelli beaker but in deepest layer 50 -70 cm we found ^{137}Cs value are $1.4 \pm 0.1 \text{ Bq kg}^{-1}$. The ^{137}Cs distributions within the soil profile in Table 3-1 we can see that the ^{137}Cs values ranged 136 ± 6 and $2277 \pm 4 \text{ Bq m}^{-2}$ referred to measuring date and corrected for Chernobyl accident the ^{137}Cs value 184 ± 8 and $3089 \pm 5 \text{ Bq m}^{-2}$, we can see also that the highest activity of ^{137}Cs in the top layer 0-15 cm is 31 % of the total activity in the soil and 2% of the total activity in the soil in the deepest layer. The ^{137}Cs found, was quite equally distributed throughout the plough layer due to cultivated practices the plough layer is about 30 cm [Nou03].

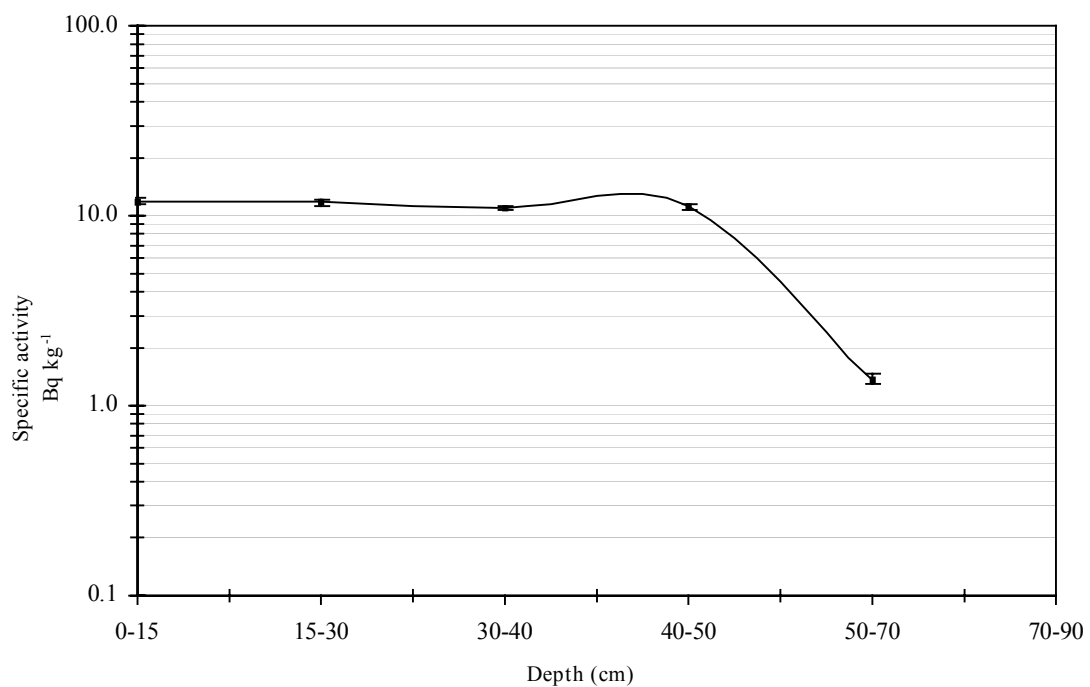


Fig. 3-1: Depth distribution of ^{137}Cs [Bq kg^{-1}] in soil profile from Klein Lobke, North Germany

Table 3 – 2: Activity concentration of ^{137}Cs [Bq kg^{-1}] in different geometry and activity concentration of layers [Bq m^{-2}] in profile samples from Twenge (field), Lower Saxony, North Germany. The numbers in parentheses give the fraction of ^{137}Cs observed in the layer

| Depth [cm] | Dry density [g cm^{-3}] | Activity concentration (Bottle) | Marinelli Beaker | | |
|------------|------------------------------------|---------------------------------|------------------------|-------------------|-----------------------|
| | | | Activity concentration | Activity of layer | |
| | | | | 01.09.1999 | 01.09.1999 |
| 0-15 | 1.346 | 13 ± 0.5 | 13.1 ± 0.43 | 2640 ± 4 | 3581 ± 6 (46.7 %) |
| 15-30 | 1.380 | 12 ± 0.4 | 12.1 ± 0.4 | 2506 ± 4 | 3398 ± 6 (44.4 %) |
| 30-40 | 1.372 | 3 ± 0.1 | 3.3 ± 0.12 | 457 ± 3 | 620 ± 4 (8.1 %) |
| 40-50 | 1.290 | 0.07 ± 0.03 | 0.1 ± 0.02 | 12 ± 3 | 16 ± 3 (0.2 %) |
| 50-60 | 1.382 | nd | 0.06 ± 0.01 | 8 ± 3 | 10 ± 4 (0.14 %) |
| 60-75 | 1.304 | nd | 0.02 ± 0.01 | 4 ± 4 | 6 ± 5 (0.07 %) |
| 75-100 | 1.464 | nd | 0.06 ± 0.01 | 21 ± 8 | 29 ± 11 (0.37 %) |
| 100-125 | 1.683 | nd | 0.0042 ± 0.0076 | 1.8 ± 8 | 2 ± 11 (0.03 %) |
| 125-150 | 1.746 | nd | nd | nd | nd |

The ^{137}Cs distributions within the soil profile in Table 3-2, we can see that the ^{137}Cs values ranged 1.8 ± 8 and $2640 \pm 4 \text{ Bq m}^{-2}$ referred to measuring date and corrected for Chernobyl accident the ^{137}Cs value 2 ± 11 and $3581 \pm 6 \text{ Bq m}^{-2}$, we can see also that the highest activity of ^{137}Cs in the top layer 0-15 cm is 46 % of the total activity in the soil and 0.03 % of the total activity in the soil in the deepest layer, 100-125 cm, we found ^{137}Cs in marinelli beaker $0.0042 \pm 0.0076 \text{ Bq kg}^{-1}$ this value less than detection limit, and was measured 7 days.

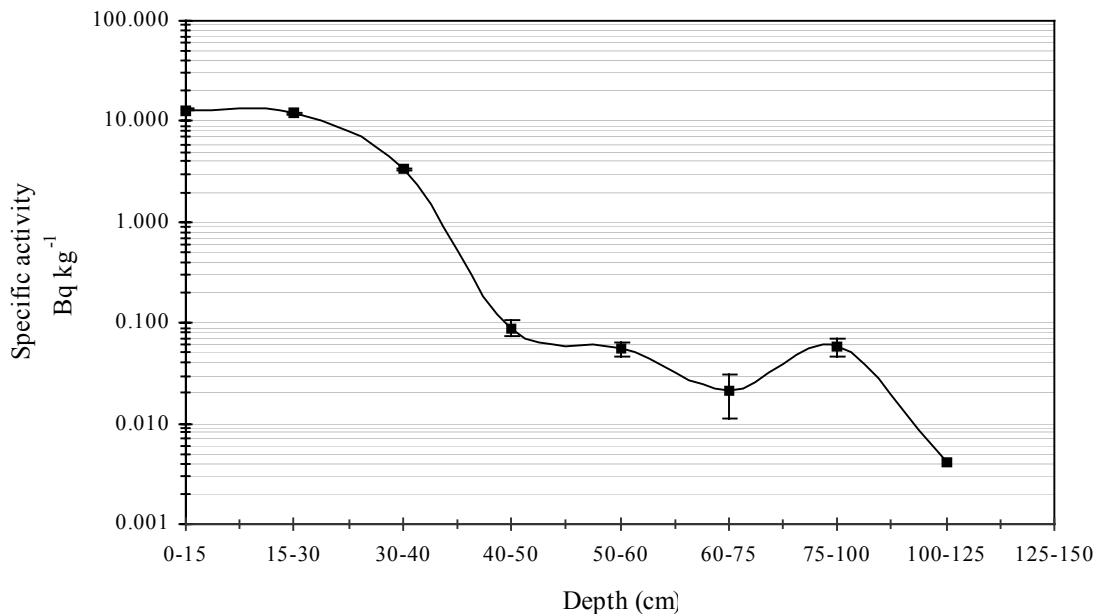


Fig. 3-2: Depth distribution of ^{137}Cs [Bq kg^{-1}] in soil profile from Twenge, (field) North Germany.

The depth distribution of anthropogenic ^{137}Cs is influenced initially by the type of management of the soil (agricultural or forested/never cultivated). Figure 3-2 -3-3 shows the distributions of ^{137}Cs from a tilled agricultural soil and a never-cultivated forested profile from Twenge and Eileniede, respectively.

Table 3 – 3: Data of the specimen place “acre Twenge”

| specimen interval cm | horizon German [9] | horizon FAO | texture | characteristics | sand % | silt % | clay % |
|----------------------|--------------------|-------------|-----------------------------|--------------------------------------------------------------------------------------------------------------------------------------------------------------------------------------------|--------|--------|--------|
| 0-15 | Ap | Ap | fine sand medium sand | wownish black, medium humus, minor compactness of the packing coherent structure rownish black, humus , minor compactness of the packing, coherent structures, charcoal and clay bricks | 88.7 | 6 | 5.3 |
| 15-30 | | | | | | | |
| 30-40 | | | | | | | |
| 40-50 | E | E | | | 86.2 | 8.7 | 5.1 |
| 50-60 | fAe | Bh (Abh) | medium sand fine sandy | dark rust-coloured brown, weak humus, middle compactness of the packing | n.b. | n.b. | n.b. |
| 60-75 | Bs/Bhs | | | rust-coloured brown, middle compactness of the packing | 89.1 | 5.9 | 4.1 |
| 75-100 | Bs | Bl | medium sand | yellow gray, weak iron blotched, middle compactness of the packing | 91.0 | 4.9 | 4.1 |
| 100-125 | Go | Bc2 | medium sand coarse sandy | in nutty aggregates silt sandy, yellow gray, in nutty aggregates gray, weak iron blotched, middle com pactness of the packing | 95.3 | 3.0 | 1.7 |
| 125-150 | | | medium sand | weak pebbly, yellow gray, weak iron blotched, mid dle compactness of the packing | 99.5 | 0.5 | 0 |

The ^{137}Cs distribution in the agricultural soil is an indicator of the depth of tillage as the tilled layer becomes homogenized due to annually ploughing (Fig. 3-2). However, the effective depth of tillage can also be indicating a deposition of redistributed soil materials if the depth of the layer is greater than the depth the plough can attain. There is a deepening of the plough layer due to annual deposition of eroded soil materials from upper slope positions. After implementing conservation management practices, the ^{137}Cs distribution with depth is only altered in the top 3 or 4 cm of the profile, which is a function of the lack of erosion influenced by soil stability, annual additions of soil organic matter to the surface.

The distribution of ^{137}Cs in the forest soil shows the migration in this soils seems to be much faster with depth (Fig. 3-3). However the distribution in the top 30 cm or so is influenced, at least partially by the soil organic matter decomposition cycle, biopedoturbation from agents such as earthworms and possibly ^{137}Cs leaching, in which there is some homogenization of the ^{137}Cs with soil depth [Van99].

Table 3 – 4: Activity concentration of ^{137}Cs [Bq kg^{-1}] in different geometry and activity concentration of layers [Bq m^{-2}] in profile samples from Eilenriede (Forest), North Germany. The numbers in parentheses give the fraction of ^{137}Cs observed in the layer

| Depth [cm] | Dry density [g cm^{-3}] | Activity concentration (Bottle) | Marinelli Beaker | | |
|------------|------------------------------------|---------------------------------|------------------------|-------------------|-----------------------|
| | | | Activity concentration | Activity of layer | |
| | | | | 01.09.1999 | 01.09.1999 |
| 0-10 | 1.133 | 48.4 ± 1.6 | 44 ± 1.4 | 4950 ± 3 | 6713 ± 4 (87.1 %) |
| 10-20 | 1.286 | 5.3 ± 0.2 | 5 ± 0.2 | 600 ± 3 | 814 ± 3 (10.6 %) |
| 20-30 | 1.334 | 0.7 ± 0.1 | 0.4 ± 0.04 | 55 ± 3 | 74 ± 4 (0.9 %) |
| 30-40 | 1.407 | 0.6 ± 0.04 | 0.5 ± 0.03 | 63 ± 3 | 86 ± 4 (1.1 %) |
| 40-50 | 1.349 | 0.2 ± 0.03 | 0.1 ± 0.01 | 13 ± 3 | 18 ± 4 (0.3 %) |
| 50-70 | 1.373 | nd | nd | nd | nd |
| 70-100 | 1.356 | nd | nd | nd | nd |
| 100-120 | 1.536 | nd | nd | nd | nd |

The total ^{137}Cs activities in the various layers of the forest soil found in soil to a depth of 0-10 cm (Fig. 3-3). About 87.1% of the total ^{137}Cs activity in the soil. In the 10-20 cm layer, about 10.6 % of the total ^{137}Cs activity was found in the soil, and we can see that the in the Table 3-2, activity of layer ranged 13 ± 3 to $4950 \pm 3 \text{ Bq m}^{-2}$ for measuring time and also ranged 18 ± 4 to $6713 \pm 4 \text{ Bq m}^{-2}$ for Chernobyl accident. Usually the more humus, the more ^{137}Cs . This correlation to some extent seems to be misleading as both ^{137}Cs and hums contents tend to decrease with depth. On the other hand, according to many authors, [Vin03, Van99, Car03], humus is conduce to ^{137}Cs sorption in soil.

Table 3 – 5: Data of the specimen place “forest Eilenriede”

| specimen interval cm | horizon German [9] | horizon FAO | texture | characteristics | sand % | silt % | clay % |
|----------------------|--------------------|-------------|-------------------------------------------------------------------------------------------------|-----------------------------------------------------------------------------------------------|--------|--------|--------|
| 1 | L | Oi | leave mulch | | | | |
| 1 | Of | Oa | | | | | |
| 0-10 | Aeh | Ah | coarse sandy medium sand | greatly weak pebbly and stony. Brownish gray. Medium humus, middle compactness of the packing | 97.7 | | |
| 10-20 | Aeh | | medium clay sand. Greatly weak pebbly and stony | brown gray, medium humus, middle compactness of the packing | 76.1 | 13.4 | 10.5 |
| 20-30 | Ah-Go | | yellow brown, greatly weak humus, greatly weak iron blotched, middle compactness of the packing | 80.3 | 12.0 | 7.7 | |
| 30-40 | | B1 | | | | | |
| 40-50 | Go-Sw | | gray yellow, weak iron blotched, middle compactness of the packing | 83.8 | 8.8 | 7.4 | |
| 50-70 | Go-Swd | B2 | coarse sandy medium sand | Marmorate, medium iron blotched, high compactness of the packing | 97.4 | | |
| 70-100 | | | | | 97.3 | | |
| 100-150 | Gro | | sandy clay loam | greatly weak pebbly and stony, gray, weak iron blotched, middle compactness of the packing | 72.8 | 14.0 | 13.3 |

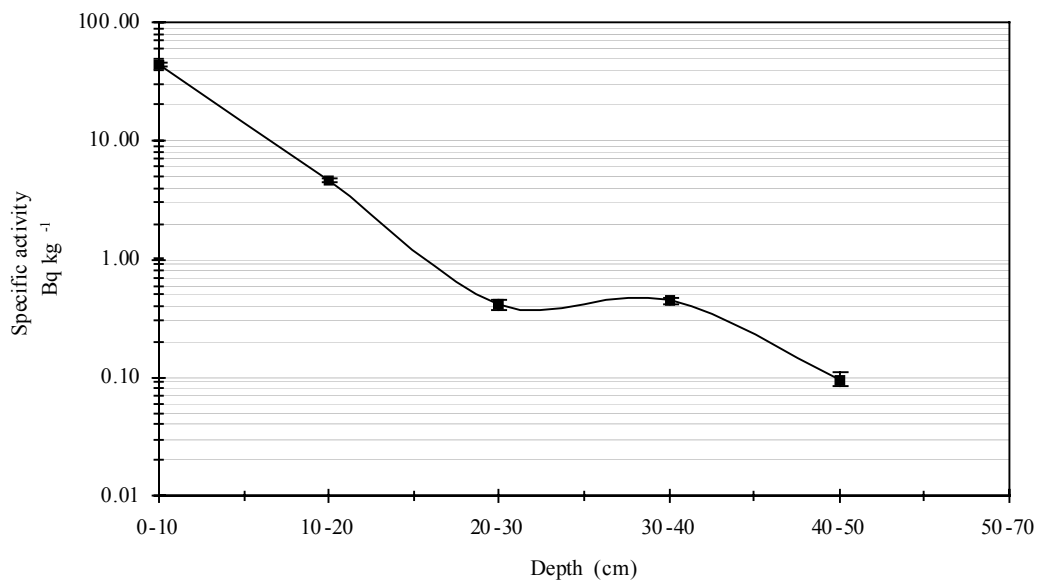


Fig. 3-3: Depth distribution of ^{137}Cs [Bq kg^{-1}] in soil profile from Eilenriede, Lower Saxony, North Germany.

In soil surfaces, Caesium has low mobility in comparison to other metals and usually does not migrate below a depth of 40 cm. The majority portion of caesium is retained in the upper 20 cm of the soil surface [Kor98; Rus00; Tak98]. Vertical migration patterns of ^{137}Cs in four agricultural soils from southern Chile indicated that approximately 90% of the applied caesium was retained in the top 40 cm of soil, and that in one soil, essentially 100% was bound in the upper 10 cm. Migration rates of radiocaesium were derived from the depth distribution profiles and were in the range of 0.11 to 0.29 cm/year [Sch02], [Chi99].

Other studies have reported that clay and zeolite minerals strongly bind caesium cations and can therefore reduce the bioavailability of caesium and the uptake in plants by irreversibly binding caesium in interlayer positions of the clay particles [Paa99].

Soils rich in organic matter adsorb caesium, but the caesium adsorbed in the organic fraction is readily exchangeable and highly available for plant uptake [San99]. Regions in Venezuela, Brazil, and Russia have been identified where a great deal of rain is encountered, the soil is peaty or podzolic (a type of forest soil characterized by high leachability) , and the mobility of caesium is considerably greater than in other soils [LaB96].

Soils rich in organic matter adsorb caesium, but the caesium adsorbed in the organic fraction is readily exchangeable and highly available for plant uptake [San99]. Regions in Venezuela, Brazil, and Russia have been identified where a great deal of rain is encountered, the soil is peaty or podzolic (a type of forest soil characterized by high leachability) , and the mobility of caesium is considerably greater than in other soils [LaB96].

Table 3 – 6: Activity concentration of ^{137}Cs [Bq kg^{-1}] in different geometry and activity concentration of layers [Bq m^{-2}] in profile samples from Neßmerpolder (meadow), North Germany

| Depth (cm) | Dry density [g cm^{-3}] | Activity concentration | Activity of layer | |
|------------|------------------------------------|------------------------|-------------------|----------------------|
| | | | 01.04.2002 | 26.04.1986 |
| 0-1 | 1.00 | 16 ± 0.6 | 164 ± 9 | 322 ± 18 (7 %) |
| 1-2 | 0.98 | 20 ± 0.7 | 194 ± 13 | 380 ± 26 (8 %) |
| 2-3 | 1.05 | 21 ± 0.7 | 223 ± 15 | 436 ± 29 (9 %) |
| 3-5 | 1.04 | 23 ± 0.7 | 482 ± 19 | 945 ± 35 (20 %) |
| 5-10 | 1.11 | 15 ± 0.5 | 833 ± 8 | 1632 ± 15 (34 %) |
| 10-15 | 1.15 | 7 ± 0.3 | 404 ± 2 | 791 ± 4 (16 %) |
| 15-20 | 1.16 | 3 ± 0.1 | 177 ± 0.4 | 347 ± 1 (7 %) |
| 20-25 | 1.23 | 2 ± 0.1 | 110 ± 0.2 | 215 ± 0.4 (4 %) |
| 25-30 | 1.29 | 1 ± 0.1 | 42 ± 0.1 | 82 ± 0.1 (2 %) |

Caesium distribution within the soil profiles are shown in Fig. 3-4. All of the detected ^{137}Cs occurred within the topmost 0-1, 1-2, and 2-3 cm at Neßmerpolder, concentrations in the near surface ranged 15 ± 0.5 – 23 ± 0.7 Bq kg^{-1} of soil Table 3-4. Disturbance by burrowing animals probably caused the animals incorporation of ^{137}Cs at Neßmerpolder, Ricklingen and Vestrup, Lower Saxony, Germany. The soil at Neßmerpolder had 24 % of ^{137}Cs inventory confined to the first interval (0-3 cm) but showed some ^{137}Cs activity in the 3-5 to 5-10 cm increment. Penetration may occur during heavy rainfall events when water containing ^{137}Cs adsorbed on suspended soil particles flow into the soil profile. Such a flow occurs in sandy soil with large pores or in clayey soils that have deep cracks that open seasonally [Arn89].

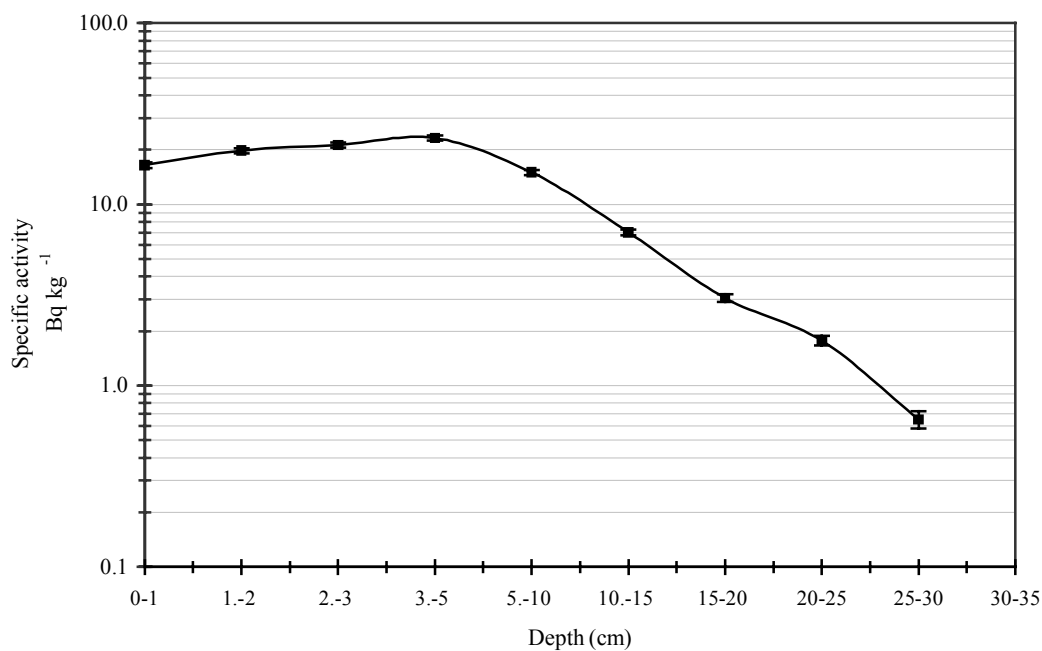


Fig. 3-4: Depth distribution of ^{137}Cs [Bq kg $^{-1}$] in soil profile from Neßmerpolder, (meadow), North Germany.

3.1.1.1 ^{137}Cs deposition densities in soil samples from Lower Saxony, North Germany.

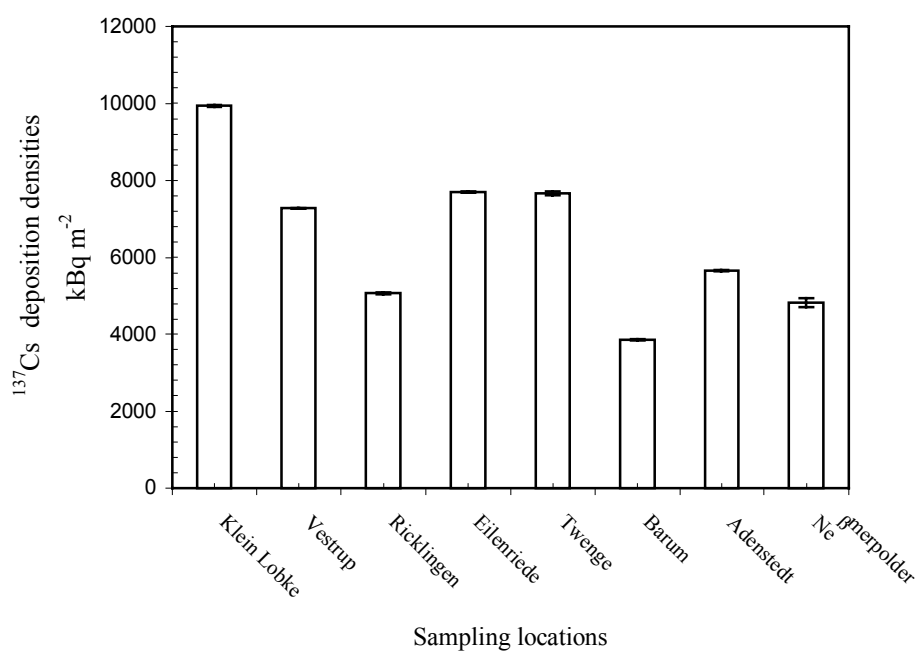
Total ^{137}Cs activity densities, as measured in the 8 sampling sites, ranged from 3845 to 9934 Bq m $^{-2}$ (Table 3-5). In general, data show in (Fig. 3-5). The high variation in the activity density determined in high precipitation sites (sampling site Klein Lobke, Eilenriede, Twenge and Vestrup, located in Lower Saxony, North Germany). The deposit of radionuclides in the area investigated, in accordance with previous reported results [Sch89].

The ^{137}Cs areal concentration is shown for each sampling sites in Fig. 3-5, the mean inventory for all of the sites is 6737 Bq m $^{-2}$ (Table 3-5), the greatest total ^{137}Cs occurs in the soils of the Klein Lobke 9934 \pm 25 Bq m $^{-2}$. This site has a highest precipitation of all the sites and highest areal ^{137}Cs concentration.

The analysis of the Chernobyl ^{137}Cs deposited in Austria illustrated the large variability of the deposition patterns low (<5 kBq m $^{-2}$) and high (>40 kBq m $^{-2}$) [Dub03]. Deposition of ^{137}Cs from Chernobyl at Munich-Neuherberg amounted to 20 kBq m $^{-2}$ [Ste98]. In Juelich, Germany the mean deposition of ^{137}Cs was 45 MBq m $^{-2}$ in the German silt loam [For00].

Table 3 – 7: ^{137}Cs deposition densities [Bq m^{-2}] in soil were taken from different sites in Lower Saxony, Germany.

| Sites | deposition densities [Bq m^{-2}] | |
|---------------------|------------------------------------------------|----------------|
| | 01.09.1999 | 26.04.1986 |
| Klein Lobke | 7324 ± 18 | 9934 ± 25 |
| Vestrup | 5367 ± 9 | 7279 ± 12 |
| Ricklingen | 3739 ± 13 | 5071 ± 18 |
| Eilenriede | 5681 ± 13 | 7705 ± 18 |
| Twenge | 5649 ± 36 | 7662 ± 49 |
| Barum | 2835 ± 14 | 3845 ± 19 |
| Adenstedt | 4175 ± 12 | 5663 ± 16 |
| Neßmerpolder | 3342 ± 76 | 4829 ± 110 |
| Range (min. – max.) | 2835-7324 | 3845-9934 |
| mean | 4967 | 6737 |
| S.D. | 1493 | 2025 |

Fig. 3-5: ^{137}Cs deposition densities [kBq m^{-2}] in soil taken from sites in Lower Saxony, North Germany.

3.1.1.2 Activity concentration of ^{137}Cs and ^{40}K [Bq kg^{-1}] in surface soil samples from different sites in Lower Saxony, North Germany.

Table 3 – 8: Activity concentration of ^{137}Cs and ^{40}K [Bq kg^{-1}] in soil were collected from Lower Saxony, North Germany.

| Location | Soil sample code | Dry density [g cm^{-2}] | Cs-137 | K-40 |
|-----------------|------------------|------------------------------------|----------------|--------------|
| Jeinsen | JeBoEPKr01 | 1.37 | 13.7 ± 0.5 | 496 ± 17 |
| | JeBoEPKs01 | 1.35 | 10.3 ± 0.4 | 597 ± 21 |
| | JeBoEPRb01 | 1.28 | 11.0 ± 0.4 | 186 ± 7 |
| | JeBoEPMa01 | 1.21 | 12.1 ± 0.5 | 359 ± 13 |
| | JeBoEPBr01 | 1.45 | 12.3 ± 0.4 | 555 ± 19 |
| | JeBoEPLa01 | 1.44 | 9.8 ± 0.3 | 558 ± 19 |
| | JeBoEPWk01 | 1.33 | 11.6 ± 0.4 | 581 ± 20 |
| | JeBoEPEg01 | 1.37 | 10.0 ± 0.3 | 539 ± 18 |
| | JeBoEPRo01 | 1.37 | 10.9 ± 0.4 | 547 ± 19 |
| | JeBoEPWeK01 | 1.34 | 11.4 ± 0.4 | 544 ± 18 |
| | JeBoEKP1 | 1.37 | 12.5 ± 0.4 | 557 ± 19 |
| | JeBoEPPe01 | 1.38 | 8.6 ± 0.3 | 510 ± 17 |
| | JeBoEPGk01 | 1.27 | 10.0 ± 0.3 | 577 ± 20 |
| Neßmerpolder | PoBoEPLu01 | 1.33 | 6.6 ± 0.3 | 511 ± 18 |
| | PoBoEPWe01 | 1.33 | 6.5 ± 0.3 | 522 ± 18 |
| | PoBoEPWe02 | 1.35 | 4.3 ± 0.2 | 526 ± 18 |
| | PoBoMPHa02 | 1.38 | 5.2 ± 0.2 | 508 ± 18 |
| | PoBoEPRa01 | 1.19 | 6.5 ± 0.3 | 503 ± 18 |
| | PoBoEPLu02 | 1.29 | 6.0 ± 0.2 | 527 ± 18 |
| | PoBoMPHa01 | 1.43 | 5.9 ± 0.2 | 496 ± 17 |
| | PoBoMPWe01 | 1.39 | 5.1 ± 0.2 | 476 ± 16 |
| | PoBoMPHe01 | 1.18 | 5.5 ± 0.2 | 382 ± 13 |
| | PoBoEPHa02 | 1.31 | 6.6 ± 0.3 | 506 ± 21 |
| | PoBoEPHe02 | 1.20 | 10.3 ± 0.4 | 612 ± 21 |
| | PoBoMPGe01 | 1.35 | 5.2 ± 0.2 | 458 ± 16 |
| | PoBoMPLu1 | 1.26 | 6.0 ± 0.2 | 475 ± 16 |
| Schessinghausen | ScBoMPRo01 | 1.39 | 10.0 ± 0.4 | 159 ± 6 |
| | ScBoMPTr02 | 1.37 | 10.2 ± 0.4 | 151 ± 6 |
| | ScBoMPRa01 | 1.39 | 9.8 ± 0.3 | 284 ± 10 |
| | ScBoMPWe01 | 1.40 | 10.3 ± 0.4 | 356 ± 13 |
| | ScBoMPTr01 | 1.46 | 10.3 ± 0.4 | 225 ± 8 |
| | ScBoMPWe02 | 1.39 | 9.5 ± 0.3 | 309 ± 11 |
| | ScBoEPKa01 | 1.38 | 10.4 ± 0.4 | 282 ± 10 |
| | ScBoEPMa01 | 1.31 | 10.8 ± 0.4 | 292 ± 10 |
| Schlewecke | SiBoEPRa01 | 1.34 | 13.3 ± 0.4 | 580 ± 20 |
| | SiBoEZu01 | 1.29 | 16.0 ± 0.5 | 545 ± 18 |
| | SiBoMPGe01 | 1.28 | 13.8 ± 0.5 | 535 ± 18 |
| | SiBoMPGe02 | 1.14 | 15.6 ± 0.5 | 852 ± 29 |
| | SiBoMPRa01 | 1.28 | 12.5 ± 0.4 | 609 ± 21 |
| | SiBoMPWe01 | 1.15 | 21.3 ± 0.7 | 771 ± 26 |
| | SiBoMPWe02 | 1.21 | 16.9 ± 0.6 | 752 ± 25 |
| SiBoEPWe01 | 1.15 | 35.7 ± 1.2 | 1332 ± 45 | |

| Location | Soil sample code | Dry density [g cm ⁻²] | Cs-137 | K-40 |
|--------------------------------------|------------------|-----------------------------------|------------|------------|
| Gestorf | GeBMPWe01 | 1.27 | 12.8 ± 0.5 | 565 ± 20 |
| | GeBoEPKa01 | 1.31 | 12.9 ± 0.5 | 390 ± 14 |
| | GeBoEPZu01 | 1.31 | 13.5 ± 0.5 | 583 ± 20 |
| Gümmmer | GuBoEPrh01a | 1.25 | 23.5 ± 0.8 | 457 ± 16 |
| | GuBoEPrh01b | 1.22 | 25.9 ± 0.9 | 469 ± 16 |
| Hermannsdorfes Landwerkstätten (HLW) | HLWBoEPHe01 | 1.22 | 18.4 ± 0.6 | 503 ± 17 |
| | RhBoEPWa01 | 1.12 | 47.8 ± 1.6 | 806 ± 27 |
| Range (Min.-Max.) | | | 4.3 - 47.8 | 151 - 1331 |
| Mean | | | 12.4 | 508 |
| S.D. | | | 7.8 | 17 |

As shown in Table 3-8, the surface concentrations of ¹³⁷Cs and ⁴⁰K in soil samples from Lower Saxony, North Germany were in the range of 4.3 ± 0.2 – 47.8 ± 1.6 Bq kg⁻¹ for ¹³⁷Cs and of 151 ± 6 – 1331 ± 45 Bq kg⁻¹ for ⁴⁰K which is relatively similar the reported values in neighboring countries and in the north hemisphere. In UK, the highest ¹³⁷Cs concentration observed in soil was 2000±86 during 1991 [Ead98]. The ¹³⁷Cs was measured in soil collected in 1992 these values ranged between 2 and 130 Bq kg⁻¹ from the Swiss [Alb99]. In the Norway the measured ¹³⁷Cs concentration have a mean value 34.8 Bq kg⁻¹ dry and for ⁴⁰K mean value is 282.7 Bq kg⁻¹ weight soil samples that were collected in 2002 [Dow03]. From different regions of Yugoslavia showed a high level of contamination for the fission product ¹³⁷Cs that has ranged from 2 to 21 Bq kg⁻¹ of 230 Bq kg⁻¹ [Esp02]. In Turkey the activity concentration of ¹³⁷Cs was found to range between 2.8 ± 0.17 and 20.75 ± 0.29 Bq kg⁻¹ [Asl03].

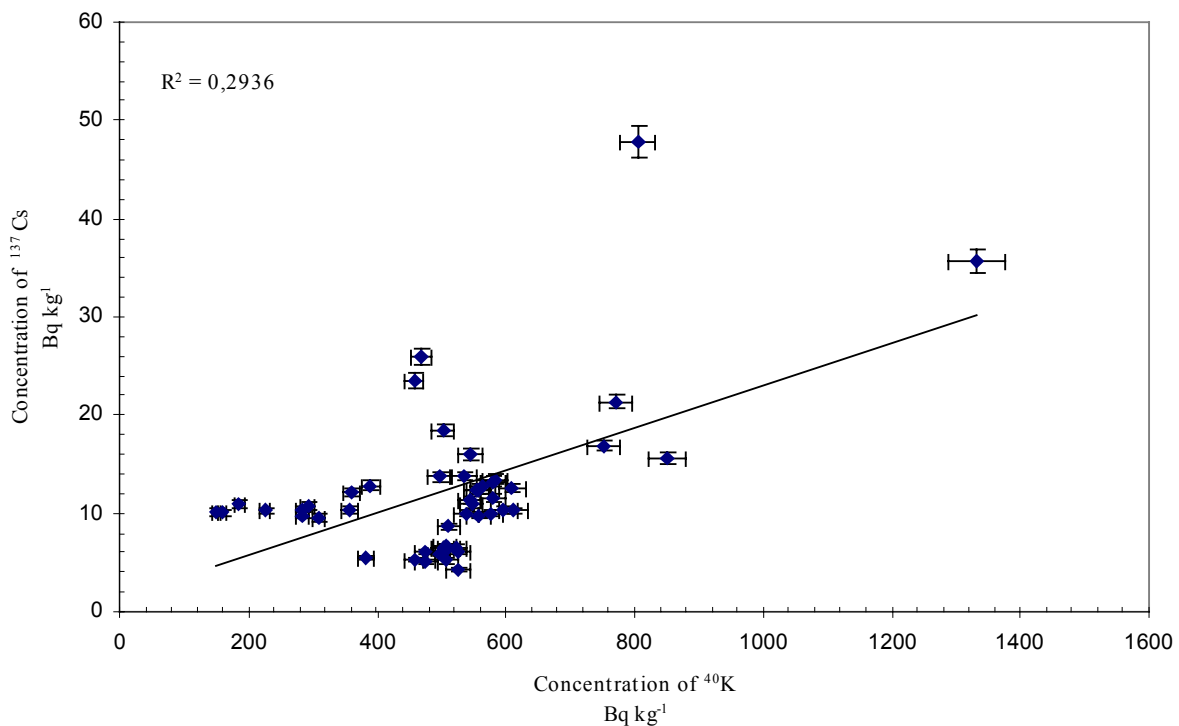


Fig. 3-6: Correlation between ¹³⁷Cs and ⁴⁰K in soil samples from Lower Saxony, North Germany.

The linear correlation between ^{137}Cs and ^{40}K concentrations in soil samples from different sites in Lower Saxony, North Germany (Fig. 3-6) with correlation factor ($R = 0.2936$).

3.1.2 ^{137}Cs in depth profile soil samples from Lippe, North Rhine-Westphalia, Germany.

The results of ^{137}Cs concentration in 2 depth profile soil samples from two locations along river Lippe show in Tables 3 –7 Tables B - 4 in appendix B.

Table 3 – 9: Activity concentration of ^{137}Cs [Bq kg^{-1}] in different geometry and activity concentration of layers [Bq m^{-2}] in profile samples Lippe (North Rhine-Westphalia), Germany.

| Code of Sample | Depth [cm] | Dry density [g cm^{-3}] | Activity concentration | Activity of layer | |
|------------------|------------|------------------------------------|------------------------|-------------------|-----------------------|
| | | | | 01.09.2000 | 26.04.1986 |
| BP 4-14. 0-2cm | 0-2 | 0.95 | 34 ± 2 | 640 ± 34 | 888 ± 47 (6 %) |
| BP 4-14. 2-4cm | 2-4 | 0.93 | 38 ± 2 | 715 ± 36 | 992 ± 50 (7 %) |
| BP 4-14. 4-6cm | 4-6 | 0.91 | 38 ± 2 | 689 ± 35 | 956 ± 48 (6 %) |
| BP 4-14. 6-10cm | 6-10 | 0.91 | 52 ± 3 | 1896 ± 95 | 2631 ± 132 (17 %) |
| BP 4-14. 10-15cm | 10-15 | 0.93 | 81 ± 4 | 3751 ± 188 | 5206 ± 261 (34 %) |
| BP 4-14. 15-20cm | 15-20 | 1.01 | 47 ± 2 | 2385 ± 120 | 3310 ± 166 (22 %) |
| BP 4-14. 20-30cm | 20-30 | 0.95 | 19 ± 1 | 898 ± 46 | 1247 ± 64 (8 %) |

The ^{137}Cs activity concentration value (Table 3-7) at the surface are $34 \pm 2 \text{ Bq kg}^{-1}$ but in deepest layer 20-30 cm we found ^{137}Cs value of $19 \pm 1 \text{ Bq kg}^{-1}$. The ^{137}Cs distributions within the soil profile in Table 3-7 we can see that the ^{137}Cs values ranged 898 ± 46 and $3751 \pm 188 \text{ Bq m}^{-2}$ referred to measuring date and corrected for Chernobyl accident the ^{137}Cs value 1247 ± 64 and $5206 \pm 261 \text{ Bq m}^{-2}$, we can see also that the highest activity of ^{137}Cs in the layer 10-15 cm is 34 % of the total activity in the soil and 6% of the total activity in the soil in the top layer.

3.1.2.1 ^{137}Cs deposition densities in soil samples from Lippe, (North Rhine-Westphalia), Germany.

Table 3 – 10: ^{137}Cs deposition densities [Bq m^{-2}] in soil were taken from different sites in Lippe, (North Rhine-Westphalia), Germany

| Site | Deposition densities [Bq m^{-2}] | |
|---------|---------------------------------------------|-----------------|
| | 01.09.2000 | 26.04.1986 |
| Bp3-30 | 9063 ± 409 | 12578 ± 567 |
| Bp 4-14 | 10974 ± 554 | 15230 ± 769 |

Total ^{137}Cs activity densities, as measured in the 2 sampling sites Bp3-30 and Bp4-14 in Lippe, (North Rhine-Westphalia),Germany are 12578 ± 567 and $15230 \pm 769 \text{ Bq m}^{-2}$ back to Chernobyl accident respectively.

3.1.2.2 Activity concentration of ^{137}Cs and ^{40}K [Bq kg^{-1}] in surface soil samples from Lippe (North Rhine-Westphalia, NRW), Germany.

Table 3 – 11: Activity concentration of ^{137}Cs and ^{40}K [Bq kg^{-1}] in soil were collected from Lippe, North Rhine -Westphalia, Germany.

| Soil sample No. | Dry density [g cm^{-3}] | Cs-137 | K-40 |
|-----------------|------------------------------------|-----------|-----------|
| BP 2-04f | 0.97 | 244 ± 7.8 | 283 ± 11 |
| BP 2-05f | 0.88 | 32 ± 1.2 | 359 ± 14 |
| BP 2-06f | 1.02 | 40 ± 1.4 | 451 ± 17 |
| BP 2-07f | 1.05 | 8 ± 0.5 | 262 ± 14 |
| BP 2-11f | 0.93 | 29 ± 1.2 | 376 ± 20 |
| BP 2-12f | 1.09 | 36 ± 14 | 401 ± 15 |
| BP 2-13f | 1.17 | 8 ± 0.5 | 259 ± 10 |
| BP 2-17f | 1.09 | 27 ± 1.1 | 334 ± 14 |
| BP 2-23f | 0.90 | 23 ± 1 | 185 ± 11 |
| BP 2-24f | 1.12 | 15 ± 0.6 | 399 ± 21 |
| BP 2-25f | 1.27 | 10 ± 0.5 | 268 ± 10 |
| BP 2-33f | 1.13 | 163 ± 0.6 | 307 ± 12 |
| BP 2-34f | 1.27 | 9 ± 0.5 | 175 ± 10 |
| BP 2-35f | 1.19 | 9 ± 0.5 | 218 ± 12 |
| BP 2-36f | 1.12 | 39 ± 1.4 | 334 ± 13 |
| BP 3-01 | 1.08 | 20 ± 1 | 318 ± 16 |
| BP 3-02 | 1.08 | 20 ± 1 | 298 ± 15 |
| BP 3-03 | 1.30 | 3 ± 0.2 | 352 ± 18 |
| BP 3-04 | 0.96 | 48 ± 2.4 | 340 ± 17 |
| BP 3-05 | 0.89 | 57 ± 2.9 | 346 ± 18 |
| BP 3-06 | 1.11 | 5 ± 0.23 | 579 ± 22 |
| BP 3-09 | 1.24 | 4 ± 0.2 | 331 ± 7 |
| BP 3-07 | 0.94 | 98 ± 3.2 | 387 ± 13 |
| BP 3-08 | 1.02 | 36 ± 1.2 | 373 ± 13 |
| BP 3-10 | 0.86 | 26 ± 0.9 | 375 ± 20 |
| BP 3-11 | 0.90 | nd | 1104 ± 37 |
| BP 3-12 | 0.97 | 21 ± 0.7 | 327 ± 11 |
| BP 3-13 | 0.98 | 205 ± 0.8 | 435 ± 15 |
| BP 3-14 | 1.19 | 10 ± 0.3 | 326 ± 11 |
| BP 3-15 | 0.98 | 78 ± 2.5 | 385 ± 13 |
| BP 3-16 | 1.10 | 10 ± 0.4 | 206 ± 7 |
| BP 3-17 | 1.09 | 17 ± 0.6 | 237 ± 8 |
| BP 3-18 | 0.81 | 35 ± 1.1 | 254 ± 9 |
| BP 3-21 | 1.38 | 7 ± 0.23 | 169 ± 3 |
| BP 3-22 | 1.04 | nd | 296 ± 15 |
| BP 3-23 | 19.90 | 20 ± 0.65 | 261 ± 9 |
| BP 3-24 | 1.11 | nd | 238 ± 12 |
| BP 3-25 | 1.04 | 18 ± 0.6 | 258 ± 6 |
| BP 3-26 | 1.19 | 12 ± 0.4 | 240 ± 5 |
| BP 3-28 | 1.10 | 18 ± 0.6 | 304 ± 10 |
| BP 3-29 | 0.99 | 28 ± 0.9 | 297 ± 10 |

| Soil sample No. | Dry density [g cm ⁻³] | Cs-137 | K-40 |
|------------------|-----------------------------------|---------------------|---------------------|
| BP 4-01 | 0.88 | 59 ± 1.9 | 424 ± 16 |
| BP 4-05 | 0.83 | 52 ± 1.7 | 387 ± 12 |
| BP 4-06 | 0.97 | 27 ± 0.9 | 651 ± 22 |
| BP 4-09 | 1.16 | 15 ± 0.5 | 341 ± 12 |
| BP 4-10 | 1.18 | 22 ± 0.7 | 304 ± 10 |
| BP 4-11 | 1.07 | 23 ± 0.8 | 312 ± 11 |
| BP 4-12 | 1.29 | 9 ± 0.3 | 281 ± 10 |
| BP 4-15 | 0.90 | 55 ± 1.8 | 413 ± 14 |
| BP 4-16 | 1.22 | 7 ± 0.2 | 267 ± 9 |
| BP Sicking. (71) | 0.95 | 32 ± 1.6 | 256 ± 13 |
| BPVorfluter(70) | 1.31 | 12 ± 0.7 | 214 ± 11 |
| BP 5-01 | 0.95 | 32 ± 1.6 | 265 ± 14 |
| BP 5-02 | 1.21 | 17 ± 0.9 | 259 ± 13 |
| BP 5-03 | 0.97 | 45 ± 2.3 | 324 ± 17 |
| BP 5-04 | 0.96 | 50 ± 2.5 | 324 ± 17 |
| BP 5-05 (Sedi) | 1.50 | 3 ± 0.2 | 196 ± 10 |
| BP 5-06 | 0.88 | 51 ± 2.5 | 387 ± 20 |
| BP 5-07 | 0.93 | 51 ± 2.6 | 353 ± 18 |
| BP 5-08 | 1.04 | 46 ± 2.3 | 312 ± 16 |
| BP 5-09 | 0.99 | 45 ± 2.2 | 369 ± 19 |
| BP 5-10 | 0.95 | 43 ± 2.2 | 381 ± 19 |
| BP 5-11 | 14.70 | 15 ± 0.8 | 199 ± 16 |
| Range(Min.-Max.) | | 3 ± 0.2 – 244 ± 7.8 | 169 ± 3 – 1104 ± 37 |
| Mean | | 34 | 320 |
| S.D. | | 41 | 130 |

The ¹³⁷Cs and ⁴⁰K activity concentrations in surface soil samples are shown in table 3-9. The ranges, the mean values and the standard deviations of ¹³⁷Cs and the ⁴⁰K concentrations were $3 \pm 0.2 - 244 \pm 7.8$ Bq kg⁻¹, 34 Bq kg⁻¹ and 41 Bq kg⁻¹, and $169 \pm 3 - 1104 \pm 37$ Bq kg⁻¹, 320 Bq kg⁻¹ and 130 Bq kg⁻¹ respectively.

The linear correlation between ¹³⁷Cs and ⁴⁰K concentrations in soil samples from different locations along Lippe river (Fig. 3-7) showed a weak correlation factor ($R = 0.0605$). Nevertheless, the positive slope means that ¹³⁷Cs activities grow with increasing ⁴⁰K activities, and this revealed the linear relationship between accumulation of ¹³⁷Cs and the presence of clay minerals, which are capable of sorbing cations like ¹³⁷Cs through ion exchange processes [Ham03].

3.1.3 ¹³⁷Cs concentrations in depth profile soil samples from Ukraine.

The ¹³⁷Cs as an ordinary fission-product is produced in nuclear reactors as well as in nuclear weapons explosions. The ¹³⁴Cs is, however, produced within the nuclear reactors only, not as a result of uranium or plutonium fission but as a result of neutron activation of the ¹³³Cs, the daughter of the fission-product ¹³³Xe [Che93].

The results of ^{137,134}Cs concentration in 22 depth profile soil samples from different locations in Ukraine show in Tables 3 -12 to 3 -16 and Tables B -5 to B - 22 in appendix B and all the results of concentrations of ^{137, 134}Cs referred to Chernobyl accident and the characteristics of soil samples from Ukraine, Zone II in Table 3-12.

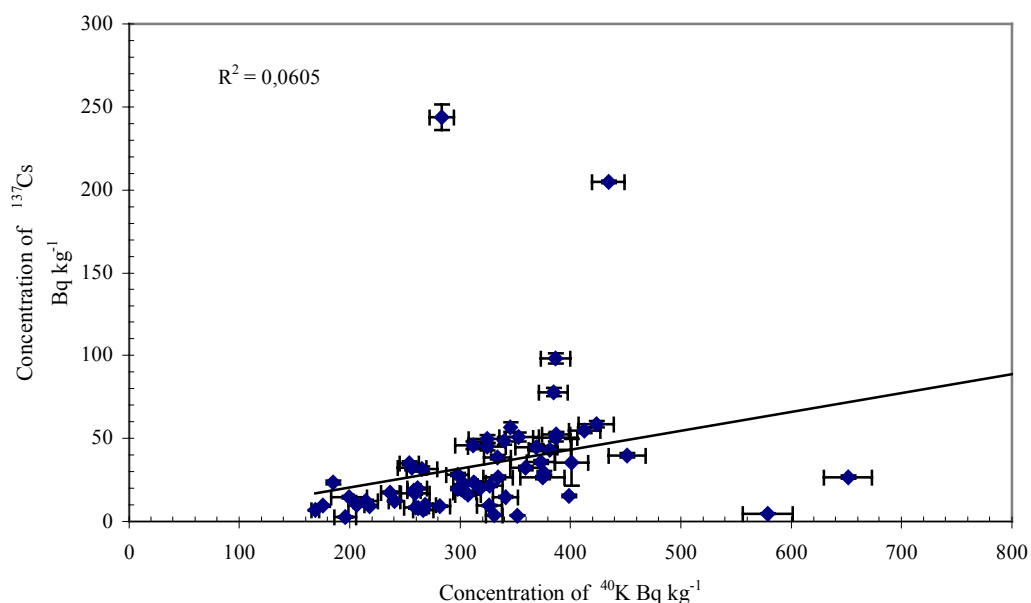


Fig. 3-7: The linear correlation between ^{137}Cs and ^{40}K concentrations in surface soil samples from Lippe, North Rhine-Westphalia, Germany.

Table 3 – 12: Characteristic of soil from zone II, Ukraine.

| Sampling sites | Description of soil | Depths (cm) | Type of soil | Soil parameters | | | | | | |
|---------------------|-------------------------------------------------------|-------------|----------------------|-----------------|----------|----------|---------------------|-------|--------------|-------------------------|
| | | | | Clay | Silt [%] | Sand [%] | CO ₃ [%] | C [%] | Org.Mat. [%] | pH (CaCl ₂) |
| Nosdristsche | Fresh humus(H ₀) | 0-2 | Eutric podzoluvisols | 2.07 | 19.04 | 77.69 | 0 | 0.93 | 0.93 | 4.76 |
| | Humus horizon(HE) | 2-27 | | 2.21 | 24.91 | 72.42 | 0 | 0.39 | 0.36 | 4.1 |
| | SiO ₂ € | 27-46 | | 3.89 | 20.88 | 74.07 | 0 | 0.05 | 0.05 | 4.49 |
| | SiO ₂ +Fe ₂ O ₃ (El) | > 46 | | Not analysis | | | | | | |
| Nove Scharno | Fresh humus(H ₀) | 0-7 | Eutric podzoluvisols | 5.96 | 41.87 | 51.83 | 0.7 | 1.92 | 1.78 | 6.81 |
| | Humus horizon(HE) | 7-23 | | 4.49 | 44.81 | 50.42 | 0 | 0.73 | 0.73 | 4.84 |
| | SiO ₂ € | > 23 | | 3.57 | 47.65 | 48.96 | 0 | 0.15 | 0.15 | 4.55 |
| Christinovka shore | Frisher humus(H ₀) | 0-6 | Fluvisols | 20.06 | 78.8 | 3.55 | 1.6 | 5.22 | 4.91 | 7.02 |
| | Humus horizon(HE) | 6-19 | | 13.95 | 83.94 | 4.11 | 2.9 | 1.72 | 1.15 | 7.53 |
| | SiO ₂ € | 19-34 | | 9.22 | 87.65 | 3.45 | 4.5 | 1.05 | 0.15 | 7.55 |
| | SiO ₂ +Fe ₂ O ₃ (El) | 34-40 | | 9.82 | 79.3 | 4.67 | 4.8 | 1.12 | 0.15 | 7.57 |
| Christinovka meadow | Fresh humus(H ₀) | 0-6 | Eutric podzoluvisols | 12.73 | 37.01 | 50.52 | 0.6 | 2.53 | 2.42 | 7.15 |
| | Humus horizon(HE) | 6-22 | | 12.45 | 36.42 | 50.23 | 0.6 | 2.36 | 2.24 | 7.25 |
| | Gleyic camb | 22-42 | | 5.19 | 48.33 | 44.98 | 0 | 0.12 | 0.12 | 6.85 |
| | Gleyic | > 42 | | Not analysis | | | | | | |

3.1.3.1 Highly contaminated (Zone II)

Table 3 – 13: Activity concentration [Bq kg^{-1}] and deposition densities [Bq m^{-2}] of ^{137}Cs in depth profile soil samples from Nosdrischtsche II, Ukraine.

| Depth [cm] | Dry density [g cm^{-3}] | Specific activity Bq kg^{-1} | | Deposition densities kBq m^{-2} | | $^{134}\text{Cs}/^{137}\text{Cs}$ Decay- corrected to 1986 |
|------------|------------------------------------|---------------------------------------|-------------------|------------------------------------------|-------------------|---------------------------------------------------------------|
| | | ^{137}Cs | ^{134}Cs | ^{137}Cs | ^{134}Cs | |
| humus/soil | 1.20 | 8200 ± 236 | 4348 ± 358 | 5003.5 ± 160 | 2729 ± 176 | 0.55 |
| 0-1 | 1.18 | 16954 ± 545 | 8083 ± 355 | 4922.4 ± 158 | 2686 ± 173 | 0.55 |
| 1-2 | 1.63 | 11642 ± 374 | 6421 ± 256 | 4722.6 ± 152 | 2591 ± 169 | 0.55 |
| 2-3 | 1.46 | 11318 ± 363 | 6620 ± 512 | 4532.7 ± 146 | 2486 ± 164 | 0.55 |
| 3-5 | 1.77 | 8481 ± 272 | 3895 ± 362 | 4367.2 ± 140 | 2390 ± 157 | 0.55 |
| 5-10 | 1.78 | 30384 ± 975 | 16658 ± 905 | 4066.4 ± 131 | 2251 ± 144 | 0.55 |
| 10-15 | 1.84 | 13519 ± 434 | 7372 ± 479 | 1362.5 ± 44 | 769 ± 64 | 0.56 |
| 15-20 | 1.84 | 1121 ± 36 | 788 ± 118 | 115.5 ± 4 | 89 ± 19 | 0.77 |
| 20-25 | 1.91 | 69 ± 2.3 | 62 ± 23 | 12.4 ± 0.4 | 17 ± 9 | 1.34 |
| 25-40 | 1.90 | 21 ± 0.8 | 37 ± 22 | 5.8 ± 0.2 | 11 ± 6 | 1.82 |

The radiocaesium analytical data are present in Table 3-13 and the specific activity profiles plotted in Fig. 3-8, ^{137}Cs , ^{134}Cs were detectable to a depth of 40 cm and the profile displayed peaks at 5-10 cm, with a maximum specific activity $30384 \pm 975 \text{ Bq kg}^{-1}$.

The upper peak can be identified as originating from Chernobyl fallout by the presence of ^{134}Cs , within a maximum specific activity of $16658 \pm 905 \text{ Bq kg}^{-1}$, coincident with the maximum ^{137}Cs activity. On the basis of the observed activity ratio of about 0.55 and the Chernobyl fallout at the time of deposition [Pat94]. The ratio between the activity of ^{134}Cs and ^{137}Cs at the time of accident Chernobyl are found in Lund region [Erl86].

Table 3-13 present data on the depth distribution of ^{137}Cs in the Chiristinovka meadow. These data indicate a clear trend as the activity concentrations for ^{134}Cs and ^{137}Cs decline with increasing depth. This decline has been reported by a number of authors [Arn89; Cop00]. ^{137}Cs is an artificial radionuclide originating from Chernobyl nuclear power plant accident. The activity of ^{137}Cs observed in the depth profile soil ranged from 21 ± 0.8 to $30384 \pm 975 \text{ Bq kg}^{-1}$. The activity of ^{134}Cs observed in the depth profile soil ranged from 37 ± 22 to $16658 \pm 905 \text{ Bq kg}^{-1}$. In the Table 3-13 we can see that the activity for ^{137}Cs of layer ranged 5.8 ± 0.2 to $5003.5 \pm 160 \text{ Bq m}^{-2}$ and for ^{134}Cs of layer ranged 11 ± 6 to $2729 \pm 176 \text{ Bq m}^{-2}$ for Chernobyl accident.

The bulk of the radioactivity was found within the top 20 cm of the 40 cm profile. This has important implications for the food chain transfer of radionuclides because it is within these upper horizons that the majority of any herbaceous plants will root and it is where most small mammals burrow and forage.

The decay-corrected $^{134}\text{Cs}/^{137}\text{Cs}$ ratio shows good agreement with that measured by [Ead98] shortly after the Chernobyl deposition. The ratio between the activity of ^{134}Cs and ^{137}Cs at the time of the Chernobyl accident was found to be 0.56 in the Lund region [Isa97]. During the Chernobyl failure, in April-May 1986, the ratio of ^{134}Cs to ^{137}Cs activities in the air and in the fallout at Cracow was nearly constant in time and equal to approximately 0.49 [Che93].

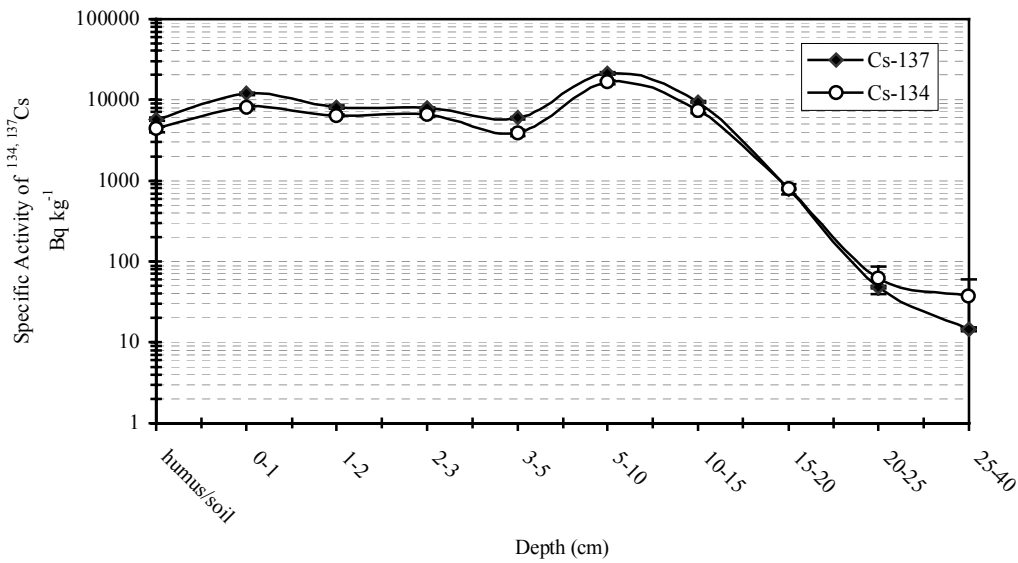


Fig. 3-8: Depth distribution of ^{134,137}Cs [Bq kg⁻¹] in soil profile from Nosdrischtsche II, Ukraine.

The vertical mobility of ¹³⁷Cs in the soil profile in Fig. 3-8 giving the distribution of ^{134,137}Cs between the humus layer and the underlying mineral soil the same studying in literature [And01].

Table 3 – 14: Activity concentration [Bq kg⁻¹] and deposition densities [Bq m⁻²] of ¹³⁷Cs in depth profile soil samples from Chirstinovka meadow, Ukraine.

| Depth [cm] | Dry density [g cm ⁻³] | Specific activity [Bq kg ⁻¹] | | Deposition densities [kBq m ⁻²] | | ¹³⁴ Cs/ ¹³⁷ Cs Decay- corrected to 1986 |
|------------|-----------------------------------|------------------------------------------|-------------------|---------------------------------------------|-------------------|------------------------------------------------------------------|
| | | ¹³⁷ Cs | ¹³⁴ Cs | ¹³⁷ Cs | ¹³⁴ Cs | |
| humus/soil | 1.21 | 1838 ± 59 | 1135 ± 90 | 822 ± 65 | 524 ± 61 | 0.64 |
| 0-1 | 1.32 | 1907 ± 61 | 1152 ± 93 | 807 ± 26 | 514 ± 60 | 0.64 |
| 1-2 | 1.43 | 2059 ± 66 | 1233 ± 102 | 781 ± 25 | 499 ± 59 | 0.64 |
| 2-3 | 1.41 | 2209 ± 71 | 1489 ± 103 | 752 ± 24 | 481 ± 57 | 0.64 |
| 3-5 | 1.40 | 2206 ± 71 | 1258 ± 99 | 720 ± 23 | 460 ± 56 | 0.64 |
| 5-10 | 1.47 | 2037 ± 66 | 1275 ± 95 | 659 ± 21 | 425 ± 53 | 0.65 |
| 10-15 | 1.44 | 2115 ± 68 | 1377 ± 97 | 509 ± 16 | 332 ± 46 | 0.65 |
| 15-20 | 1.57 | 2280 ± 73 | 1356 ± 96 | 357 ± 12 | 232 ± 39 | 0.65 |
| 20-25 | 1.47 | 2107 ± 68 | 1329 ± 251 | 178 ± 6 | 126 ± 32 | 0.71 |
| 25-40 | 1.74 | 88 ± 3 | 107 ± 50 | 23 ± 1 | 28 ± 13 | 1.22 |

The anthropogenic radionuclide ¹³⁷Cs, deposited in the soil of Ukraine is as a result of fallout of radioactivity from the atmosphere following the nuclear power plant accident at Chernobyl on 26 April 1986. The ¹³⁷Cs activities varied from 88 ± 3 to 2280 ± 73 Bq kg⁻¹ as compared with the ¹³⁷Cs levels in the soil samples of the UK which varied from 260 to 440 Bq kg⁻¹ and 1.1 to 3.4 Bq kg⁻¹ for ¹³⁴Cs [Cop01], that of Urbino soil (Marche region, Central Italy), ranging from 26.1 ± 3 to 143 ± 9 Bq kg⁻¹ [Guo99].

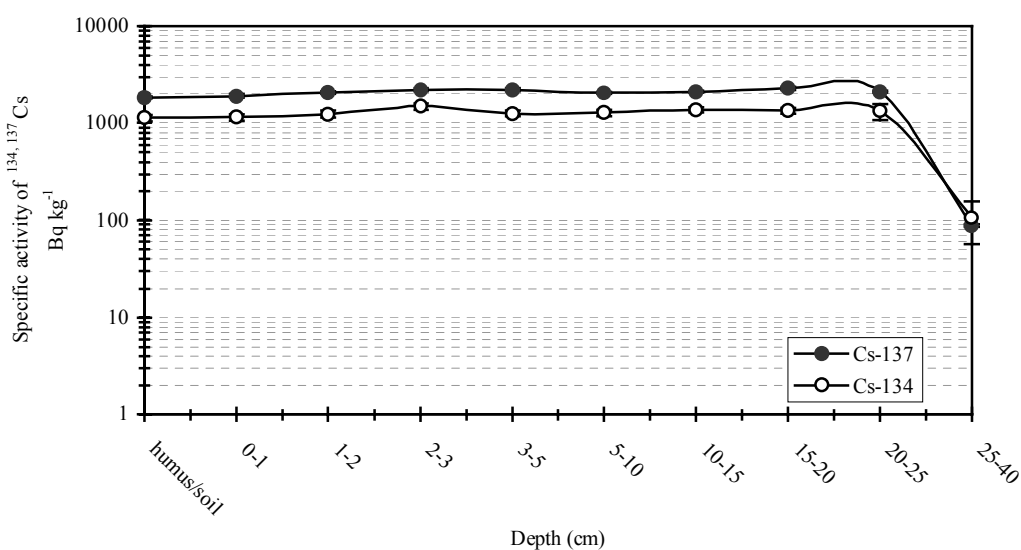


Fig. 3-9: Depth distribution of ^{137,134}Cs [Bq kg⁻¹] in soil profile from Chirstinovka meadow, Ukraine.

3.1.3.2 Medium contaminated (ZoneIII)

Table 3 – 15: Activity concentration [Bq kg⁻¹] and deposition densities [Bq m⁻²] of ¹³⁷Cs in depth profile soil samples from Tschigiri 1, Ukraine.

| Depth [cm] | Dry density [g cm ⁻³] | Specific activity Bq kg ⁻¹ | | Deposition densities kBq m ⁻² | | ¹³⁴ Cs/ ¹³⁷ Cs Decay- corrected to 1986 |
|------------|-----------------------------------|---------------------------------------|-------------------|------------------------------------------|-------------------|------------------------------------------------------------------|
| | | ¹³⁷ Cs | ¹³⁴ Cs | ¹³⁷ Cs | ¹³⁴ Cs | |
| humus/soil | 0.40 | 44598 ± 1432 | 22920 ± 955 | 368.3 ± 11.9 | 199.8 ± 24.2 | 0.54 |
| 0-1 | 0.60 | 19047 ± 612 | 9850 ± 713 | 238.8 ± 7.8 | 133.3 ± 21.4 | 0.56 |
| 1-2 | 0.96 | 5411 ± 174 | 3312 ± 328 | 124.5 ± 4.1 | 74.2 ± 17.2 | 0.60 |
| 2-3 | 1.32 | 1282 ± 41 | 910 ± 72 | 72.5 ± 2.4 | 42.3 ± 14.0 | 0.58 |
| 3-5 | 1.44 | 414 ± 13 | 335 ± 37 | 55.5 ± 1.9 | 30.3 ± 13.1 | 0.55 |
| 5-10 | 1.49 | 191 ± 6 | 227 ± 42 | 43.6 ± 1.5 | 24.3 ± 12.1 | 0.56 |
| 10-15 | 1.54 | 145 ± 5 | 286 ± 44 | 29.4 ± 1 | 15.4 ± 9.1 | 0.52 |
| 15-20 | 1.55 | 106 ± 3.5 | 243 ± 38 | 18.3 ± 0.6 | 7.6 ± 5.7 | 0.42 |
| 20-25 | 1.58 | 61 ± 2.1 | 223 ± 35 | 10.0 ± 0.4 | 3.0 ± 2.8 | 0.30 |
| 25-40 | 1.61 | 21 ± 0.8 | nd | 5.2 ± 0.2 | nd | - |

The concentration of ¹³⁷Cs in soils of the Tschigiri 1, Ukraine in Table 3-15 ranged from 21 ± 0.2 to 44598 ± 1432 Bq kg⁻¹ and the concentration of ¹³⁴Cs ranged from about 244 ± 38 to 25058 ± 1044 Bq kg⁻¹, with most of the fallout attributed to the accident at the Chernobyl nuclear power plant [Pap89]. The concentration of ¹³⁷Cs in 10 uncultivated fields from southern England ranged from 0 to 25567 Bq kg⁻¹, with the highest levels contained in the top 10 cm of the soil surface. The concentration of ¹³⁷Cs in five cultivated fields ranged from 0 to 14594 Bq kg⁻¹, and the concentrations were well distributed from the surface to the plough layer [Owe96].

The level and distribution of fallout attributable to the 26 April 1986 Chernobyl nuclear power station accident in the Ukraine, at Zhitomir and at Katyuzhanka in the Ukraine and measured the radioactivity of ¹³⁷Cs and ¹³⁴Cs. The substances investigated were soil, the activity

of ^{137}Cs was 960 and 1210 Bq kg^{-1} in two soil samples. The activity of ^{134}Cs was 15 % of ^{137}Cs in the two soil samples [Mas94].

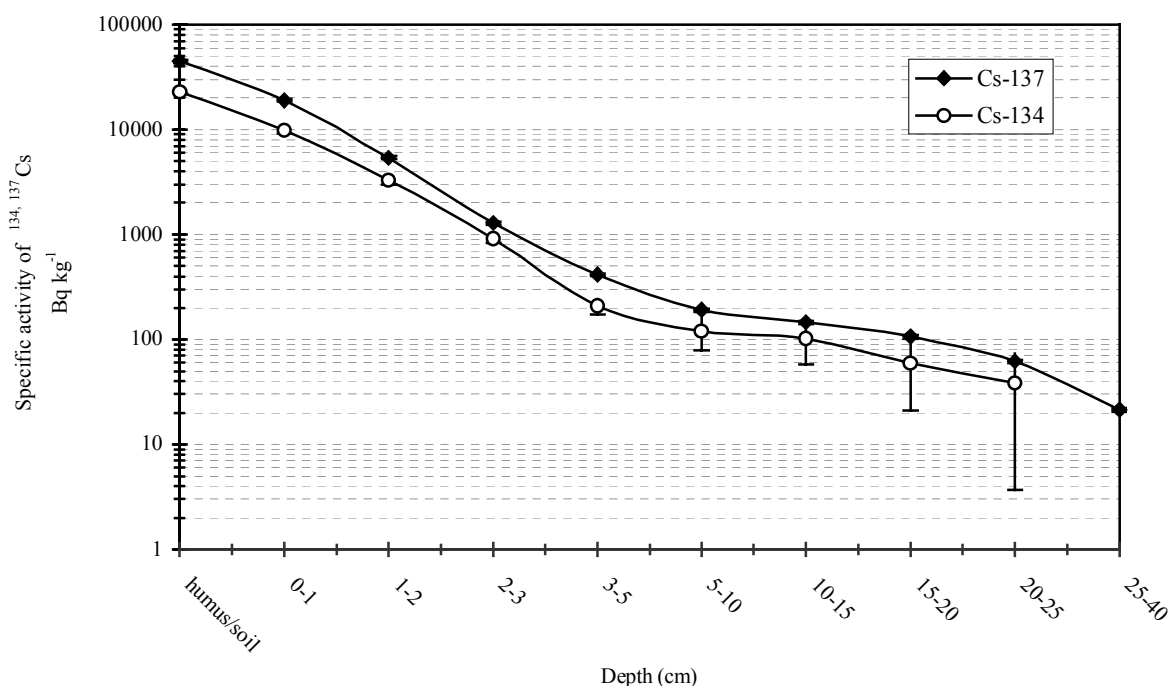


Fig. 3-10: Depth distribution of $^{137,134}\text{Cs}$ [Bq kg^{-1}] in soil profile from Tschigiri 1, Ukraine.

3.1.3.3 Not contaminated

Table 3- 16: Activity concentration [Bq kg^{-1}] and deposition densities [Bq m^{-2}] of ^{137}Cs in depth profile soil samples from Oserjanka 1, Ukraine.

| Depth [cm] | Dry density [g cm^{-3}] | Specific activity [Bq kg^{-1}] | | deposition densities [kBq m^{-2}] | |
|------------|------------------------------------|-------------------------------------------|-------------------|----------------------------------------------|-------------------|
| | | ^{137}Cs | ^{134}Cs | ^{137}Cs | ^{134}Cs |
| humus/soil | 0.66 | 69 ± 3 | | 11.8 ± 0.8 | |
| 0-1 | 0.68 | 82 ± 3 | | 11.7 ± 0.8 | |
| 1-2 | 0.97 | 75 ± 3 | | 11.2 ± 0.7 | |
| 2-3 | 0.85 | 66 ± 2 | | 10.6 ± 0.7 | |
| 3-5 | 0.88 | 52 ± 2 | | 10.0 ± 0.7 | |
| 5-10 | 0.82 | 17 ± 1 | | 8.9 ± 0.3 | |
| 10-15 | 0.79 | 12 ± 1 | | 7.7 ± 0.6 | |
| 15-20 | 0.86 | 24 ± 1 | | 6.9 ± 0.5 | |
| 20-25 | 0.85 | 30 ± 1 | | 5.2 ± 0.4 | |
| 25-40 | 0.77 | 12 ± 1 | | 3.1 ± 0.3 | |

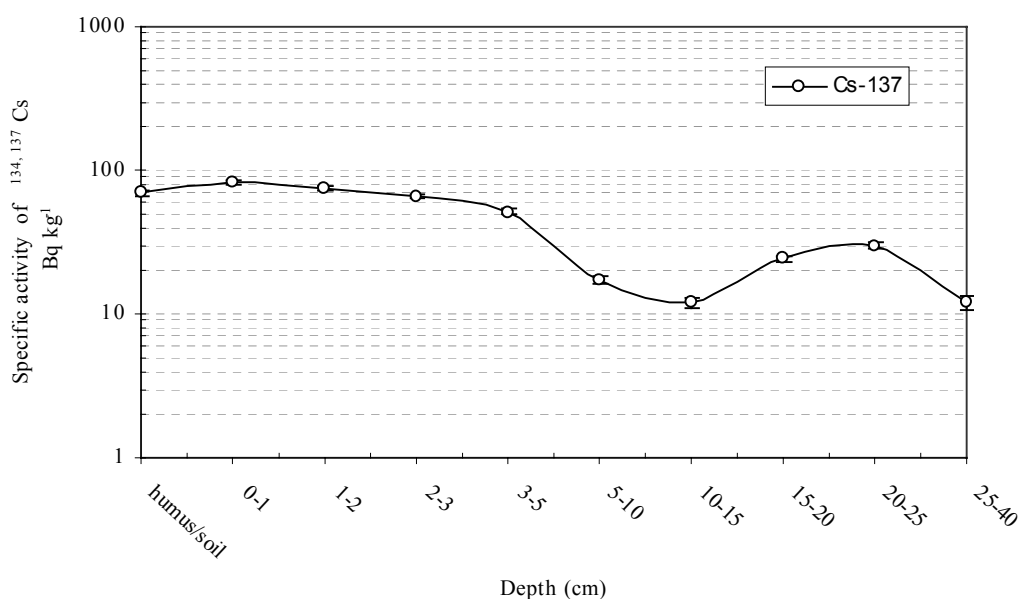


Fig. 3-11: Depth distribution of ¹³⁷Cs [Bq kg⁻¹] in soil profile from Oserjanka 1, Ukraine.

The concentration of ¹³⁷Cs in soils of the Oserjanka 1, Ukraine ranged from 12 ± 1 to 82 ± 3 Bq kg⁻¹ and the ¹³⁴Cs was not found in these samples.

3.1.3.4 ¹³⁷Cs and ¹³⁴Cs deposition densities [Bq m⁻²] in soil taken from different sites in Ukraine.

The results summarized in Table 3-17 and Fig. 3-12 show that, in general, the averages and standard deviation ranges of the concentrations of ¹³⁷Cs in soil in most autonomous regions and nationally are higher than the world figures reported in [UNS88]. The low and high ¹³⁷Cs activities at different locations in the Ukraine vary from 588 ± 68 to 2729 ± 176 kBq m⁻² in zone II but in zone III the medium contamination so the range of densities deposits is 151 ± 13 and 558 ± 41 and the third region is not contaminated and ¹³⁷Cs ranged between 2.2 ± 0.2 and 7.9 ± 0.5 kBq m⁻² calculated back to April 1986.

Calculated deposition densities of ¹³⁷Cs in various latitude regions in 1998 were given in the UNSCEAR report as about 1.40 and 2.50 kBq m⁻² for 20°-30° and 40°-50°, respectively [UNS00]. These levels were perturbed by an additional deposition from the Chernobyl accident in 1986, especially in European countries. Nabyvanets et al. indicated that a high variability of ¹³⁷Cs activity on a small area occurs usually as a result of water and, particularly wind erosion, which tends to remove and redistribute fine contaminated particles and to a smaller degree vertical migration of pollutants in soil. However, the concentrations and distribution of radionuclide can be modified significantly by cultivation. Cultivation decreases concentrations of the radionuclide in the upper layer and causes re-distribution toward deeper layers [Nab00]. In this study, most of the fields in this region are irrigated during the cultivation season. It was even difficult to identify the pathways of ¹³⁷Cs inflow to the agricultural fields. The soil is stirred by farmers with tractors. The fields in the Buyuk Menderes Delta are washed by water during spring due to the salinity of the soil in this region. The water is outlet drainage through the sea after the washing process.

Table 3 - 17: ^{137}Cs and ^{134}Cs deposition densities [kBq m^{-2}] in soil were taken from different sites in Ukraine.

| sites | deposition densities | |
|--------------------------------|------------------------------------------|------------------------------------------|
| | ^{137}Cs kBq m^{-2} | ^{134}Cs kBq m^{-2} |
| Highly contaminated (Zone II) | | |
| Nosdristsche 2 | 5003 ± 160 | 2729 ± 176 |
| Christinowka Flußufer | 4679 ± 43 | 1812 ± 126 |
| Christinowka Wiese | 822 ± 26 | 588 ± 68 |
| Nowe Scharno 3 | 3549 ± 114 | 2168 ± 176 |
| mean values | 3143 | 1805 |
| S.D. | 1786 | 942 |
| Medium contaminated (Zone III) | | |
| Tschigiri 1 | 368 ± 12 | 278 ± 27 |
| Tschigiri 2 | 371 ± 12 | 292 ± 44 |
| Tschigiri 3 | 352 ± 11 | 151 ± 13 |
| Tschigiri – Zwintor 1 | 477 ± 15 | 405 ± 52 |
| Woronowo 1 | 540 ± 17 | 351 ± 37 |
| Woronowo 2 | 200 ± 7 | 175 ± 14 |
| Woronowo 3 | 444 ± 14 | 236 ± 32 |
| Woronowo 4 | 795 ± 26 | 558 ± 41 |
| Woronowo 5 | 560 ± 18 | 215 ± 44 |
| Woronowo 6 | 540 ± 17 | 320 ± 27 |
| Woronowo 7 | 267 ± 9 | 251 ± 33 |
| mean values | 447 | 557 |
| S.D. | 163 | 890 |
| Not contaminated | | |
| Baraschewka 1 | 2.8 ± 0.2 | nd |
| Osernjanka 1 | 7.9 ± 0.5 | nd |
| Osernjanka 2 | 2.2 ± 0.2 | nd |
| Osernjanka 3 | 2.8 ± 0.2 | nd |
| Dawidowka 1 | 2.8 ± 0.2 | 68 ± 20 |
| Lewkow 1 | 5.1 ± 0.3 | nd |
| Lewkow 2 | 2.6 ± 0.1 | 47 ± 9 |
| mean values | 4 | nd |
| S.D. | 2 | nd |

The distribution of ^{137}Cs in undisturbed soil was characterized by an accumulation in the upper 10–15 cm layer due to the high affinity of ^{137}Cs for the constituents of soil and found that ^{137}Cs derived from the Chernobyl accident remained practically fixed in the upper 30 cm of the soil since 1997 reported by [Nab00]. Studies on the distribution of ^{137}Cs in the environment and the parameters affecting its behaviour in soil are important. The results of these studies indicate the importance and usefulness of regional surveys and evaluation to estimate region-wide exposure to outdoor external gamma radiation derived ^{137}Cs in soils.

In Russian, the ground deposition of long-lived fission products determined by γ -spectrometry was (recalculated to 26 April 1986) 1600 $\text{kBq }^{137}\text{Cs m}^{-2}$, 900 $\text{kBq }^{134}\text{Cs m}^{-2}$ and 60

kBq $^{125}\text{Sb m}^{-2}$. Of these radionuclides, ^{137}Cs shows the dominating activity at the present time [Car03].

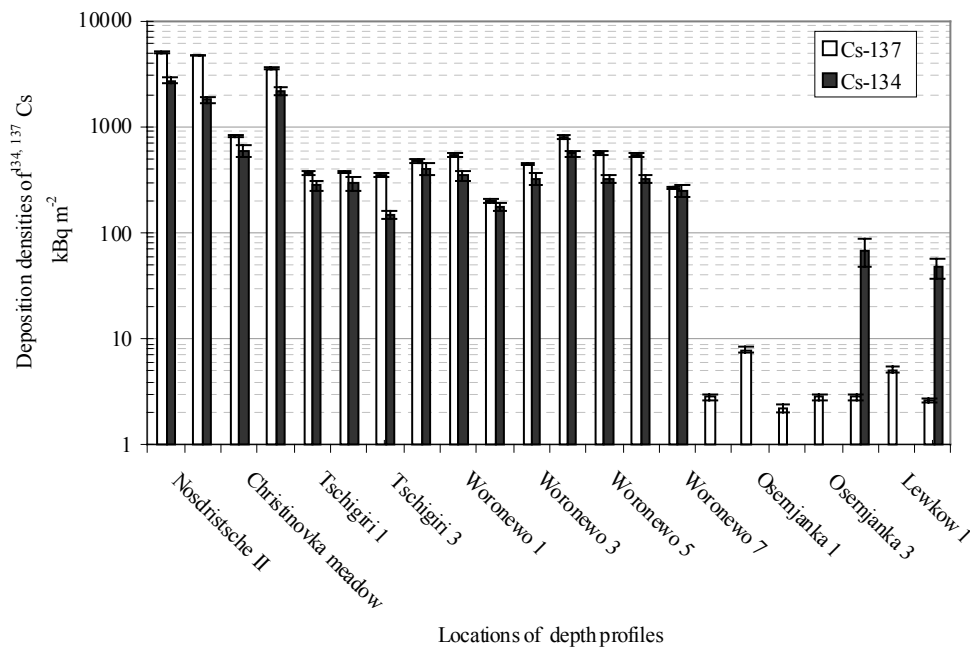


Fig. 3-12: ^{137}Cs and ^{134}Cs deposition densities [kBq m⁻²] in soil were taken from different sites in Ukraine.

3.2 Concentration of natural radionuclides in depth profile and surface soil samples

Radionuclides ^{238}U , ^{226}Ra , ^{210}Pb , ^{235}U , ^{40}K , ^{228}Ra , ^{228}Th , and ^{232}Th concentration obtained in different soil samples from different sites in Germany and Ukraine, and calculated specific concentration for radionuclides by eq. 2-5 [Dow02, Sie96]. But to calculate specific activity of ^{235}U by

$$^{235}\text{U} = ^{238}\text{U}/21.7 \quad (3 - 5)$$

3.2.1 Natural radionuclides in soil samples from Lower Saxony, North Germany.

The results of soil samples were collected from different sites in Lower Saxony see Fig 2-4 and Tables A-1, A-3, depth profiles and surface soil. Here about characteristic of soil from Ricklingen, Eilenriede and Twenge.

3.2.1.1 Natural radionuclides in depth profiles soil samples from Lower Saxony, North Germany.

The results of the depth profiles studies of radionuclides ^{238}U , ^{226}Ra , ^{210}Pb , ^{235}U , ^{40}K , ^{228}Ra , ^{228}Th , and ^{232}Th are presented in Tables 3-18, 3-19 and 3-20, for different depths from Ricklingen, Eilenriede, and Twenge, respectively.

From the results in Tables show the similar trend of variation in activity. Therefore, only the range, mean value and standard deviation for entire study region are presented at the bottom

of the respective Tables. The ^{238}U activity in the depth profile soil 0-5 to 120-170 cm varies from 10 ± 7.08 to 26 ± 6.74 Bq kg^{-1} with mean value of 21.7 Bq kg^{-1} . The ^{226}Ra activity varies from 14 ± 0.75 to 21 ± 1.33 Bq kg^{-1} , with a mean value of 19.0 Bq kg^{-1} . The ^{210}Pb activity varies from 19.9 ± 2 to 33.1 ± 2 Bq kg^{-1} , with a mean value of 27.2 Bq kg^{-1} . The ^{235}U activity varies from 0.47 ± 0.3 to 1.2 ± 0.31 Bq kg^{-1} , with a mean value of 1.0 Bq kg^{-1} . The ^{40}K activity varies from 417 ± 14 to 449 ± 15 Bq kg^{-1} , with a mean value of 430 Bq kg^{-1} . The ^{228}Ra activity varies from 17 ± 1 to 26 ± 2 Bq kg^{-1} , with a mean value of 22.7 Bq kg^{-1} . The ^{228}Th activity varies from 15 ± 1 to 23 ± 4 Bq kg^{-1} , with a mean value of 19.6 Bq kg^{-1} . The ^{232}Th activity varies from 16 ± 1 to 25 ± 3 Bq kg^{-1} , with a mean value of 21.3 Bq kg^{-1} . It is clear the result of different depth presented in Table 3-18 and Fig. 3- 13.

Table 3 – 18: Activity concentration [Bq kg^{-1}] of ^{238}U , ^{226}Ra , ^{210}Pb , ^{235}U , ^{40}K , ^{228}Ra , ^{228}Th , and ^{232}Th in soil profile samples collected from Ricklingen (meadow), North Germany.

| Depth [cm] | Dry density [g cm^{-3}] | U-238 | Ra-226 | Pb-210 | U-235 | K-40 | Ra-228 | Th-228 | Th-232 |
|-------------------|------------------------------------|---------------|---------------|--------------|-----------------|--------------|------------|------------|------------|
| 0-5 | 1.29 | 24 ± 11.4 | 17 ± 0.85 | 28.3 ± 2 | 1.12 ± 0.53 | 419 ± 14 | 22 ± 1 | 20 ± 3 | 21 ± 2 |
| 5-10 | 1.30 | 24 ± 6.28 | 19 ± 0.78 | 29.0 ± 2 | 1.11 ± 0.29 | 434 ± 15 | 22 ± 2 | 20 ± 3 | 21 ± 2 |
| 10-15 | 1.27 | 25 ± 6.61 | 20 ± 1.02 | 28.6 ± 2 | 1.17 ± 0.3 | 422 ± 14 | 23 ± 2 | 21 ± 2 | 22 ± 2 |
| 15-20 | 1.23 | 24 ± 7.88 | 20 ± 1.29 | 33.1 ± 2 | 1.09 ± 0.36 | 431 ± 14 | 23 ± 2 | 20 ± 2 | 22 ± 2 |
| 20-25 | 1.27 | 22 ± 2.7 | 21 ± 1.15 | 31.1 ± 2 | 0.99 ± 0.12 | 432 ± 15 | 24 ± 2 | 20 ± 3 | 22 ± 2 |
| 25-33 | 1.26 | 26 ± 6.74 | 20 ± 1.14 | 29.9 ± 2 | 1.20 ± 0.31 | 437 ± 15 | 23 ± 3 | 18 ± 7 | 20 ± 4 |
| 33-50 | 1.33 | 19 ± 1.19 | 19 ± 1.16 | 26.5 ± 2 | 0.89 ± 0.05 | 446 ± 15 | 24 ± 2 | 21 ± 3 | 23 ± 3 |
| 50-75 | 1.28 | 18 ± 3.55 | 16 ± 1.03 | 20.2 ± 2 | 0.84 ± 0.16 | 449 ± 15 | 21 ± 2 | 18 ± 3 | 20 ± 2 |
| 75-100 | 1.36 | 10 ± 7.08 | 14 ± 0.75 | 19.9 ± 2 | 0.47 ± 0.33 | 421 ± 14 | 17 ± 1 | 15 ± 1 | 16 ± 1 |
| 120-170 | 1.39 | 24 ± 6.65 | 21 ± 1.33 | 24.9 ± 2 | 1.12 ± 0.31 | 417 ± 14 | 26 ± 2 | 23 ± 4 | 25 ± 3 |
| Range (Min.-Max.) | | 10 – 26 | 14 – 21 | 19 – 33 | 0.47 – 1.2 | 417 – 449 | 17 – 26 | 15 – 23 | 16 – 25 |
| Mean | | 21.7 | 19.0 | 27.2 | 1.0 | 430.9 | 22.7 | 19.6 | 21.3 |
| S.D. | | 4.7 | 2.3 | 4.4 | 0.2 | 11.1 | 2.4 | 2.2 | 2.4 |

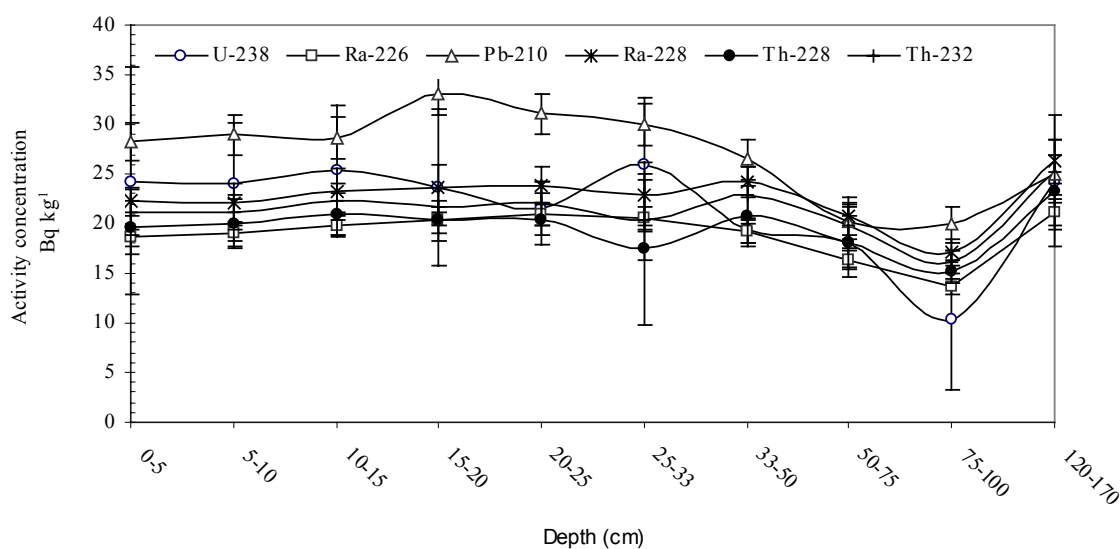


Fig. 3-13: Variation of Natural radionuclides with depth in depth profile soil from Ricklingen, Lower Saxony, North Germany.

The presents data on the distributions of radionuclides with depth in the activity levels of natural radioactive elements are given in Table 3-20 and Fig. 3-14, where the levels were found to be normally distributed. The concentrations of ^{238}U , ^{226}Ra , ^{210}Pb , ^{235}U , ^{40}K , ^{228}Ra , ^{228}Th , and ^{232}Th found in the soil samples ranged from 9 - 24 , 9 - 21, 15 - 28, 0.43 - 1.1, 253 - 401, 12 - 26, 10 - 23, and 11 - 25 Bq kg^{-1} , respectively, with an average value of 21.7, 19.0, 27.2, 306, 22.7, 19.6, and 21.3 Bq kg^{-1} , respectively.

Low values of concentrations of the naturally occurring radionuclides of uranium and thorium series at this particular depth at the Meitze, in Lower Saxony are the same range reported in [Sch89].

Table 3 - 19: Activity concentration of ^{238}U , ^{226}Ra , ^{210}Pb , ^{235}U , ^{40}K , ^{228}Ra , ^{228}Th , and ^{232}Th [Bq kg^{-1}] in soil profile samples collected from Eilenrede (forest), North Germany.

| Depth [cm] | Dry density [g cm^{-3}] | U-238 | Ra-226 | Pb-210 | U-235 | K-40 | Ra-228 | Th-228 | Th-232 |
|-------------------|------------------------------------|--------|----------|----------|-------------|-----------|----------|------------|----------|
| 0-10 | 1.133 | 17 ± 5 | 11 ± 0.6 | 33 ± 1.5 | 0.8 ± 0.25 | 253 ± 9 | 14 ± 0.7 | 12.6 ± 1.3 | 13 ± 1.1 |
| 10-20 | 1.286 | 22 ± 6 | 12 ± 0.9 | 17 ± 0.9 | 1 ± 0.27 | 283 ± 10 | 16 ± 1.8 | 14.1 ± 1.4 | 15 ± 1.2 |
| 20-30 | 1.334 | 24 ± 8 | 14 ± 1.8 | 16 ± 1.6 | 1.1 ± 0.36 | 297 ± 10 | 16 ± 1.4 | 13.9 ± 2 | 15 ± 1.8 |
| 30-40 | 1.407 | 18 ± 4 | 12 ± 0.8 | 19 ± 1 | 0.84 ± 0.21 | 300 ± 1 | 15 ± 1.3 | 13.6 ± 1.2 | 14 ± 1.1 |
| 40-50 | 1.349 | 13 ± 1 | 12 ± 0.7 | 16 ± 0.9 | 0.62 ± 0.06 | 307 ± 10 | 16 ± 1.7 | 14 ± 1.4 | 15 ± 1.3 |
| 50-70 | 1.373 | 9 ± 6 | 13 ± 0.8 | 16 ± 0.9 | 0.41 ± 0.26 | 324 ± 11 | 18 ± 0.7 | 11.8 ± 7 | 15 ± 4.4 |
| 70-100 | 1.356 | 24 ± 6 | 21 ± 1.1 | 28 ± 1.3 | 1.12 ± 0.26 | 401 ± 13 | 26 ± 2.2 | 23.7 ± 2.4 | 25 ± 1.8 |
| 100-120 | 1.536 | 9 ± 6 | 9 ± 0.5 | 15 ± 1 | 0.43 ± 0.29 | 285 ± 10 | 12 ± 0.7 | 10.2 ± 1.6 | 11 ± 1.4 |
| Range (Min.-Max.) | | 9 - 24 | 9 - 21 | 15 - 28 | 0.43 - 1.1 | 253 - 401 | 12 - 26 | 10 - 23 | 11 - 25 |
| Mean | | 21.7 | 19.0 | 27.2 | 1.0 | 306 | 22.7 | 19.6 | 21.3 |
| S.D. | | 4.7 | 2.3 | 4.4 | 0.2 | 11.1 | 2.4 | 2.2 | 2.4 |

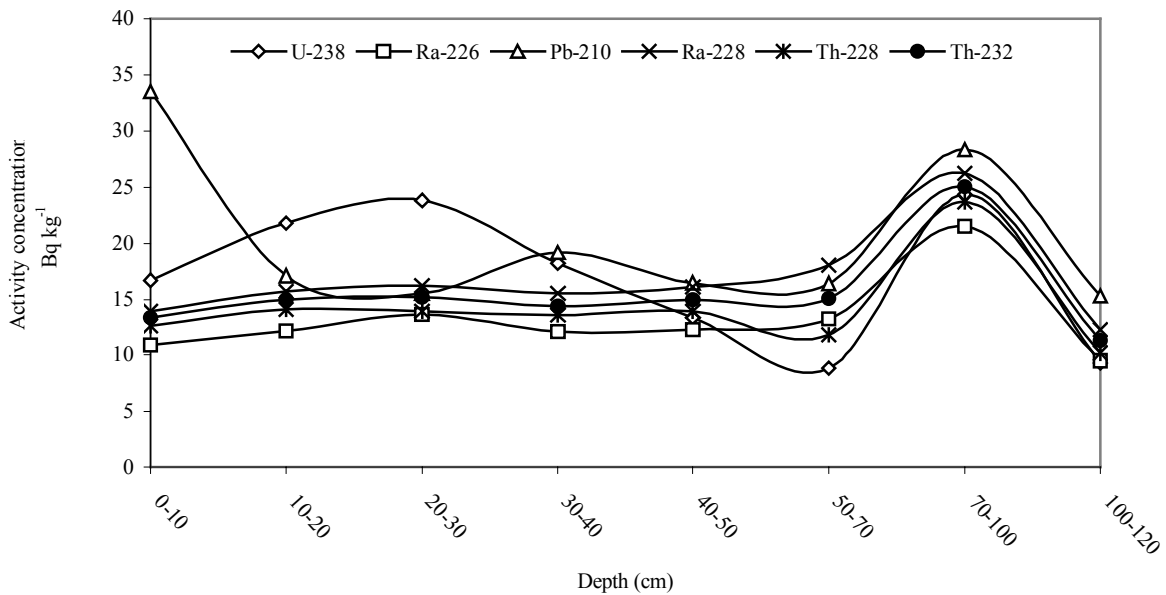
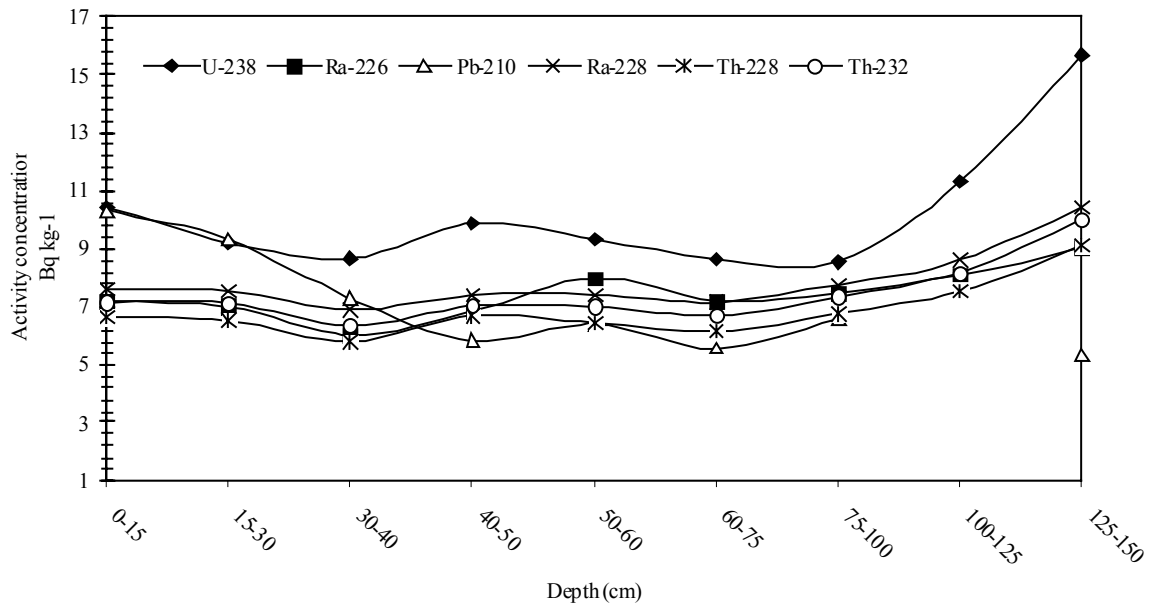


Fig. 3-14: Variation of Natural radionuclides with depth in depth profile soil from Eilenriede, Lower Saxony, North Germany.

The results of measurements for nine soil samples, collected at different depths from Twenge, Lower Saxony, Germany, are shown in Table 3-19. In all cases specific activities are quite homogenous, showing no more than a few Bq kg^{-1} for ^{238}U , ^{226}Ra and ^{232}Th . Differences in the lower activity limits for some samples mostly depend on the sample amount and counting time. The presents data on the distributions of radionuclides with depth in the activity levels of natural radioactive elements are given in Table 3-20 and Fig. 3-15, where the levels were found to be normally distributed. The concentrations of ^{238}U , ^{226}Ra , ^{210}Pb , ^{235}U , ^{40}K , ^{228}Ra , ^{228}Th , and ^{232}Th found in the soil samples ranged from 9 - 10, 6 - 9, 7 - 18, 0.4 - 0.55, 179 - 319, 16.9 - 10, 5.8 - 9.1, and 6 - 10 Bq kg^{-1} , respectively, with an average value of 9.8, 7.6, 10.1, 0.5, 245.5, 7.9, 6.9, and 7.4 Bq kg^{-1} , respectively.

Table 3 - 20: Activity concentration of ^{238}U , ^{226}Ra , ^{210}Pb , ^{235}U , ^{40}K , ^{228}Ra , ^{228}Th , and ^{232}Th , [Bq kg^{-1}] in soil profile samples collected from Twenge, North Germany.

| Depth [cm] | Dry density [g cm^{-3}] | U-238 | Ra-226 | Pb-210 | U-235 | K-40 | Ra-228 | Th-228 | Th-232 |
|-------------------|------------------------------------|--------------|-------------|----------------|-----------------|--------------|----------------|---------------|-------------|
| 0-15 | 1.346 | 10 ± 0.4 | 7 ± 0.7 | 10.3 ± 1.8 | 0.48 ± 0.02 | 209 ± 7 | 7.6 ± 0.47 | 6.6 ± 0.8 | 7 ± 0.7 |
| 15-30 | 1.380 | 9 ± 0.1 | 7 ± 0.7 | 9.3 ± 1.8 | 0.43 ± 0.01 | 206 ± 97 | 7.5 ± 0.7 | 6.5 ± 0.9 | 7 ± 0.8 |
| 30-40 | 1.372 | 9 ± 2.03 | 6 ± 0.6 | 7.3 ± 1.6 | 0.40 ± 0.09 | 195 ± 13 | 6.9 ± 0.33 | 5.8 ± 0.9 | 6 ± 0.7 |
| 40-50 | 1.290 | 10 ± 5.3 | 7 ± 0.6 | 5.9 ± 1.6 | 0.45 ± 0.25 | 179 ± 3 | 7.4 ± 0.63 | 6.7 ± 0.9 | 7 ± 0.4 |
| 50-60 | 1.382 | 9 ± 3.6 | 9 ± 3.7 | 6.4 ± 1.3 | 0.43 ± 0.17 | 214 ± 7 | 7.4 ± 0.61 | 6.5 ± 0.8 | 7 ± 0.7 |
| 60-75 | 1.304 | 9 ± 4.7 | 7 ± 0.6 | 5.6 ± 1.3 | 0.40 ± 0.22 | 262 ± 9 | 7.1 ± 0.65 | 6.2 ± 0.7 | 7 ± 0.7 |
| 75-100 | 1.464 | 9 ± 2.3 | 7 ± 0.7 | 6.6 ± 1.4 | 0.39 ± 0.1 | 314 ± 10 | 7.8 ± 0.65 | 6.8 ± 0.8 | 7 ± 0.8 |
| 100-125 | 1.683 | 11 ± 3.3 | 8 ± 0.9 | - | 0.52 ± 0.15 | 319 ± 11 | 8.6 ± 0.69 | 7.5 ± 1 | 8 ± 0.9 |
| 125-150 | 1.746 | 12 ± 6.1 | 9 ± 0.4 | 5.3 ± 1.5 | 0.55 ± 0.28 | 309 ± 10 | 10 ± 0.38 | 9.1 ± 1.3 | 10 ± 1 |
| Range (Min.-Max.) | | 9 - 10 | 6 - 9 | 5.3 - 10 | 10.3 | 179 - 319 | 6.9 - 10 | 5.8 - 9.1 | 6 - 10 |
| Mean | | 9.8 | 7.6 | 7.1 | 9.3 | 245.2 | 7.9 | 6.9 | 7.4 |



| | | | | | | | | |
|------|-----|-----|-----|-----|------|-----|-----|-----|
| S.D. | 1.2 | 1.1 | 1.8 | 7.3 | 56.3 | 1.1 | 1.0 | 1.1 |
|------|-----|-----|-----|-----|------|-----|-----|-----|

Fig. 3-15: Variation of natural radionuclides with depth in depth profile soil from Twenge, Lower Saxony, North Germany.

3.2.1.2 Natural radionuclides in surface soil from Lower Saxony, North Germany.

Table 3 - 21: Activity concentration of ²³⁸U, ²²⁶Ra, ²¹⁰Pb, ²³⁵U, ²²⁸Ra, ²²⁸Th, and ²³²Th, [Bq kg⁻¹] in soil were collected from Lower Saxony, North Germany.

| Site | soil sample Code | Dry density [g cm ⁻³] | U-238 | Ra-226 | Pb-210 | U-235 | Ra-228 | Th-228 | Th -232 |
|--------------|------------------|-----------------------------------|------------|------------|-----------|------------|------------|------------|------------|
| Jeinsen | JeBoEPKr01 | 1.37 | 31 ± 3 | 32.9 ± 1.2 | 84 ± 10 | 1.4 ± 0.1 | 26.2 ± 1.3 | 29.9 ± 1.3 | 28.1 ± 1.3 |
| | JeBoEPKs01 | 1.35 | 18 ± 3 | 33.2 ± 1.2 | 73 ± 9 | 0.8 ± 0.1 | 29.7 ± 1.5 | 28.8 ± 1.3 | 29.2 ± 1.4 |
| | JeBoEPRb01 | 1.28 | 26 ± 3 | 33.9 ± 1.2 | 11 ± 8 | 1.2 ± 0.1 | 33.1 ± 1.5 | 31.7 ± 1.2 | 32.4 ± 1.3 |
| | JeBoEPMa01 | 1.21 | 12 ± 1 | 36.1 ± 1.3 | 2 ± 0.4 | 0.6 ± 0.1 | 28.9 ± 1.3 | 31.8 ± 1.2 | 30.3 ± 1.3 |
| | JeBoEPBr01 | 1.45 | 26 ± 3 | 33.2 ± 1.1 | 57 ± 8 | 1.2 ± 0.1 | 31.9 ± 1.2 | 28.8 ± 1.1 | 30.3 ± 1.1 |
| | JeBoEPLa01 | 1.44 | 26 ± 3 | 33.1 ± 1.1 | 60 ± 7 | 1.2 ± 0.1 | 27.8 ± 1.1 | 28.3 ± 1 | 28.0 ± 1.1 |
| | JeBoEPWk01 | 1.33 | 33 ± 3 | 34.6 ± 1.2 | 55 ± 7 | 1.5 ± 0.1 | 34.0 ± 1.3 | 30.4 ± 1.1 | 32.2 ± 1.2 |
| | JeBoEPEg01 | 1.37 | 27 ± 2 | 32.1 ± 1.1 | 51 ± 4 | 1.2 ± 0.1 | 30.8 ± 1.2 | 31.4 ± 1.6 | 31.1 ± 1.4 |
| | JeBoEPRo01 | 1.37 | 27 ± 2 | 33.2 ± 1.2 | 47 ± 4 | 1.3 ± 0.1 | 32.7 ± 1.3 | 31.4 ± 1.6 | 32.0 ± 1.4 |
| | JeBoEPWeK01 | 1.34 | 30 ± 2 | 32.8 ± 1.2 | 49 ± 4 | 1.4 ± 0.1 | 31.8 ± 1.2 | 32.9 ± 1.6 | 32.3 ± 1.4 |
| | JeBoEKP1 | 1.37 | 54 ± 3 | 31.7 ± 1.1 | 46 ± 4 | 2.5 ± 0.1 | 26.9 ± 1.1 | 26.8 ± 1 | 26.9 ± 1 |
| | JeBoEPPe01 | 1.38 | 51 ± 3 | 30.2 ± 1 | 46 ± 4 | 2.4 ± 0.1 | 25.9 ± 1 | 25.6 ± 1 | 25.7 ± 1 |
| JeBoEPGk01 | 1.27 | 56 ± 3 | 32.5 ± 1.1 | 43 ± 4 | 2.6 ± 0.1 | 28.0 ± 1.1 | 28.5 ± 1.1 | 28.3 ± 1.1 | |
| Neßmerpolder | PoBoEPWe01 | 1.33 | 25 ± 3 | 22.7 ± 0.8 | 41 ± 4 | 1.1 ± 0.1 | 22.9 ± 1.2 | 23.1 ± 0.9 | 23.0 ± 1.1 |
| | PoBoEPWe02 | 1.35 | 23 ± 3 | 23.8 ± 0.9 | 36 ± 4 | 1.1 ± 0.1 | 29.4 ± 1.4 | 26.6 ± 1 | 28.0 ± 1.2 |
| | PoBoMPHa02 | 1.38 | 27 ± 2 | 23.6 ± 0.9 | 41 ± 4 | 1.2 ± 0.1 | 22.8 ± 1.2 | 22.8 ± 0.9 | 22.8 ± 1.1 |
| | PoBoEPRa01 | 1.19 | 26 ± 2 | 26.0 ± 0.9 | 43 ± 5 | 1.2 ± 0.1 | 27.1 ± 1.2 | 27.0 ± 1.1 | 27.1 ± 1.1 |
| | PoBoEPLu02 | 1.29 | 34 ± 3 | 24.2 ± 0.8 | 49 ± 7 | 1.6 ± 0.1 | 30.2 ± 1.1 | 27.6 ± 1 | 28.9 ± 1.1 |

| | PoBoMPHa01 | 1.43 | 27 ± 3 | 26.9 ± 0.9 | 37 ± 7 | 1.3 ± 0.1 | 28.6 ± 1.1 | 28.0 ± 1 | 28.3 ± 1.1 |
|--------------------------------------|------------------|-----------------------------------|---------|------------|----------|-----------|------------|------------|------------|
| Site | soil sample Code | Dry density [g cm ⁻³] | U-238 | Ra-226 | Pb-210 | U-235 | Ra-228 | Th-228 | Th-232 |
| Neßmerpolder | PoBoMPWe01 | 1.39 | 28 ± 3 | 22.8 ± 0.8 | 44 ± 6 | 1.3 ± 0.1 | 24.3 ± 1 | 24.2 ± 0.9 | 24.3 ± 1 |
| | PoBoMPHe01 | 1.18 | 25 ± 2 | 19.5 ± 0.7 | 34 ± 5 | 1.2 ± 0.1 | 24.4 ± 1 | 20.5 ± 0.8 | 22.4 ± 0.9 |
| | PoBoEPHa02 | 1.31 | 30 ± 2 | 25.5 ± 0.9 | 48 ± 4 | 1.4 ± 0.1 | 30.3 ± 1.2 | 30.8 ± 1.6 | 30.5 ± 1.4 |
| | PoBoEPHe02 | 1.20 | 30 ± 3 | 27.3 ± 0.9 | 54 ± 5 | 1.4 ± 0.1 | 33.8 ± 1.3 | 32.8 ± 3.1 | 33.3 ± 2.2 |
| | PoBoMPGe01 | 1.35 | 46 ± 2 | 20.2 ± 0.7 | 34 ± 3 | 2.1 ± 0.1 | 22.6 ± 0.9 | 22.6 ± 0.8 | 22.6 ± 0.9 |
| | PoBoMPLu1 | 1.26 | 47 ± 2 | 21.6 ± 0.7 | 34 ± 3 | 2.2 ± 0.1 | 24.7 ± 1 | 23.9 ± 0.9 | 24.3 ± 1 |
| Schessinghausen | ScBoMPRo01 | 1.39 | 16 ± 2 | 13.9 ± 0.6 | 51 ± 7 | 0.8 ± 0.1 | 13.4 ± 0.8 | 12.1 ± 0.5 | 12.7 ± 0.6 |
| | ScBoMPTr02 | 1.37 | 11 ± 2 | 14.6 ± 0.6 | 5 ± 6 | 0.5 ± 0.1 | 11.1 ± 0.9 | 12.9 ± 0.6 | 12.0 ± 0.7 |
| | ScBoMPRa01 | 1.39 | 33 ± 2 | 13.5 ± 0.5 | 25 ± 2 | 1.5 ± 0.1 | 11.4 ± 0.6 | 10.9 ± 0.4 | 11.2 ± 0.5 |
| | ScBoMPWe01 | 1.40 | 15 ± 2 | 15.9 ± 0.6 | 33 ± 4 | 0.7 ± 0.1 | 14.3 ± 0.8 | 12.4 ± 0.5 | 13.4 ± 0.6 |
| | ScBoMPTr01 | 1.46 | 14 ± 1 | 10.9 ± 0.4 | 23 ± 3 | 0.6 ± 0.1 | 9.3 ± 0.5 | 10.1 ± 0.7 | 9.7 ± 0.6 |
| | ScBoMPWe02 | 1.39 | 16 ± 2 | 16.1 ± 0.6 | 37 ± 4 | 0.8 ± 0.1 | 15.2 ± 0.7 | 15.0 ± 0.9 | 15.1 ± 0.8 |
| | ScBoEPKa01 | 1.38 | 15 ± 1 | 15.1 ± 0.6 | 38 ± 4 | 0.7 ± 0.1 | 15.0 ± 0.7 | 14.0 ± 0.9 | 14.5 ± 0.8 |
| | ScBoEPMa01 | 1.31 | 13 ± 1 | 14.7 ± 0.6 | 39 ± 4 | 0.6 ± 0.1 | 13.3 ± 0.6 | 14.2 ± 1 | 13.8 ± 0.8 |
| Schlewecke | SiBoEPRa01 | 1.34 | 20 ± 2 | 28.5 ± 1 | 37 ± 4 | 0.9 ± 0.1 | 31.4 ± 1.2 | 29.3 ± 1.6 | 30.4 ± 1.4 |
| | SiBoEZu01 | 1.29 | 27 ± 2 | 32.3 ± 1.1 | 58 ± 5 | 1.2 ± 0.1 | 31.3 ± 1.2 | 31.1 ± 1.1 | 31.2 ± 1.2 |
| | SiBoMPGe01 | 1.28 | 52 ± 3 | 29.5 ± 1 | 43 ± 4 | 2.4 ± 0.1 | 28.4 ± 1.8 | 27.0 ± 1 | 27.7 ± 1.1 |
| | SiBoMPGe02 | 1.14 | 37 ± 3 | 41.6 ± 1.4 | 62 ± 6 | 1.7 ± 0.1 | 44.8 ± 1.8 | 46.5 ± 2.2 | 45.7 ± 2 |
| | SiBoMPRa01 | 1.28 | 28 ± 2 | 30.8 ± 1.1 | 41 ± 4 | 1.3 ± 0.1 | 33.9 ± 1.3 | 33.5 ± 1.7 | 33.7 ± 1.5 |
| | SiBoMPWe01 | 1.15 | 36 ± 3 | 40.3 ± 1.4 | 71 ± 6 | 1.6 ± 0.1 | 45.3 ± 1.8 | 42.0 ± 2.1 | 43.6 ± 1.9 |
| | SiBoMPWe02 | 1.21 | 36 ± 3 | 39.5 ± 1.3 | 71 ± 6 | 1.6 ± 0.1 | 42.0 ± 1.6 | 41.0 ± 2.1 | 41.5 ± 1.9 |
| | SiBoEPWe01 | 1.15 | 69 ± 6 | 66.4 ± 2.2 | 139 ± 12 | 3.2 ± 0.3 | 76.1 ± 2.9 | 69.7 ± 3.5 | 72.9 ± 3.2 |
| Gestorf | GeBMPWe01 | 1.27 | 15 ± 1 | 34.2 ± 1.2 | 4 ± 0.5 | 0.7 ± 0.1 | 34.0 ± 1.5 | 33.8 ± 1.3 | 33.9 ± 1.4 |
| | GeBoEPKa01 | 1.31 | 23 ± 3 | 34.2 ± 1.2 | 111 ± 12 | 1.1 ± 0.1 | 30.7 ± 1.4 | 30.8 ± 1.2 | 30.7 ± 1.3 |
| | GeBoEPZu01 | 1.31 | 34 ± 3 | 32.3 ± 1.1 | 60 ± 8 | 1.6 ± 0.2 | 29.5 ± 1.2 | 28.2 ± 1.1 | 28.9 ± 1.1 |
| Gümmer | GuBoEPrh01a | 1.25 | 19 ± 2 | 20.5 ± 0.7 | 53 ± 4 | 0.9 ± 0.1 | 20.2 ± 0.9 | 19.3 ± 1.3 | 19.7 ± 1.1 |
| | GuBoEPrh01b | 1.22 | 21 ± 2 | 22.4 ± 0.8 | 47 ± 4 | 1.0 ± 0.1 | 19.7 ± 0.9 | 19.8 ± 1.3 | 19.7 ± 1.1 |
| Hermannsdorfes LandWerkstätten (HLW) | HLWBoEPHe01 | 1.22 | 25 ± 3 | 29.5 ± 1.1 | 40 ± 5 | 1.1 ± 0.1 | 31.0 ± 1.5 | 31.9 ± 1.2 | 31.5 ± 1.4 |
| | RhBoEPWa01 | 1.12 | 32 ± 3 | 33.1 ± 1.1 | 86 ± 7 | 1.5 ± 0.1 | 36.4 ± 1.5 | 34.2 ± 1.9 | 35.3 ± 1.7 |
| Range (Min.-Max.) | | | 11 - 69 | 10.9 - 66 | 5 - 139 | 0.5 - 3.2 | 9 - 76 | 10 - 69 | 9 - 72 |
| Mean | | | 28.9 | 27.9 | 48.1 | 1.3 | 27.9 | 27.3 | 27.6 |
| S.D. | | | 12.4 | 9.6 | 23.3 | 0.6 | 10.8 | 10.1 | 10.4 |

Fortynine samples of soil at depth of 0 cm - 30 cm were analysed; the activities of radionuclides being given in Table 3-21. The mean activities of ²³⁸U, ²²⁶Ra, ²¹⁰Pb, ²³⁵U, ²²⁸Ra, ²²⁸Th, and ²³²Th were 28.9, 27.9, 48.1, 1.3, 27.9, 27.3, and 27.6 Bq kg⁻¹, respectively.

3.2.2 Natural radionuclides in soil samples from Lippe, North Rhine-Westphalia, Germany.

3.2.2.1 Natural radionuclides in depth profiles soil from Lippe, (North Rhine-Westphalia), Germany.

Results were obtained for two depth sections taken from a selected region of elevated natural radioactivity. Two sample sites were selected from within the region, the sites being denoted as Bp3-30 and Bp4-14.

Table 3 - 22: Bp 4 -14 Activity concentration of ^{238}U , ^{226}Ra , ^{210}Pb , ^{235}U , ^{40}K , ^{228}Ra , ^{228}Th , and ^{232}Th [Bq kg^{-1}] in soil collected from Lippe, North Rhine-Westphalia, Germany.

| Depth [cm] | Dry density [g cm^{-3}] | U-238 | Ra-226 | Pb-210 | U-235 | K-40 | Ra-228 | Th-228 | Th-232 |
|-------------------|------------------------------------|---------|-----------|-----------|---------|-----------|----------|----------|----------|
| 0-2 | 0.95 | 29 | 319 ± 16 | 138 ± 26 | 0.7 | 424 ± 175 | 117 ± 12 | 96 ± 9 | 106 ± 10 |
| 2-4 | 0.93 | 22 | 385 ± 19 | 158 ± 28 | 1.0 | 362 ± 166 | 133 ± 13 | 116 ± 11 | 125 ± 12 |
| 4-6 | 0.91 | 43 | 413 ± 21 | 175 ± 29 | 0.8 | 369 ± 172 | 131 ± 13 | 121 ± 12 | 126 ± 12 |
| 6-10 | 0.91 | 23 | 417 ± 21 | 193 ± 31 | 0.8 | 403 ± 179 | 101 ± 10 | 116 ± 11 | 108 ± 11 |
| 10-15 | 0.93 | 23 | 363 ± 18 | 195 ± 29 | 0.7 | 357 ± 199 | 69 ± 7 | 83 ± 8 | 76 ± 8 |
| 15-20 | 1.01 | 23 | 280 ± 14 | 200 ± 29 | 0.9 | 346 ± 189 | 46 ± 5 | 52 ± 5 | 49 ± 5 |
| 20-30 | 0.95 | 22 | 267 ± 13 | 217 ± 30 | 0.9 | 359 ± 198 | 33 ± 4 | 37 ± 4 | 35 ± 4 |
| Range (Min.-Max.) | | 22 - 43 | 280 - 417 | 138 - 200 | 0.7 - 1 | 346 - 424 | 33 - 133 | 37 - 121 | 35 - 126 |
| Mean | | 26.5 | 349.1 | 182.4 | 0.8 | 374.2 | 90.1 | 88.5 | 89.3 |
| S.D. | | 7.4 | 61.4 | 27.1 | 0.1 | 28.4 | 40.8 | 33.3 | 36.5 |

Samples of soil at different depths were analysed; the activities of given in Table 3-22. The mean activities of ^{238}U , ^{226}Ra , ^{210}Pb , ^{235}U , ^{40}K , ^{228}Ra , ^{228}Th and ^{232}Th , were 26.5, 349.1, 182.4, 0.8, 374.2, 90.1, 88.5, and 89.3 Bq kg^{-1} , respectively. The concentrations of U and Th-series radionuclides were observed to be higher at the 4-6 cm depth than that of 0-2 cm depth, but the concentrations of potassium were almost equal in both layers of soil. The activity of ^{232}Th was higher than that of ^{238}U in all the samples,

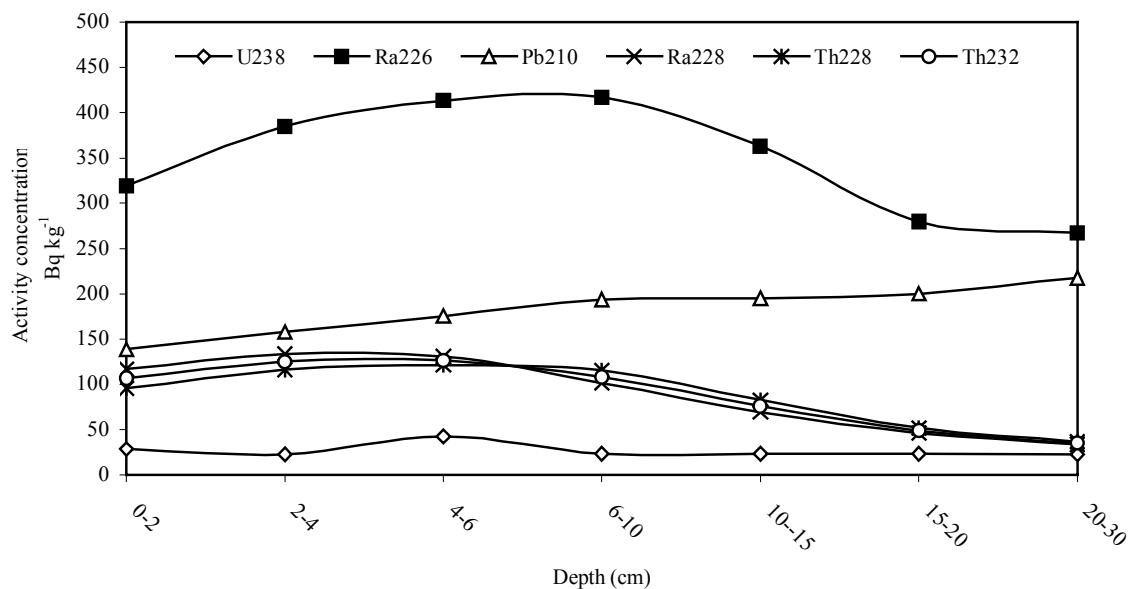


Fig. 3-16: Variation of natural radionuclides with depth in depth profile soil from Lippe (North Rhine-Westphalia), Germany.

The concentrations of ^{226}Ra , ^{210}Pb , and uranium in the soil of each sites are given in the top portions of Tables 3-22 and B-11. It can be seen that most of the soil activity was concentrated in the upper 15 cm (humus layer), with intermediate values in the middle layer.

Concentrations in the deepest layer generally differed little from those in the top layers. This suggests that the excess activity was introduced by contaminated top soil brought in from other sites within the community. The upper layer of soil showed an excess of ^{226}Ra with respect to its precursor ^{238}U and its descendant, ^{210}Pb . This disequilibrium in the ^{238}U series was confirmed by γ spectroscopic studies [Tra83]. As the activity of ^{226}Ra is less variable with depth given the generally accepted concept that radium is less mobile than uranium in the surface environment, it would initially appear that uranium mobilisation and loss relative to radium is the cause of the disequilibrium exhibited at these sites [Dow02].

Greeman and Rose [Gre90] studied radioactive disequilibrium in the ^{238}U series for a number of soils and concluded that, in the surface horizons of some soils, ^{226}Ra excess could be attributed to the cycling of ^{226}Ra by plants, leading to an increase in the isotope relative to ^{238}U . Von Gunten, Surbeck, and Rossler [Gun96] observed ^{226}Ra activities a factor of 20 above the activity of ^{238}U in a Karst region of Switzerland and proposed that, following continuous weathering of calcite particles, uranium was lost from the soil as the soluble carbonate complex, ^{226}Ra being retained within the soil. De Jong, Acton and Kozak [Jon93] hypothesised that the $^{226}\text{Ra}/^{238}\text{U}$ disequilibrium in a Saskatchewan soil was probably due to the mode of deposition of the parent material rather than subsequent selective leaching of members of the series.

3.2.2.2 Natural radionuclides in surface soil samples from Lippe, (North Rhine-Westphalia), Germany.

Table 3 - 23: Activity concentration of ^{238}U , ^{226}Ra , ^{210}Pb , ^{235}U , ^{228}Ra , ^{228}Th , and ^{232}Th [Bq kg^{-1}] in soil collected from Lippe, North Rhine-Westphalia, Germany.

| Soil sample No. | Dry density [g cm^{-3}] | U-238 | Ra-226 | Pb-210 | U-235 | Ra-228 | Th-228 | Th-232 |
|-----------------|------------------------------------|-------|----------|----------|-------|-----------|---------|---------|
| BP 2-04f | 1.0 | - | 344 ± 8 | 176 ± 23 | - | 111 ± 3.3 | 92 ± 2 | 101 ± 3 |
| BP 2-05f | 0.9 | - | 155 ± 4 | 203 ± 23 | - | 76 ± 1.2 | 48 ± 8 | 62 ± 5 |
| BP 2-06f | 1.0 | - | 170 ± 3 | 93 ± 15 | - | 65 ± 0.1 | 56 ± 2 | 61 ± 1 |
| BP 2-07f | 1.1 | 11.5 | 67 ± 4 | 74 ± 13 | 0.53 | 22 ± 3.3 | 21 ± 2 | 21 ± 3 |
| BP 2-11f | 0.9 | 13.0 | 123 ± 7 | 143 ± 21 | 0.60 | 67 ± 6.3 | 51 ± 5 | 59 ± 6 |
| BP 2-12f | 1.1 | - | 164 ± 3 | 85 ± 20 | - | 50 ± 2.3 | 49 ± 4 | 50 ± 3 |
| BP 2-13f | 1.2 | - | 88 ± 3 | 50 ± 15 | - | 26 ± 1.3 | 24 ± 1 | 25 ± 1 |
| BP 2-17f | 1.1 | - | 342 ± 7 | 96 ± 22 | - | 146 ± 6 | 101 ± 3 | 123 ± 5 |
| BP 2-23f | 0.9 | 18.5 | 197 ± 11 | 143 ± 24 | 0.85 | 88 ± 8.5 | 63 ± 7 | 76 ± 8 |
| BP 2-24f | 1.1 | - | 259 ± 14 | 122 ± 22 | - | 102 ± 8.7 | 83 ± 8 | 93 ± 8 |
| BP 2-25f | 1.3 | - | 44 ± 2 | 52 ± 13 | - | 19 ± 1.5 | 22 ± 2 | 21 ± 2 |
| BP 2-33f | 1.1 | - | 55 ± 3 | 30 ± 11 | - | 35 ± 2.2 | 31 ± 4 | 33 ± 3 |
| BP 2-34f | 1.3 | 9.6 | 21 ± 1 | 40 ± 9 | 0.44 | 16 ± 2.4 | 13 ± 2 | 15 ± 2 |
| BP 2-35f | 1.2 | 12.3 | 26 ± 1 | 47 ± 10 | 0.57 | 20 ± 2.6 | 14 ± 2 | 17 ± 2 |
| BP 2-36f | 1.1 | - | 272 ± 4 | 84 ± 20 | 0.00 | 62 ± 6.4 | 63 ± 5 | 63 ± 6 |
| BP 3-01 | 1.1 | 19.2 | 278 ± 14 | 149 ± 21 | 0.89 | 96 ± 9.4 | 75 ± 7 | 85 ± 8 |
| BP 3-02 | 1.1 | 19.3 | 71 ± 4 | 93 ± 12 | 0.89 | 21 ± 2.3 | 20 ± 2 | 20 ± 2 |
| BP 3-03 | 1.3 | 14.6 | 23 ± 1 | 24 ± 12 | 0.67 | 20 ± 2.2 | 19 ± 2 | 20 ± 2 |
| BP 3-04 | 1.0 | 15.9 | 239 ± 12 | 150 ± 25 | 0.73 | 61 ± 6.1 | 63 ± 6 | 62 ± 6 |
| BP 3-05 | 0.9 | 13.4 | 208 ± 10 | 129 ± 23 | 0.62 | 54 ± 5.5 | 56 ± 5 | 55 ± 5 |
| BP 3-06 | 1.1 | 26.8 | 34 ± 2 | 81 ± 12 | 1.24 | 37 ± 3.9 | 34 ± 3 | 36 ± 3 |

| Soil sample No. | Dry density [g cm ⁻³] | U-238 | Ra-226 | Pb-210 | U-235 | Ra-228 | Th-228 | Th-232 |
|-------------------|-----------------------------------|-----------|----------|----------|------------|------------|------------|----------|
| BP 3-09 | 1.2 | 21.6 | 29 ± 2 | 48 ± 6 | 1.00 | 22 ± 2.3 | 20 ± 2 | 21 ± 2 |
| BP 3-07 | 0.9 | 20.2 ± 5 | 520 ± 28 | 372 ± 30 | 0.93 | 96 ± 5 | 105 ± 5 | 100 ± 5 |
| BP 3-08 | 1.0 | 23.8 ± 4 | 189 ± 10 | 277 ± 21 | 1.09 | 35 ± 1.5 | 33 ± 6 | 34 ± 4 |
| BP 3-10 | 0.9 | 20.4 ± 4 | 225 ± 9 | 244 ± 21 | 0.94 | 48 ± 5 | 41 ± 6 | 45 ± 6 |
| BP 3-11 | 0.9 | 17.5 ± 2 | 82 | 205 ± 17 | 0.81 | 61 ± 4.3 | 64 ± 8 | 62 ± 6 |
| BP 3-12 | 1.0 | 13.5 ± 4 | 380 ± 21 | 305 ± 23 | 0.62 | 45 ± 5.8 | 51 ± 5 | 48 ± 5 |
| BP 3-13 | 1.0 | 22.1 ± 3 | 194 ± 8 | 318 ± 23 | 1.02 | 40 ± 10.2 | 28 ± 3 | 34 ± 7 |
| BP 3-14 | 1.2 | 16.6 ± 20 | 37 ± 2 | 50 ± 7 | 0.76 | 18 ± 1.1 | 17 ± 1 | 17 ± 1 |
| BP 3-15 | 1.0 | 34.0 ± 5 | 343 ± 20 | 310 ± 25 | 1.56 | 63 ± 3.2 | 70 ± 1 | 67 ± 2 |
| BP 3-16 | 1.1 | 12.4 ± 3 | 238 ± 12 | 169 ± 15 | 0.57 | 54 ± 3.6 | 50 ± 2 | 52 ± 3 |
| BP 3-17 | 1.1 | 14.2 ± 16 | 15 ± 1 | 53 ± 7 | 0.65 | 12 ± 0.4 | 10 ± 1 | 11 ± 1 |
| BP 3-18 | 0.8 | 23.9 ± 2 | 37 ± 3 | 103 ± 10 | 1.10 | 20 ± 1.4 | 20 ± 3 | 20 ± 2 |
| BP 3-21 | 1.4 | 15.7 ± 2 | 89 ± 4 | 90 ± 12 | 0.72 | 13 ± 1.5 | 13 ± 1 | 13 ± 1 |
| BP 3-22 | 1.0 | 22.9 | 81 ± 4 | 103 ± 17 | 1.06 | 22 ± 2.4 | 20 ± 2 | 21 ± 2 |
| BP 3-23 | 1.0 | 9.9 ± 3 | 179 ± 11 | 208 ± 17 | 0.46 | 20 ± 1.2 | 21 ± 2 | 21 ± 2 |
| BP 3-24 | 1.1 | 17.2 | 36 ± 2 | 64 ± 9 | 0.79 | 15 ± 1.7 | 13 ± 1 | 14 ± 1 |
| BP 3-25 | 1.0 | 15.2 ± 3 | 182 ± 9 | 193 ± 17 | 0.70 | 29 ± 3.1 | 30 ± 3 | 29 ± 3 |
| BP 3-26 | 1.2 | 17.5 ± 2 | 74 ± 4 | 111 ± 11 | 0.81 | 17 ± 1.8 | 15 ± 2 | 16 ± 2 |
| BP 3-28 | 1.1 | 14.2 ± 2 | 99 ± 5 | 139 ± 12 | 0.65 | 18 ± 1.4 | 20 ± 1 | 19 ± 1 |
| BP 3-29 | 1.0 | 10.3 ± 3 | 151 ± 8 | 178 ± 15 | 0.47 | 23 ± 1.7 | 23 ± 2 | 23 ± 2 |
| BP 4-01 | 0.9 | 40.6 | 214 ± 11 | 170 ± 25 | 1.87 | 42 ± 4.3 | 47 ± 4.1 | 44 ± 4 |
| BP 4-05 | 0.8 | 17.2 ± 5 | 545 ± 31 | 274 ± 24 | 0.79 | 108 ± 6.2 | 115 ± 13.1 | 112 ± 10 |
| BP 4-06 | 1.0 | 36.7 ± 3 | 87 ± 5 | 122 ± 12 | 1.69 | 46 ± 3 | 45 ± 1.1 | 45 ± 2 |
| BP 4-09 | 1.2 | 15.3 ± 2 | 77 ± 4 | 102 ± 10 | 0.71 | 14 ± 1.3 | 14 ± 0.6 | 14 ± 1 |
| BP 4-10 | 1.2 | 25.5 ± 3 | 164 ± 10 | 165 ± 14 | 1.17 | 22 ± 2.1 | 25 ± 2.2 | 24 ± 2 |
| BP 4-11 | 1.1 | 14.6 ± 3 | 222 ± 12 | 163 ± 15 | 0.67 | 34 ± 4.1 | 39 ± 0.5 | 37 ± 2 |
| BP 4-12 | 1.3 | 23.1 ± 2 | 35 ± 2 | 59 ± 7 | 1.06 | 17 ± 1.7 | 18 ± 1.4 | 18 ± 2 |
| BP 4-15 | 0.9 | 25.8 ± 3 | 193 ± 11 | 269 ± 21 | 1.19 | 47 ± 2.8 | 46 ± 7.3 | 46 ± 5 |
| BP 4-16 | 1.2 | 20.5 ± 3 | 38 ± 2 | 45 ± 6 | 0.94 | 14 ± 1.2 | 11 ± 1.1 | 13 ± 1 |
| BP Sicking. (71) | 1.0 | 16.1 | 572 ± 28 | 190 ± 27 | 0.74 | 139 ± 9.7 | 134 ± 12.6 | 137 ± 11 |
| BP Vorfluter (70) | 1.3 | - | 741 ± 36 | 215 ± 28 | - | 159 ± 11.1 | 149 ± 14 | 154 ± 13 |
| BP 5-01 | 0.9 | 8.1 | 201 ± 4 | 197 ± 3 | 0.37 | 28 ± 0.7 | 29 ± 1 | 29 ± 1 |
| BP 5-02 | 1.2 | 8.2 | 161 ± 8 | 150 ± 22 | 0.38 | 24 ± 2.6 | 27 ± 2.5 | 25 ± 3 |
| BP 5-03 | 1.0 | 19.0 | 218 ± 4 | 185 ± 3 | 0.88 | 41 ± 0.1 | 46 ± 0.8 | 43 ± 1 |
| BP 5-04 | 1.0 | 27.8 | 238 ± 12 | 197 ± 28 | 1.28 | 43 ± 4.6 | 46 ± 4.5 | 45 ± 5 |
| BP 5-05 (Sedi) | 1.5 | - | 73 ± 4 | 82 ± 16 | - | 19 ± 2 | 16 ± 1.5 | 17 ± 2 |
| BP 5-06 | 0.9 | 22.4 | 257 ± 13 | 188 ± 28 | 1.03 | 56 ± 5.8 | 61 ± 5.8 | 59 ± 6 |
| BP 5-07 | 0.9 | 20.6 | 191 ± 10 | 156 ± 24 | 0.95 | 41 ± 4.3 | 45 ± 4.2 | 43 ± 4 |
| BP 5-08 | 1.0 | 14.0 | 265 ± 13 | 167 ± 26 | 0.65 | 54 ± 5.5 | 62 ± 5.9 | 58 ± 6 |
| BP 5-09 | 1.0 | 13.6 | 243 ± 12 | 155 ± 25 | 0.62 | 58 ± 5.9 | 63 ± 6 | 61 ± 6 |
| BP 5-10 | 1.0 | 13.2 | 391 ± 19 | 183 ± 30 | 0.61 | 105 ± 10.5 | 109 ± 10.2 | 107 ± 10 |
| BP 5-11 | 1.3 | 13.5 | 13 ± 1 | 33 ± 9 | 0.62 | 11 ± 1.3 | 10 ± 1 | 10 ± 1 |
| Range (Min.-Max.) | | 8 - 36.7 | 13 - 572 | 30 - 372 | 0.37 - 1.8 | 11 - 159 | 10 - 149 | 10 - 154 |

The results for 49 soil samples from Lippe are shown in Table 3-23. No equilibrium between uranium isotopes and its daughters is evident. The 'uranium series disequilibrium ratio' (i.e. the ratio of ²²⁶Ra soil activity concentration to ²³⁸U soil activity concentration) was also

measured, and the results are plotted in Figure 3-16. These values are a measure of the degree of uranium series disequilibrium in soils, and are in the range 8-36.7, with most of the country lying in the interval 0.5-2.0. It is interesting to note that the strongest disequilibrium lies in areas where ^{226}Ra concentrations are highest.

The reasons for elevated ^{226}Ra and uranium series disequilibrium are very complex and are not well understood at this time. However, qualitative associations may be made with local geological structures [McA92].

3.2.3 Natural radionuclides in depth profiles from Ukraine

Table 3- 24: Activity concentration of ^{238}U , ^{226}Ra , ^{210}Pb , ^{235}U , ^{40}K , ^{228}Ra , ^{228}Th , and ^{232}Th [Bq kg^{-1}] in soil collected from Tschigiri 2, Ukraine.

| Depth [cm] | Dry density [g cm^{-3}] | U-238 | Ra-226 | Pb-210 | U-235 | K-40 | Ra-228 | Th-228 | Th-232 |
|-------------------|------------------------------------|------------|---------|----------|------------|-----------|---------|---------|---------|
| humus soil | 0.89 | 30.9 ± 14 | 26 ± 4 | 128 ± 23 | 1.43 ± 0.6 | 324 ± 14 | 21 ± 6 | 18 ± 3 | 20 ± 5 |
| 0-1 | 1.15 | 20.0 ± 11 | 19 ± 3 | 41 ± 16 | 0.92 ± 0.5 | 321 ± 13 | 24 ± 6 | 13 ± 2 | 22 ± 5 |
| 1-2 | 2.20 | 18.7 ± 11 | 17 ± 2 | 51 ± 20 | 0.86 ± 0.5 | 306 ± 12 | 20 ± 3 | 22 ± 5 | 19 ± 3 |
| 2-3 | 1.40 | nd | 20 ± 2 | 69 ± 17 | 0.05 ± 0.4 | 325 ± 13 | 25 ± 3 | 20 ± 2 | 23 ± 2 |
| 3-5 | 1.56 | 8.6 ± 5 | 25 ± 2 | 23 ± 6 | 0.40 ± 0.2 | 342 ± 13 | 21 ± 2 | 22 ± 3 | 22 ± 3 |
| 5-10 | 1.56 | 16.2 ± 4 | 18 ± 2 | 26 ± 5 | 0.75 ± 0.2 | 340 ± 13 | 22 ± 2 | 23 ± 4 | 22 ± 3 |
| 15-10 | 1.59 | 7.5 ± 4 | 21 ± 2 | 21 ± 4 | 0.34 ± 0.2 | 349 ± 13 | 21 ± 2 | 21 ± 4 | 21 ± 3 |
| 15-20 | 1.73 | 7.5 ± 3 | 19 ± 1 | 22 ± 5 | 0.35 ± 0.1 | 333 ± 12 | 21 ± 2 | 17 ± 2 | 19 ± 2 |
| 20-25 | 1.71 | nd | 22 ± 2 | 24 ± 5 | 0.04 ± 0.1 | 366 ± 14 | 21 ± 3 | 21 ± 5 | 21 ± 4 |
| 25-40 | 1.83 | 14.4 ± 3 | 19 ± 1 | 17 ± 5 | 0.66 ± 0.1 | 389 ± 14 | 23 ± 2 | 22 ± 2 | 23 ± 2 |
| Range (Min.-Max.) | | 7.5 – 30.9 | 17 - 26 | 17 - 128 | 0.04 - 1.4 | 306 - 389 | 20 - 25 | 13 - 23 | 19 - 23 |
| Mean | | | 20 ± 4 | 42 ± 10 | 0.58 ± 0.3 | 340 ± 13 | 21 ± 3 | 20 ± 3 | 21 ± 3 |

The activity of ^{40}K in the depth profile soil ranged from 306 ± 12 to $389 \pm 14 \text{ Bq kg}^{-1}$ with a mean activity of $340 \pm 13 \text{ Bq kg}^{-1}$.

The study shows that the concentrations of Th and U-series radionuclides and ^{40}K in the Tschigiri2 depth profile soil is higher than the Christinovka meadow depth profile soil. The concentration of ^{232}Th is the same range that of ^{238}U in this site.

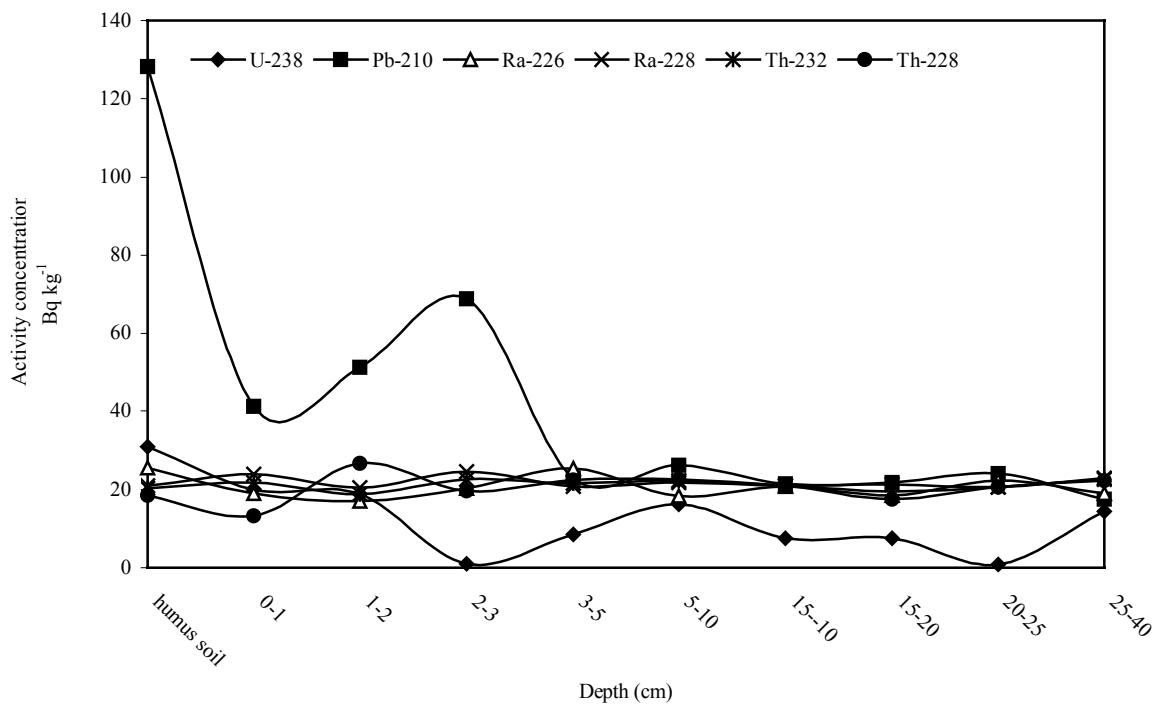


Fig. 3-17: Variation of natural radionuclides with depth in depth profile soil from Tschigiri 2, Ukraine.

Table3-25: Activity concentration of ^{238}U , ^{226}Ra , ^{210}Pb , ^{235}U , ^{40}K , ^{228}Ra , ^{228}Th , and ^{232}Th [Bq kg^{-1}] in soil collected from Oserjanka 1, Ukraine.

| Depth [cm] | Dry density [g cm^{-3}] | U-238 | Ra-226 | Pb-210 | U-235 | K-40 | Ra-228 | Th-228 | Th-232 |
|-------------------|------------------------------------|------------|------------|--------------|----------------|--------------|------------|------------|------------|
| humus soil | 0.62 | 28 ± 9 | 19 ± 3 | 177 ± 18 | 1.3 ± 0.4 | 236 ± 13 | 19 ± 4 | 17 ± 2 | 18 ± 3 |
| 0-1 | 0.68 | 53 ± 9 | 17 ± 2 | 189 ± 23 | 2.4 ± 0.4 | 280 ± 14 | 25 ± 3 | 22 ± 4 | 23 ± 4 |
| 1-2 | 0.97 | 37 ± 8 | 14 ± 1 | 146 ± 17 | 1.7 ± 0.4 | 233 ± 11 | 18 ± 3 | 15 ± 1 | 17 ± 2 |
| 2-3 | 0.85 | 25 ± 6 | 15 ± 2 | 92 ± 13 | 1.2 ± 0.3 | 204 ± 10 | 20 ± 3 | 18 ± 1 | 19 ± 2 |
| 3-5 | 0.88 | 54 ± 7 | 21 ± 3 | 90 ± 13 | 2.5 ± 0.3 | 284 ± 13 | 27 ± 3 | 25 ± 2 | 26 ± 2 |
| 5-10 | 0.82 | 53 ± 8 | 16 ± 2 | 87 ± 16 | 2.5 ± 0.4 | 238 ± 12 | 23 ± 3 | 16 ± 1 | 20 ± 2 |
| 15-10 | 0.79 | 37 ± 7 | 17 ± 2 | 86 ± 16 | 1.7 ± 0.3 | 194 ± 11 | 22 ± 3 | 15 ± 1 | 19 ± 2 |
| 15-20 | 0.86 | 35 ± 8 | 18 ± 2 | 82 ± 18 | 1.6 ± 0.4 | 255 ± 13 | 18 ± 3 | 18 ± 1 | 18 ± 3 |
| 20-25 | 0.85 | 32 ± 7 | 14 ± 1 | 30 ± 11 | 1.5 ± 0.3 | 247 ± 12 | 13 ± 3 | 13 ± 1 | 13 ± 2 |
| 25-40 | 0.77 | 35 ± 8 | 16 ± 2 | 48 ± 12 | 1.6 ± 0.4 | 189 ± 11 | 25 ± 4 | 20 ± 1 | 24 ± 4 |
| Range (Min.-Max.) | | 25 - 54 | 14 - 21 | 30 - 189 | 1.5 - 2.5 | 189 - 284 | 13 - 27 | 13 - 25 | 13 - 26 |
| mean | | 38 ± 8 | 17 ± 2 | 102 ± 15 | 1.78 ± 0.3 | 236 ± 12 | 18 ± 2 | 18 ± 2 | 20 ± 3 |

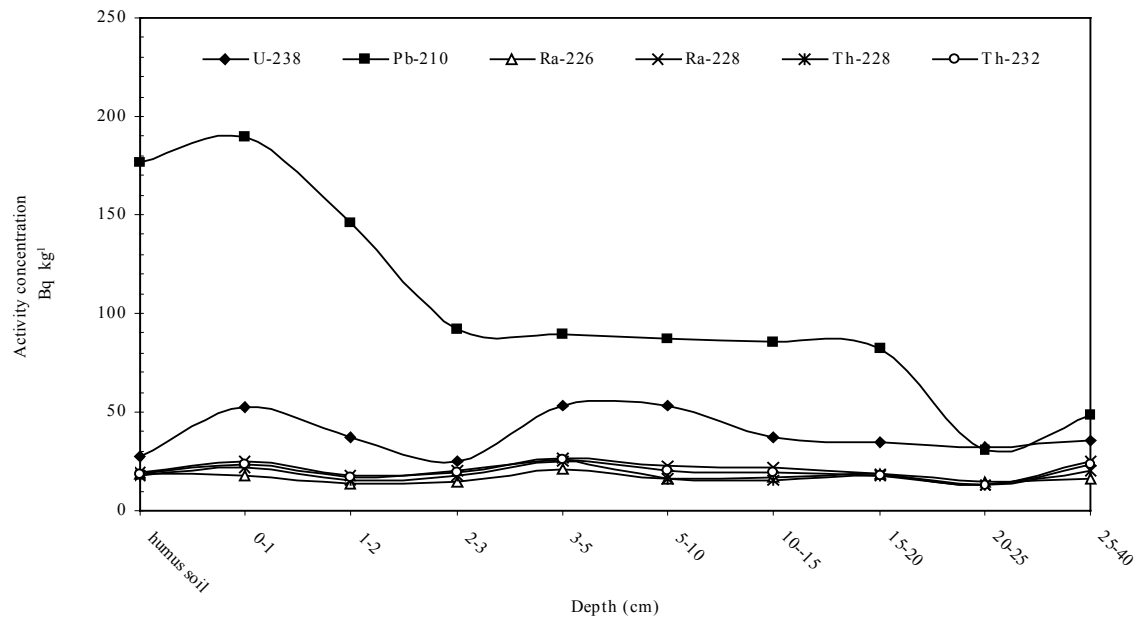


Fig. 3-18: Variation of natural radionuclides with depth in depth profile soil from Oserjanke1, Ukraine.

The soil properties prevent the radionuclides of the ^{238}U -series from reaching deeper soil profiles. The same behaviour was observed for ^{40}K as well. No influence was observed for ^{232}Th , which was found in low concentrations in the coal [Flu02].

Table 3 - 26: Natural radionuclide content in soil from UNSEARA 2000 [UNS00].

| Region/country | Concentration in soil (Bq kg^{-1}) | | | | | | | |
|--------------------|-----------------------------------------------|------------|------------------|----------|-------------------|----------|-------------------|----------|
| | ^{40}K | | ^{238}U | | ^{226}Ra | | ^{232}Th | |
| | Mean | Range | Mean | Range | Mean | Range | Mean | Range |
| Africa | | | | | | | | |
| Algeria | 370 | 66 - 1150 | 30 | 2 - 110 | 50 | 5 - 180 | 25 | 2 - 140 |
| Egypt | 320 | 29 - 650 | 37 | 6 - 120 | 17 | 5 - 64 | 18 | 2 - 96 |
| North America | | | | | | | | |
| Costa Rica | 140 | 6 - 380 | 46 | 11 - 130 | 46 | 11 - 130 | 11 | 1 - 42 |
| United States [M7] | 370 | 100 - 700 | 35 | 4 - 140 | 40 | 8 - 160 | 35 | 4 - 130 |
| South America | | | | | | | | |
| Argentina | 650 | 540 - 750 | - | - | - | - | - | - |
| East Asia | | | | | | | | |
| Bangladesh | 350 | 130 - 610 | - | - | 34 | 21 - 43 | - | - |
| China [PI 6, Z5] | 440 | 9 - 1800 | 33 | 2 - 690 | 32 | 2 - 440 | 41 | 1 - 360 |
| -HongKongSAR[W12] | 530 | 80 - 1100 | 84 | 25 - 130 | 59 | 20 - 110 | 95 | 16 - 200 |
| India | 400 | 38 - 760 | 29 | 7 - 81 | 29 | 7 - 81 | 64 | 14 - 160 |
| Japan [M5] | 310 | 15 - 990 | 29 | 2 - 59 | 33 | 6 - 98 | 28 | 2 - 88 |
| Kazakstan | 300 | 100 - 1200 | 37 | 12 - 120 | 35 | 12 - 120 | 60 | 10 - 220 |
| Korea, Rep. of | 670 | 17 - 1500 | - | - | - | - | - | - |
| Malaysia | 310 | 170 - 430 | 66 | 49 - 86 | 67 | 38 - 94 | 82 | 63 - 110 |
| Thailand | 230 | 7 - 712 | 114 | 3 - 370 | 48 | 11 - 78 | 51 | 7 - 120 |

3.3 Elemental correlation, equilibrium and disequilibrium for natural radionuclides in depth profile and surface soil samples.

The results of soil samples were collected from different sites in Lower Saxony, Germany, (see Fig 2-4 and Tables A-1, A-3 in appendix A), depth profiles and surface soil.

3.3.1 Elemental correlation for natural radionuclides in depth profile and surface soil samples from Lower Saxony, North Germany.

The results of the depth profiles studies of radionuclides correlation between of ^{238}U , ^{226}Ra , ^{210}Pb , ^{40}K , ^{228}Ra , ^{228}Th , and ^{232}Th are presented in Tables 3-26, 3-27 and 3-28, of Ricklingen, Eilenriede, and Twenge, respectively, for different depths profiles.

3.3.1.1 Depth profiles soil samples from Lower Saxony, North Germany.

Table 3 - 27: Elemental correlation between natural radionuclides in soil samples from Lower Klein Lobke, Saxony, North Germany.

| Depth (cm) | Dry density [g cm ⁻³] | $^{238}\text{U}/^{40}\text{K}$ | $^{232}\text{Th}/^{40}\text{K}$ | $^{232}\text{Th}/^{238}\text{U}$ | $^{228}\text{Ra}/^{228}\text{Th}$ | $^{210}\text{Pb}/^{226}\text{Ra}$ | $^{226}\text{Ra}/^{238}\text{U}$ |
|------------|-----------------------------------|--------------------------------|---------------------------------|----------------------------------|-----------------------------------|-----------------------------------|----------------------------------|
| 0-15 | 1.28 | 0.06 | 0.05 | 0.86 | 1.1 | 1.56 | 0.74 |
| 15-30 | 1.25 | 0.05 | 0.05 | 1.14 | 1.0 | 1.68 | 0.99 |
| 30-40 | 1.18 | 0.04 | 0.06 | 1.32 | 1.1 | 1.72 | 1.11 |
| 40-50 | 1.25 | 0.04 | 0.05 | 1.60 | 1.1 | 1.51 | 1.29 |
| 50-70 | 1.48 | 0.04 | 0.04 | 1.20 | 1.1 | 1.30 | 0.93 |
| 70-90 | 1.27 | 0.04 | 0.07 | 1.32 | 1.1 | 1.21 | 0.92 |
| 90-105 | 1.36 | 0.04 | 0.04 | 1.35 | 1.1 | 1.15 | 1.09 |
| 105-130 | 1.24 | 0.03 | 0.06 | 1.27 | 1.1 | 1.38 | 1.05 |
| 130-150 | 1.27 | 0.04 | 0.06 | 1.36 | 1.1 | 1.48 | 1.10 |
| 150-200 | 1.29 | 0.05 | 0.04 | 1.18 | 1.1 | 1.09 | 1.03 |
| 200-250 | 1.35 | 0.05 | 0.04 | 0.93 | 1.1 | 1.62 | 0.85 |
| Mean | | 0.04 | 0.05 | 1.23 | 1.09 | 1.43 | 1.01 |

Relationships between the concentration of ^{238}U , ^{226}Ra , ^{210}Pb , ^{40}K , ^{228}Ra , ^{228}Th , and ^{232}Th are shown in Fig.3-19 and Table 3-27. Although Fig. 3-19(a) and (b) show some scatter in the concentrations of ^{232}Th and ^{238}U versus the ^{40}K content. The concentrations of ^{232}Th and ^{238}U increase with increase in the ^{40}K content. The scattering of the concentration of ^{232}Th and ^{238}U to the ^{40}K content may be explained by the surface area of soil particles [Meg88].

Fig. 3-19(d) and (f) the $^{228}\text{Ra}/^{228}\text{Th}$ and $^{226}\text{Ra}/^{238}\text{U}$ concentration ratios were evaluated from the measured values of activity concentrations. Although the activity ratios are found to have a wide range, the mean values for eleven different depths are almost the same. The mean values $^{228}\text{Ra}/^{228}\text{Th}$ and $^{226}\text{Ra}/^{238}\text{U}$ ratios for different depth soils of Klein Lobke are 1.09 there is equilibrium between thorium series and the mean $^{226}\text{Ra}/^{238}\text{U}$ ratio 1.01 in the depth profile soil samples indicate the status of the radioactive secular equilibrium between ^{226}Ra and ^{238}U in these soil.. The mean ratio $^{232}\text{Th}/^{238}\text{U}$ is and 1.23 for the Klein Lobke soil.

The highly significant correlation occurring between uranium and thorium is consistent with the geochemical behaviour of their complexes, namely, the tendency of uranium and thorium to concentrate in the fluid phase during magma tic differentiation. Uranium and thorium,

with their daughters present in rock and soil, are the main contributors to the absorbed dose rate in air and, hence, to the dose absorbed by the population [Bra92].

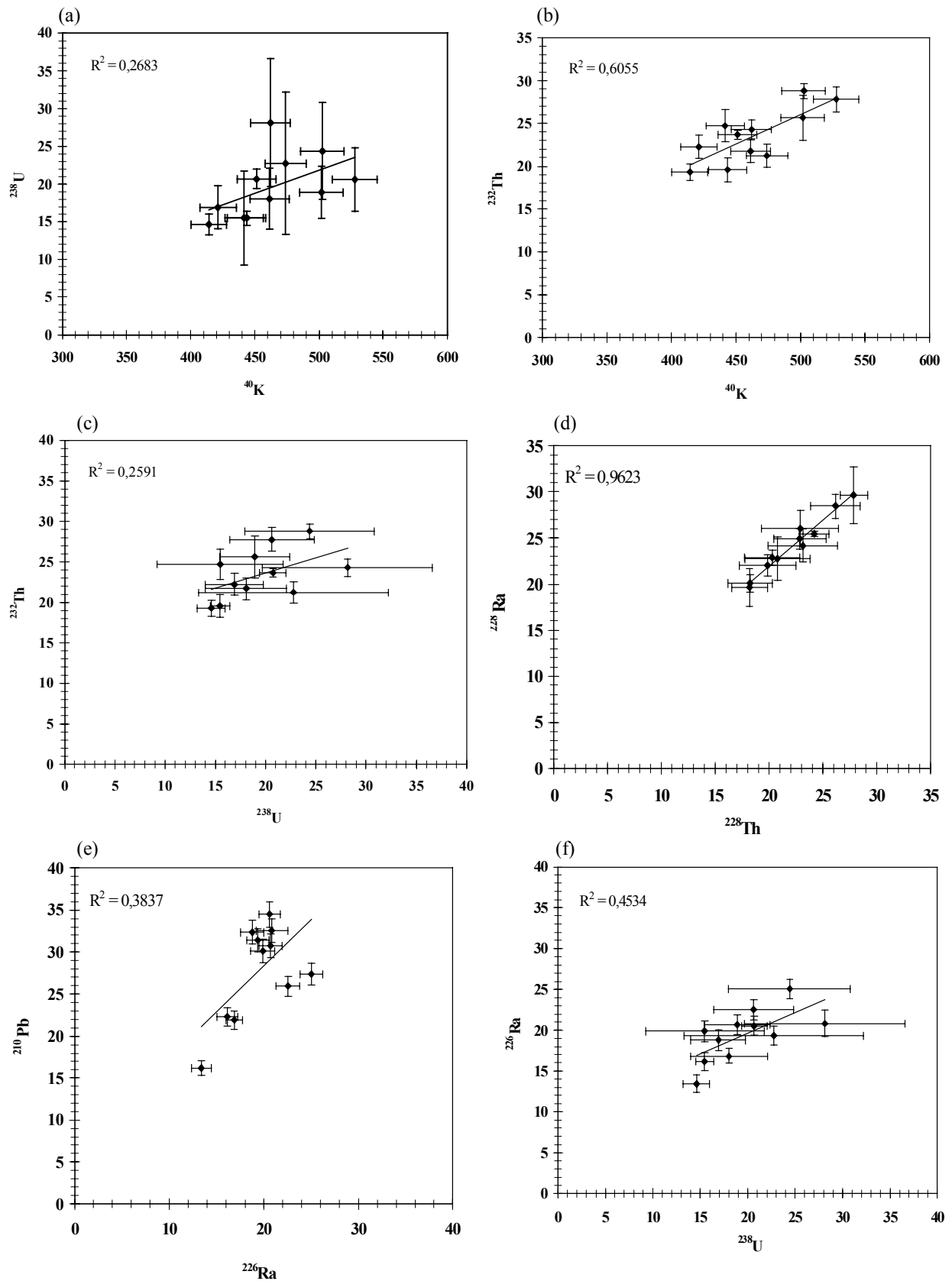


Fig. 3-19: Elemental correlation between natural radionuclides in soil samples from Klein Lobke, Lower Saxony, North Germany.

Table 3 - 28: Elemental correlation between natural radionuclides in soil samples from Ricklingen, Lower Saxony, North Germany.

| Depth (cm) | Dry density [g cm ⁻³] | ²³⁸ U/ ⁴⁰ K | ²³² Th/ ⁴⁰ K | ²³² Th/ ²³⁸ U | ²²⁸ Ra/ ²²⁸ Th | ²¹⁰ Pb/ ²²⁶ Ra | ²²⁶ Ra/ ²³⁸ U |
|------------|-----------------------------------|-----------------------------------|------------------------------------|-------------------------------------|--------------------------------------|--------------------------------------|-------------------------------------|
| 0-5 | 1.29 | 0.06 | 0.05 | 0.87 | 1.1 | 1.52 | 0.76 |
| 5-10 | 1.30 | 0.06 | 0.05 | 0.88 | 1.1 | 1.53 | 0.79 |
| 10-15 | 1.27 | 0.06 | 0.05 | 0.88 | 1.1 | 1.45 | 0.78 |
| 15-20 | 1.23 | 0.05 | 0.05 | 0.92 | 1.2 | 1.62 | 0.86 |
| 20-25 | 1.27 | 0.05 | 0.05 | 1.03 | 1.2 | 1.49 | 0.97 |
| 25-33 | 1.26 | 0.06 | 0.05 | 0.79 | 1.3 | 1.46 | 0.79 |
| 33-50 | 1.33 | 0.04 | 0.04 | 1.18 | 1.2 | 1.37 | 1.00 |
| 50-75 | 1.28 | 0.04 | 0.04 | 1.09 | 1.1 | 1.23 | 0.90 |
| 75-100 | 1.36 | 0.02 | 0.06 | 1.57 | 1.1 | 1.45 | 1.33 |
| 120-170 | 1.39 | 0.06 | 0.02 | 1.04 | 1.1 | 1.18 | 0.87 |
| Mean | | 0.05 | 0.05 | 1.02 | 1.16 | 1.43 | 0.91 |

The activity ratio's of natural radionuclides in depth profile from Ricklingen, Lower Saxony, North Germany are presented in Table 3-28 and Fig. 3-20. The ratios ²²⁶Ra/²³⁸U indicate that for some samples the activities of ²²⁶Ra and, ²³⁸U deviate slightly from secular equilibrium; but the value approaches unity for most of the samples.

Relationships between the concentration of ²³⁸U, ²²⁶Ra, ²¹⁰Pb, ⁴⁰K, ²²⁸Ra, ²²⁸Th, and ²³²Th are shown in Fig.3-20 and Table 3-28. Although Fig. 3-20(a) and (b) show some scatter in the concentrations of ²³²Th and ²³⁸U versus the ⁴⁰K content. The concentrations of ²³²Th and ²³⁸U increase with increase in the ⁴⁰K content. The scattering of the concentration of ²³²Th and ²³⁸U to the ⁴⁰K content may be explained by the surface area of soil particles. The ²³⁸U/⁴⁰K and ²³²Th/⁴⁰K ratios are 0.05 and 0.05, respectively, the world average for both quotients being 0.067 (UNS88).

The mean ²³²Th and ²³⁸U quotients is the 1.02 for the Ricklingen, Lower Saxony, North Germany. The activity of ²³²Th in these depth profile are nearly similar ²³⁸U activity. The world ratio ²³²Th/²³⁸U is 1.0 [UNS88].

Fig. 3-20(d) and (f) and Table 3-27 the ²²⁸Ra/²²⁸Th and ²²⁶Ra/²³⁸U concentration ratios were evaluated from the measured values of activity concentrations. Although the activity ratios are found to have a wide range, the mean values for eleven different depths are almost the same. The mean values ²²⁸Ra/²²⁸Th and ²²⁶Ra/²³⁸U ratios for different depth soils of Ricklingen are 1.16 and 0.91 respectively

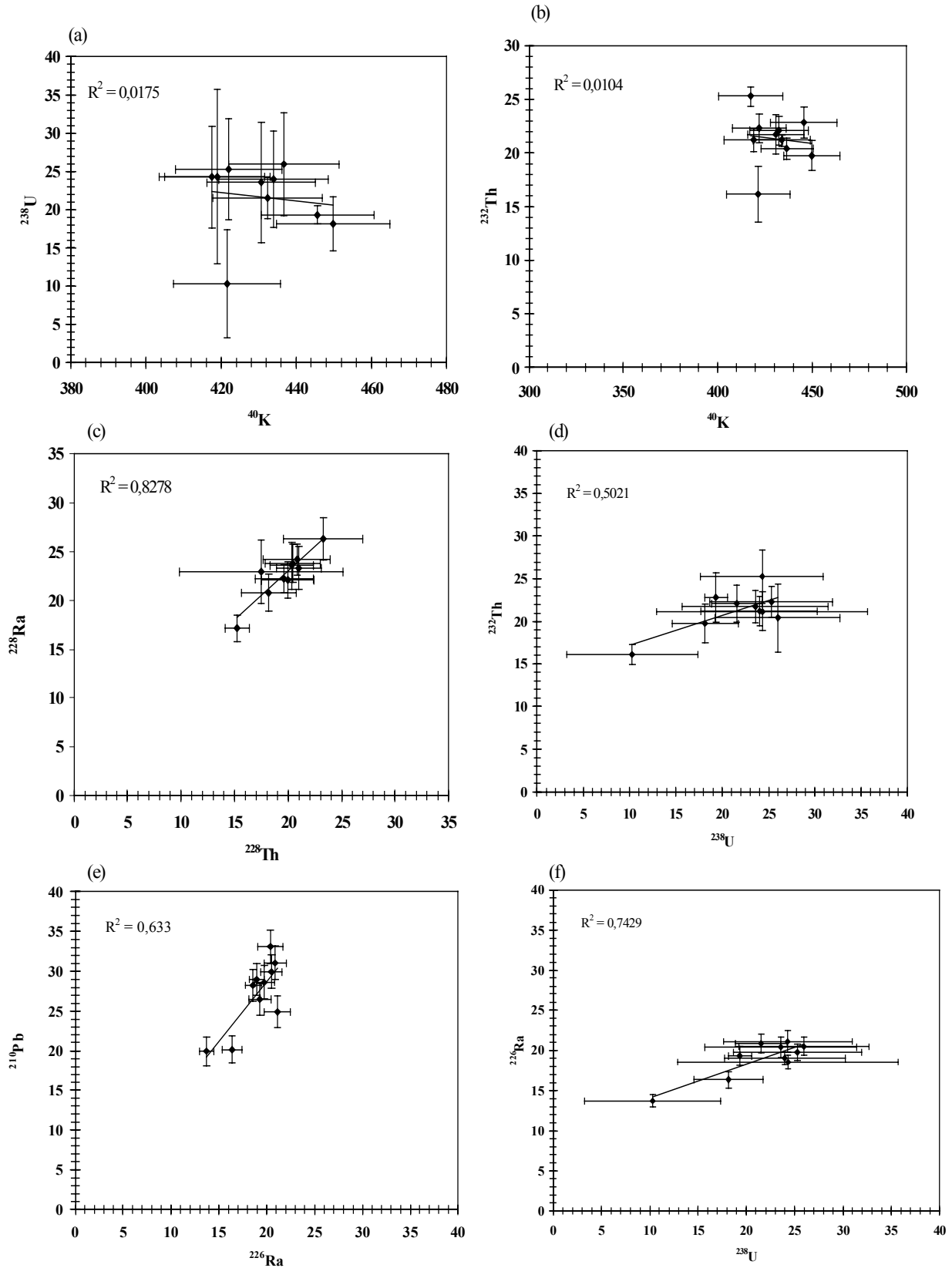


Fig. 3-20: Elemental correlation between natural radionuclides in soil samples from Ricklingen, Lower Saxony, North Germany.

Table 3 - 29: Elemental correlation between natural radionuclides in soil samples from Twenge, Lower Saxony, North Germany.

| Depth (cm) | Dry density [g cm ⁻³] | ²³⁸ U/ ⁴⁰ K | ²³² Th/ ⁴⁰ K | ²³² Th/ ²³⁸ U | ²²⁸ Ra/ ²²⁸ Th | ²¹⁰ Pb/ ²²⁶ Ra | ²²⁶ Ra/ ²³⁸ U |
|------------|-----------------------------------|-----------------------------------|------------------------------------|-------------------------------------|--------------------------------------|--------------------------------------|-------------------------------------|
| 0-15 | 1.346 | 0.05 | 0.03 | 0.68 | 1.1 | 2.15 | 0.69 |
| 15-30 | 1.380 | 0.04 | 0.03 | 0.77 | 1.2 | 2.60 | 0.76 |
| 30-40 | 1.372 | 0.04 | 0.04 | 0.73 | 1.2 | 1.42 | 0.69 |
| 40-50 | 1.290 | 0.06 | 0.04 | 0.71 | 1.1 | 1.10 | 0.69 |
| 50-60 | 1.382 | 0.04 | 0.03 | 0.75 | 1.1 | 0.84 | 1.00 |
| 60-75 | 1.304 | 0.03 | 0.03 | 0.77 | 1.2 | 2.18 | 0.83 |
| 75-100 | 1.464 | 0.03 | 0.03 | 0.86 | 1.1 | 1.20 | 0.87 |
| 100-125 | 1.683 | 0.04 | 0.03 | 0.72 | 1.1 | - | 0.72 |
| 125-150 | 1.746 | 0.04 | 0.10 | 0.83 | 1.1 | 0.97 | 0.75 |
| Mean | | 0.04 | 0.04 | 0.76 | 1.15 | 1.38 | 0.78 |

Relationships between the concentration of ²³⁸U, ²²⁶Ra, ²¹⁰Pb, ⁴⁰K, ²²⁸Ra, ²²⁸Th, and ²³²Th are shown in Fig.3-21 and Table 3-29. Although Fig. 3-19(a) and (b) show some scatter in the concentrations of ²³²Th and ²³⁸U versus the ⁴⁰K content. The concentrations of ²³²Th and ²³⁸U increase with increase in the ⁴⁰K content. The scattering of the concentration of ²³²Th and ²³⁸U to the ⁴⁰K content may be explained by the surface area of soil particles

The mean value of ratios ²³⁸U/⁴⁰K and ²³²Th/⁴⁰K are equal 0.04. The activity ratios of ²³⁸U/⁴⁰K and ²³²Th/⁴⁰K are same for both layers. The mean ratios ²²⁶Ra/²³⁸U is the 0.78 for some samples the activities of ²²⁶Ra and ²³⁸U, deviate slightly from secular equilibrium; but the value approaches unity for most of the samples.

The ratios ²²⁶Ra/²³⁸U indicate that for some samples the activities of ²²⁶Ra and, ²³⁸U deviate slightly from secular equilibrium; but the value approaches unity for most of the samples.

The ratios between ²²⁸Th and ²³²Th concentrations in the air samples are about 1, indicating radiological equilibrium between these radionuclides [Dia02].

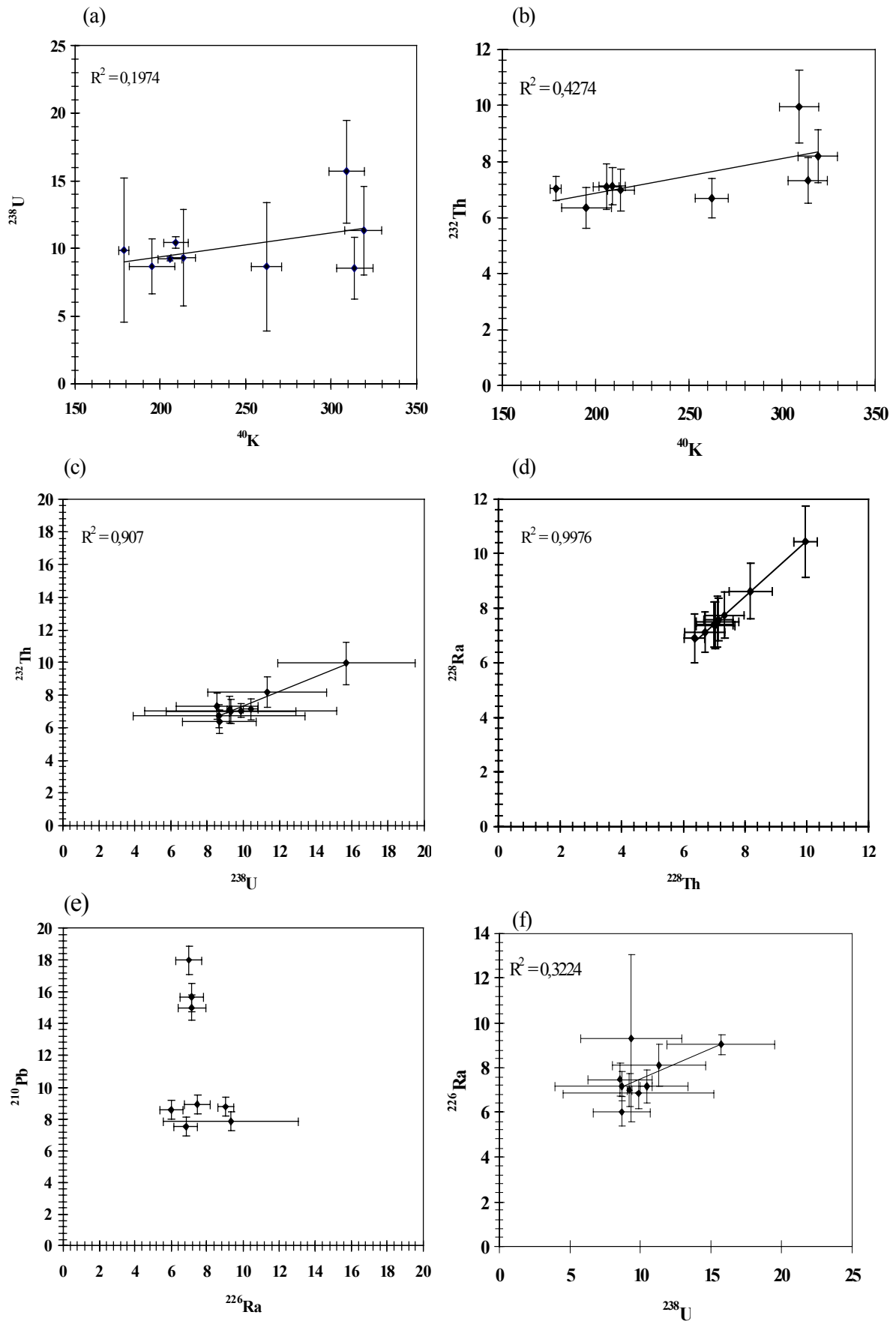


Fig. 3-21: Elemental correlation between natural radionuclides in soil samples from Iwenge, Lower Saxony, North Germany.

3.3.1.2 Surface soil samples From Lower Saxony, North Germany.

Table 3 - 30: Elemental correlation between natural radionuclides in soil samples from Lower Saxony, North Germany.

| Location | soil sample Code | Dry density [g cm ⁻³] | ²³⁸ U/ ⁴⁰ K | ²³² Th/ ⁴⁰ K | ²³² Th/ ²³⁸ U | ²²⁸ Ra/ ²²⁸ Th | ²¹⁰ Pb/ ²²⁶ Ra | ²²⁶ Ra/ ²³⁸ U |
|-----------------|------------------|-----------------------------------|-----------------------------------|------------------------------------|-------------------------------------|--------------------------------------|--------------------------------------|-------------------------------------|
| Jeinsen | JeBoEPKr01 | 1.37 | 0.06 | 0.06 | 0.91 | 0.9 | 2.55 | 1.07 |
| | JeBoEPKs01 | 1.35 | 0.03 | 0.05 | 1.58 | 1.0 | 2.21 | 1.80 |
| | JeBoEPRb01 | 1.28 | 0.14 | 0.17 | 1.24 | 1.0 | 0.33 | 1.29 |
| | JeBoEPMa01 | 1.21 | 0.03 | 0.08 | 2.48 | 0.9 | 0.07 | 2.95 |
| | JeBoEPBr01 | 1.45 | 0.05 | 0.05 | 1.16 | 1.1 | 1.70 | 1.28 |
| | JeBoEPLa01 | 1.44 | 0.05 | 0.05 | 1.06 | 1.0 | 1.80 | 1.26 |
| | JeBoEPWk01 | 1.33 | 0.06 | 0.06 | 0.98 | 1.1 | 1.59 | 1.05 |
| | JeBoEPEg01 | 1.37 | 0.05 | 0.06 | 1.15 | 1.0 | 1.58 | 1.18 |
| | JeBoEPRo01 | 1.37 | 0.05 | 0.06 | 1.17 | 1.0 | 1.43 | 1.21 |
| | JeBoEPWeK01 | 1.34 | 0.06 | 0.06 | 1.08 | 1.0 | 1.48 | 1.09 |
| | JeBoEKPI | 1.37 | 0.10 | 0.05 | 0.50 | 1.0 | 1.47 | 0.58 |
| | JeBoEPPe01 | 1.38 | 0.10 | 0.05 | 0.50 | 1.0 | 1.51 | 0.59 |
| | JeBoEPGk01 | 1.27 | 0.10 | 0.05 | 0.51 | 1.0 | 1.33 | 0.58 |
| Neßmerpolder | PoBoEPLu01 | 1.33 | 0.04 | 0.04 | 1.01 | 1.0 | 1.53 | 0.98 |
| | PoBoEPWe01 | 1.33 | 0.05 | 0.04 | 0.92 | 1.0 | 1.81 | 0.91 |
| | PoBoEPWe02 | 1.35 | 0.04 | 0.05 | 1.22 | 1.1 | 1.50 | 1.03 |
| | PoBoMPHa02 | 1.38 | 0.05 | 0.04 | 0.86 | 1.0 | 1.73 | 0.88 |
| | PoBoEPRa01 | 1.19 | 0.05 | 0.05 | 1.05 | 1.0 | 1.65 | 1.01 |
| | PoBoEPLu02 | 1.29 | 0.06 | 0.05 | 0.86 | 1.1 | 2.04 | 0.72 |
| | PoBoMPHa01 | 1.43 | 0.05 | 0.06 | 1.04 | 1.0 | 1.39 | 0.99 |
| | PoBoMPWe01 | 1.39 | 0.06 | 0.05 | 0.88 | 1.0 | 1.94 | 0.83 |
| | PoBoMPHe01 | 1.18 | 0.07 | 0.06 | 0.89 | 1.2 | 1.72 | 0.77 |
| | PoBoEPHa02 | 1.31 | 0.06 | 0.06 | 1.02 | 1.0 | 1.90 | 0.85 |
| | PoBoEPHe02 | 1.20 | 0.05 | 0.05 | 1.10 | 1.0 | 1.99 | 0.90 |
| | PoBoMPGe01 | 1.35 | 0.10 | 0.05 | 0.49 | 1.0 | 1.67 | 0.44 |
| | PoBoMPLu1 | 1.26 | 0.10 | 0.05 | 0.51 | 1.0 | 1.56 | 0.46 |
| Schessinghausen | ScBoMPRo01 | 1.39 | 0.10 | 0.08 | 0.78 | 1.1 | 3.70 | 0.85 |
| | ScBoMPTr02 | 1.37 | 0.07 | 0.08 | 1.11 | 0.9 | 2.43 | 1.35 |
| | ScBoMPRa01 | 1.39 | 0.12 | 0.04 | 0.34 | 1.0 | 1.84 | 0.40 |
| | ScBoMPWe01 | 1.40 | 0.04 | 0.04 | 0.87 | 1.2 | 2.06 | 1.04 |
| | ScBoMPTr01 | 1.46 | 0.06 | 0.04 | 0.71 | 0.9 | 2.16 | 0.80 |
| | ScBoMPWe02 | 1.39 | 0.05 | 0.05 | 0.92 | 1.0 | 2.32 | 0.98 |
| | ScBoEPKa01 | 1.38 | 0.05 | 0.05 | 0.96 | 1.1 | 2.52 | 1.01 |
| | ScBoEPMa01 | 1.31 | 0.04 | 0.05 | 1.05 | 0.9 | 2.66 | 1.13 |
| Schlewecke | SIBoEPRa01 | 1.34 | 0.03 | 0.05 | 1.54 | 1.1 | 1.29 | 1.45 |
| | SIBoEZu01 | 1.29 | 0.05 | 0.06 | 1.17 | 1.0 | 1.79 | 1.21 |
| | SiBoMPGe01 | 1.28 | 0.10 | 0.05 | 0.53 | 1.1 | 1.46 | 0.57 |
| | SIBoMPGe02 | 1.14 | 0.04 | 0.05 | 1.25 | 1.0 | 1.49 | 1.14 |
| | SIBoMPRa01 | 1.28 | 0.05 | 0.06 | 1.19 | 1.0 | 1.33 | 1.08 |
| | SIBoMPWe01 | 1.15 | 0.05 | 0.06 | 1.22 | 1.1 | 1.77 | 1.13 |
| | SIBoMPWe02 | 1.21 | 0.05 | 0.06 | 1.16 | 1.0 | 1.78 | 1.11 |
| SiBoEPWe01 | 1.15 | 0.05 | 0.05 | 1.06 | 1.1 | 2.10 | 0.97 | |

| Location | soil sample Code | Dry density [g cm ⁻³] | ²³⁸ U/ ⁴⁰ K | ²³² Th/ ⁴⁰ K | ²³² Th/ ²³⁸ U | ²²⁸ Ra/ ²²⁸ Th | ²¹⁰ Pb/ ²²⁶ Ra | ²²⁶ Ra/ ²³⁸ U |
|--------------------------------------|------------------|-----------------------------------|-----------------------------------|------------------------------------|-------------------------------------|--------------------------------------|--------------------------------------|-------------------------------------|
| Gestorf | GeBMPWe01 | 1.27 | 0.03 | 0.06 | 2.27 | 1.0 | 0.12 | 2.29 |
| | GeBMPWe01 | 1.27 | 0.03 | 0.06 | 2.27 | 1.0 | 0.12 | 2.29 |
| Gümmer | GeBoEPKa01 | 1.31 | 0.06 | 0.08 | 1.32 | 1.0 | 3.23 | 1.47 |
| | GeBoEPZu01 | 1.31 | 0.06 | 0.05 | 0.86 | 1.0 | 1.85 | 0.96 |
| | GuBoEPrh01a | 1.25 | 0.04 | 0.04 | 1.05 | 1.0 | 2.58 | 1.10 |
| | GuBoEPrh01b | 1.22 | 0.04 | 0.04 | 0.96 | 1.0 | 2.09 | 1.09 |
| Hermannsdorfes LandWerkstätten (HLW) | HLWBoEPHe01 | 1.22 | 0.05 | 0.06 | 1.28 | 1.0 | 1.36 | 1.20 |
| | RhBoEPWa01 | 1.12 | 0.04 | 0.04 | 1.10 | 1.1 | 2.61 | 1.03 |
| Mean | | | 0.06 | 0.05 | 1.03 | 1.02 | 1.7 | 1.06 |

Relationships between the concentration of ²³⁸U, ²²⁶Ra, ²¹⁰Pb, ⁴⁰K, ²²⁸Ra, ²²⁸Th, and ²³²Th are shown in Fig. 3-22 and Table 3-30. Although Fig. 3-22(a) and (b) show some scatter in the concentrations of ²³²Th and ²³⁸U versus the ⁴⁰K content. The concentrations of ²³²Th and ²³⁸U increase with increase in the ⁴⁰K content. The scattering of the concentration of ²³²Th and ²³⁸U to the ⁴⁰K content may be explained by the surface area of soil particles. A more detailed analysis of the results from individual measurements shows that there is some degree of correlation between the concentrations of ²³⁸U and ⁴⁰K in soil and between ²³²Th and ⁴⁰K. Fig.3-22 indicate that both correlations are weak, though significant because of the large number of measurements. Individual results for any one of the three radionuclide concentrations are not, therefore, good predictors of individual values for the other two. Although some scatter in the concentrations of ²³⁸U and ²³²Th vs. the ⁴⁰K content is noted, the activity concentrations of ²³⁸U and ²³²Th in soil appear to increase as the ⁴⁰K content increases.

The concentrations of ²³⁸U, ²³²Th, and ⁴⁰K vary with soil particle size for the most representative lithotypes of soil in Spain and, subsequently, to investigate whether the scattering of the ²³⁸U and ²³²Th concentrations vs. ⁴⁰K content can be explained by differences in soil particle size, as suggested by other authors [Kva86; Qui94].

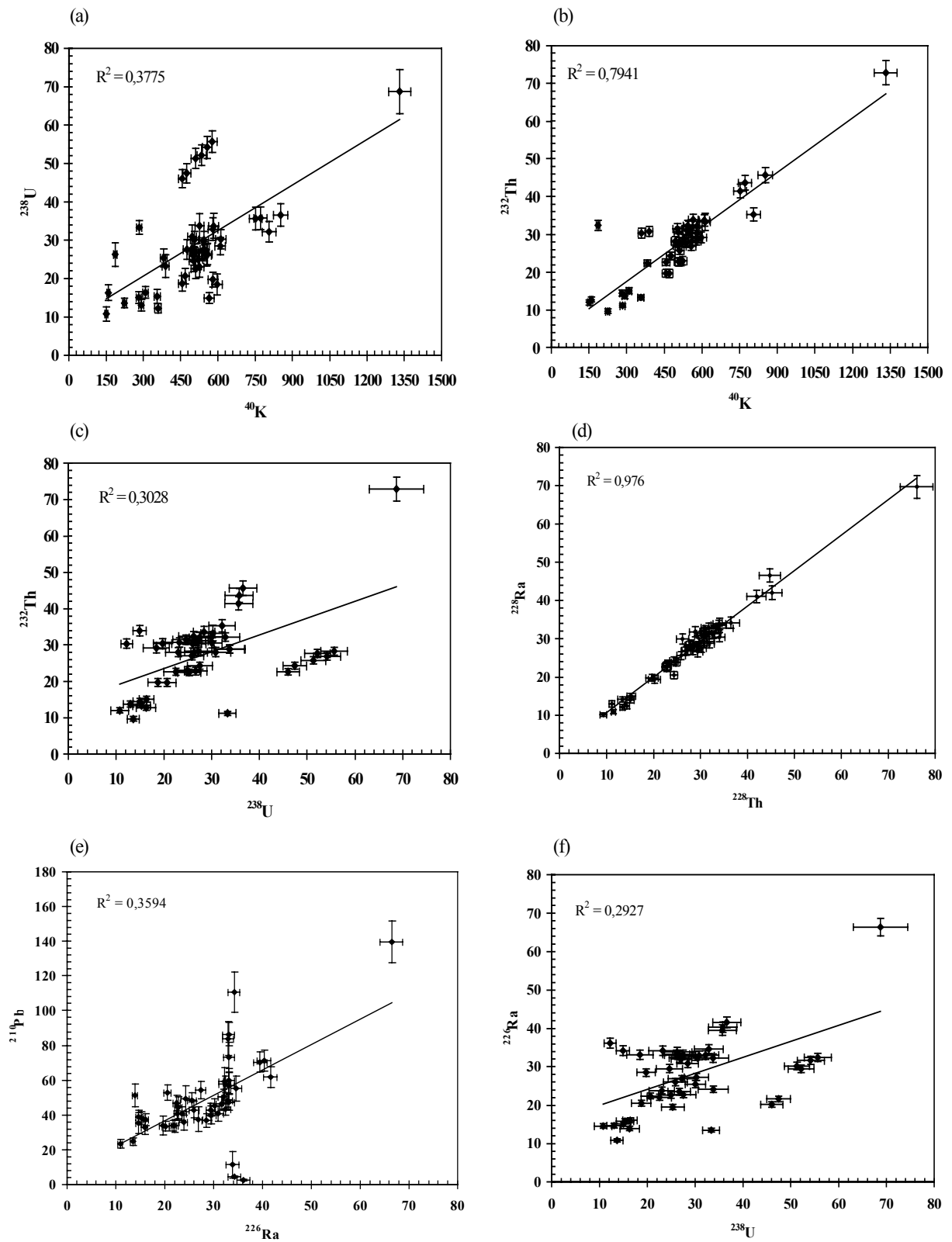


Fig. 3-22: Elemental correlation between natural radionuclides in soil samples from different sites in Lower Saxony, North Germany.

3.3.2 Elemental correlation, equilibrium and disequilibrium for natural radionuclides in surface soil samples form Lippe, (North Rhine-Westphalia), Germany.

3.3.2.1 Depth profiles form Lippe, (North Rhine-Westphalia), Germany.

Table 3 - 31: Elemental correlation between natural radionuclides in soil samples from Lippe, (North Rhine-Westphalia), Germany.

| Depth cm | Dry density [g cm ⁻³] | ²³⁸ U/ ⁴⁰ K | ²³² Th/ ⁴⁰ K | ²³² Th/ ²³⁸ U | ²²⁸ Ra/ ²²⁸ Th | ²¹⁰ Pb/ ²²⁶ Ra | ²²⁶ Ra/ ²³⁸ U |
|-------------|-----------------------------------------|-----------------------------------|------------------------------------|-------------------------------------|--------------------------------------|--------------------------------------|-------------------------------------|
| 0-2 | 0.95 | 0.07 | 0.25 | 3.72 | 1.2 | 0.43 | 11.16 |
| 2-4 | 0.93 | 0.06 | 0.34 | 5.55 | 1.2 | 0.41 | 17.14 |
| 4-6 | 0.91 | 0.12 | 0.34 | 2.97 | 1.1 | 0.42 | 9.72 |
| 6-10 | 0.91 | 0.06 | 0.27 | 4.71 | 0.9 | 0.46 | 18.12 |
| 10--15 | 0.93 | 0.06 | 0.21 | 3.28 | 0.8 | 0.54 | 15.67 |
| 15-20 | 1.01 | 0.07 | 0.14 | 2.10 | 0.9 | 0.71 | 11.98 |
| 20-30 | 0.95 | 0.06 | 0.10 | 1.57 | 0.9 | 0.81 | 12.00 |
| Mean | | 0.07 | 0.24 | 3.41 | 1.0 | 0.54 | 13.68 |

From the Table 3-31 we can noted that there is no equilibrium between uranium isotopes and its daughters is evident. The mean value of ratios ²³⁸U/⁴⁰K and ²³²Th/⁴⁰K are 0.07 and 0.24 respectively. The maximum ²³²Th/²³⁸U quotients are 2.9 and 2.5 and the mean are 1.97 and 2.28. for the Karnaphuli and Shango river sediments, respectively. The ²³⁸U/⁴⁰K and ²³⁸Th/⁴⁰K ratios ranged from 0.07 to 0.33 and 0.18 to 0.38, respectively [Man99]. The mean values ²²⁸Ra/²²⁸Th, ²¹⁰Pb/²²⁶Ra and ²²⁶Ra/²³⁸U ratios for different depth soils are 1.0, 0.54 and 13.68 respectively. When the natural uranium concentrations are converted to activities of ²³⁸U, then ²³⁸Ra to ²³⁸U ratios of 9.72-18.12, with a mean of 13.68, are obtained. The activity ratios of ²¹⁰Pb to ²²⁶Ra varied from 0.41 to 0.81 with a mean of 0.54.

3.3.2.2 Surface soil from Lippe, (North Rhine-Westphalia), Germany.

Table 3 - 32: Elemental correlation between natural radionuclides in soil samples from Lippe, North Rhine-Westphalia, Germany.

| Soil sample No. | Dry density [g cm ⁻³] | ²³⁸ U/ ⁴⁰ K | ²³² Th/ ⁴⁰ K | ²³² Th/ ²³⁸ U | ²²⁸ Ra/ ²²⁸ Th | ²¹⁰ Pb/ ²²⁶ Ra | ²²⁶ Ra/ ²³⁸ U |
|-----------------|-----------------------------------|-----------------------------------|------------------------------------|-------------------------------------|--------------------------------------|--------------------------------------|-------------------------------------|
| BP 2-04f | 0.97 | - | 0.357 | - | 1.2 | 0.5 | - |
| BP 2-05f | 0.88 | - | 0.173 | - | 1.6 | 1.3 | - |
| BP 2-06f | 1.02 | - | 0.135 | - | 1.2 | 0.5 | - |
| BP 2-07f | 1.05 | 0.044 | 0.082 | 1.865 | 1.0 | 1.1 | 5.887 |
| BP 2-11f | 0.93 | 0.035 | 0.158 | 4.566 | 1.3 | 1.2 | 9.455 |
| BP 2-12f | 1.09 | - | 0.124 | - | 1.0 | 0.5 | - |
| BP 2-13f | 1.17 | - | 0.098 | - | 1.1 | 0.6 | - |
| BP 2-17f | 1.09 | - | 0.369 | - | 1.4 | 0.3 | - |
| BP 2-23f | 0.90 | 0.100 | 0.408 | 4.089 | 1.4 | 0.7 | 10.650 |
| BP 2-24f | 1.12 | - | 0.232 | - | 1.2 | 0.5 | - |
| BP 2-25f | 1.27 | - | 0.077 | - | 0.9 | 1.2 | - |
| BP 2-33f | 1.13 | - | 0.108 | - | 1.1 | 0.5 | - |
| BP 2-34f | 1.27 | 0.055 | 0.084 | 1.525 | 1.3 | 1.9 | 2.175 |
| BP 2-35f | 1.19 | 0.057 | 0.078 | 1.383 | 1.4 | 1.8 | 2.077 |
| BP 2-36f | 1.12 | - | 0.187 | - | 1.0 | 0.3 | - |
| BP 3-01 | 1.08 | 0.060 | 0.268 | 4.431 | 1.3 | 0.5 | 14.475 |
| BP 3-02 | 1.08 | 0.065 | 0.069 | 1.062 | 1.0 | 1.3 | 3.681 |
| BP 3-03 | 1.30 | 0.042 | 0.056 | 1.342 | 1.0 | 1.0 | 1.551 |
| BP 3-04 | 0.96 | 0.047 | 0.182 | 3.873 | 1.0 | 0.6 | 14.992 |
| BP 3-05 | 0.89 | 0.039 | 0.158 | 4.064 | 1.0 | 0.6 | 15.447 |
| BP 3-06 | 1.11 | 0.046 | 0.062 | 1.334 | 1.1 | 2.4 | 1.275 |
| BP 3-09 | 1.24 | 0.065 | 0.062 | 0.956 | 1.1 | 1.7 | 1.343 |
| BP 3-07.Jos | 0.94 | 0.047 | 0.310 | 6.657 | 0.9 | 0.5 | 29.596 |
| BP 3-07 | 0.94 | 0.052 | 0.259 | 4.957 | 0.9 | 0.7 | 25.698 |
| BP 3-08 | 1.02 | 0.064 | 0.091 | 1.431 | 1.1 | 1.5 | 7.937 |
| BP 3-10 | 0.86 | 0.055 | 0.119 | 2.181 | 1.2 | 1.1 | 11.010 |
| BP 3-11 | 0.90 | 0.016 | 0.057 | 3.571 | 2.505 | 2.5 | 4.682 |
| BP 3-12 | 0.97 | 0.041 | 0.147 | 3.559 | 0.803 | 0.8 | 28.132 |
| BP 3-13 | 0.98 | 0.051 | 0.078 | 1.546 | 1.642 | 1.6 | 8.786 |
| BP 3-14 | 1.19 | 0.051 | 0.053 | 1.051 | 1.348 | 1.3 | 2.255 |
| BP 3-15 | 0.98 | 0.088 | 0.173 | 1.959 | 0.902 | 0.9 | 10.114 |
| BP 3-16 | 1.10 | 0.060 | 0.253 | 4.194 | 0.710 | 0.7 | 19.102 |
| BP 3-17 | 1.09 | 0.060 | 0.047 | 0.787 | 3.471 | 3.5 | 1.075 |
| BP 3-18 | 0.81 | 0.094 | 0.079 | 0.833 | 2.799 | 2.8 | 1.538 |
| BP 3-21 | 1.38 | 0.093 | 0.076 | 0.823 | 1.018 | 1.0 | 5.658 |
| BP 3-22 | 1.04 | 0.077 | 0.071 | 0.913 | 1.260 | 1.3 | 3.554 |
| BP 3-23 | 1.03 | 0.038 | 0.079 | 2.088 | 1.158 | 1.2 | 18.144 |
| BP 3-24 | 1.11 | 0.072 | 0.058 | 0.804 | 1.777 | 1.8 | 2.084 |
| BP 3-25 | 1.04 | 0.059 | 0.114 | 1.926 | 1.059 | 1.1 | 11.969 |
| BP 3-26 | 1.19 | 0.073 | 0.067 | 0.923 | 1.510 | 1.5 | 4.206 |
| BP 3-28 | 1.10 | 0.047 | 0.063 | 1.352 | 1.409 | 1.4 | 6.964 |

| Soil sample No. | Dry density [g cm ⁻³] | ²³⁸ U/ ⁴⁰ K | ²³² Th/ ⁴⁰ K | ²³² Th/ ²³⁸ U | ²²⁸ Ra/ ²²⁸ Th | ²¹⁰ Pb/ ²²⁶ Ra | ²²⁶ Ra/ ²³⁸ U |
|-------------------|-----------------------------------|-----------------------------------|------------------------------------|-------------------------------------|--------------------------------------|--------------------------------------|-------------------------------------|
| BP 3-29 | 0.99 | 0.035 | 0.078 | 2.250 | 1.177 | 1.2 | 14.688 |
| BP 4-01 | 0.88 | 0.096 | 0.104 | 1.089 | 0.794 | 0.8 | 5.266 |
| BP 4-05 | 0.83 | 0.044 | 0.288 | 6.477 | 0.503 | 0.5 | 31.623 |
| BP 4-06 | 0.97 | 0.056 | 0.070 | 1.237 | 1.409 | 1.4 | 2.365 |
| BP 4-09 | 1.16 | 0.045 | 0.041 | 0.910 | 1.328 | 1.3 | 5.039 |
| BP 4-10 | 1.18 | 0.084 | 0.078 | 0.930 | 1.008 | 1.0 | 6.443 |
| BP 4-11 | 1.07 | 0.047 | 0.117 | 2.499 | 0.733 | 0.7 | 15.212 |
| BP 4-12 | 1.29 | 0.082 | 0.063 | 0.763 | 1.666 | 1.7 | 1.530 |
| BP 4-15 | 0.90 | 0.063 | 0.112 | 1.795 | 1.392 | 1.4 | 7.495 |
| BP 4-16 | 1.22 | 0.077 | 0.047 | 0.613 | 1.181 | 1.2 | 1.843 |
| BP Sicking. (71) | 0.95 | 0.063 | 0.533 | 8.462 | 0.332 | 0.3 | 35.427 |
| BP Vorfluter (70) | 1.31 | - | 0.719 | - | 0.291 | 0.3 | - |
| BP 5-01 | 0.95 | 0.030 | 0.108 | 3.565 | 0.977 | 1.0 | 24.979 |
| BP 5-02 | 1.21 | 0.032 | 0.098 | 3.097 | 0.931 | 0.9 | 19.684 |
| BP 5-03 | 0.97 | 0.059 | 0.134 | 2.287 | 0.849 | 0.8 | 11.467 |
| BP 5-04 | 0.96 | 0.086 | 0.138 | 1.604 | 0.828 | 0.8 | 8.574 |
| BP 5-05 (Sedi) | 1.50 | - | 0.088 | - | 1.116 | 1.1 | - |
| BP 5-06 | 0.88 | 0.058 | 0.152 | 2.621 | 0.730 | 0.7 | 11.484 |
| BP 5-07 | 0.93 | 0.058 | 0.121 | 2.070 | 0.818 | 0.8 | 9.269 |
| BP 5-08 | 1.04 | 0.045 | 0.185 | 4.119 | 0.631 | 0.6 | 18.890 |
| BP 5-09 | 0.99 | 0.037 | 0.164 | 4.470 | 0.637 | 0.6 | 17.962 |
| BP 5-10 | 0.95 | 0.034 | 0.281 | 8.159 | 0.469 | 0.5 | 29.672 |
| BP 5-11 | 1.27 | 0.067 | 0.052 | 0.773 | 2.541 | 2.5 | 0.960 |
| Mean | | 0.047 | 0.14 | 2.53 | 1.05 | 1.103 | 10.87 |

This hypothesis is also supported by the relationship between the ratios $^{232}\text{Th}/^{238}\text{U}$ and $^{226}\text{Ra}/^{238}\text{U}$, (Fig. 3-23). Using ^{228}Ra as an indicator for ^{232}Th , which may be considered very immobile [Lan86]. It is possible to conclude that uranium is similarly depleted relative to thorium. Samples displaying low $^{226}\text{Ra}/^{238}\text{U}$ ratios all contain significant amounts of labile ^{238}U or U associated with the non-resistant fractions of the soil. The highest disequilibrium values are associated with low levels of labile ^{238}U , a fact which also supports the depletion of ^{238}U in samples with high $^{226}\text{Ra}/^{238}\text{U}$ ratios. Adopting an average $^{226}\text{Ra}/^{238}\text{U}$ ratio of 10.87 for the soil of Lippe, (North Rhine-Westphalia), Germany, allows for division of the data set on the basis of the samples $^{226}\text{Ra}/^{238}\text{U}$ ratios being above or below average for the soil samples.

Samples exhibiting lower than average $^{226}\text{Ra}/^{238}\text{U}$ ratios indicating the probable loss of ^{238}U compound to samples exhibiting greater than average $^{226}\text{Ra}/^{238}\text{U}$ ratios. The apparent loss of ^{238}U relative to ^{226}Ra in these samples appears related to the positions of the samples relative to the soil level. samples that remain saturated for much of the year exhibiting the higher $^{226}\text{Ra}/^{238}\text{U}$ ratios.

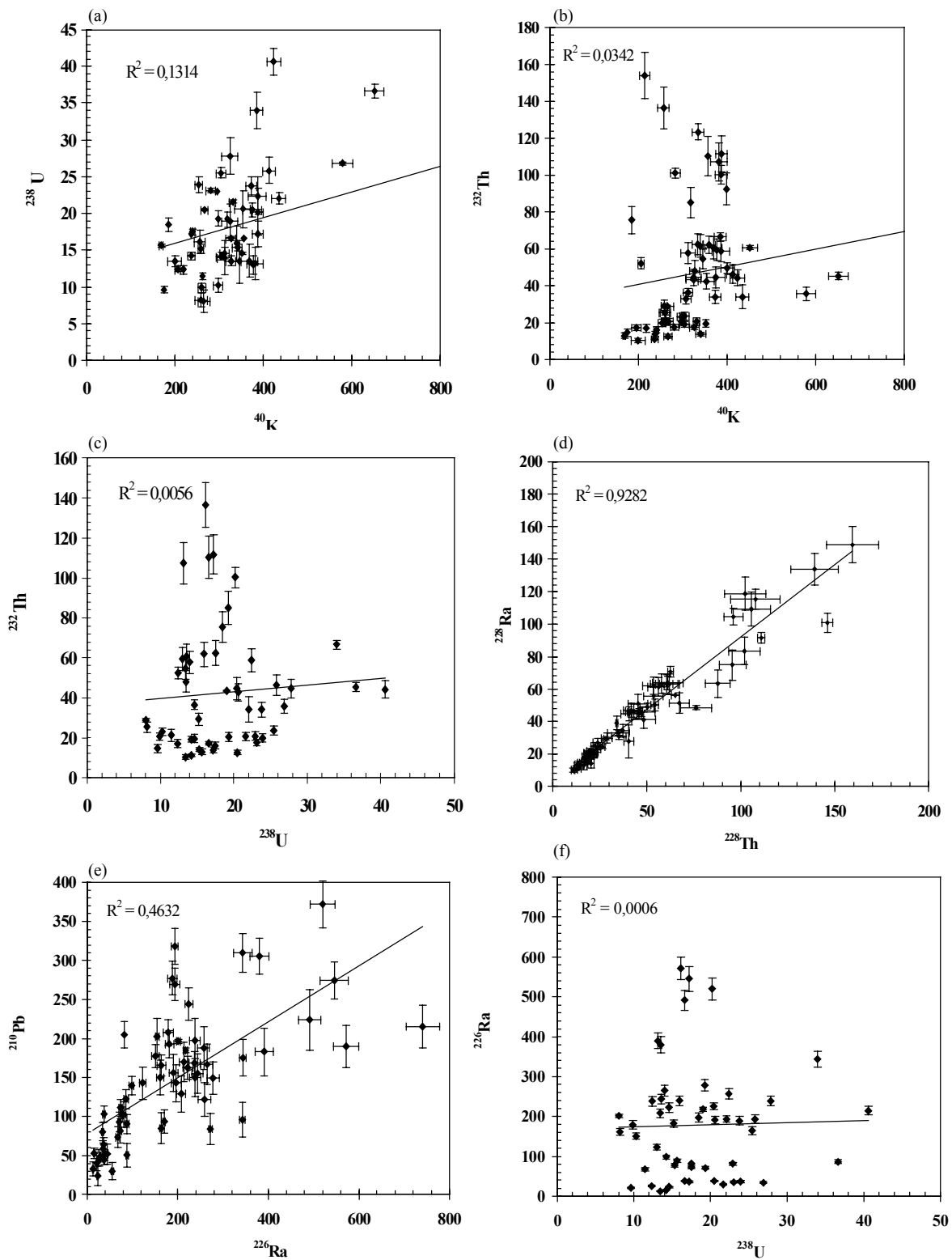


Fig. 3-23: Elemental correlation between natural radionuclides in soil samples from Lippe, (North Rhine-Westphalia), Germany.

This fact provides further evidence that the better drained/less saturated, and hence, more oxidising soil levels, exhibit greater depletion of ^{238}U relative to ^{226}Ra . This view is supported by the disequilibrium values of the series of random samples taken from the vicinity of sites (Table 3-32, Fig. 3-23).

Relationships between the concentration of ^{238}U , ^{226}Ra , ^{210}Pb , ^{40}K , ^{228}Ra , ^{228}Th , and ^{232}Th are shown in Fig. 3-23 and Table 3-32. Although Fig. 3-19(a) and (b) show some scatter in the concentrations of ^{232}Th and ^{238}U versus the ^{40}K content. The concentrations of ^{232}Th and ^{238}U increase with increase in the ^{40}K content. The scattering of the concentration of ^{232}Th and ^{238}U to the ^{40}K content may be explained by the surface area of soil particles.

3.3.3 Elemental correlation, equilibrium and disequilibrium for natural radionuclides in soil samples from depth profiles from Ukraine.

Table 3 - 33: Elemental correlation between natural radionuclides in soil samples from Chirstinovka meadow, Ukraine.

| Depth [cm] | Dry density [g cm ⁻³] | $^{238}\text{U}/^{40}\text{K}$ | $^{232}\text{Th}/^{40}\text{K}$ | $^{232}\text{Th}/^{238}\text{U}$ | $^{228}\text{Ra}/^{228}\text{Th}$ | $^{210}\text{Pb}/^{226}\text{Ra}$ | $^{226}\text{Ra}/^{238}\text{U}$ |
|------------|-----------------------------------|--------------------------------|---------------------------------|----------------------------------|-----------------------------------|-----------------------------------|----------------------------------|
| humus soil | 1.41 | 0.02 | 0.07 | 3.57 | 1.4 | 1.3 | 4.07 |
| 0-1 | 1.32 | 0.01 | 0.07 | 10.86 | 1.4 | 2.1 | 12.73 |
| 1-2 | 1.43 | 0.10 | 0.08 | 0.76 | 1.1 | 1.6 | 0.75 |
| 2-3 | 1.41 | - | 0.08 | - | 1.1 | 1.3 | - |
| 3-5 | 1.40 | 0.05 | 0.08 | 1.48 | 1.0 | 0.4 | 1.24 |
| 5-10 | 1.47 | 0.08 | 0.08 | 0.98 | 1.1 | 1.0 | 1.00 |
| 15-10 | 1.44 | 0.06 | 0.07 | 1.25 | 1.4 | 2.2 | 1.34 |
| 15-20 | 1.57 | 0.03 | 0.08 | 3.01 | 1.1 | 2.0 | 3.03 |
| 20-25 | 1.47 | 0.07 | 0.07 | 1.05 | 1.4 | 0.6 | 1.10 |
| 25-40 | 1.74 | 0.06 | 0.05 | 0.91 | 1.0 | 0.6 | 0.97 |
| Mean | | 0.05 | 0.07 | 1.63 | 1.2 | 1.3 | 1.7 |

Relationships between the concentration of ^{238}U , ^{226}Ra , ^{210}Pb , ^{235}U , ^{40}K , ^{228}Ra , ^{228}Th , and ^{232}Th are shown in Fig. 3-24 and Table 3-33. Although Fig. 3-24(a) and (b) show some scatter in the concentrations of ^{232}Th and ^{238}U versus the ^{40}K content. The concentrations of ^{232}Th and ^{238}U increase with increase in the ^{40}K content. The scattering of the concentration of ^{232}Th and ^{238}U to the ^{40}K content may be explained by the surface area of soil particles.

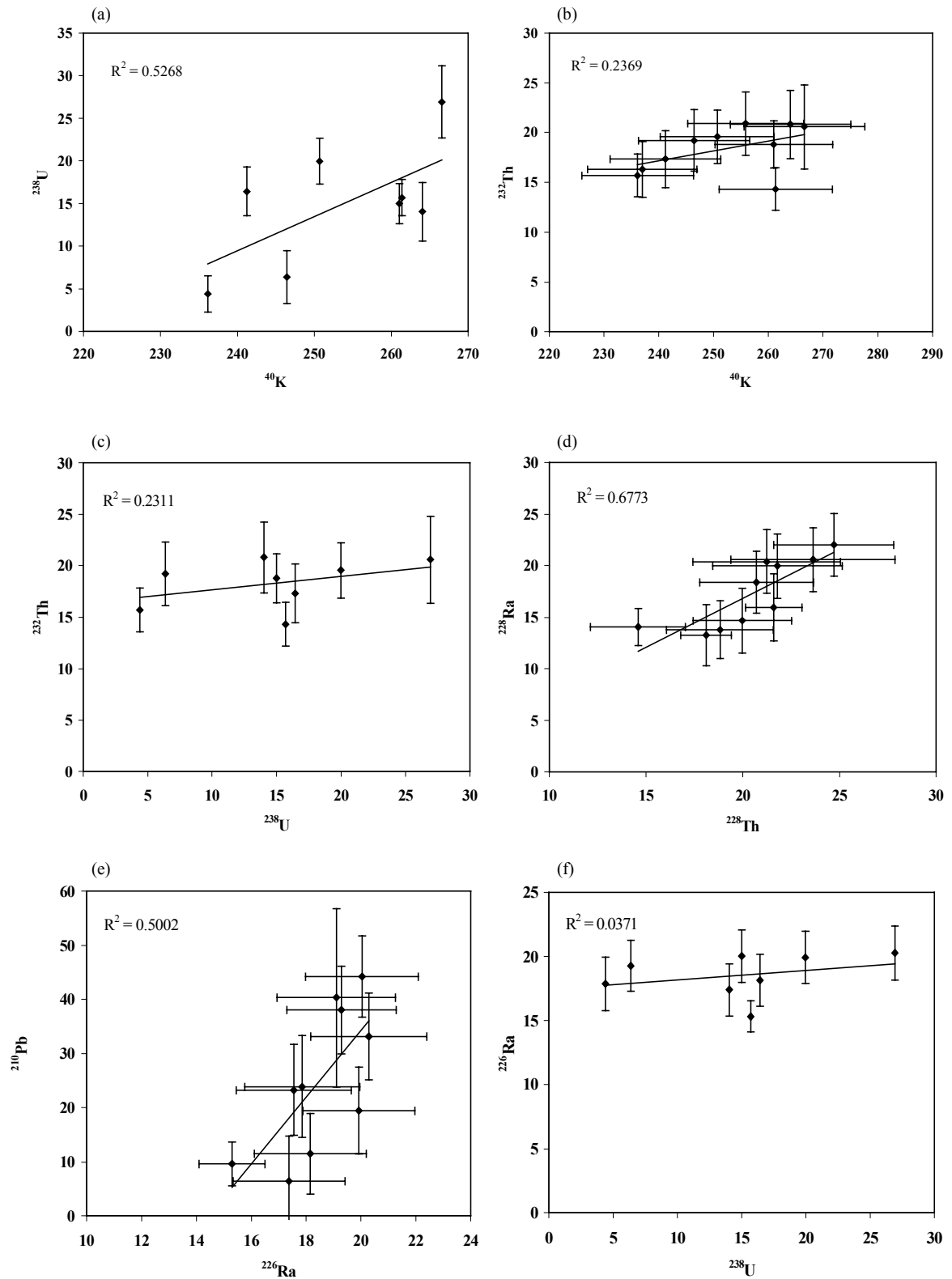


Fig. 3-24: Elemental correlation between natural radionuclides in soil samples from Chirstinovka meadow, Ukraine.

Table 3 - 34: Elemental correlation between natural radionuclides in soil samples from schigiri2, Ukraine.

| Depth [cm] | Dry density [g cm ⁻³] | ²³⁸ U/ ⁴⁰ K | ²³² Th/ ⁴⁰ K | ²³² Th/ ²³⁸ U | ²²⁸ Ra/ ²²⁸ Th | ²¹⁰ Pb/ ²²⁶ Ra | ²²⁶ Ra/ ²³⁸ U |
|------------|-----------------------------------|-----------------------------------|------------------------------------|-------------------------------------|--------------------------------------|--------------------------------------|-------------------------------------|
| humus soil | 0.89 | 0.10 | 0.06 | 0.66 | 1.1 | 9.4 | 0.83 |
| 0-1 | 1.15 | 0.06 | 0.07 | 1.09 | 1.8 | 10.9 | 0.95 |
| 1-2 | 2.20 | 0.06 | 0.06 | 1.00 | 0.9 | 10.6 | 0.91 |
| 2-3 | 1.40 | 0.00 | 0.07 | 23.07 | 1.3 | 6.3 | 20.66 |
| 3-5 | 1.56 | 0.03 | 0.06 | 2.52 | 0.9 | 4.3 | 2.96 |
| 5-10 | 1.56 | 0.05 | 0.07 | 1.37 | 1.0 | 5.4 | 1.13 |
| 15-10 | 1.59 | 0.02 | 0.06 | 2.81 | 1.0 | 5.1 | 2.79 |
| 15-20 | 1.73 | 0.02 | 0.06 | 2.59 | 1.2 | 4.5 | 2.47 |
| 20-25 | 1.71 | 0.00 | 0.06 | 23.03 | 1.0 | 2.1 | 24.97 |
| 25-40 | 1.83 | 0.04 | 0.06 | 1.56 | 1.0 | 3.0 | 1.31 |
| Mean | | 0.03 | 0.06 | 1.07 | 1.11 | 2.01 | 1.67 |

Relationships between the concentration of ²³⁸U, ²²⁶Ra, ²¹⁰Pb, ⁴⁰K, ²²⁸Ra, ²²⁸Th, and ²³²Th are shown in Table 3-34. The concentrations of ²³²Th and ²³⁸U increase with increase in the ⁴⁰K content. The scattering of the concentration of ²³²Th and ²³⁸U to the ⁴⁰K content may be explained by the surface area of soil particles.

Table 3 - 35: Elemental correlation between natural radionuclides in soil samples from Oserjanka 1, Ukraine.

| Depth [cm] | Dry density [g cm ⁻³] | ²³⁸ U/ ⁴⁰ K | ²³² Th/ ⁴⁰ K | ²³² Th/ ²³⁸ U | ²²⁸ Ra/ ²²⁸ Th | ²¹⁰ Pb/ ²²⁶ Ra | ²²⁶ Ra/ ²³⁸ U |
|------------|-----------------------------------|-----------------------------------|------------------------------------|-------------------------------------|--------------------------------------|--------------------------------------|-------------------------------------|
| humus soil | 0.62 | 0.12 | 0.08 | 0.67 | 1.0 | 9.4 | 0.68 |
| 0-1 | 0.68 | 0.19 | 0.08 | 0.45 | 1.2 | 10.9 | 0.33 |
| 1-2 | 0.97 | 0.16 | 0.07 | 0.45 | 1.2 | 10.6 | 0.37 |
| 2-3 | 0.85 | 0.12 | 0.09 | 0.76 | 0.9 | 6.3 | 0.58 |
| 3-5 | 0.88 | 0.19 | 0.09 | 0.48 | 0.9 | 4.3 | 0.39 |
| 5-10 | 0.82 | 0.22 | 0.09 | 0.38 | 1.0 | 5.4 | 0.31 |
| 15-10 | 0.79 | 0.19 | 0.10 | 0.52 | 0.9 | 5.1 | 0.45 |
| 15-20 | 0.86 | 0.14 | 0.07 | 0.52 | 1.1 | 4.5 | 0.53 |
| 20-25 | 0.85 | 0.13 | 0.05 | 0.40 | 1.1 | 2.1 | 0.45 |
| 25-40 | 0.77 | 0.19 | 0.13 | 0.67 | 0.9 | 3.0 | 0.46 |
| Mean | | 0.16 | 0.08 | 0.53 | 1.1 | 6.16 | 0.05 |

Relationships between the concentration of ²³⁸U, ²²⁶Ra, ²¹⁰Pb, ²³⁵U, ⁴⁰K, ²²⁸Ra, ²²⁸Th, and ²³²Th are shown in Table 3-35. The concentrations of ²³²Th and ²³⁸U increase with increase in the ⁴⁰K content. The scattering of the concentration of ²³²Th and ²³⁸U to the ⁴⁰K content may be explained by the surface area of soil particles.

4 Modeling of ambient dose rates from radionuclide concentrations in soil

Major contribution to the ambient dose equivalent rate is caused by radiation of natural radionuclides present in soil. The ambient dose equivalent rate depends on their concentrations in soil. The territory of Lower Saxony, North Germany and Ukraine were contaminated with artificial radionuclides due to both nuclear weapon tests and the Chernobyl NPP accident. ^{137}Cs is a principal artificial long-lived radionuclide, which influenced the ambient dose equivalent rate after the Chernobyl accident. Concentrations of ^{137}Cs and natural radionuclides in soil were measured in the different sites of Lower Saxony, North Germany, Lippe, North Rhine-Westphalia, Germany and Ukraine.

4.1 External gamma-dose rate of ^{137}Cs in soil

The observed vertical distribution of ^{137}Cs in the soil and the corresponding bulk densities of the soil layers were used to calculate the resulting gamma-dose rates of this radionuclide in air (1 m height above the surface) according to [Bel98, Bot00]. These dose rates were calculated separately for all sites, and separately for ^{137}Cs from the global fallout and from the Chernobyl fallout. To facilitate a comparison, the dose rates were always calculated in n Sv h^{-1} per Bq radiocesium deposited per square meter.

4.1.1 External gamma-dose rate of ^{137}Cs in soil from Lower Saxony, North Germany.

Table 4 - 1: External gamma-dose rate of ^{137}Cs in n Sv h^{-1} and densities deposition of ^{137}Cs in different sites in Lower Saxony, North Germany.

| No of profile | Sites | Cs-137 deposits in Bq m^{-2} | | Dose rate [n Sv h^{-1}] |
|---------------|--------------|---------------------------------------|-------------|---------------------------------------|
| | | 01.09.1999 | 26.04.19986 | |
| 1 | Klein Lobke | 7324 ± 18 | 9934 ± 25 | 19.7 |
| 2 | Vestrup | 5367 ± 9 | 7279 ± 12 | 17.37 |
| 3 | Ricklingen | 3739 ± 13 | 5071 ± 18 | 7.41 |
| 4 | Eilenriede | 5681 ± 13 | 7705 ± 18 | 20.06 |
| 5 | Twenge | 5649 ± 36 | 7662 ± 49 | 17.61 |
| 6 | Barum | 2835 ± 14 | 3845 ± 19 | 9.16 |
| 7 | Adenstedt | 4175 ± 12 | 5663 ± 16 | 13.43 |
| 8 | Neßmerpolder | 3342 ± 76 | 4885 ± 112 | 5.74 |
| Min. | | 2835 ± 14 | 3845 ± 19 | 5.74 |
| Max. | | 7324 ± 18 | 9934 ± 25 | 20.06 |
| Mean | | 4967 ± 17 | 6736 ± 22 | 14.9 |

The resulting values revealed that the dose rates for ^{137}Cs from the global fallout are at all sites in n Sv h^{-1} Table 4-1 and Fig 4-1. The minimum and maximum of the dose rate at site Neßmerpolder and Eilenriede are 5.74 and 20.06 n Sv h^{-1} respectively. The mean dose rate of 14.9 n Sv h^{-1} is obtained.

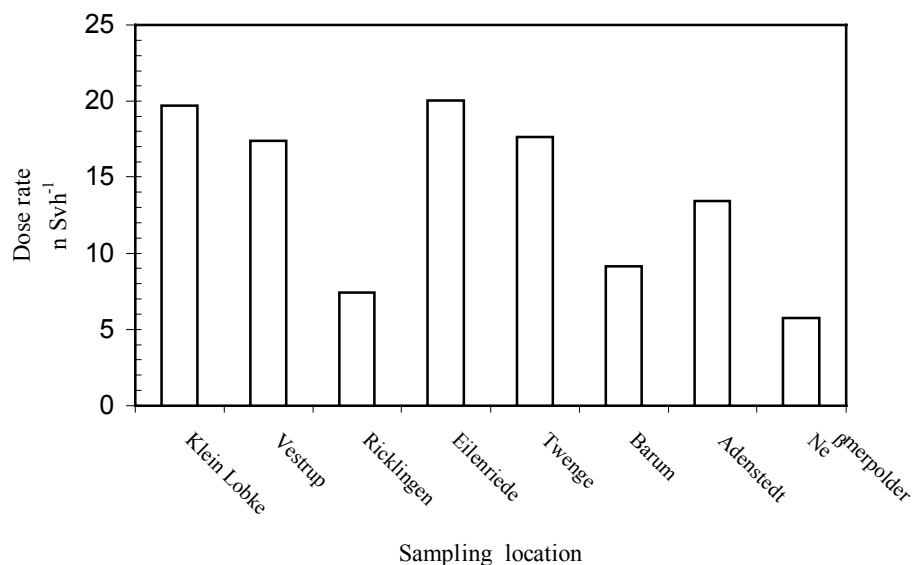


Fig. 4-1: External gamma-dose rate (n Sv h⁻¹) of ¹³⁷Cs from Chernobyl-derived and past atmosphere in different locations in Lower Saxony, North Germany.

In Bavaria, Germany the dose rate of the external gamma-radiation due to ¹³⁷Cs from global fallout in the soil determined from the depth distributions varied between 0.34 and 0.57 (mean: 0.45 ± 0.07) n Gy h⁻¹ per kBq m⁻² [Sch98].

4.1.2 External gamma-dose rate of ¹³⁷Cs in soil from Lippe, North Rhine-Westphalia, Germany.

Table 4 - 2: External gamma-dose rate of ¹³⁷Cs in n Sv h⁻¹ and densities deposition of ¹³⁷Cs in different sites in Lippe, North Rhine-Westphalia, Germany.

| No of profile | sites | Cs-137 deposits in Bq m ² | | Dose rate [n Sv h ⁻¹] |
|---------------|---------|--------------------------------------|-------------|-----------------------------------|
| | | 01.09.2000 | 26.04.1986 | |
| 1 | Bp3-30 | 9063 ± 409 | 12578 ± 567 | 14.96 |
| 2 | Bp 4-14 | 10974 ± 554 | 15230 ± 769 | 16.51 |

External gamma-dose rate of ¹³⁷Cs in n Sv h⁻¹ and deposition densities of ¹³⁷Cs of different sites in Bp 3-30 and Bp 4-14, Lippe, North Rhine-Westphalia, Germany are 14.96 n Sv h⁻¹ and 16.51 n Sv h⁻¹ respectively, Table 4-2.

4.1.3 External gamma-dose rate of ^{137}Cs in soil from Ukraine (Chernobyl)

Table 4 - 3: External gamma-dose rate of ^{137}Cs in $\mu\text{Sv h}^{-1}$ and densities deposition of ^{137}Cs in different sites in Ukraine.

| No of profile | sites | Cs-137 deposits in k Bq m^{-2} | | Dose rate $\mu\text{Sv h}^{-1}$ | |
|---------------|--------------------------|-----------------------------------------|-------------|---------------------------------|--------------------------|
| | | 01.09.2001 | 26.04.19986 | Calculated Referred 1986 | Measured 1995[Bel 98] |
| 1 | Nosdristsche 2 | 3500 ± 112 | 5003 ± 160 | 3.55557 | 4.69 |
| 2 | Christinovka river shore | 3273 ± 229 | 4679 ± 43 | 6.0904 | - |
| 3 | Christinovka meadow | 580 ± 19 | 822 ± 26 | 0.43978 | - |
| 4 | Nowe Scharno 3 | 2502 ± 80 | 3549 ± 114 | 3.5691 | 5.33 |
| 5 | Woronewo 1 | 380 ± 12 | 540 ± 17 | 0.68006 | 0.872 |
| 6 | Woronewo 2 | 141 ± 5 | 200 ± 7 | 0.39905 | 1.310 |
| 7 | Woronewo 3 | 313 ± 10 | 444 ± 14 | 0.74128 | 1.130 |
| 8 | Woronewo 4 | 560 ± 18 | 795 ± 25 | 1.39847 | 1.800 |
| 9 | Woronewo 5 | 394 ± 13 | 560 ± 18 | 1.22632 | 1.540 |
| 10 | Woronewo 6 | 380 ± 12 | 540 ± 17 | 0.64261 | 1.170 |
| 11 | Woronewo 7 | 188 ± 6 | 267 ± 9 | 0.14943 | 0.728 |
| 12 | Tschigiri 1 | 259 ± 8 | 368 ± 12 | 0.71451 | 0.974 |
| 13 | Tschigiri 2 | 261 ± 8 | 371 ± 12 | 0.65457 | 0.938 |
| 14 | Tschigiri 3 | 247 ± 8 | 352 ± 11 | 0.58822 | 1.080 |
| 15 | Tschigiri - Zwintor 1 | 362 ± 11 | 505 ± 15 | 1.62 | 1.030 |
| 16 | Osernjanka 1 | 6 ± 0.3 | 7.9 ± 0.5 | 0.0055 | - |
| 17 | Osernjanka 2 | 2 ± 0.2 | 2.2 ± 0.2 | 0.005 | - |
| 18 | Osernjanka 3 | 2 ± 0.1 | 2.8 ± 0.2 | 0.002 | - |
| 19 | Baraschewka 1 | 2 ± 0.1 | 2.8 ± 0.2 | 0.00387 | - |
| 20 | Dawidowka 1 | 4 ± 0.2 | 5.2 ± 0.3 | 0.00547 | - |
| 21 | Lewkow 1 | 4 ± 0.2 | 5.0 ± 0.3 | 0.00475 | - |
| 22 | Lewkow 2 | 2 ± 0.1 | 2.6 ± 0.1 | - | - |

According to [Bel98, Bot00], the external gamma dose rate of ^{137}Cs from global fallout in air (1 m height above soil surface) can be calculated from its depth distribution in the soil.

From the Table 4-3 we can see that the external gamma-dose rate of ^{137}Cs from global fallout varied between not contaminated, medium (Zone III) and high contaminated (Zone II) in Ukraine. With respect to the total activity of ^{137}Cs from global fallout in the soil at each site (kBq m^{-2}) the range of the values external gamma dose rate of ^{137}Cs is: 0.002 – 6.0904 $\mu\text{Sv h}^{-1}$.

In Fig. 4-3, the external dose rates of ^{137}Cs from global fallout are compared with those of the Chernobyl-derived ^{137}Cs , both related to the corresponding total activities, at the twenty two sampling sites. As expected, the dose rate of Chernobyl-derived ^{137}Cs was larger than that of ^{137}Cs from global fallout at all sites, because the activity of Chernobyl-derived ^{137}Cs was concentrated nearer to the soil surface.

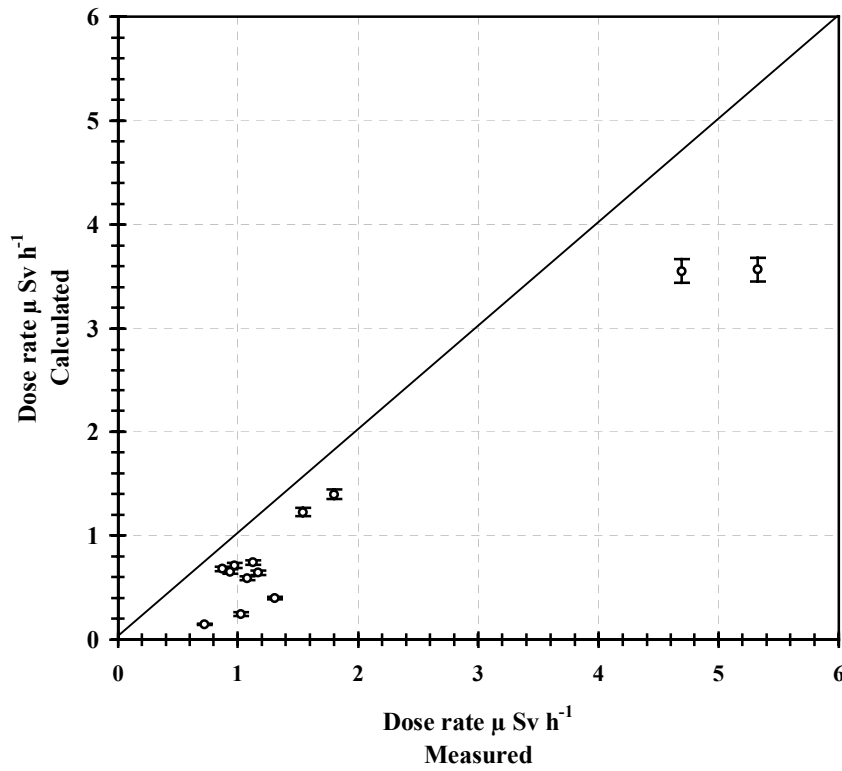


Fig. 4-2: Correlation between results of measurements and calculations dose rates in different sites in Ukraine.

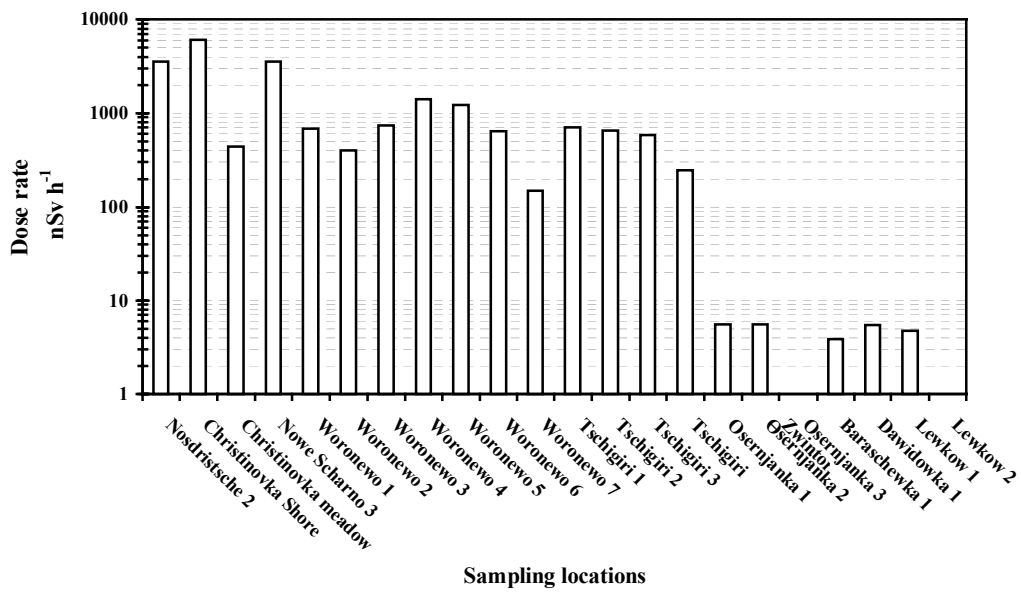


Fig. 4-3: Calculated external gamma-dose rate (n Sv h⁻¹) of ¹³⁷Cs from Chernobyl-fellout in different locations in Ukraine.

4.2 Ambient dose rates from natural radionuclides in soil at height of 1 m above ground in investigation sites.

The ambient dose equivalent rate has been measured using the device: FH 40 G-L System-Radiometer the company ESM Eberline Instruments [Wah02]. The results have been used for theoretical evaluation of the external dose rate on the basis of the relation eq. (4-1) below [UNS82]:

$$D = a \cdot C_U + b \cdot C_{Th} + c \cdot C_k \quad (4-1)$$

where D the absorbed dose rate in air for one meter above the soil surface (nGyh^{-1}), a the dose rate per unit ^{238}U activity mass concentration in soil = $0.462 \text{ n Gyh}^{-1}/\text{Bqkg}^{-1}$, C_U the concentration of ^{226}Ra in the soil (Bq kg^{-1}), taken as the ^{226}Ra concentration, b the dose rate per unit ^{232}Th activity mass concentration in soil = $0.604 \text{ n Gyh}^{-1}/\text{Bqkg}^{-1}$. C_{Th} the concentration of ^{232}Th in the soil (Bq kg^{-1}), taken as the ^{228}Ra concentration. c the dose rate per unit ^{40}K activity mass concentration in soil = $0.0417 \text{ n Gyh}^{-1}/\text{Bqkg}^{-1}$ C_k the concentration of ^{40}K in the soil (Bq kg^{-1}). The conversion factors used to compute the absorbed dose rate in air per unit of specific activity concentration in soil for ^{40}K , ^{226}Ra , and ^{232}Th [ICR94]. The conversion factor for photon equivalent dose rate in air kirma is 1.15 Sv Gy^{-1} [Kem96].

4.2.1 Ambient dose rate in air from gamma-radiation 1 m above the ground surface in Lower Saxony, Germany.

Table 4 - 4: Absorbed dose rate in air from gamma-radiation 1 m above the ground surface in Lower Saxony, Germany.

| Sites | Ra-226 [Bq/kg] | K-40 [Bq/kg] | Th-232 [Bq/kg] | Dose rate [n Sv h ⁻¹] |
|--------------|-------------------|-----------------|-------------------|--------------------------------------|
| Klein Lobke | 21 ± 1.7 | 462 ± 16 | 24.3 ± 1.1 | 50 ± 2.4 |
| Ricklingen | 19 ± 1.0 | 419 ± 14 | 21.2 ± 2.3 | 44.9 ± 2.8 |
| Twenge | 7 ± 0.7 | 209 ± 7 | 7.1 ± 0.7 | 18.7 ± 1.2 |
| Adenstedt | 26 ± 1.5 | 496 ± 17 | 31.7 ± 2.6 | 59.6 ± 3.4 |
| Eilenriede | 11 ± 0.7 | 253 ± 9 | 13.4 ± 1.0 | 27.2 ± 1.5 |
| Barum | 21 ± 1.5 | 315 ± 11 | 22.6 ± 2.9 | 42.0 ± 3.3 |
| Vestrup | 9 ± 0.7 | 139 ± 5 | 8.4 ± 1.0 | 17.3 ± 1.3 |
| Neßmerpolder | 23.5 ± 1.5 | 390 ± 46 | 26.5 ± 1.2 | 49.5 ± 2.5 |
| Min. | 7 ± 0.7 | 139 ± 5 | 7.1 ± 0.7 | 17.3 ± 1.3 |
| Max. | 26 ± 1.5 | 496 ± 17 | 31.7 ± 2.6 | 59.6 ± 3.4 |
| Mean | 17.2 ± 1.2 | 335.4 ± 15.4 | 19.4 ± 1.6 | 38.7 ± 2.5 |

Table 4-4 gives the absorbed dose rates calculated from a height of 1 m above the ground surface calculated from the activity concentrations of the radionuclides measured. The mean dose rate at Lower Saxony $38.7 \pm 2.5 \text{ n Sv h}^{-1}$ is less than that from the other sites in Lippe, NRW $126 \pm 12.6 \text{ n Sv h}^{-1}$, probably due to its higher natural radionuclide content in soils. Minimum and maximum dose rate are $17.3 \pm 1.3 \text{ n Sv h}^{-1}$ and $59.6 \pm 3.4 \text{ n Sv h}^{-1}$ respectively.

The ambient dose equivalent rate (ADER) was measured at a height of 1 m above the ground surface during sampling of under investigation sites. The ADER caused by radionuclides

in soil was determined. The largest part of ADER is caused by ^{40}K (41% on average), 24% is due to ^{226}Ra and its progeny, and 35% is due to ^{232}Th and its progeny.

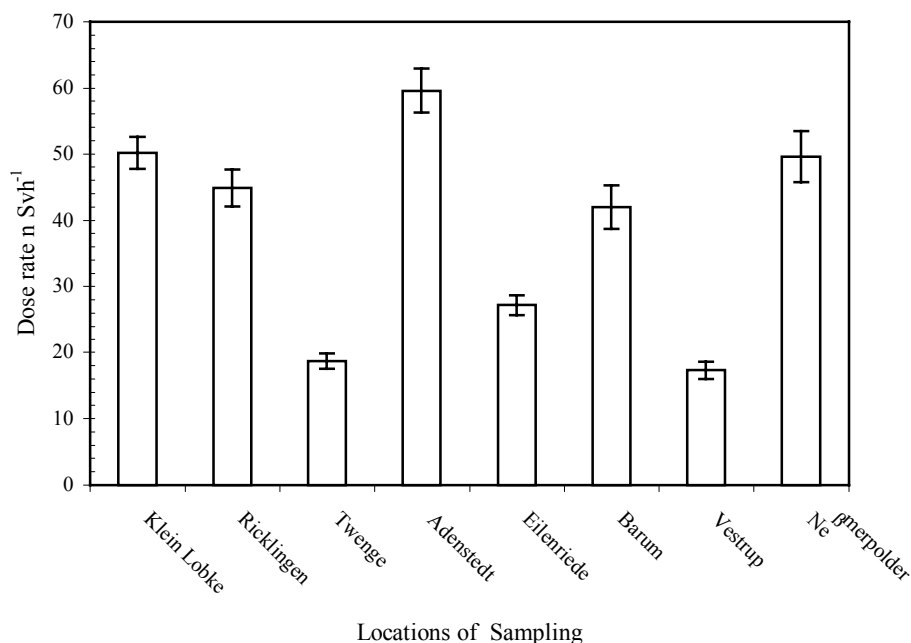


Fig. 4-4: Calculated dose rates from natural radionuclides in soil samples from different locations in Lower Saxony, North Germany.

The composition of the various soil samples is shown in Table 4 - 4 and Fig 4 - 4, summarize the measured concentrations of the naturally occurring radioactive elements ^{226}Ra , ^{232}Th , ^{40}K in soils in Lower Saxony North Germany. The results indicated that the main contribution to the background gamma-radiation in soils is the radiation from the natural radioactive series notably ^{40}K , ^{226}Ra and ^{232}Th . The ^{40}K content of the soil samples ranged from 139 to 496 Bq kg⁻¹. In the soil samples ^{232}Th content ranged from 7.1 to 31.7 Bq kg⁻¹ and 7 to 26 Bq kg⁻¹. Samples from Adenstedt were found to contain the highest concentration of ^{232}Th for both soils while Twenge and Westrup gave the lowest value among the soil samples. The ^{226}Ra content in soil samples ranged from 7 to 26 Bq kg⁻¹. The highest concentration of ^{226}Ra was found in the soil from Adenstedt. In the same table, the absorbed doses in air due to the natural gamma terrestrial radiation are also reported. Data are calculations absorbed dose in air, namely $(38.7 \pm 2.5) \text{ n Sv h}^{-1}$

The absorbed doses in air due to the natural gamma terrestrial radiation are also reported. Data are thermoluminescent-measured absorbed dose in air corrected for the cosmic-ray contribution at sea level in Italy, namely 0.28 m Gy y^{-1} . The experimental thermoluminescent data are compared with absorbed doses in air calculated from the concentration values of natural radionuclides. The conversion factors used to compute the absorbed dose rate in air per unit of specific activity concentration in soil (1 Bq kg^{-1}) were 43 p Gy h^{-1} for ^{40}K , 427 p Gy h^{-1} for ^{238}U , and 662 p Gy h^{-1} for ^{232}Th (UNS88) considering a homogeneous distribution of radionuclides in a semi-infinite plane [Bra92].

Table 4 - 5: Calculated absorbed dose rate in air from gamma-radiation 1 m above the ground surface in Lower Saxony.

| Location | soil sample No | Ra-226 (Bq/Kg) | K-40 (Bq/Kg) | Th-232 (Bq/Kg) | Dose rate [$n \cdot Sv h^{-1}$] |
|--------------|-----------------|----------------|--------------|----------------|-----------------------------------|
| Jeinsen | JeBoEPKr01 | 33 ± 1 | 496 ± 17 | 28 ± 1 | 61 ± 2 |
| | JeBoEPKs01 | 33 ± 1 | 597 ± 21 | 29 ± 1 | 67 ± 3 |
| | JeBoEPRb01 | 34 ± 1 | 186 ± 7 | 32 ± 1 | 49 ± 2 |
| | JeBoEPMa01 | 36 ± 1 | 359 ± 13 | 30 ± 1 | 57 ± 2 |
| | JeBoEPBr01 | 33 ± 1 | 555 ± 19 | 30 ± 1 | 65 ± 2 |
| | JeBoEPLa01 | 33 ± 1 | 558 ± 19 | 28 ± 1 | 64 ± 2 |
| | JeBoEPWk01 | 35 ± 1 | 581 ± 20 | 32 ± 1 | 69 ± 2 |
| | JeBoEPEg01 | 32 ± 1 | 539 ± 18 | 31 ± 1 | 64 ± 2 |
| | JeBoEPRo01 | 33 ± 1 | 547 ± 19 | 32 ± 1 | 66 ± 2 |
| | JeBoEPWeK01 | 33 ± 1 | 544 ± 18 | 32 ± 1 | 66 ± 2 |
| | JeBoEKPI | 32 ± 1 | 557 ± 19 | 27 ± 1 | 62 ± 2 |
| | JeBoEPPe01 | 30 ± 1 | 510 ± 17 | 26 ± 1 | 58 ± 2 |
| | JeBoEPGk01 | 32 ± 1 | 577 ± 20 | 28 ± 1 | 65 ± 2 |
| Neßmerpolder | PoBoEPLu01 | 22 ± 1 | 511 ± 18 | 23 ± 1 | 52 ± 2 |
| | PoBoEPWe01 | 23 ± 1 | 522 ± 18 | 23 ± 1 | 53 ± 2 |
| | PoBoEPWe02 | 24 ± 1 | 526 ± 18 | 28 ± 1 | 57 ± 2 |
| | PoBoMPHa02 | 24 ± 1 | 508 ± 18 | 23 ± 1 | 53 ± 2 |
| | PoBoEPRa01 | 26 ± 1 | 503 ± 18 | 27 ± 1 | 57 ± 2 |
| | PoBoEPLu02 | 24 ± 1 | 527 ± 18 | 29 ± 1 | 58 ± 2 |
| | PoBoMPHa01 | 27 ± 1 | 496 ± 17 | 28 ± 1 | 58 ± 2 |
| | PoBoMPWe01 | 23 ± 1 | 476 ± 16 | 24 ± 1 | 52 ± 2 |
| | PoBoMPHe01 | 20 ± 1 | 382 ± 13 | 22 ± 1 | 44 ± 2 |
| | PoBoEPHa02 | 26 ± 1 | 506 ± 17 | 31 ± 1 | 59 ± 2 |
| | PoBoEPHe02 | 27 ± 1 | 612 ± 21 | 33 ± 1 | 67 ± 3 |
| | PoBoMPGe01 | 20 ± 1 | 458 ± 16 | 23 ± 1 | 48 ± 2 |
| | PoBoMPLu1 | 22 ± 1 | 475 ± 16 | 24 ± 1 | 51 ± 2 |
| | Schessinghausen | ScBoMPRo01 | 14 ± 1 | 159 ± 6 | 13 ± 1 |
| ScBoMPTr02 | | 15 ± 1 | 151 ± 6 | 12 ± 1 | 23 ± 1 |
| ScBoMPRa01 | | 13 ± 1 | 284 ± 10 | 11 ± 1 | 29 ± 1 |
| ScBoMPWe01 | | 15 ± 1 | 253 ± 9 | 13 ± 1 | 29 ± 1 |
| ScBoMPTr01 | | 11 ± 1 | 225 ± 8 | 10 ± 1 | 23 ± 1 |
| ScBoMPWe02 | | 16 ± 1 | 309 ± 11 | 15 ± 1 | 34 ± 1 |
| ScBoEPKa01 | | 15 ± 1 | 282 ± 10 | 15 ± 1 | 32 ± 1 |
| ScBoEPMa01 | | 15 ± 1 | 292 ± 10 | 14 ± 1 | 31 ± 1 |
| Schlewecke | SiBoEPRa01 | 29 ± 1 | 580 ± 20 | 30 ± 1 | 64 ± 2 |
| | SiBoEZu01 | 32 ± 1 | 545 ± 18 | 31 ± 1 | 65 ± 2 |
| | SiBoMPGe01 | 29 ± 1 | 535 ± 18 | 28 ± 1 | 61 ± 2 |
| | SiBoMPGe02 | 42 ± 1 | 852 ± 29 | 46 ± 2 | 95 ± 4 |
| | SiBoMPRa01 | 31 ± 1 | 609 ± 21 | 34 ± 1 | 69 ± 3 |
| | SiBoMPWe01 | 40 ± 1 | 771 ± 26 | 44 ± 2 | 89 ± 3 |
| | SiBoMPWe02 | 40 ± 1 | 752 ± 25 | 41 ± 2 | 86 ± 3 |
| | SiBoEPWe01 | 66 ± 2 | 1332 ± 45 | 73 ± 2 | 150 ± 6 |

| Location | soil sample No | Ra-226 (Bq/Kg) | K-40 (Bq/Kg) | Th-232 (Bq/Kg) | Dose rate [n Sv h ⁻¹] |
|--------------------------------------|----------------|----------------|--------------|----------------|-----------------------------------|
| Gestorf | GeBMPWe01 | 34 ± 1 | 565 ± 20 | 34 ± 1 | 69 ± 3 |
| | GeBoEPKa01 | 34 ± 1 | 390 ± 14 | 31 ± 1 | 58 ± 2 |
| | GeBoEPZu01 | 32 ± 1 | 583 ± 20 | 29 ± 1 | 65 ± 2 |
| Gümmer | GuBoEPrh01a | 21 ± 1 | 457 ± 16 | 20 ± 1 | 47 ± 2 |
| | GuBoEPrh01b | 22 ± 1 | 469 ± 16 | 20 ± 1 | 48 ± 2 |
| Hermannsdorfes Landwerkstätten (HLW) | HLWBoEPHe01 | 30 ± 1 | 503 ± 17 | 31 ± 1 | 62 ± 2 |
| | RhBoEPWa01 | 33 ± 1 | 806 ± 27 | 35 ± 2 | 81 ± 3 |
| Min. | | 11 ± 1 | 151 ± 6 | 10 ± 1 | 23.3 ± 1 |
| Max. | | 66 ± 2 | 1332 ± 45 | 73 ± 2 | 150 ± 6 |
| Mean | | 27.9 ± 1 | 508 ± 17 | 27.6 ± 1 | 58.3 ± 2 |

The results of specific activities of ⁴⁰K, ²²⁶Ra and ²³²Th are given in Table 4-5. All results of specific activities are expressed on the dry weight bases in Bq kg⁻¹. The results indicate that ⁴⁰K is the only radionuclide present in a significant amount in all soil samples while the other radionuclides are present in very small concentrations. The specific activity of ⁴⁰K ranges from (151 ± 6) to (1332 ± 45) with an average of (508 ± 17) Bq kg⁻¹. that of ²²⁶Ra ranges from (11 ± 1) to (66 ± 2) with an average of (27.9 ± 1) Bq kg⁻¹ and that of ²³²Th ranges from (10 ± 1) to (73 ± 2) Bq kg⁻¹ with an average specific activity of (27.6 ± 1) Bq kg⁻¹. It can be seen from the results that the distribution of these naturally occurring radionuclides in the soil samples analyzed are not uniform and even.

The results calculated for absorbed gamma-ray dose rate are summarized in Table 4-5. The highest value of absorbed dose rate was found for Schlewecke area (sample No. SIBoEPWe01). i.e., (150 ± 6) n Sv h⁻¹ while the lowest for Schessinghausen (sample No. ScBoMPTr01) area, i.e., (23.3 ± 1) n Sv h⁻¹. The overall mean absorbed dose rate in air of the selected areas was calculated to be (58.3 ± 2) n Sv h⁻¹. The outdoor dose rate calculated for Jhangar valley is relatively higher than the world average terrestrial dose rate of 65.5 n Sv h⁻¹ and also from the value reported for Brunei Darrussalam (39 n Sv h⁻¹) [Lai99]. However, this dose rate in air was comparable to that reported for Denver (USA), i.e., a range of 67 to 162 n Sv h⁻¹ and mean absorbed dose rate of 108 n Sv h⁻¹. These values for Denver were, however, much higher than the values found for other areas of Atlantic. Gulf coastal plains and non-coastal plains of USA [Sto99]. This relatively higher terrestrial dose rate in air is consistent with the higher terrestrial radionuclide activity in the soil of the selected area, such as higher activity and large variations of ⁴⁰K as reported in Table 4-5.

4.2.2 Ambient dose rates at Lippe, North Rhine-Westphalia, Germany.

Ambient dose rates were measured using the instrument FH 40 G-L System-Radiometer (the manufactured by the company ESM Eberline Instruments).

Table 4 - 6: ^{226}Ra , ^{232}Th and ^{40}K concentrations in soil samples and measured and calculated values of the external Gamma dose rates in n Sv h^{-1} at Lippe, NRW, Germany.

| Soil sample No | Ra226 [Bq/kg] | K40 [Bq/kg] | Th232 [Bq/kg] | Dose rate [n Sv h ⁻¹] measured | Dose rate [n Sv h ⁻¹] Calculated |
|----------------|---------------|-------------|---------------|--------------------------------------------|----------------------------------------------|
| BP 2-04f | 344 ± 8 | 283 ± 11 | 101 ± 3 | 137 ± 13 | 266 ± 7 |
| BP 2-05f | 155 ± 4 | 359 ± 14 | 62 ± 5 | 111 ± 11 | 143 ± 6 |
| BP 2-06f | 170 ± 3 | 451 ± 17 | 61 ± 1 | 106 ± 10 | 154 ± 3 |
| BP 2-07f | 67 ± 4 | 262 | 21 ± 3 | 103 ± 10 | 63 ± 4 |
| BP 2-11f | 123 ± 7 | 376 | 59 ± 6 | 87 ± 9 | 125 ± 8 |
| BP 2-12f | 164 ± 3 | 401 ± 15 | 50 ± 3 | 127 ± 12 | 141 ± 4 |
| BP 2-13f | 88 ± 3 | 259 ± 10 | 25 ± 1 | 88 ± 9 | 77 ± 3 |
| BP 2-17f | 342 ± 7 | 334 ± 14 | 123 ± 5 | 197 ± 19 | 284 ± 8 |
| BP 2-23f | 197 ± 11 | 185 | 76 ± 8 | 142 ± 14 | 166 ± 11 |
| BP 2-24f | 259 ± 14 | 399 | 93 ± 8 | 190 ± 19 | 221 ± 13 |
| BP 2-25f | 44 ± 2 | 268 ± 10 | 21 ± 2 | 84 ± 8 | 50 ± 3 |
| BP 2-33f | 55 ± 3 | 307 ± 12 | 33 ± 3 | - | 67 ± 4 |
| BP 2-34f | 21 ± 1 | 175 | 15 ± 2 | - | 30 ± 2 |
| BP 2-35f | 26 ± 1 | 218 | 17 ± 2 | - | 36 ± 2 |
| BP 2-36f | 272 ± 4 | 334 ± 127 | 63 ± 6 | - | 204 ± 7 |
| BP 3-01 | 278 ± 14 | 318 | 85 ± 8 | - | 222 ± 13 |
| BP 3-02 | 71 ± 4 | 298 | 20 ± 2 | 150 ± 15 | 66 ± 4 |
| BP 3-03 | 23 ± 1 | 352 | 20 ± 2 | 115 ± 11 | 43 ± 2 |
| BP 3-04 | 239 ± 12 | 340 | 62 ± 6 | 96 ± 9 | 186 ± 11 |
| BP 3-05 | 208 ± 10 | 346 | 55 ± 5 | 128 ± 13 | 165 ± 9 |
| BP 3-06 | 34 ± 2 | 579 ± 22 | 36 ± 3 | 122 ± 12 | 71 ± 4 |
| BP 3-09 | 29 ± 2 | 331 ± 7 | 21 ± 2 | 81 ± 8 | 46 ± 3 |
| BP 3-07 | 520 ± 28 | 387 ± 13 | 100 ± 5 | 194 ± 19 | 364 ± 19 |
| BP 3-08 | 189 ± 10 | 373 ± 13 | 34 ± 4 | 119 ± 19 | 142 ± 9 |
| BP 3-10 | 225 ± 9 | 375 ± 20 | 45 ± 6 | 136 ± 12 | 169 ± 10 |
| BP 3-11 | 82 | 1104 ± 37 | 62 ± 6 | 137 ± 13 | 140 ± 6 |
| BP 3-12 | 380 ± 21 | 327 ± 11 | 48 ± 5 | 111 ± 11 | 251 ± 10 |
| BP 3-13 | 194 ± 8 | 434 ± 15 | 34 ± 7 | 106 ± 10 | 147 ± 10 |
| BP 3-14 | 37 ± 2 | 326 ± 11 | 17 ± 1 | 103 ± 10 | 48 ± 2 |
| BP 3-15 | 343 ± 20 | 385 ± 13 | 67 ± 2 | 87 ± 9 | 247 ± 13 |
| BP 3-16 | 238 ± 12 | 206 ± 7 | 52 ± 3 | 127 ± 12 | 172 ± 9 |
| BP 3-17 | 15 ± 1 | 237 ± 8 | 11 ± 1 | 88 ± 9 | 27 ± 2 |
| BP 3-18 | 37 ± 3 | 2547 ± 9 | 20 ± 2 | 197 ± 19 | 46 ± 3 |
| BP 3-21 | 89 ± 4 | 169 ± 3 | 13 ± 1 | 142 ± 14 | 64 ± 3 |
| BP 3-22 | 81 ± 4 | 296 | 21 ± 2 | 190 ± 19 | 72 ± 4 |
| BP 3-23 | 179 ± 11 | 261 ± 9 | 21 ± 2 | 84 ± 8 | 122 ± 8 |
| BP 3-24 | 36 ± 2 | 238 | 14 ± 1 | - | 40 ± 2 |
| BP 3-25 | 182 ± 9 | 258 ± 6 | 29 ± 3 | - | 129 ± 7 |
| BP 3-26 | 74 ± 4 | 240 ± 5 | 16 ± 2 | - | 62 ± 4 |

| Soil sample No | Ra226 [Bq/kg] | K40 [Bq/kg] | Th232 [Bq/kg] | Dose rate [n Sv h ⁻¹] measured | Dose rate [n Sv h ⁻¹] Calculated |
|-------------------|---------------|--------------|---------------|--------------------------------------------|----------------------------------------------|
| BP 3-28 | 99 ± 5 | 304 ± 10 | 19 ± 1 | - | 80 ± 4 |
| BP 3-29 | 151 ± 8 | 297 ± 10 | 23 ± 2 | - | 111 ± 5 |
| BP 4-01 | 214 ± 11 | 424 ± 16 | 44 ± 4 | 74 ± 13 | 165 ± 9 |
| BP 4-05 | 545 ± 31 | 387 ± 12 | 112 ± 10 | 148 ± 7 | 386 ± 24 |
| BP 4-06 | 87 ± 5 | 651 ± 22 | 45 ± 2 | 107 ± 15 | 109 ± 5 |
| BP 4-09 | 77 ± 4 | 341 ± 12 | 14 ± 1 | 62 ± 10 | 67 ± 3 |
| BP 4-10 | 164 ± 10 | 304 ± 10 | 24 ± 2 | 179 ± 6 | 118 ± 7 |
| BP 4-11 | 222 ± 12 | 312 ± 11 | 37 ± 2 | 118 ± 18 | 158 ± 8 |
| BP 4-12 | 35 ± 2 | 281 ± 10 | 18 ± 2 | 47 ± 12 | 44 ± 3 |
| BP 4-15 | 193 ± 11 | 413 ± 14 | 46 ± 5 | 56 ± 5 | 155 ± 10 |
| BP 4-16 | 38 ± 2 | 267 ± 9 | 13 ± 1 | 72 ± 5 | 42 ± 2 |
| BP Sicking. (71) | 572 ± 28 | 256 | 137 ± 11 | 72 ± 7 | 411 ± 23 |
| BP Vorfluter (70) | 741 ± 36 | 214 | 154 ± 13 | 100 ± 7 | 511 ± 28 |
| BP 5-01 | 201 ± 4 | 265 | 29 ± 1 | 53 ± 10 | 140 ± 3 |
| BP 5-02 | 161 ± 8 | 259 | 25 ± 3 | 100 ± 5 | 116 ± 6 |
| BP 5-03 | 218 ± 4 | 324 | 43 ± 1 | 65 ± 10 | 161 ± 3 |
| BP 5-04 | 238 ± 12 | 324 | 45 ± 5 | 85 ± 6 | 173 ± 10 |
| BP 5-05 (Sedi) | 73 ± 4 | 196 | 17 ± 2 | 78 ± 8 | 60 ± 4 |
| BP 5-06 | 257 ± 13 | 387 | 59 ± 6 | 115 ± 8 | 196 ± 11 |
| BP 5-07 | 191 ± 10 | 353 | 43 ± 4 | 169 ± 11 | 148 ± 8 |
| BP 5-08 | 265 ± 13 | 312 | 58 ± 6 | 103 ± 17 | 196 ± 11 |
| BP 5-09 | 243 ± 12 | 369 | 61 ± 6 | 78 ± 10 | 189 ± 11 |
| BP 5-10 | 391 ± 19 | 382 | 107 ± 10 | 98 ± 8 | 300 ± 17 |
| BP 5-11 | 13 ± 1 | 199 | 10 ± 1 | 101 ± 10 | 24 ± 1 |
| Min. | 13 ± 1 | 175 | 10 ± 1 | 53 ± 10 | 24 ± 1 |
| Max. | 741 ± 36 | 1104 ± 37 | 154 ± 13 | 179 ± 6 | 511 ± 28 |
| Mean | 187 ± 9 | 331.6 ± 12.5 | 47 ± 4 | 126 ± 12 | 148 ± 7 |

The results calculated for absorbed gamma-ray dose rate for different sites in Lippe, NRW, Germany are summarized in Table 4-6. The highest value of absorbed dose rate was found for sample No. BP5-01 i.e., 511 ± 28 n Sv h⁻¹ while the lowest for sample No. BP5-11, i.e., 24 ± 1 n Sv h⁻¹. The overall mean absorbed dose rate in air of the selected areas was calculated to be 148 ± 7 n Sv h⁻¹. The mean outdoor dose rate measured for the same areas is 126 ± 12 n Sv h⁻¹.

The results of this experiment are shown in Fig.4-5, as a correlation between actual dose rate data (measurement) and inferred dose rate data (calculation). The result showed a positive correlation. i.e. the dose rates inferred are nearly equal to the dose rates measured. This supports the contention that dose rates remotely measured can be representative of the activity per unit of surface area in the soil, though a source distribution has to be presumed.

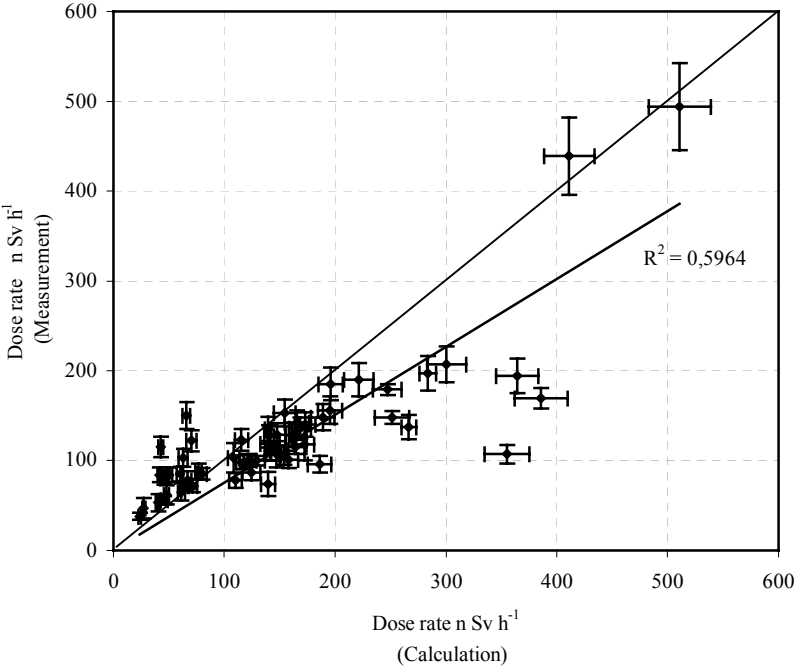


Fig. 4-5: Correlation between results of measurements and calculations dose rates at Lippe, NRW, Germany.

4.2.3 ^{226}Ra , ^{232}Th and ^{40}K concentrations in soil samples and calculated values of the external Gamma dose rates in n Sv h^{-1} at Ukraine.

Calculated external Gamma dose rates (n Sv h^{-1}) from soil at different sites in Ukraine by using ^{226}Ra , ^{232}Th and ^{40}K concentrations in Bq kg^{-1} . The results in table 4-7 obtained from eq. 4-1.

Table 4 - 7: Absorbed dose rate in air from gamma-radiation 1 m above the ground surface in Ukraine.

| No of profile | sites | Ra-226 | K-40 | Th-232 | External dose rates [n Sv h^{-1}] |
|---------------|-----------------------|----------------|------------------|----------------|----------------------------------------------|
| 1 | Nosdriutsche 2 | 5.9 ± 1.8 | 204.6 ± 8.4 | 7.7 ± 1.7 | 18.3 ± 2.5 |
| 2 | Christinovka shore | 29.7 ± 3.6 | 523.7 ± 19.7 | 33.0 ± 3.5 | 63.8 ± 5.3 |
| 3 | Christinovka meadow | 18.8 ± 2.1 | 251.0 ± 10.4 | 18.8 ± 3.0 | 35.1 ± 3.7 |
| 4 | Nowe Scharno 3 | 17.4 ± 2.7 | 317.3 ± 12.1 | 17.8 ± 3.8 | 36.8 ± 4.6 |
| 5 | Woronewo 1 | 23.7 ± 2.6 | 322.6 ± 13.4 | 21.8 ± 2.6 | 43.2 ± 3.8 |
| 6 | Woronewo 2 | 20.8 ± 2.2 | 334.0 ± 13.1 | 20.9 ± 3.4 | 41.6 ± 4.2 |
| 7 | Woronewo 3 | 19.0 ± 1.5 | 236.5 ± 10.4 | 20.0 ± 1.6 | 35.3 ± 2.4 |
| 8 | Woronewo 4 | 20.6 ± 3.4 | 344.6 ± 14.3 | 17.9 ± 2.5 | 39.9 ± 4.2 |
| 9 | Woronewo 5 | 19.0 ± 1.9 | 415.4 ± 15.9 | 18.8 ± 2.0 | 43.1 ± 3.1 |
| 10 | Woronewo 6 | 15.9 ± 1.1 | 245.5 ± 10.4 | 19.1 ± 1.5 | 33.5 ± 2.1 |
| 11 | Woronewo 7 | 20.3 ± 2.3 | 235.3 ± 12.1 | 25.2 ± 3.1 | 39.5 ± 4.0 |
| 12 | Tschigiri 1 | 15.5 ± 8.0 | 336.5 ± 13.1 | 17.2 ± 1.6 | 36.3 ± 6.0 |
| 13 | Tschigiri 2 | 22.8 ± 2.4 | 321.5 ± 13.6 | 21.7 ± 2.4 | 42.6 ± 3.6 |
| 14 | Tschigiri 3 | 19.0 ± 1.5 | 294.0 ± 12.4 | 18.8 ± 1.7 | 37.3 ± 2.6 |
| 15 | Tschigiri – Zwintor 1 | 21.0 ± 1.8 | 343.6 ± 13.1 | 21.2 ± 2.6 | 42.3 ± 3.4 |
| 16 | Osernjanka 1 | 12.7 ± 1.7 | 97.2 ± 7.3 | 10.5 ± 1.9 | 18.7 ± 2.6 |
| 17 | Osernjanka 2 | 16.8 ± 2.0 | 241.5 ± 12.1 | 19.3 ± 2.5 | 33.9 ± 3.4 |
| 18 | Osernjanka 3 | 22.4 ± 5.0 | 307.7 ± 13.0 | 28.2 ± 1.7 | 46.2 ± 4.4 |
| 19 | Baraschewka 1 | 20.3 ± 1.2 | 361.5 ± 14.1 | 24.1 ± 1.9 | 44.9 ± 2.6 |
| 20 | Dawidowka 1 | 38.5 ± 3.3 | 324.2 ± 13.8 | 37.7 ± 4.2 | 62.2 ± 5.3 |
| 21 | Lewkow 1 | 65.7 ± 2.7 | 264.1 ± 14.1 | 27.7 ± 1.9 | 66.8 ± 3.4 |
| 22 | Lewkow 2 | 32.3 ± 1.5 | 326.5 ± 12.4 | 21.0 ± 1.4 | 47.4 ± 2.3 |
| Min. | | 5.9 ± 1.8 | 97.2 ± 7.3 | 7.7 ± 1.7 | 18.3 ± 2.5 |
| Max. | | 65.7 ± 2.7 | 523.7 ± 19.7 | 37.7 ± 4.2 | 66.8 ± 3.4 |
| Mean | | 22.6 ± 2.6 | 302.2 ± 12.7 | 21.3 ± 2.4 | 41.3 ± 3.6 |

Tables 4-7 and Fig. 4-6 show the calculated exposure rate (n Sv h^{-1}) due to the terrestrial radionuclides at one meter above ground. In soil, the exposure rate ranged from 18.3 ± 2.5 to $66.8 \pm 3.4 \text{ n Sv h}^{-1}$ and the average dose rate is $41.3 \pm 3.6 \text{ n Sv h}^{-1}$.

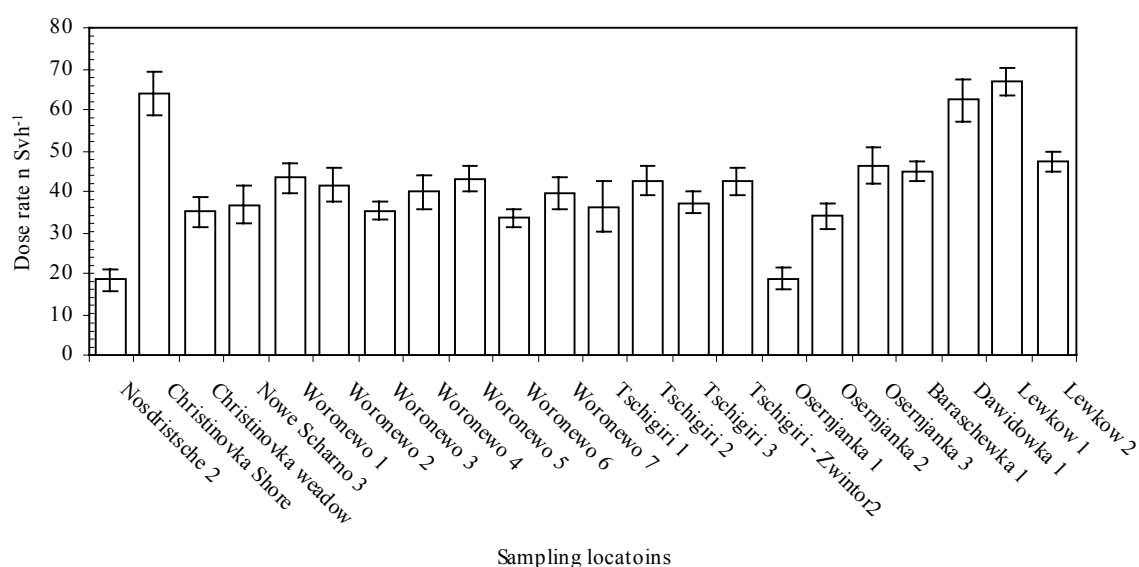


Fig. 4-6: Dose rate from natural radionuclides in soil samples from different sites in Ukraine

4.3 External gamma dose rate of natural and artificial radionuclides in North Germany.

Gamma dose levels were also investigated at Lower Saxony and Lippe (Table 4-8). The mean dose rate at Lippe 131 n Sv h⁻¹ is higher than that from the other sites 69 n Sv h⁻¹, probably, due to its higher natural radionuclide content in soils. This can be confirmed by applying eq. (4-2) below [God98]:

$$D = a \times C_U + b \times C_{Th} + c \times C_K + C_{Cs} + 34 \text{ n Gy h}^{-1} \quad (4-2)$$

where D the absorbed dose rate in air for one meter above the soil surface (n Gy h⁻¹), a the dose rate per unit ²³⁸U activity mass concentration in soil = 0.462 n Gy h⁻¹ / Bq kg⁻¹, C_U the concentration of ²²⁶Ra in the soil (Bq kg⁻¹), taken as the ²²⁶Ra concentration. b the dose rate per unit ²³²Th activity mass concentration in soil = 0.604 n Gy h⁻¹ / Bq kg⁻¹. C_{Th} the concentration of ²³²Th in the soil (Bq kg⁻¹), taken as the ²²⁸Ra concentration. c the dose rate per unit ⁴⁰K activity mass concentration in soil = 0.0417 n Gy h⁻¹ / Bq kg⁻¹, C_K the concentration of ⁴⁰K in the soil (Bq kg⁻¹). The conversion factor for photon equivalent dose rate in air kirma is 1.15 Sv Gy⁻¹ [Kem96], C_{Cs} the Dose rate of ¹³⁷Cs in the soil n Sv h⁻¹ which calculate according to [Bel98, Bot00], 34 n Gy h⁻¹ the cosmic ray contribution for the gamma dose level for latitudes higher than 50° [UNS82].

Table 4 - 8: External gamma dose rates in n Sv h⁻¹ for two sites in Germany.

| Sites | U series (Ra-226) | K-40 | Th series (Th-232) | Cs-137 | Cosmic ray [n Sv h ⁻¹] | Dose rate |
|--------------|-------------------|------|--------------------|--------|------------------------------------|-----------|
| Lippe | 100 | 16 | 33 | 16 | 39 | 131 |
| Lower Saxony | 9 | 16 | 13 | 15 | 39 | 69 |

The ambient dose equivalent rate (ADER) was measured at a height of 1 m above the ground surface during sampling of under investigation sites. The ADER caused by radionuclides

in soil was determined. The part of ADER is caused by ^{40}K 17% on average, 10% is due to ^{226}Ra and its progeny, 15% is due to ^{232}Th and its progeny, 16% for ^{137}Cs and the largest part 42% for cosmic ray for Lower Saxony and (ADER) for Lippe is caused by ^{40}K 8% on average. 49% is due to ^{226}Ra and its progeny, 16% is due to ^{232}Th and its progeny, 8% for ^{137}Cs and the 19% for cosmic ray Fig. 4-7.

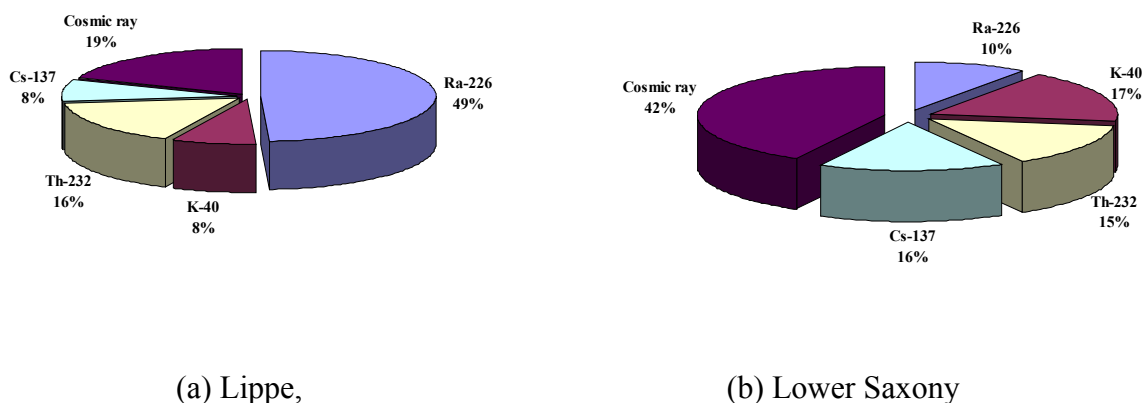


Fig. 4-7: The total external gamma dose rate in different sites, (a) Lippe (b) Lower Saxony

The calculated values shown in Table 4 - 8 are in good agreement with the measured values. As a result of the low uranium and thorium content in soil, for the locations, Lippe and Lower Saxony, it can be seen that the measured dose rates are basically determined by the cosmic-ray contribution. Similar results were obtained by [Ryb02].

Average external dose rate on Swiss territory outdoors is 147 n Sv h^{-1} (1.29 m Sv y^{-1}). The largest part of the Swiss population is exposed to an outdoors dose rate between 85 and 120 n Sv y^{-1} . The highest contribution of the sources considered comes from the natural terrestrial and cosmic radiation, respectively 54 and 46 n Sv h^{-1} . The average dose rate of Swiss population is 108 n Sv y^{-1} (0.95 m Sv y^{-1}) per capita [Ryb02].

5 Internal and external gamma radiation exposure from soil

The following are potential pathways of exposure to radioactive soil contaminants in a residential setting and are addressed by this guidance document:

- External radiation exposure from radionuclides in soil
- Direct ingestion of soil
- Inhalation of dusts

As usually observed in environmental samples, the concentrations of the radionuclides were better represented by the log-normal distribution, and the central tendency thus is represented by the geometric average. When the number of samples was less than three, the geometric average was determined by considering the similarity with the other results [san02].

5.1 Realistic Modeling of transfer of radionuclides from soils to man

Surface soil can become contaminated with radionuclides through: many different mechanisms such as airborne deposition spills and leaching from contaminated material stored above ground. Current activities associated with the cleanup of contaminated weapons production and storage facilities might result in additional soil contamination as well as in the discovery of past contamination. Even after cleanup of known contaminated land, some residual contamination will remain. The calculated doses are deliberately designed to conservatively represent the maximum dose to any individual. Thus, these doses are inappropriate for use in calculating population exposures or to estimate health effects. The calculation of doses to actual individuals requires the use of site-specific and individual specific parameters in the formulas used for the calculations.

Only surface soil contamination refers only to depths comprising the plow layer. i.e., down to a depth of about 30 cm. The guidance here in is not intended to be used for evaluating the implications of an ongoing contamination episode such as a continuing airborne deposition. All other important dose pathways are considered including external radiation exposure, ingestion of contaminated foodstuffs, direct and indirect ingestion of soil by humans and animals, and both indoor and outdoor inhalation of resuspended material. Examples of contamination scenarios for which these limits are applicable include widespread contamination from fallout from weapons tests and nuclear facility accidents (such as occurred at Chernobyl) as well as more localized contamination resulting from nuclear facility operations and/or decontamination and decommissioning [NCR99].

Exposures to radionuclides may be internal or external, and effects are caused by energetic particles or rays released as part of the decay of atoms. Decay energies of particles or rays emitted by each radionuclide must be accounted for. The internal and external doses from all radionuclides present must be summed to arrive at the appropriate exposure dose for a given organism. In addition, a number of radionuclides have daughter products that must also be included in the exposure calculations. Internal exposures result from ingestion of contaminated food, soil, or water or inhalation of contaminated soil or dust. External exposures result from direct exposure to radiation from the soil and may occur either above or below ground. In all cases, the radiation source must be known in terms of the quantity of each specific radionuclide (Bq kg^{-1}) [Sam97].

5.1.1 External gamma radiation exposure from soil

One of the principal dose pathways resulting from contaminated surface soil is external exposure from radiation emitted from the radionuclides present in the surface soil. The dose to individuals from external exposure will depend on a number of factors including the type and energy of the emitted radiations, the distribution of the source with depth in the soil, the relative amount of time spent outdoors versus indoors, the amount of shielding provided by on-site structures and the body itself, and even the moisture content of the soil.

The dose from external irradiation is caused by the photons penetrating the human body from gamma emitting radionuclides. Therefore, the relation between dose and radioactivity is more complicated, depending not only on the radioactivity, but also on the geometry in which the radioactivity is distributed, on shielding effects, on self absorption effects and on the distance to the source. Dose coefficients for external irradiation are expressed in dose rate (i.e. m Sv per hour, m Sv h⁻¹) per activity content of the source (i.e. Bq per kilogram, Bq kg⁻¹). In the present case, suitable dose coefficients are calculated for each nuclide and age group, the dose coefficients are given in tables in [BfS99].

The annual effective dose from external gamma radiation.

$$H_{\text{Ext, a}} = f_{\text{Con, a}} \sum \left(H_{x,s}^{\cdot} - H_x^{\text{U}} \right) \cdot t_{\text{Exp, a, s}} \cdot a_{x,s} \quad (5-1)$$

where:

- $H_{E,a}$ annual effective dose from external gamma radiation for reference man in Sv
 $H_{x,s}^{\cdot}$ Photon - equivalent dose in air at 1 m above ground in exposure work place in Sv
 H_x^{U} Photon - equivalent dose for natural gamma radiation in air at a height of 1 m above ground in Sv h⁻¹
 $f_{\text{con, a}}$ Conversion factor from photon-equivalent dose to effective dose for reference man
 $t_{\text{Exp, a, s}}$ the annual spent time on the exposure site s in h
 $a_{x, s}$ factor for consideration of the shield (protection) on the exposure site s for gamma radiation in air non-dimensional.

$$H_{x,s}^{\cdot} = C_{\text{soil, s}} \cdot g_{\text{ext}}$$

$$H_x^{\text{U}} = C_{\text{Soil}}^{\text{U}} \cdot g_{\text{ext}}$$

where:

- $C_{\text{soil, s}}$ Specific activity for radionuclide where the Uranium-Radium series in radioactive equilibrium for surface soil layers (0-30 cm) for the exposure site s in Bq kg⁻¹ for dry soil
 $C_{\text{Soil}}^{\text{U}}$ Specific natural subsurface activity for radionuclide where the Uranium-Radium series in radioactive equilibrium for surface soil layers (0-30 cm) for the exposure site s in Bq kg⁻¹ for dry soil

g_{ext} Conversion factor for the conversion the Specific activity of soil Uranium-Radium series in radioactive equilibrium) to the photon-equivalent dose in air at a height of 1 m above ground in Sv kg Bq⁻¹ h⁻¹

$$g_{\text{ext}} = 5.3 \cdot 10^{-10} \text{ Sv kg Bq}^{-1} \text{ h}^{-1}$$

5.1.2 Internal gamma radiation exposure from inhalation dust

Another potential pathway for human doses from contaminated sites is inhalation of airborne radionuclides on soil. The potential exposure from this pathway depends on a number of factors including the average activity of the soil, the length of time exposed either inside or outdoors, the particle size distribution of the suspended soil, the nuclide and its chemical form, and the age and breathing rate of the person exposed.

Dose coefficients for inhalation dust are also contained in the [BfS99] with table III-2 applying to 6 age groups of the general population. The dose coefficients relate the individual effective dose (in μSv) to the ingested quantity of radioactivity (in Bq kg⁻¹).

Annual effective dose from inhalation dust $H_{\text{Inh}, a}$ is calculated as the following:-

$$H_{\text{Inh}, a} = \dot{V}_a \sum_s \sum_r (C_{\text{air}, r, s} - C_{\text{air}, r}^U) g_{\text{Inh}, r, a} \cdot t_{\text{Exp}, a, s} \cdot a_{\text{air}, s} \quad (5-2)$$

where

H_{Inh} annual effective dose from inhalation of dust for reference man a in Sv.
 $C_{\text{air}, r, s}$ activity concentration of dust for radionuclide r in external air for for the exposure site s in Bq m⁻³

$C_{\text{air}, r}^U$ natural subsoil-activity concentration of the dust for radionuclide r in external air for the exposure site s in Bq m⁻³

$$C_{\text{air}, r}^U = 0$$

\dot{V}_a breath rate for reference man a in m³ h⁻¹

$g_{\text{Inh}, r, a}$ coefficient of inhalation dose for radionuclide r and reference man a in Sv Bq⁻¹

$t_{\text{Exp}, a, s}$ the annual time spent on the exposure site s in h

$a_{\text{air}, s}$ factor to determine the concentration of dust on exposure site s from concentration of dust in are, non dimensional ($a_{\text{air}, s} = 1$ for spent in outdoor and $a_{\text{air}, s} = 0.5$ for spent in indoor) in the investigation, the radiation exposure for the following radionuclides: (²³⁸U, ²³⁴U, ²³⁰Th, ²²⁶Ra, ²¹⁰Pb, ²¹⁰Po, ²³⁵U, ²³¹Pa and ²²⁷Ac)

$$C_{\text{air}, r, s} = (C_{\text{soil}(0.02), r, s} - C_{\text{soil}(0.02), r}^U) S_{\text{dust}}$$

$C_{\text{soil}(0.02), r, s}$ Specific activity of radionuclids r in the fraction of dust (<0.02 mm) which the surface soil layers for exposure site in Bq kg⁻¹ for dry soil.

$C_{\text{soil}(0.02), r}^U$ Specific natural subsoil - activity for radionuclids r in the fraction of dust (<0.02 mm) which the surface soil layers for exposure site in Bq kg⁻¹ for dry soil

S_{dust} Reference value of the concentration of dust = $5 \cdot 10^{-8} \text{ kg m}^{-3}$

$$C_{\text{soil}(0.02),r,s} = (C_{\text{soil},r,s} - C_{\text{soil},r}^U) AF_{0.02,r}$$

$C_{\text{soil},r,s}$ Specific activity of radionuclides r in all samples which the surface soil layers for exposure site in Bq kg^{-1} for dry soil

$C_{\text{soil},r}^U$ Specific natural subsoil-activity for radionuclides in all samples which the surface soil layers in Bq kg^{-1} for dry soil
 $AF_{0.02,r} \approx 4$ for all radionuclide r

5.1.3 Internal gamma radiation exposure from ingestion direct soil.

Dose coefficients for ingestion are contained in the [BfS99]. The dose coefficients in Tables of [BfS99], apply for 6 age groups of the general population. The dose coefficients relate the individual effective dose (in Sv) to the ingested quantity of radioactivity (in Bq kg^{-1}).

Annual effective dose $H_{\text{ing,soil},a}$ for reference man from direct ingestion soil

$$H_{\text{ing,soil},a} = U_{\text{soil},a} \sum_s t_{\text{Exp},a,s} \sum_r (C_{\text{soil}(0.5),r,s} - C_{\text{soil}(0.5),r}^U) g_{\text{ing},r,a} \quad (5-3)$$

Where:

$H_{\text{ing,soil},a}$ annual effective dose from direct ingestion of soil for reference man per year in Sv

$C_{\text{soil}(0.5),r,s}$ Specific activity of radionuclides r in fine particles (<0.5 mm) which the surface soil layers for exposure site in Bq kg^{-1} for dry soil.

$C_{\text{soil}(0.5),r}^U$ Specific natural subsoil-activity for radionuclides r in fine particles (<0.5 mm) which the surface soil layers for exposure site in Bq kg^{-1} for dry soil.

$U_{\text{soil},a}$ Taking rate of soil for reference man a in kg h^{-1} exposure site in h

$t_{\text{Exp},a,s}$ annual spent time on the exposure site s in h

$g_{\text{ing},r,a}$ Coefficient of ingestion dose for the radionuclide r and reference man a in Sv Bq^{-1} in the investigation. the radiation exposure for the following radionuclides: (^{238}U , ^{234}U , ^{230}Th , ^{226}Ra , ^{210}Pb , ^{210}Po , ^{235}U , ^{231}Pa and ^{227}Ac)

$$C_{\text{soil}(0.05),r,s} = (C_{\text{soil},r,s} - C_{\text{soil},r}^U) AF_{0.02,r}$$

$C_{\text{soil},r,s}$ Specific activity of radionuclides r in all samples which the surface soil layers for exposure site in Bq kg^{-1} for dry soil

$C_{\text{soil},r}^U$ Specific natural subsoil-activity for radionuclides in all samples which the surface soil layers in Bq kg^{-1} for dry soil

$AF_{0.05,r} \approx 2$ for all radionuclide r

5.2 External exposure from radionuclides in soil from Lower Saxony, Lippe (Germany) and Ukraine.

Exposure situations in which external irradiation is relevant are in outdoor, the dose from external irradiation is calculated according to eq. 5-1. The exposure time for outdoor external irradiation was assumed to be (2000 h a^{-1}).

Table 5- 1: External exposure (in m Sv) from U-series and Th-series in soil from Lower Saxony, North Germany.

| Radionuclides | <1 a | 1-2 a | 2-7 a | 7-12a | 12-17 a | >17 a |
|--------------------|--------|--------|--------|--------|---------|--------|
| U series (Ra-226) | 0.0208 | 0.0182 | 0.0182 | 0.0182 | 0.0156 | 0.0156 |
| Th series (Ra-228) | 0.0275 | 0.0240 | 0.0240 | 0.0240 | 0.0206 | 0.0206 |
| Total | 0.0482 | 0.0422 | 0.0422 | 0.0422 | 0.0362 | 0.0362 |

The calculated effective dose of external exposure in a single year for the ^{226}Ra (U-series) and ^{228}Ra (Th-series) radionuclides in soil from Table 5-1 were obtained as 0.0208 m Sv. for infants (<1 a), 0.0182 m Sv for children (2-7 a) and 0.0156 m Sv for adults (>17 a) and 0.0275 m Sv, for infants (<1 a), 0.0240 m Sv for children (2-7 a), 0.0206 m Sv for adults (>17 a) and the total external exposure are 0.0482 m Sv, for infants (<1 a), 0.0422 m Sv for children (2-7 a), 0.0362 m Sv for adults (>17 a) for ^{226}Ra (U-series) and ^{228}Ra (Th-series) radionuclides respectively.

Table 5-1 and Fig. 5-1 show that the biggest annual external dose for infants (<1 a), from 1-2 a to 7-12 a the same exposed external dose and 12-17 a and adults (>17 a) also the same exposed external dose for U-series and Th-series.

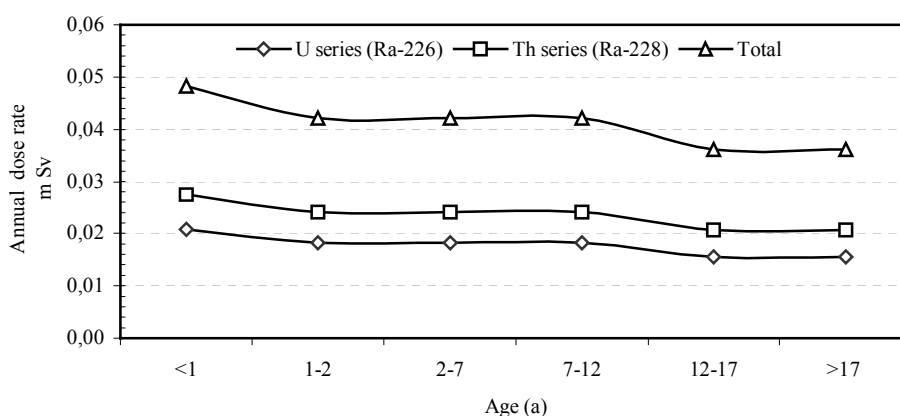


Fig. 5-1: Relation between different ages and external exposure from natural radionuclides in soil from Lower Saxony, North Germany.

Table 5- 2: External exposure (in m Sv) from U-series and Th-series in soil from Lippe, NRW, Germany.

| Radionuclides | <1 a | 1-2 a | 2-7 a | 7-12a | 12-17 a | >17 a |
|--------------------|--------|--------|--------|--------|---------|--------|
| U series (Ra-226) | 0.1122 | 0.0982 | 0.0982 | 0.0982 | 0.0841 | 0.0841 |
| Th series (Ra-228) | 0.0428 | 0.0374 | 0.0374 | 0.0374 | 0.0321 | 0.0321 |
| Total | 0.1550 | 0.1356 | 0.1356 | 0.1356 | 0.1162 | 0.1162 |

The calculated effective dose of external exposure in a single year for the ^{226}Ra (U-series) and ^{228}Ra (Th-series) radionuclides in soil from Table 5-2 were obtained as 0.1122 m Sv. for infants (<1 a), 0.0982 m Sv for children (2-7 a) and 0.0841 m Sv for adults (>17 a), and 0.0428 m Sv, for infants (<1 a), 0.0374 m Sv for children (2-7 a). 0.0321 m Sv for adults (>17 a) and the total external exposure are 0.1550 m Sv. for infants (<1 a), 0.1356 m Sv for children (2-7 a).

0.1162 mSv for adults (>17 a) for ^{226}Ra (U-series) and ^{228}Ra (Th-series) radionuclides respectively.

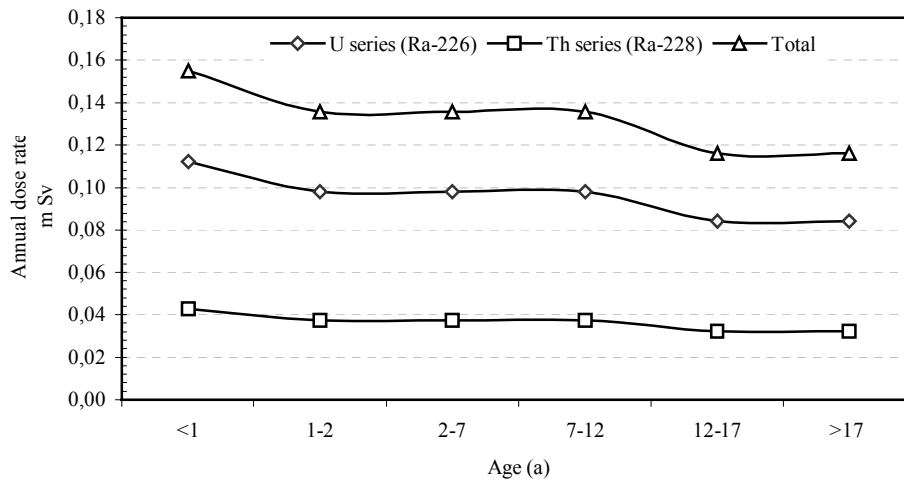


Fig. 5-2: Relation between different ages and external exposure from natural radionuclides in soil from Lippe, NRW, Germany.

Table 5- 3: Ages and external exposure(in m Sv) from U-series and Th-series in soil from Ukraine.

| Radionuclides | <1 a | 1-2 a | 2-7 a | 7-12a | 12-17 a | >17 a |
|--------------------|--------|--------|--------|--------|---------|--------|
| U series (Ra-226) | 0.0175 | 0.0153 | 0.0153 | 0.0153 | 0.0131 | 0.0131 |
| Th series (Ra-228) | 0.0237 | 0.0207 | 0.0207 | 0.0207 | 0.0178 | 0.0178 |
| Total | 0.0412 | 0.0360 | 0.0360 | 0.0360 | 0.0309 | 0.0309 |

The calculated effective dose of external exposure in a single year for the ^{226}Ra (U-series) and ^{228}Ra (Th-series) radionuclides in soil from Table 5-3 were obtained as 0.0175 m Sv. for infants (<1 a), 0.0153 m Sv for children (2-7 a) and 0.0131 m Sv for adults (>17 a), and 0.0237 m Sv. for infants (<1 a), 0.0207 m Sv for children (2-7 a), 0.0178 m Sv for adults (>17 a) and the total external exposure are 0.0412 m Sv, for infants (<1 a), 0.0360 m Sv for children (2-7 a), 0.0309 m Sv for adults (>17 a) for ^{226}Ra (U-series) and ^{228}Ra (Th-series) radionuclides respectively.

In generally, Table 5-1 to 5-3 and Fig. 5-1 to 5-3 show that the largest annual external dose for infants (<1 a), from 1-2a to 7-12 a the same exposed external dose and 12-17 a and adults (>17 a) also the same exposed external dose for U-series and Th-series.

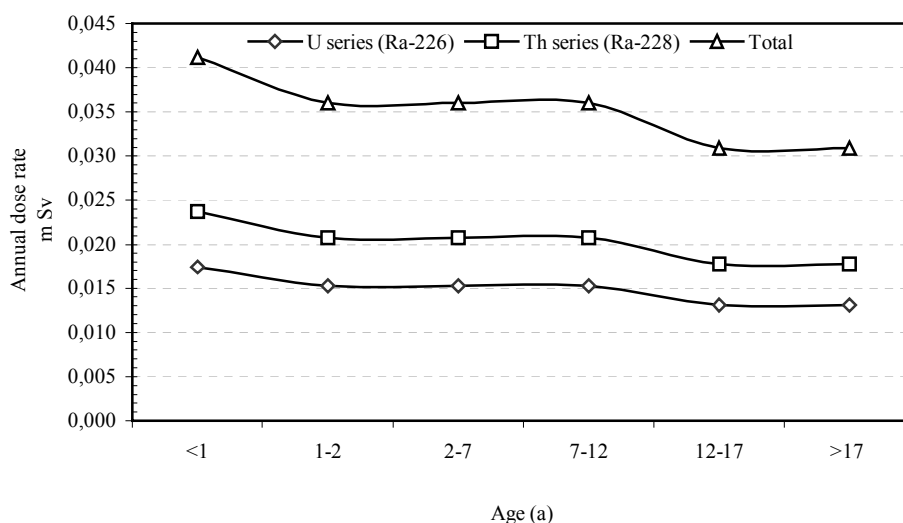


Fig. 5-3: Relation between different ages and external exposure from natural radionuclides in soil from Ukraine.

5.3 Internal exposure from inhalation of radionuclides in soil (dust) from Lower Saxony, Lippe, (NRW), (Germany) and Ukraine.

Inhalation intake of natural radionuclides other than radon and its decay products makes only a minor contribution to internal exposure. Broadly representative breathing rates are listed in Table II-1 [BfS99] for group age. Results of measurements of the concentrations of uranium- and thorium-series radionuclides in soil are listed in Tables in appendix B. Exposure situations in which the internal exposure is relevant are in outdoor, the internal exposure from inhalation of radionuclides in soil is calculated from the geometric mean values of the radioactive concentrations in the soil studied according to eq. 5-2. The most restrictive mixtures are thorium-232 and radium-228 in equilibrium with their decay products. Uranium-238 in equilibrium with its decay products is the most restrictive [Dix84].

Dose conversion factors (DCF) can be obtained from literature [BfS99]. The applicable data for the radionuclides from the natural uranium, and thorium decay series are presented in Tables 5-4 to 5-6 and 5-8 to 5-10 for exposure of the general public due to inhalation and ingestion respectively. It should be emphasised that the DCFs are age related and dependent on particle size.

Table 5- 4: Relation between internal exposure (in μ Sv) from inhalation of natural radionuclides in soil (dust) from Lower Saxony (Germany) and age group.

| Radionuclides | Annual effective dose in μ Sv | | | | | |
|---------------|-----------------------------------|-------|-------|--------|---------|-------|
| | <1 a | 1-2 a | 2-7 a | 7-12 a | 12-17 a | >17 a |
| U-series | | | | | | |
| Ra-226 | 0.018 | 0.024 | 0.025 | 0.031 | 0.037 | 0.032 |
| Pb-210 | 0.009 | 0.013 | 0.012 | 0.015 | 0.017 | 0.016 |
| U-238 | 0.015 | 0.021 | 0.022 | 0.026 | 0.029 | 0.027 |
| Th-series | | | | | | |
| Ra-228 | 0.018 | 0.022 | 0.022 | 0.029 | 0.037 | 0.024 |
| Th-228 | 0.186 | 0.277 | 0.286 | 0.341 | 0.383 | 0.361 |
| Th-232 | 0.063 | 0.107 | 0.130 | 0.162 | 0.205 | 0.227 |
| Total | 0.309 | 0.464 | 0.497 | 0.604 | 0.707 | 0.686 |

Fig. 5 - 4 and Table 5 – 4, showing the relationship between the group age and annual dose equivalents from gamma radiation from U-series and Th-series, enable exposures to be estimated in outdoor from inhalation soil of various specific activities.

The highest total inhalation exposure was $0.707 \mu\text{Sv a}^{-1}$ for age 12-17 a old compared to another total inhalation exposure for different ages and also the total inhalation exposure from ^{228}Th and ^{232}Th are more higher than from the radionuclides ^{226}Ra , ^{210}Pb , ^{228}Ra and ^{238}U . Tables and Figs from 5 - 4 to 5 - 6 shows that the total inhalation exposure from radionuclides ^{226}Ra , ^{210}Pb , ^{228}Ra and ^{238}U for all age group are nearly the same values. Intakes of ^{238}U and ^{232}Th based on measured airborne concentrations at Femald for the 3rd quarter and inhalation dose factors give effective dose equivalent (EDE) of $0.27 \mu\text{Sv}$ from ^{238}U and $0.46 \mu\text{Sv}$ from ^{232}Th . for a total of $0.73 \mu\text{Sv}$ [Lei02].

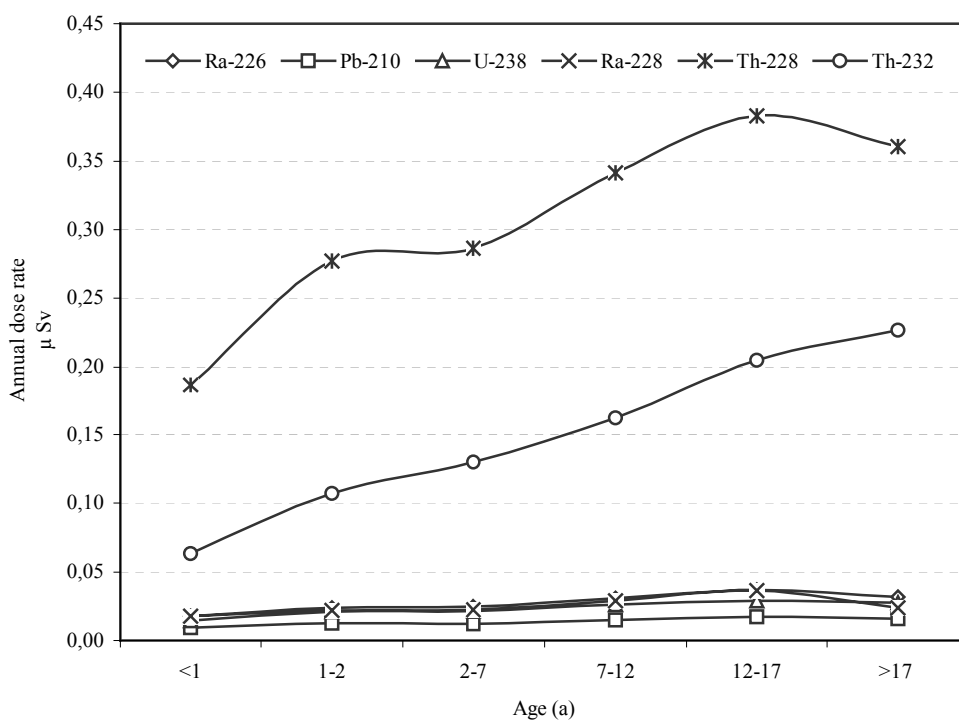


Fig. 5-4: Relation between different ages internal exposure (in μSv) from inhalation of natural radionuclides in soil (dust) from Lower Saxony, Germany.

Recently, Layton proposed a different approach for the estimation of average inhalation rates at different ages. The inhalation rates is vary with age. Daily inhalation peaks at 15 to 17 a [Lay93].

Table 5- 5: Relation between internal exposure (in μ Sv) from inhalation of natural radionuclides in soil (dust) from Lippe, (Germany) and age group.

| Radionuclides | Annual effective dose in μ Sv | | | | | |
|---------------|-----------------------------------|-------|-------|-------|---------|-------|
| | <1 a | 1-2 a | 2-7 a | 7-12a | 12-17 a | >17 a |
| U-series | | | | | | |
| Ra-226 | 0.095 | 0.128 | 0.133 | 0.166 | 0.200 | 0.172 |
| Pb-210 | 0.030 | 0.040 | 0.039 | 0.047 | 0.054 | 0.050 |
| U-238 | 0.010 | 0.015 | 0.015 | 0.018 | 0.020 | 0.019 |
| Th-series | | | | | | |
| Ra-228 | 0.028 | 0.034 | 0.035 | 0.045 | 0.057 | 0.037 |
| Th-228 | 0.283 | 0.422 | 0.435 | 0.519 | 0.582 | 0.548 |
| Th-232 | 0.098 | 0.166 | 0.201 | 0.251 | 0.317 | 0.351 |
| Total | 0.543 | 0.804 | 0.858 | 1.047 | 1.230 | 1.178 |

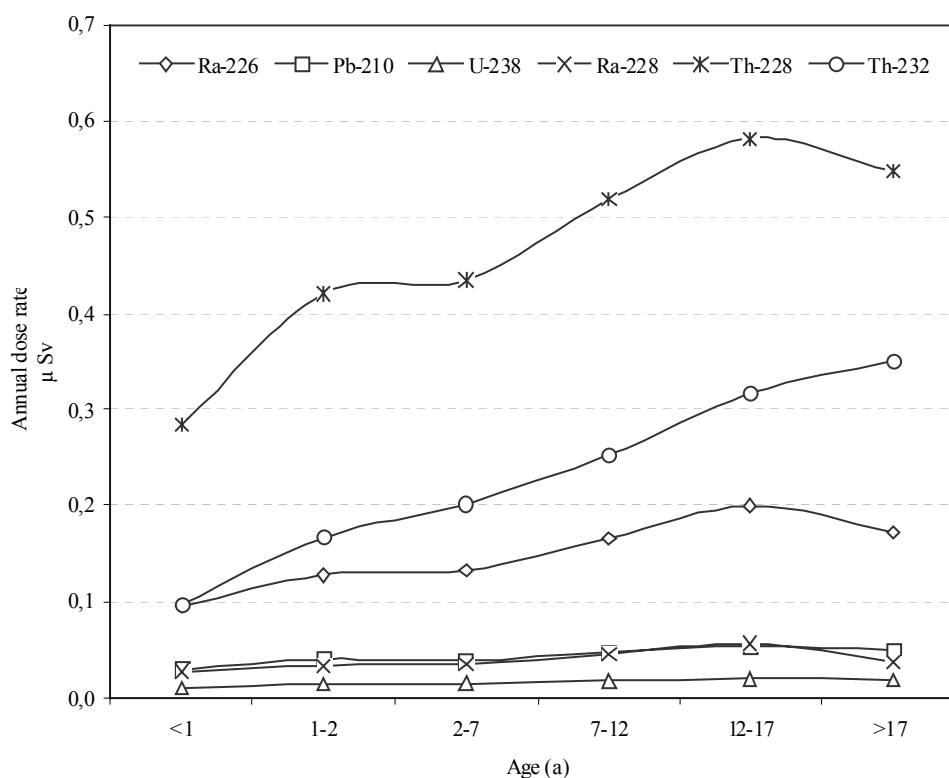
Fig. 5-5: Relation between different ages internal exposure (in μ Sv) from inhalation of natural radionuclides in soil (dust) from Lippe, (Germany).

Fig. 5-5 and Table 5-5, showing the relationship between the group age and annual dose equivalents from gamma radiation from U-series and Th-series. enable exposures to be estimated in outdoor from inhalation soil of various specific activities.

The highest total inhalation exposure was 0.707μ Sv a^{-1} for age 12-17 a old compared to another total inhalation exposure for different ages and also the total inhalation exposure from ^{228}Th and ^{232}Th are more higher than from the radionuclides ^{226}Ra , ^{210}Pb , ^{228}Ra , and ^{238}U .

Table 5- 6: Relation between internal exposure (in μ Sv) from inhalation of natural radionuclides in soil (dust) from Ukraine and age group.

| Radionuclides | Annual effective dose in μ Sv | | | | | |
|---------------|-----------------------------------|--------|---------|----------|-----------|--------|
| | < 1 a | 1- 2 a | 2 - 7 a | 7 - 12 a | 12 - 17 a | > 17 a |
| U-series | | | | | | |
| Ra-226 | 0.015 | 0.020 | 0.021 | 0.026 | 0.031 | 0.027 |
| Pb-210 | 0.015 | 0.020 | 0.019 | 0.023 | 0.026 | 0.025 |
| U-238 | 0.010 | 0.015 | 0.015 | 0.018 | 0.020 | 0.019 |
| Th-series | | | | | | |
| Ra-228 | 0.015 | 0.019 | 0.019 | 0.025 | 0.032 | 0.021 |
| Th-228 | 0.164 | 0.244 | 0.252 | 0.300 | 0.337 | 0.317 |
| Th-232 | 0.053 | 0.089 | 0.108 | 0.135 | 0.170 | 0.189 |
| Total | 0.271 | 0.406 | 0.434 | 0.527 | 0.616 | 0.597 |

The results obtained for the geometric mean, and annual effective dose are presented in Table 5-6. The total annual effective dose ranged from 0.271 to 0.616 μ Sv for group age from <1 to >17 year old. In general, the highest annual effective dose values were found for ^{228}Th and ^{232}Th and the lowest for ^{238}U , ^{210}Pb , ^{226}Ra and ^{228}Ra . For all group ages, a relatively large variability in annual effective dose for different radionuclide was found even within the same age we can see that clearly in Fig 5-6.

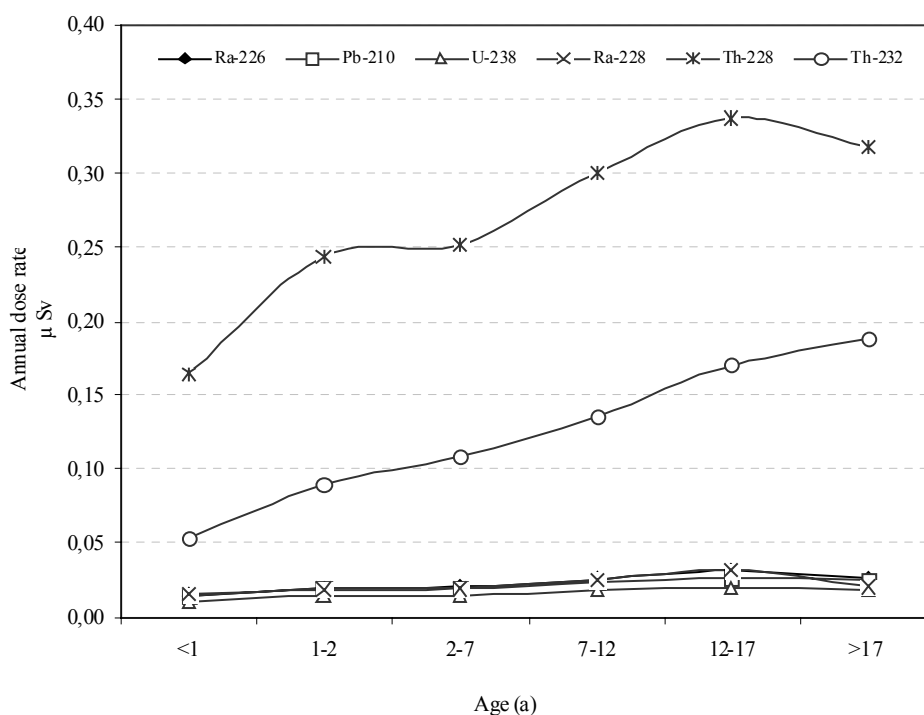
Fig. 5-6: Relation between different ages internal exposure (in μ Sv) from inhalation of natural radionuclides in soil (dust) from Ukraine.

Table 5- 7: Annual effective dose from inhalation of uranium and thorium series radionuclides [UNS00].

| Radionuclide | Committed effective dose (μSv) | | |
|-------------------|---------------------------------------------|------------------------|---------------|
| | Infants (1 a old) | Children (10 a old) | Adults >17 |
| U-series | | | |
| ^{238}U | 0.018 | 0.022 | 0.021 |
| ^{234}U | 0.021 | 0.027 | 0.026 |
| ^{230}Th | 0.033 | 0.045 | 0.051 |
| ^{226}Ra | 0.021 | 0.027 | 0.026 |
| ^{210}Pb | 3.5 | 4.2 | 4 |
| ^{210}Po | 1 | 1.3 | 1.2 |
| Th-series | | | |
| ^{232}Th | 0.048 | 0.073 | 0.091 |
| ^{228}Ra | 0.019 | 0.026 | 0.019 |
| ^{228}Th | 0.25 | 0.31 | 0.29 |
| ^{235}U | 0.001 | 0.001 | 0.001 |
| Total | 5 | 6 | 5.8 |

The evaluation of the internal doses from inhalation of U-series and Th-series in studied soil is presented in Tables 5 - 4 to 5 - 6. Revised dose coefficients taken from BFS [BFS99] are used. The age-weighted annual effective dose, generally, is less than from inhalation of uranium- and thorium-series radionuclides in soil. which may be compared to the annual effective dose in the UNSCEAR 2000 Table 17 annex B [UNS00].

5.3.1 Internal exposure from direct ingestion of radionuclides in soil from Lower Saxony, Lippe, NRW, (Germany) and Ukraine.

Humans may coincidentally ingest soil [zac91]. This occurs through transfer from the hands and other objects to the mouth, and through food ingestion, particularly vegetables. Small children are especially prone to soil ingestion through hand-to-mouth transfer. Vegetables and other plant foods may retain considerable amounts of soil even after routine cleaning for these reasons we can see that the all of the results in present work. Generally, the children under 1 year not ingestion soil so they don't exposed internal exposure from direct ingestion of soil but the children 1-2 year ingested soil more than age group so that the internal exposure for them more than age group. Exposure situations in which internal exposure from direct ingestion of radionuclides in soil in outdoor is calculated from the geometric mean values of the radioactive concentrations in the soil studied according to eq. 5-3.

Tables 5-8 to 5- 10 list the internal exposure from direct ingestion of radionuclides in soil (dust) from Lower Saxony, Lippe (NRW), Germany and Ukraine, respectively, with different ages. The highest annual exposure for 1-2 year old for all radionuclides and for all different locations and from the Figs.5-7 to 5-9 we can see that the same behaviour for internal exposure from direct ingestion of radionuclides in soil for all radionuclides and ages. Table 5-8 shows the annual direct ingestion of radionuclides in soil in μSv . Also shown are the annual internal exposures due to direct ingestion of dust as a function of age groups. We can see that annual exposure ingestion for baby less than 1 year is zero, and the maximum annual exposure direct ingestion for age 1-2 year for all radionuclides see Fig. 5-8.

For the U-series annual direct ingestion annual exposure are 4.69 for ^{226}Ra , 28.06 for ^{210}Pb and 18.17 for ^{238}U only for 1-2 year old and for greater than 17 year old are 0.16, 0.65 and 0.42 for ^{226}Ra , ^{210}Pb and ^{238}U , respectively

For the Th-series annual direct ingestion exposure are 27.72 for ^{228}Ra , 1.79 for ^{228}Th and 2.19 for ^{232}Th only for 1-2 year old and for greater than 17 year old are 0.40, 0.04 and 0.13 for ^{228}Ra , ^{228}Th , and ^{232}Th , respectively.

Table 5- 8: Internal exposure from direct ingestion of radionuclides in soil from Lower Saxony, (Germany) and age group.

| Radionuclides | Annual effective dose in μSv | | | | | |
|---------------|-----------------------------------------|-------|-------|-------|---------|-------|
| | <1 a | 1-2 a | 2-7 a | 7-12a | 12-17 a | >17 a |
| U-series | | | | | | |
| Ra-226 | 0 | 4.69 | 1.82 | 0.47 | 0.88 | 0.16 |
| Pb-210 | 0 | 28.06 | 10.29 | 1.78 | 1.78 | 0.65 |
| U-238 | 0 | 18.17 | 6.66 | 1.15 | 1.15 | 0.42 |
| Th-series | | | | | | |
| Ra-228 | 0 | 27.72 | 9.92 | 2.28 | 3.09 | 0.40 |
| Th-228 | 0 | 1.79 | 0.64 | 0.09 | 0.05 | 0.04 |
| Th-232 | 0 | 2.19 | 1.02 | 0.17 | 0.15 | 0.13 |
| Total | 0 | 82.62 | 30.35 | 5.93 | 7.10 | 1.81 |

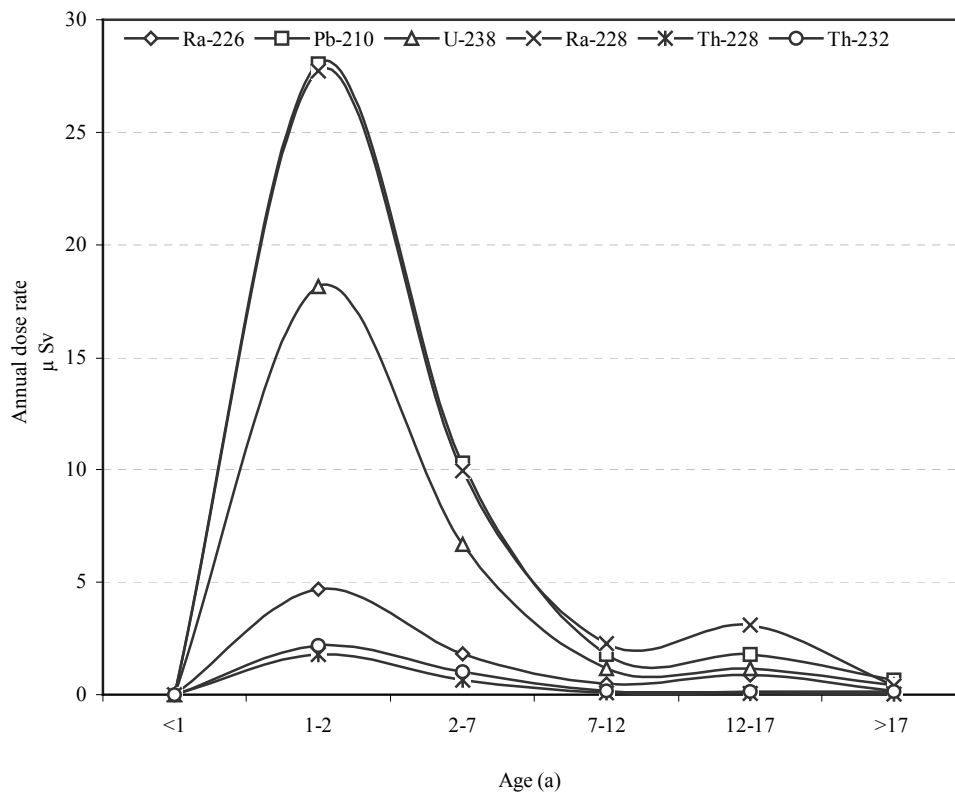


Fig. 5-7: Internal exposure from direct ingestion of radionuclides in soil from Lower Saxony, (Germany) and age group.

Table 5- 9: Internal exposure from direct ingestion of radionuclides in soil from Lippe, NRW, (Germany) and age group.

| Radionuclides | Annual effective dose in μSv | | | | | |
|---------------|-----------------------------------------|--------|-------|-------|---------|-------|
| | <1 a | 1-2 a | 2-7 a | 7-12a | 12-17 a | >17 a |
| U-series | | | | | | |
| Ra-226 | 0 | 25.34 | 9.82 | 2.53 | 4.75 | 0.89 |
| Pb-210 | 0 | 88.71 | 32.53 | 5.62 | 5.62 | 2.04 |
| U-238 | 0 | 12.67 | 4.65 | 0.80 | 0.80 | 0.29 |
| Th-series | | | | | | |
| Ra-228 | 0 | 43.90 | 15.71 | 3.60 | 4.90 | 0.64 |
| Th-228 | 0 | 2.73 | 0.97 | 0.13 | 0.08 | 0.06 |
| Th-232 | 0 | 12.67 | 4.65 | 0.80 | 0.80 | 0.29 |
| Total | 0 | 186.02 | 68.32 | 13.49 | 16.96 | 4.21 |

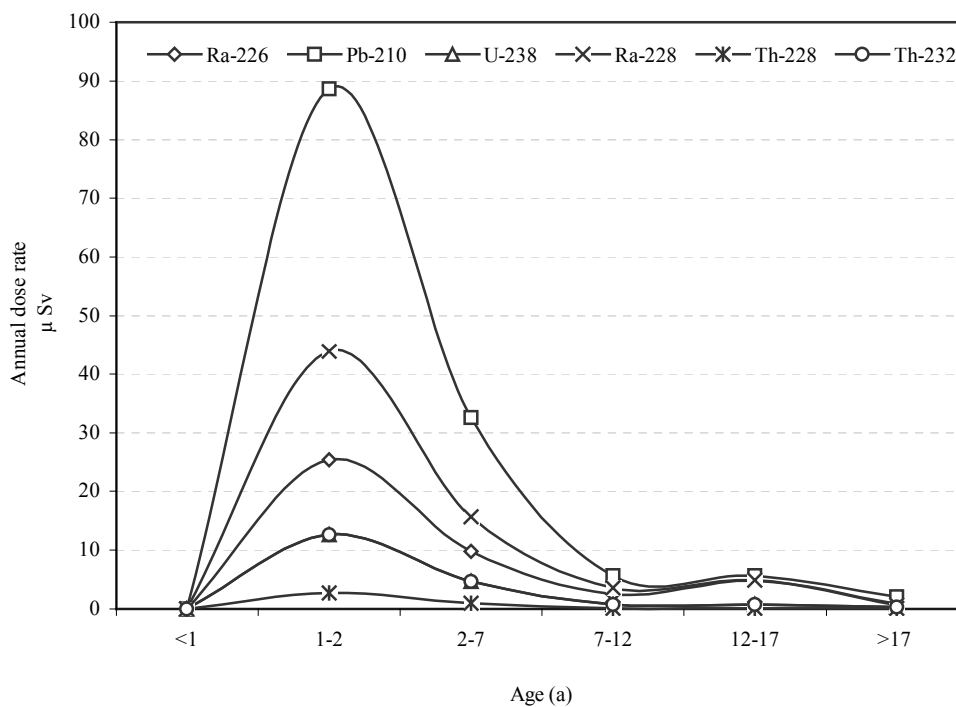


Fig. 5-8: Internal exposure from direct ingestion of radionuclides in soil from Lippe, (Germany) and age group.

Table 5- 10: Internal exposure from direct ingestion of radionuclides in soil from Ukraine and age group.

| Radionuclides | Annual effective dose in μ Sv | | | | | |
|---------------|-----------------------------------|-------|-------|--------|---------|-------|
| | <1 a | 1-2 a | 2-7 a | 7-12 a | 12-17 a | >17 a |
| U-series | | | | | | |
| Ra-226 | 0 | 3.94 | 1.53 | 0.39 | 0.74 | 0.14 |
| Pb-210 | 0 | 43.56 | 15.97 | 2.76 | 2.76 | 1.00 |
| U-238 | 0 | 12.65 | 4.64 | 0.80 | 0.80 | 0.29 |
| Th-series | | | | | | |
| Ra-228 | 0 | 24.32 | 8.70 | 2.00 | 2.71 | 0.35 |
| Th-228 | 0 | 1.42 | 0.51 | 0.07 | 0.04 | 0.03 |
| Th-232 | 0 | 1.82 | 0.85 | 0.14 | 0.12 | 0.11 |
| Total | 0 | 87.72 | 32.20 | 6.16 | 7.18 | 1.93 |

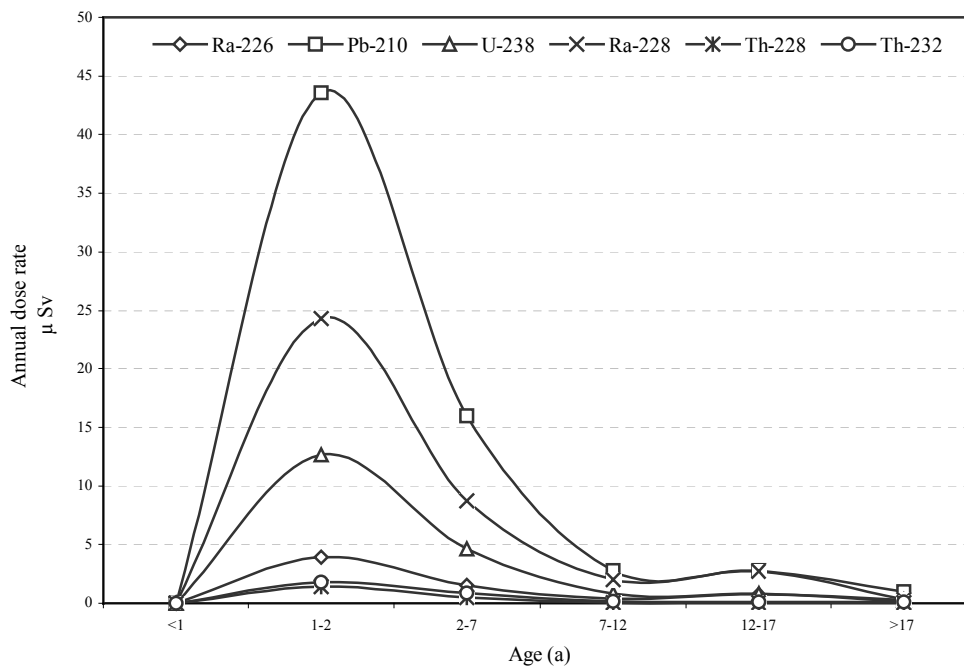


Fig. 5-9: Internal exposure from direct ingestion of radionuclides in soil from Ukraine.

Table 5- 11: Annual intake and effective dose from ingestion of uranium and thorium series radionuclides [UNS00].

| Radionuclide | Committed effective dose (μSv) | | |
|-------------------|---------------------------------------------|------------------------|---------------|
| | Infants (1 a old) | Children (10 a old) | Adults >17 |
| U-series | | | |
| ^{238}U | 0.23 | 0.26 | 0.25 |
| ^{234}U | 0.25 | 0.28 | 0.28 |
| ^{230}Th | 0.42 | 0.48 | 0.64 |
| ^{226}Ra | 7.5 | 12 | 6.3 |
| ^{210}Pb | 40 | 40 | 21 |
| ^{210}Po | 180 | 100 | 70 |
| Th-series | | | |
| ^{232}Th | 0.26 | 0.32 | 0.38 |
| ^{228}Ra | 31 | 40 | 11 |
| ^{228}Th | 0.38 | 0.3 | 0.22 |
| ^{235}U | 0.011 | 0.012 | 0.012 |
| Total | 260 | 200 | 110 |

Notwithstanding issues of variability of intake, [UNS00] has developed reference values for intakes of uranium and thorium series radionuclides in the diet. Reference annual intakes are given in Table 5-11. Annual intakes estimated in different surveys typically vary by up to a factor of five above or below these reference values (see table 18 of annex B of UNSCEAR 2000 for a detailed comparison). Based on these reference intakes, UNSCEAR (2000) provides estimates of the effective dose rates associated with intakes by ingestion of uranium and thorium series radionuclides. These estimates are summarised in Tables 5-8 to 5-10. Overall, the worldwide average effective dose rate from natural background is about 2.4 mSv a^{-1} [Tho03].

Legislation in South Africa addresses the allowed yearly radiation dose to registered radiation workers and the general public, and adheres to the most common internationally accepted standards of 20 mSv a^{-1} and 1 mSv a^{-1} , respectively, for these categories. The yearly dose is obviously the sum of the contributions from every individual nuclide from all possible sources. Accordingly, for members of the public, the individual sources are to be evaluated at the (South African) guideline level of $25 \mu\text{Sv a}^{-1}$. This imposes severe constraints on the radioanalytical laboratory to offer an affordable routine service due to the required sensitivity to analyse these NORMs and the variety of matrices involved. Evaluation of the available radioanalytical infrastructure, the yearly intake and the generally accepted dose conversion factors allow the laboratory to provide proper service designs to enable meaningful radiological hazard evaluation [Faa00].

5.4 Comparison between external and internal exposure from radionuclides in soil from different locations: Lower Saxony, Lippe (Germany) and Ukraine.

In Fig. 5–10 the annual external gamma radiation exposure (m Sv) is shown for three different locations, Lower Saxony, Lippe, (Germany) and Ukraine. It is clear from Fig. 5-10 that the total (U-series and Th-series) annual external gamma radiation exposure calculate for three different locations is the highest value for Lippe, and for Lower Saxony and Ukraine nearly the same vales of annual external gamma radiation exposure (m Sv) for group age.

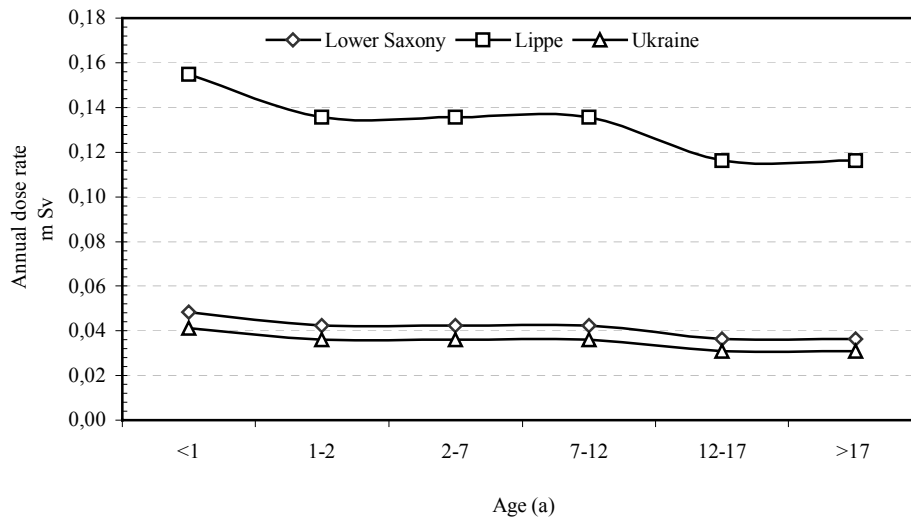


Fig. 5-10: Annual external gamma radiation exposure (m Sv) from radionuclides in soil from Lower Saxony, Lippe, (Germany) and Ukraine.

The measured values of outdoor gamma radiation have not changed. modification of the factors for shielding by housing and by body have increased the estimate of mean dose equivalent rate for U.S. from the 0.26 m Sv a^{-1} to 0.28 m Sv a^{-1} given in report [NCR75a].

In Figs. 5–11 the total annual internal gamma radiation exposure ($\mu \text{ Sv}$) from inhalation is shown for three different locations, Lower Saxony, Lippe, (Germany) and Ukraine. It is clear from Fig.5-11 that the total (U-series and Th-series) annual external gamma radiation exposure calculate for three different locations is the highest value for Lippe, and for Lower Saxony and Ukraine nearly the same vales of annual internal gamma radiation exposure ($\mu \text{ Sv}$) from inhalation for group age.

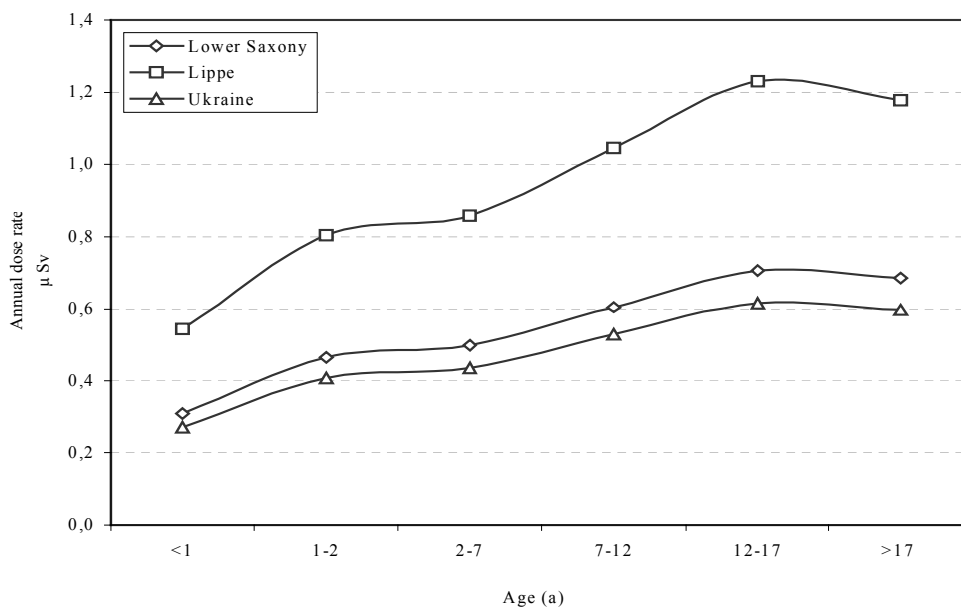


Fig. 5-11: Annual internal gamma radiation exposure ($\mu \text{ Sv}$) from inhalation of radionuclides in soil from Lower Saxony, Lippe, (Germany) and Ukraine.

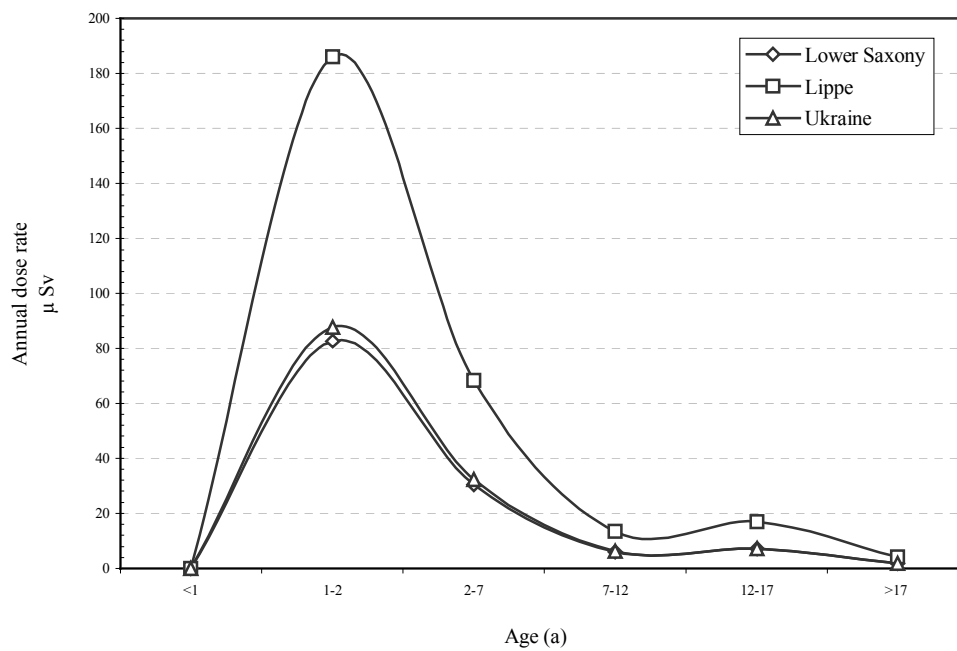


Fig. 5-12: Annual internal gamma radiation exposure (μSv) from direct ingestion of soil (dust) from Lower Saxony, Lippe (Germany), and Ukraine.

In Fig. 5–12 the total internal gamma radiation exposure (μSv) from direct ingestion of soil (dust) is shown for three different locations, Lower Saxony, Lippe, (Germany) and Ukraine. It is clear from Fig.5-12 that the total (U-series and Th-series) annual internal gamma radiation exposure (μSv) from direct ingestion of soil calculate for three different locations is the highest value for Lippe, and for Lower Saxony and Ukraine nearly the same values of internal gamma radiation exposure (μSv) from direct ingestion of soil for group age.

6 Appendices

6.1 Appendix A

Table A- 1: of description of sites of soil samples profiles from Lower Saxony on September 1999:-

| No. of depth profile | Locations | Latitude (N) | Longitude (E) | No. of soil samples |
|----------------------|--------------------|--------------|---------------|---------------------|
| 1 | Klein Lobke | 52 19 98 | 09 00 38 | 11 |
| 2 | Ricklinger Fredhof | 52 19 98 | 09 42 20 | 10 |
| 3 | Twenge | 52 29 39 | 09 44 98 | 9 |
| 4 | Badenstedt | 52 14 76 | 10 08 81 | 9 |
| 5 | Eilenriede | 52 19 29 | 09 41 30 | 8 |
| 6 | Barum | 53 03 46 | 10 31 30 | 9 |
| 7 | Vestrup | 45 50 05 | 07 06 61 | 6 |
| 8 | Neßmerpolder | 53 40 11 | 07 31 35 | 9 |

Table A- 2: The soil profiles from Chernobyl, Ukraine were taken in 1995

| No. Of Profiles | Location | No. of Samples |
|-----------------|--------------------------|----------------|
| 1 | Baraschewka1 | 10 |
| 2 | Oserjanka1 | 10 |
| 3 | Oserjanka2 | 10 |
| 4 | Oserjanka3 | 10 |
| 5 | Dawidowka1 | 10 |
| 6 | Lewkow1 | 10 |
| 7 | Lewkow2 | 10 |
| 8 | Woronewo1 | 10 |
| 9 | Woronewo2 | 10 |
| 10 | Woronewo3 | 10 |
| 11 | Woronewo4 | 10 |
| 12 | Woronewo 5 | 10 |
| 13 | Woronewo6 | 10 |
| 14 | Woronewo7 | 10 |
| 15 | Tschigiri1 | 10 |
| 16 | Tschigiri2 | 10 |
| 17 | Tschigiri3 | 10 |
| 18 | Tschigiri Zwintor1 | 10 |
| 19 | Norsdrischtsche II | 10 |
| 20 | Nove Scharno 3 | 10 |
| 21 | Christinovka river shore | 10 |
| 22 | Christinovka meadow | 10 |

Table A- 3: description of Locations of soil samples from Lower Saxony

| No. of Samples | Date of Sampling | Sample code | Sites of samples | Latitude (N) | Longitude (E) |
|----------------|------------------|-------------|------------------|--------------|---------------|
| 1 | 25.05.2001 | PoBoMPHe01 | Neßmerpolder | 53 40 11 | 07 31 35 |
| 2 | 25.05.2001 | PoBoEPHe01 | Neßmerpolder | 53 40 11 | 07 31 35 |
| 3 | 21.07.2001 | SiBoMPGe01 | Schlewecke | 52 02 41 | 10 07 55 |
| 4 | 21.07.2001 | SiBoMPGe02 | Schlewecke | 52 02 41 | 10 07 55 |
| 5 | 27.07.2001 | SiBoMPRa01 | Schlewecke | 52 02 41 | 10 07 55 |
| 6 | 27.07.2001 | SiBoEPRa01 | Schlewecke | 52 02 41 | 10 07 55 |
| 7 | 06.08.2001 | SiBoMPWe01 | Schlewecke | 52 02 41 | 10 07 55 |
| 8 | 06.08.2001 | SiBoEPWe01 | Schlewecke | 52 02 41 | 10 07 55 |
| 9 | 14.08.2001 | JeBoEPKs01 | Jeinsen | 52 13 30 | 09 46 50 |
| 10 | 14.08.2001 | JeBoEPKp01 | Jeinsen | 52 13 30 | 09 46 50 |
| 11 | 14.08.2001 | JeBoEPRb01 | Jeinsen | 52 13 30 | 09 46 50 |
| 12 | 14.08.2001 | JeBoEPMa01 | Jeinsen | 52 13 30 | 09 46 50 |
| 13 | 14.08.2001 | JeBoEPKr01 | Jeinsen | 52 13 30 | 09 46 50 |
| 14 | 14.08.2001 | JeBoEPEg01 | Jeinsen | 52 13 30 | 09 46 50 |
| 15 | 15.08.2001 | GeBoMPWe01 | Gestorf | 52 11 03 | 10 04 50 |
| 16 | 15.08.2001 | GeBoEPKa01 | Gestorf | 52 11 03 | 10 04 50 |
| 17 | 16.08.2001 | ScBoMPRa01 | Schessinghausen | 52 22 42 | 09 49 54 |
| 18 | 16.08.2001 | ScBoMPRo01 | Schlewecke | 52 13 10 | 10 07 55 |
| 19 | 20.08.2001 | SiBoMPWe02 | Schlewecke | 52 35 16 | 10 07 55 |
| 20 | 20.08.2001 | SiBoEPZu01 | Schlewecke | 52 35 16 | 10 07 55 |
| 21 | 27.08.2001 | PoBoMPHe02 | Neßmerpolder | 53 40 11 | 07 31 35 |
| 22 | 27.08.2001 | PoBoMPHa01 | Neßmerpolder | 53 40 11 | 07 31 35 |
| 23 | 27.08.2001 | PoBoEPHa01 | Neßmerpolder | 53 40 11 | 07 31 35 |
| 24 | 27.08.2001 | PoBoEPHa02 | Neßmerpolder | 53 40 11 | 07 31 35 |
| 25 | 27.08.2001 | PoBoMIWe01 | Neßmerpolder | 53 40 11 | 07 31 35 |
| 26 | 27.08.2001 | PoBoEPWe01 | Neßmerpolder | 53 40 11 | 07 31 35 |
| 27 | 27.08.2001 | PoBoEPWe02 | Neßmerpolder | 53 40 11 | 07 31 35 |
| 28 | 27.08.2001 | PoBoMPWa02 | Neßmerpolder | 53 40 11 | 07 31 35 |
| 29 | 27.08.2001 | PoBoMPLu01 | Neßmerpolder | 53 40 11 | 07 31 35 |
| 30 | 27.08.2001 | PoBoEPLu01 | Neßmerpolder | 53 40 11 | 07 31 35 |
| 31 | 27.08.2001 | PoBoEPLu02 | Neßmerpolder | 53 40 11 | 07 31 35 |
| 32 | 27.08.2001 | PoBoMPRa01 | Neßmerpolder | 53 40 11 | 07 31 35 |
| 33 | 03.09.2001 | HLWBoEPHe01 | HLW | 52 14 76 | 10 08 81 |
| 34 | 11:09:2001 | ScBoMPWe01 | Schessinghausen | 52 22 42 | 09 49 54 |
| 35 | 11:09:2001 | ScBoMPWe01 | Schessinghausen | 52 22 42 | 09 49 54 |
| 36 | 11:09:2001 | ScBoMPTr02 | Schessinghausen | 52 22 42 | 09 49 54 |
| 37 | 13:09:2001 | JeBoEPLa01 | Jeinsen | 52 13 30 | 09 46 50 |
| 38 | 13:09:2001 | JeBoEPPe01 | Jeinsen | 52 13 30 | 09 46 50 |
| 39 | 13:09:2001 | JeBoEPWK01 | Jeinsen | 52 13 30 | 09 46 50 |
| 40 | 13:09:2001 | JEBoEPWeK01 | Jeinsen | 52 13 30 | 09 46 50 |
| 41 | 13:09:2001 | JeBoEPBk01 | Jeinsen | 52 13 30 | 09 46 50 |
| 42 | 13:09:2001 | JeBoEPBr01 | Jeinsen | 52 13 30 | 09 46 50 |
| 43 | 13:09:2001 | JeBoEPRo01 | Jeinsen | 52 13 30 | 09 46 50 |

Table A- 4: Soil depth profile from Lippe, North Rhine-West phalia, Germany

| No. of Profiles | Codes of profiles | Date of sampling | Latitude (N) | Longitude (E) | No. of samples |
|-----------------|-------------------|------------------|--------------|---------------|----------------|
| 1 | BP 3-30 | 15.08.2000 | 51 41 34 | 7 4 21 | 7 |
| 2 | BP 4-14 | 15.08.2000 | 51 41 65 | 7 4 60 | 7 |

Table A- 5: Soil samples from Lippe, North Rhine-West phalia, Germany

| No of Samples | Date of Sampling | Latitude (N) | Longitude (E) | Code of Samples |
|---------------|------------------|--------------|---------------|-----------------|
| 1 | 09.07.2000 | 51 42 12 | 7 6 39 | BP 2-04f |
| 2 | 09.07.2000 | 51 42 12 | 7 6 39 | BP 2-05f |
| 3 | 09.07.2000 | 51 42 12 | 7 6 38 | BP 2-06f |
| 4 | 09.07.2000 | 51 42 12 | 7 6 38 | BP 2-07f |
| 5 | 09.07.2000 | 51 42 12 | 7 6 32 | BP 2-11f |
| 6 | 09.07.2000 | 51 42 12 | 7 6 32 | BP 2-12f |
| 7 | 09.07.2000 | 51 42 12 | 7 6 32 | BP 2-13f |
| 8 | 09.07.2000 | 51 42 12 | 7 6 19 | BP 2-17f |
| 9 | 09.07.2000 | 51 42 5 | 7 6 13 | BP 2-23f |
| 10 | 09.07.2000 | 51 42 4 | 7 6 13 | BP 2-24f |
| 11 | 09.07.2000 | 51 42 4 | 7 6 13 | BP 2-25f |
| 12 | 09.07.2000 | 51 42 24 | 7 6 57 | BP 2-33f |
| 13 | 09.07.2000 | 51 42 24 | 7 6 58 | BP 2-34f |
| 14 | 09.07.2000 | 51 42 24 | 7 6 58 | BP 2-35f |
| 15 | 09.07.2000 | 51 41 58 | 7 5 38 | BP 2-36f |
| 16 | 09.07.2000 | 51 41 58 | 7 5 38 | BP 2-38g |
| 17 | 14.08.2000 | 51 41 57 | 7 5 25 | BP 3-01 |
| 18 | 14.08.2000 | 51 41 58 | 7 5 25 | BP 3-02 |
| 19 | 14.08.2000 | 51 41 58 | 7 5 25 | BP 3-03 |
| 20 | 14.08.2000 | 51 41 53 | 7 5 15 | BP 3-04 |
| 21 | 14.08.2000 | 51 41 56 | 7 5 15 | BP 3-05 |
| 22 | 14.08.2000 | 51 41 59 | 7 5 15 | BP 3-06 |
| 23 | 14.08.2000 | 51 41 57 | 7 4 58 | BP 3-09 |
| 24 | 14.08.2000 | 51 41 58 | 7 4 58 | BP 3-07 |
| 25 | 14.08.2000 | 51 41 58 | 7 4 60 | BP 3-08 |
| 26 | 14.08.2000 | 51 41 54 | 7 4 46 | BP 3-10 |
| 27 | 14.08.2000 | 51 41 58 | 7 4 46 | BP 3-11 |
| 28 | 14.08.2000 | 51 41 46 | 7 4 28 | BP 3-12 |
| 29 | 14.08.2000 | 51 41 48 | 7 4 21 | BP 3-13 |
| 30 | 14.08.2000 | 51 41 30 | 7 4 19 | BP 3-14 |
| 31 | 14.08.2000 | 51 41 33 | 7 4 25 | BP 3-15 |
| 32 | 14.08.2000 | 51 41 28 | 7 3 57 | BP 3-16 |
| 33 | 14.08.2000 | 51 41 25 | 7 3 55 | BP 3-17 |
| 34 | 14.08.2000 | 51 41 21 | 7 3 56 | BP 3-18 |
| 35 | 15.08.2000 | 51 40 15 | 7 1 26 | BP 3-21 |
| 36 | 15.08.2000 | 51 40 15 | 7 1 25 | BP 3-22 |
| 37 | 15.08.2000 | 51 40 2 | 6 56 11 | BP 3-23 |
| 38 | 15.08.2000 | 51 40 3 | 6 56 15 | BP 3-24 |

Table A- 5: Soil samples from North Rhine-West phalia, (Lippe) Continued

| No of Samples | Date of Sampling | Latitude (N) | Longitude (E) | Code of Samples |
|---------------|------------------|--------------|---------------|------------------|
| 39 | 15.08.2000 | 51 40 2 | 6 54 9 | BP 3-25 |
| 40 | 15.08.2000 | 51 40 25 | 6 50 58 | BP 3-26 |
| 41 | 15.08.2000 | 51 38 36 | 6 42 5 | BP 3-28 |
| 42 | 15.08.2000 | 51 38 38 | 6 41 53 | BP 3-29 |
| 43 | 26.09.2000 | 51 42 19 | 7 6 43 | BP 4-01 |
| 44 | 26.09.2000 | 51 42 6 | 7 6 4 | BP 4-05 |
| 45 | 26.09.2000 | 51 42 7 | 7 6 3 | BP 4-06 |
| 46 | 27.09.2000 | 51 39 4 | 6 38 26 | BP 4-09 |
| 47 | 27.09.2000 | 51 39 5 | 6 38 35 | BP 4-10 |
| 48 | 27.09.2000 | 51 38 55 | 6 38 42 | BP 4-11 |
| 49 | 27.09.2000 | 51 41 32 | 7 4 22 | BP 4-12 |
| 50 | 27.09.2000 | 51 41 57 | 7 4 60 | BP 4-15 |
| 51 | 27.09.2000 | 51 41 59 | 7 4 60 | BP 4-16 |
| 52 | 27.09.2000 | 51 41 57 | 7 4 60 | BPicking.(71) |
| 53 | 27.09.2000 | 51 41 58 | 7 4 60 | BPVorfluter (70) |
| 54 | 17.11.2000 | 51 41 29 | 7 4 18 | BP 5-01 |
| 55 | 17.11.2000 | 51 41 30 | 7 4 3 | BP 5-02 |
| 56 | 17.11.2000 | 51 41 35 | 7 4 26 | BP 5-03 |
| 57 | 17.11.2000 | 51 41 39 | 7 4 18 | BP 5-04 |
| 58 | 17.11.2000 | 51 41 43 | 7 4 19 | BP5-05 (Sedi) |
| 59 | 17.11.2000 | 51 41 45 | 7 4 35 | BP 5-06 |
| 60 | 17.11.2000 | 51 41 50 | 7 4 45 | BP 5-07 |
| 61 | 17.11.2000 | 51 41 55 | 7 4 50 | BP 5-08 |
| 62 | 17.11.2000 | 51 41 51 | 7 4 56 | BP 5-09 |
| 63 | 17.11.2000 | 51 41 51 | 7 5 8 | BP 5-10 |
| 64 | 17.11.2000 | 51 41 28 | 7 4 1 | BP 5-11 |

Fitting program

```
r=165
```

```
t(x)=(x>0)?1:0
```

```
w(x)=log10(x/900)
```

```
u(x)=1/x*(a+b*w(x)+c*w(x)*w(x)+d*w(x)*w(x)*w(x)+e*w(x)*w(x)*w(x)*w(x)+f*w(x)*w(x)*w(x)*w(x)*w(x)+g*w(x)*w(x)*w(x)*w(x)*w(x)*w(x)+h*w(x)*w(x)*w(x)*w(x)*w(x)*w(x)*w(x))
```

```
FIT_LIMIT=1e-10
```

```
fit [x=20:2000] u(x) 'st1200be jo.txt' using 1:2 via a.b.c.d.e.f.g.h
```

```
v(x)=exp(k*log(x)+l)
```

```
FIT_LIMIT=1e-10
```

```
fit [x=r:2000] v(x) 'st1200be jo.txt' using 1:2 via k.l
```

```
set xrange[50:1800]
```

```
#set yrange[0.0003:0.04]
```

```
set data style points
```

```
set function style dots
```

```
set logscale xy
```

```
plot'st1200be.txt'.v(x)*t(x-r).u(x)*t(r-x)
```

Line Parameters

| | |
|---|-------------|
| a | = 889.538 |
| b | = 329.768 |
| c | = 61.1956 |
| d | = -32.7598 |
| e | = 1572.66 |
| f | = 6114.79 |
| g | = 5854.18 |
| h | = 1698.75 |
| k | = -0.829291 |
| l | = 5.63433 |

6.2 Appendix B

Table B - 1: Data of the specimen place "Eilenride"

| specimen interval cm | horizon german [9] | horizon FAO | texture | characteristics | sand % | silt % | clay % |
|----------------------|--------------------|-------------|-------------------------------------------------------------------------------------------------|-----------------------------------------------------------------------------------------------|--------|--------|--------|
| 1 | L | Oi | Leave mulch | | | | |
| 1 | Of | Oa | | | | | |
| 0-10 | Aeh | Ah | coarse sandy medium sand | greatly weak pebbly and stony, brownish gray, medium humus, middle compactness of the packing | 97.7 | | |
| 10-20 | Aeh | | medium clay sand. greatly weak pebbly and stony | brown gray, medium humus, middle compactness of the packing | 76.1 | 13.4 | 10.5 |
| 20-30 | Ah-Go | | yellow brown, greatly weak humus, greatly weak iron blotched. middle compactness of the packing | 80.3 | 12.0 | 7.7 | |
| 30-40 | | Bl | | gray yellow, weak iron blotched, middle compactness of the packing | 83.8 | 8.8 | 7.4 |
| 40-50 | Go-Sw | | | | | | |
| 50-70 | Go-Swd | B2 | coarse sandy medium sand | Marmorate, medium iron blotched. high compactness of the packing | 97.4 | | |
| 70-100 | | | | | 97.3 | | |
| 100-150 | Gro | | sandy clay loam | greatly weak pebbly and stony, gray, weak iron blotched, middle compactness of the packing | 72.8 | 14.0 | 13.3 |

Table B - 2: Data of the specimen place Klein Lobke

| specimen interval cm | horizon german [9] | horizon FAO | texture | characteristics | sand % | silt % | clay % |
|----------------------|--------------------|-------------|-----------------|------------------------------------------------------------------------------------------------------------------------------------------------------------------------------------------------------------------------------------------------------------|---------------|---------------|---------------|
| 0-15 | Alp | Ahp | sandy clay silt | dark brown gray, weak humus. minor compactness of the packing | 32.3 | 54.5 | 13.2 |
| 15-30 | | | | | | | |
| 30-40 | Axh-Al | | | | | 31.5 | 55.1 |
| 40-50 | Sw-Axh-Bht | | silty clay sand | partly weak silty sand. dirty brown, greatly weak humus, greatly weak iron and manganese blotched, Konkretionen, middle compactness of the packing | 35.3 | 49.6 | 15 |
| 50-70 | | Bhtl | | | | | |
| 70-90 | Sw-Bht | | weak clay silt | with 2 cm intensely Layer of intense clay medium sand, gray ochre blotched, partly black, greatly weak humous, medium iron blotched removable with weak clay medium sand. gray dark ochre marbled, medium iron blotched. middle compactness of the packing | 69.4 | 17.8 | 12.7 |
| 90-105 | | | | | | | |
| 105-130 | | | | | 18.1 | 70.1 | 11.8 |
| 130-150 | Sw-Bhtv | Bt2 | | | 65.7 | 25.4 | 9 |
| 150-200 | Sw/fGo+Sw | | | with 1 cm intense Layer of clay sand, yellowish gray. medium iron blotched, medium carbonate containing, induration at the loess, minor compactness of the packing | 7 | 82 | 11 |
| 200-250 | Sw/Sd | Br3 | | yellowish gray, weak iron blotched, medium carbonate containing, minor compactness of the packing up to 225 cm sandy clay silt, greatly weak pebbly and stony, medium carbonate containing, minor compactness of the packing, up to 265 cm weak silty clay | 37.5/ 32.5 | 50.2/ 62.9 | 12.4/ 62.9 |

Table B - 3: Data of the specimen place Ricklingen

| specimen interval cm | horizon german [9] | horizon FAO | texture | characteristics | sand % | silt % | clay % |
|----------------------|--------------------|-------------|--------------------------|-------------------------------------------------------------------------------------------------------------------------------------------------------------------------------------------------------------|------------|-----------|---------|
| 0-5 | rAp+Ali | Apl | silty clay sand | dark brown, medium humus, middle compactness of the packing | 42.9 | 46.8 | 10.3 |
| 5-10 | | | | | | | |
| 10-15 | | | | | | | |
| 15-20 | | | | | | | |
| 20-25 | | | | | | | |
| 25-33 | | | | | | | |
| 33-60 | Al | At2 | sandy clay silt | sallow brown, greatly weak humus, middle compactness of the packing | 34.2 | 56.2 | 9.6 |
| 60-85 | II Sw-Bt | Btl | medium silty sand. | into nests intense clay sand, brownish gray, weak iron blotched, middle compactness of the packing | 58.7 | 32.9 | 8.4 |
| 85-120 | Sw | B2 | weak clay sand | partly medium sand coarse sandy, brownish gray, weak iron blotched, middle compactness of the packing | 81.5 | 13.4 | 5.1 |
| 120-170 | Sw/ Sd | B3 | medium sand coarse sandy | up to 150cm weak pebbly, brown gray, minor compactness of the packing; up to 170cm sandy clay loam, weak pebbly, partly intense clay sand and weak clay loam, yellow brown. high compactness of the packing | 98.3/ 45.2 | 1.7/ 19.4 | 0/ 35.4 |

Table B - 4: Data of the specimen place Twenge

| specimen interval cm | horizon German [9] | horizon FAO | texture | characteristics | sand % | silt % | clay % |
|----------------------|--------------------|-------------|--------------------------|------------------------------------------------------------------------------------------------------------------------------------------------------------------------------------------|--------|--------|--------|
| 0-15 | Ap | Ap | fine sand medium sand | wornish black, medium humous, minor compactness of the packing coherent structure brownish black, humus, minor compactness of the packing, coherent structures, charcoal and clay bricks | 88.7 | 6 | 5.3 |
| 15-30 | | | | | | | |
| 30-40 | | | | | | | |
| 40-50 | E | E | | | 86.2 | 8.7 | 5.1 |
| 50-60 | fAe | Bh (Abh) | medium sand fine sandy | dark rust-coloured brown. weak humus . middle compactness of the packing | n.b. | n.b. | n.b. |
| 60-75 | Bs/Bhs | | | rust-coloured brown. middle compactness of the packing | 89.1 | 5.9 | 4.1 |
| 75-100 | Bs | Bl | medium sand | yellow gray, weak iron blotched, middle compactness of the packing | 91.0 | 4.9 | 4.1 |
| 100-125 | Go | Bc2 | medium sand coarse sandy | in nutty aggregates silt sandy, yellow gray, in nutty aggregates gray, weak iron blotched, middle compactness of the packing | 95.3 | 3.0 | 1.7 |
| 125-150 | | | medium sand | weak pebbly, yellow gray, weak iron blotched. middle compactness of the packing | 99.5 | 0.5 | 0 |

Table B - 5: Data of the specimen place Vestrup

| specimen interval cm | horizon German [9] | horizon FAO | texture | characteristics | sand % | silt % | clay % | | | | |
|----------------------|--------------------|-------------|--------------------------------------------------|----------------------------------------------------------------------------------------------------------------------------------------------------------------------------------------------------------------------------------------------------------------|----------------------|--------------------|-------------------|---------------------------------------------------------------------------------------------------------------------------|------|------|------|
| 0-15 | rAep +Aeh | Ahp Bhs | sand weak silty. greatly weak pebbly | reddish dark brownish gray, intense humus, minor compactness of the packing, very weakly minted crumble structures, reddish brown. medium humus, intense iron blotched, middle corn-, pactness of the packing, weak salient coherent structures | 81.2 | 13.9 | 4.9 | | | | |
| 15-27 | Bsh | | | | 83.0 | 12.8 | 3.9 | | | | |
| 27-36 | Bhs | Bhs | sand weak silty. weak pebbly | dull brown, medium iron blotched, middle compactness of the packing, weak salient coherent structures bright reddish brown, weak iron blotched, middle compactness of the packing, par- ticulate structure. partly coherent structures; up to 45cm sand medium | 82.3 77.4 66.1 | 13.9 18.5 24 | 3.8 4.1 9.9 | | | | |
| 36-50 | Bs/ Sw | Bs | sand intense clay. greatly weak pebbly and stony | greenish bright gray, weak iron blotched, middle compactness of the packing, greenish bright gray, intense iron blotched, high compactness of the packing, diacase fill of sand weak silty, coherent structures | 70.4 | 12.6 | 17 | | | | |
| 50-75 | Sw | Bcr | | | | | | | | | |
| 75-100 | Sw | | | | | | | | | | |
| 100-140 | Go-Sd | | | | | | | nutty aggregates of fine sand weak silty, bright red dish brown., medium iron blotched. middle compactness of the packing | 72.2 | 12 | 15.8 |
| 140-180 | Go/ | | | | | | | | 74.2 | 10.8 | 15 |
| 160-180 | Gro | | | | | | | | 71.4 | 15.6 | 13 |

Table B - 6: Data of the specimen place Adenstedt

| specimen interval cm. | horizon german [9] | horizon FAO | texture | characteristics | sand % | silt % | clay % |
|-----------------------|----------------------|-------------|----------------------------------------------------------------------------------------------------------------|---------------------------------------------------------------------------------------------------------|----------------|-----------------------------------------------------------------------------------------------------------------------------------|--------|
| 0-15 | Axp | Ahp | intense clay silt | dark gray, medium humus . minor compactness of the packing | 6.8 | 75.9 | 17.3 |
| 15-30 | | | | Gray, middle compactness of the packing | 5.4 | 77.7 | 16.9 |
| 30-40 | Axh | | | | | | |
| 40-50 | Sw | Bl | medium clay silt, yellowish Gray, mar bled with Ochre, weak iron blotched | yellowish gray, to be riddled with black, medium iron Blotched, middle compactness of the packing | 3.6 | 75.8 | 20.6 |
| 50-75 | Sw | | | | | | |
| 75-100 | | Sw | fine laminated iron precipitation around Roots, medium carbonate Containing, middle compactness of the packing | 3.0 | 77.0 | 20 | |
| 100-150 | fGo+ICke-Sw/ fGo+ICc | Br2 /Cr | medium clay silt, yellowish Gray, mar bled with Ochre, weak iron blotched | partly iron precipitation around Roots. medium carbonate containing, medium compactness of the Packing. | 4 | 84 | 12 |
| 150-200 | fGo+ICv-Sw | Cr | | | | | |
| 200-250 | fGo+ICv-Sd | | | | weak clay sand | partly medium sand up to medium silty clay. down ward increasing, weak silty clay, bright gray, greatly weak carbonate containing | 45.7 |

Table B - 7: Data of the specimen place Barum

| | horizon german [9] | horizon FAO | texture | characteristics | sand % | silt % | clay % |
|---------|--------------------------|----------------|------------------------|--------------------------------------------------------------------------------------------|-----------|-----------|-----------|
| 0-20 | Ap | Apl | weak clay silt | dark brown gray. weak humus, minor compactness of the packing; alluvial deposits loess | 27.1 | 64 | 8.9 |
| 20-37 | | | | | | | |
| 37-57 | wM | Ahb2 | weak clay silt | brown. greatly weak humus . middle compactness of the packing; alluvial deposits loess | 21.6 | 68.2 | 10.3 |
| 57-73 | Al | Btl | sandy silt | sallow brown beige. middle compactness of the packing | 15 | 74.4 | 10.6 |
| 73-88 | Bt | Bt2 | clay silt | reddish brown. middle compactness of the packing; sand loess | 6.1 | 73.6 | 20.3 |
| 88-120 | Bt | Bt3 | weak clay sand | nonpoint insert sandy silt, gray brown. middle compactness of the packing; sand loess | 14.7 | 70.6 | 14.7 |
| 120-133 | | | | | | | |
| 133-143 | Bbt-Cv | Bt/C | fine sandy medium sand | intense stony; stone level, beige gray. middle compactness of the packing; wind borne sand | 79 | 16 | 5 |
| 143-160 | | | | | | | |

¹³⁷Cs in depth profile soil samples from Lower Saxony, GermanyTable B - 8: Activity concentration [Bq kg⁻¹] of ¹³⁷Cs in different geometry and activity concentration of layers [Bq m⁻²] in profile samples from Ricklingen, (meadow) North Germany.

| Depth [cm] | Dry density [g/cm ³] | Activity concentration (Bottle) | Marinelli Beaker | | |
|---------------|-------------------------------------|---------------------------------------|---------------------------|-------------------|------------|
| | | | Activity concentration | Activity of layer | |
| | | | | 01.09.1999 | 01.09.1999 |
| 0-5 | 1.29 | 10 ± 0.4 | 9 ± 0.3 | 571 ± 1 | 775 ± 2 |
| 5-10 | 1.30 | 11 ± 0.4 | 9 ± 0.3 | 610 ± 1 | 828 ± 2 |
| 10-15 | 1.27 | 11 ± 0.4 | 10 ± 0.3 | 625 ± 1 | 848 ± 2 |
| 15-20 | 1.23 | 10 ± 0.4 | 9 ± 0.3 | 560 ± 1 | 759 ± 2 |
| 20-25 | 1.27 | 10 ± 0.4 | 9 ± 0.3 | 553 ± 1 | 750 ± 2 |
| 25-33 | 1.26 | 8 ± 0.3 | 7 ± 0.2 | 725 ± 2 | 984 ± 3 |
| 33-50 | 1.33 | 0.23 ± 0.1 | 0.4 ± 0.1 | 94 ± 5 | 128 ± 6 |
| 50-75 | 1.28 | nd | nd | nd | nd |
| 75-100 | 1.36 | nd | nd | nd | nd |

Table B - 9: Activity concentration (Bqkg^{-1}) of ^{137}Cs in different geometry and activity concentration [Bq/m^2] of layers in profile samples from Barum(field), North Germany.

| Depth [cm] | Density [g/cm^3]dry | Activity concentration (Bottle) | Marinelli Beaker | | |
|------------|--------------------------------|---------------------------------|------------------------|-------------------|----------------|
| | | | Activity concentration | Activity of layer | |
| | | | | 01.09.1999 | 26.04.1986 |
| 0-20 | 1.230 | 7.3 ± 0.3 | 6.2 ± 0.2 | 1518 ± 0.5 | 2060 ± 1 |
| 20-37 | 1.195 | 7.1 ± 0.3 | 6.1 ± 0.2 | 1233 ± 0.4 | 1672 ± 1 |
| 37-57 | 1.268 | 0.33 ± 0.1 | 0.3 ± 0.03 | 83 ± 0.01 | 113 ± 0.01 |
| 57-73 | 1.275 | nd | nd | nd | nd |
| 73-88 | 1.217 | nd | nd | nd | nd |
| 88-120 | 1.233 | nd | nd | nd | nd |
| 120-133 | 1.295 | nd | nd | nd | nd |
| 133-143 | 1.501 | nd | nd | nd | nd |
| 143-160 | 1.675 | nd | nd | nd | nd |

Table B - 10: Activity concentration (Bqkg^{-1}) of ^{137}Cs in different geometry and activity concentration [Bq/m^2] of layers in profile samples from Badenstedt (field), North Germany.

| Depth [cm] | Density [g/cm^3]dry | Activity concentration (Bottle) | Marinelli Beaker | | |
|------------|--------------------------------|---------------------------------|------------------------|-------------------|--------------|
| | | | Activity concentration | Activity of layer | |
| | | | | 01.09.1999 | 26.04.1986 |
| 0-15 | 1.182 | 14 ± 0.9 | 12 ± 0.4 | 2194 ± 4 | 2975 ± 5 |
| 15-30 | 1.147 | 13 ± 0.5 | 11 ± 0.4 | 1864 ± 3 | 2528 ± 5 |
| 30-40 | 1.258 | 0.7 ± 0.1 | 0.4 ± 0.1 | 54 ± 3 | 74 ± 3 |
| 40-50 | 1.208 | nd | 0.5 ± 0.03 | 64 ± 2 | 86 ± 3 |
| 50-75 | 1.200 | nd | nd | nd | nd |
| 75-100 | 1.199 | nd | nd | nd | nd |
| 100-150 | 1.188 | nd | nd | nd | nd |
| 150-200 | 1.313 | nd | nd | nd | nd |
| 200-250 | | nd | nd | nd | nd |

^{137}Cs in depth profile soil samples from Lippe (North Rhine-Westphalia), Germany

Table B - 11: Activity concentration [Bq kg^{-1}] of ^{137}Cs in different geometry and activity concentration of layers [Bq m^{-2}] in profile sample (BP3-30), Lippe NRW, Germany.

| Code of sample | Depth (cm) | Density (g/cm^3) | Activity concentration | Activity of layer | |
|------------------|------------|-----------------------------|------------------------|-------------------|----------------|
| | | | | 01.09.2000 | 26.04.1986 |
| BP 3-30. 0-2cm | 0-2 | 0.91 | 36 ± 2 | 662 ± 33 | 919 ± 46 |
| BP 3-30. 2-4cm | 2-4 | 0.95 | 45 ± 2 | 880 ± 44 | 1221 ± 61 |
| BP 3-30. 4-6cm | 4-6 | 0.98 | 47 ± 2 | 841 ± 42 | 1167 ± 59 |
| BP 3-30. 6-10cm | 6-10 | 1.00 | 57 ± 3 | 2292 ± 114 | 3181 ± 159 |
| BP 3-30. 10-15cm | 10-15 | 0.98 | 47 ± 2 | 2099 ± 105 | 2913 ± 146 |
| BP 3-30. 15-20cm | 15-20 | 0.94 | 23 ± 1 | 1100 ± 56 | 1527 ± 78 |
| BP 3-30. 20-30cm | 20-30 | 0.92 | 26 ± 0.3 | 1189 ± 14 | 1651 ± 19 |

¹³⁷Cs in depth profile soil samples from Ukraine.

Table B - 12: Chirstinovka River shore

| Depth [cm] | Dry density [g/cm ³] | Specific activity Bq kg ⁻¹ | | deposition densities kBq m ⁻² | | ¹³⁴ Cs/ ¹³⁷ Cs |
|------------|----------------------------------|---------------------------------------|---------------|------------------------------------------|------------|--------------------------------------|
| | | Cs-137 | Cs-134 | Cs-137 | Cs-134 | |
| humus/soil | 0.66 | 28836 ± 926 | 185110 ± 1211 | 3734 ± 120 | 2053 ± 133 | 0.55 |
| 0-1 | 1.07 | 40841 ± 1311 | 24292 ± 1356 | 3563 ± 114 | 1944 ± 126 | 0.55 |
| 1-2 | 1.21 | 52282 ± 1678 | 34358 ± 1540 | 3127 ± 100 | 1685 ± 112 | 0.54 |
| 2-3 | 1.46 | 84045 ± 2697 | 30170 ± 1437 | 2493 ± 80 | 1269 ± 93 | 0.51 |
| 3-5 | 1.38 | 36203 ± 1162 | 19919 ± 1232 | 1265 ± 41 | 828 ± 72 | 0.65 |
| 5-10 | 1.45 | 2296 ± 73 | 1559 ± 63 | 262 ± 9 | 276 ± 38 | 1.05 |
| 10-15 | 1.41 | 966 ± 31 | 679 ± 88 | 96 ± 3.2 | 164 ± 33 | 1.70 |
| 15-20 | 1.52 | 171 ± 6 | 425 ± 77 | 28 ± 1 | 116 ± 27 | 4.13 |
| 20-25 | 1.47 | 68 ± 2 | 335 ± 75 | 15 ± 0.6 | 84 ± 21 | 5.57 |
| 25-40 | 1.57 | 42 ± 2 | 251 ± 66 | 10 ± 0.4 | 59 ± 16 | 5.89 |

Table B - 13: Nove Scharnow3

| Depth [cm] | Dry density [g/cm ³] | Specific activity Bq kg ⁻¹ | | deposition densities kBq m ⁻² | | ¹³⁴ Cs/ ¹³⁷ Cs |
|------------|----------------------------------|---------------------------------------|-------------|------------------------------------------|------------|--------------------------------------|
| | | Cs-137 | Cs-134 | Cs-137 | Cs-134 | |
| humus/soil | 1.37 | 16814 ± 540 | 9303 ± 774 | 3549 ± 114 | 2168 ± 176 | 0.61 |
| 0-1 | 1.49 | 18604 ± 597 | 10856 ± 803 | 3353 ± 108 | 2044 ± 166 | 0.61 |
| 1-2 | 1.54 | 18595 ± 597 | 12488 ± 753 | 3076 ± 99 | 1883 ± 154 | 0.61 |
| 2-3 | 1.55 | 19252 ± 618 | 10310 ± 776 | 2789 ± 90 | 1691 ± 143 | 0.61 |
| 3-5 | 1.81 | 17421 ± 559 | 9322 ± 699 | 2490 ± 80 | 1532 ± 131 | 0.62 |
| 5-10 | 1.64 | 16457 ± 528 | 10865 ± 779 | 1859 ± 60 | 1199 ± 105 | 0.65 |
| 10-15 | 1.68 | 4680 ± 150 | 2853 ± 365 | 512 ± 17 | 309 ± 42 | 0.61 |
| 15-20 | 1.89 | 731 ± 24 | 455 ± 67 | 119 ± 8 | 70 ± 11 | 0.59 |
| 20-25 | 1.76 | 302 ± 10 | 310 ± 55 | 50 ± 7 | 27 ± 5 | 0.55 |
| 25-40 | 1.42 | 109 ± 4 | - | 23 ± 10 | - | - |

Table B - 14: Tschigiri 2

| Depth [cm] | Dry density [g/cm ³] | Specific activity Bq kg ⁻¹ | | deposition densities kBq m ⁻² | | ¹³⁴ Cs/ ¹³⁷ Cs |
|------------|----------------------------------|---------------------------------------|------------|------------------------------------------|----------|--------------------------------------|
| | | Cs-137 | Cs-134 | Cs-137 | Cs-134 | |
| humus/soil | 0.87 | 8594 ± 276 | 6770 ± 629 | 371.1 ± 12 | 292 ± 44 | 0.79 |
| 0-1 | 1.15 | 6704 ± 215 | 3976 ± 482 | 264.5 ± 9 | 208 ± 36 | 0.79 |
| 1-2 | 2.20 | 3821 ± 123 | 3386 ± 362 | 187.4 ± 6 | 162 ± 30 | 0.87 |
| 2-3 | 1.40 | 1707 ± 55 | 1134 ± 94 | 103.2 ± 3 | 88 ± 22 | 0.85 |
| 3-5 | 1.56 | 804 ± 26 | 555 ± 82 | 79.4 ± 3 | 72 ± 21 | 0.91 |
| 5-10 | 1.56 | 344 ± 11 | 294 ± 59 | 54.3 ± 2 | 55 ± 18 | 1.01 |
| 10-15 | 1.59 | 171 ± 6 | 190 ± 61 | 27.4 ± 4 | 32 ± 14 | 1.15 |
| 15-20 | 1.73 | 68 ± 2 | 102 ± 54 | 13.8 ± 6 | 16 ± 9 | 1.19 |
| 20-25 | 1.71 | 38 ± 1 | 89 ± 51 | 8.0 ± 7 | 8 ± 4 | 0.96 |
| 25-40 | 1.83 | 17 ± 1 | - | 4.7 ± 8 | - | - |

Table B - 15: Tschigiri 3

| Depth [cm] | Dry density [g/cm ³] | Specific activity Bq kg ⁻¹ | | deposition densities kBq m ⁻² | | ¹³⁴ Cs/ ¹³⁷ Cs |
|------------|----------------------------------|---------------------------------------|------------|------------------------------------------|----------|--------------------------------------|
| | | Cs-137 | Cs-134 | Cs-137 | Cs-134 | |
| humus/soil | 0.82 | 11882 ± 382 | 6858 ± 317 | 352 ± 11 | 144 ± 13 | 0.41 |
| 0-1 | 1.04 | 8051 ± 259 | - | 261 ± 9 | 92 ± 11 | 0.35 |
| 1-2 | 1.34 | 3540 ± 114 | 2158 ± 114 | 177 ± 6 | 92 ± 11 | 0.52 |
| 2-3 | 1.40 | 1863 ± 60 | 972 ± 72 | 130 ± 4 | 63 ± 9 | 0.48 |
| 3-5 | 1.32 | 1103 ± 36 | - | 104 ± 3 | 49 ± 8 | 0.47 |
| 5-10 | 1.51 | 672 ± 22 | - | 75 ± 3 | - | - |
| 10-15 | 1.45 | 170 ± 6 | - | 24 ± 8 | - | - |
| 15-20 | 1.50 | 34 ± 1.3 | 300 ± 47 | 12 ± 13 | - | - |
| 20-25 | 1.73 | 10 ± 0.6 | 305 ± 48 | 9 ± 14 | - | - |
| 25-40 | 1.84 | 30 ± 1.2 | - | 8 ± 14 | - | - |

Table B - 16: Tschigiri Zwintor I

| Depth [cm] | Dry density [g/cm ³] | Specific activity Bq kg ⁻¹ | | deposition densities kBq m ⁻² | | ¹³⁴ Cs/ ¹³⁷ Cs |
|------------|----------------------------------|---------------------------------------|--------------|------------------------------------------|----------|--------------------------------------|
| | | Cs-137 | Cs-134 | Cs-137 | Cs-134 | |
| humus/soil | 0.40 | 73257 ± 2353 | 47149 ± 2874 | 515 ± 17 | 388 ± 54 | 0.75 |
| 0-1 | 0.76 | 20247 ± 650 | 10398 ± 715 | 286 ± 9 | 241 ± 54 | 0.84 |
| 1-2 | 1.28 | 2958 ± 95 | 1840 ± 94 | 132 ± 4 | 162 ± 32 | 1.22 |
| 2-3 | 1.48 | 1197 ± 39 | 731 ± 58 | 95 ± 3 | 138 ± 23 | 1.46 |
| 3-5 | 1.51 | 630 ± 20 | 670 ± 61 | 77 ± 3 | 127 ± 21 | 1.65 |
| 5-10 | - | 601 ± 19 | - | 58 ± 1 | 107 ± 20 | - |
| 10-15 | 1.66 | 83 ± 3 | - | 19 ± 1 | 107 ± 16 | - |
| 15-20 | 1.61 | 67 ± 2 | 199 ± 43 | 12 ± 0.5 | 107 ± 16 | - |
| 20-25 | 1.61 | 45 ± 0.5 | 358 ± 42 | 7 ± 0.3 | 91 ± 16 | - |
| 25-40 | 1.96 | 11 ± 0.5 | 212 ± 36 | 3 ± 0.2 | 62 ± 12 | - |

Table B - 17: Woronewol

| Depth [cm] | Dry density [g/cm ³] | Specific activity Bq kg ⁻¹ | | deposition densities kBq m ⁻² | | ¹³⁴ Cs/ ¹³⁷ Cs |
|------------|----------------------------------|---------------------------------------|------------|------------------------------------------|----------|--------------------------------------|
| | | Cs-137 | Cs-134 | Cs-137 | Cs-134 | |
| humus/soil | 0.71 | 6496 ± 209 | 4405 ± 215 | 540.2 ± 17 | 320 ± 34 | 0.59 |
| 0-1 | 1.18 | 7420 ± 238 | 4724 ± 203 | 517.5 ± 17 | 306 ± 33 | 0.59 |
| 1-2 | 1.01 | 6664 ± 214 | 4073 ± 408 | 429.7 ± 14 | 255 ± 31 | 0.59 |
| 2-3 | 1.08 | 8645 ± 248 | 5682 ± 452 | 362.5 ± 12 | 218 ± 27 | 0.60 |
| 3-5 | 1.41 | 6069 ± 195 | 4258 ± 351 | 268.9 ± 9 | 161 ± 23 | 0.60 |
| 5-10 | 1.62 | 1046 ± 34 | - | 98.1 ± 3 | 52 ± 14 | 0.53 |
| 10-15 | 1.66 | 135 ± 4 | - | 13.5 ± 2 | - | - |
| 15-20 | 1.70 | 24 ± 0.9 | - | 2.3 ± 5 | - | - |
| 20-25 | 1.74 | 2.7 ± 0.3 | - | 0.2 ± 5 | - | - |
| 25-40 | 1.79 | - | - | - | - | - |

Table B - 18: Woronewo 2

| Depth [cm] | Dry density [g/cm ³] | Specific activity Bq kg ⁻¹ | | deposition densities kBq m ⁻² | | ¹³⁴ Cs/ ¹³⁷ Cs |
|------------|----------------------------------|---------------------------------------|------------|------------------------------------------|----------|--------------------------------------|
| | | Cs-137 | Cs-134 | Cs-137 | Cs-134 | |
| humus/soil | 0.98 | 5057 ± 162 | 4342 ± 304 | 199.8 ± 6.6 | 156 ± 13 | 0.78 |
| 0-1 | 1.28 | 7700 ± 247 | 3695 ± 159 | 149.9 ± 5 | 113 ± 10 | 0.76 |
| 1-2 | 1.42 | 1521 ± 49 | 811 ± 63 | 51.3 ± 1.8 | 66 ± 8 | 1.29 |
| 2-3 | 1.42 | 778 ± 25 | 420 ± 49 | 29.6 ± 1.1 | 54 ± 7 | 1.84 |
| 3-5 | 1.55 | 303 ± 10 | 499 ± 50 | 18.6 ± 0.8 | 48 ± 6 | 2.60 |
| 5-10 | 1.64 | 83 ± 3 | - | 9.2 ± 0.4 | 33 ± 5 | 3.56 |
| 10-15 | 1.74 | 19 ± 0.9 | - | 2.4 ± 3.9 | - | - |
| 15-20 | 1.77 | 2.2 ± 0.3 | - | 0.7 ± 6 | - | - |
| 20-25 | 1.83 | 1.9 ± 0.3 | - | 0.5 ± 7.8 | - | - |
| 25-40 | 1.88 | 1.3 ± 0.3 | - | 0.4 ± 0.1 | - | - |

Table B - 19: Woronewo3

| Depth [cm] | Dry density [g/cm ³] | Specific activity Bq kg ⁻¹ | | deposition densities kBq m ⁻² | | ¹³⁴ Cs/ ¹³⁷ Cs |
|------------|----------------------------------|---------------------------------------|-------------|------------------------------------------|----------|--------------------------------------|
| | | Cs-137 | Cs-134 | Cs-137 | Cs-134 | |
| humus/soil | 0.63 | 16937 ± 545 | 7398 ± 1002 | 444 ± 14.4 | 291 ± 38 | 0.66 |
| 0-1 | 0.91 | 7392 ± 237 | 4279 ± 178 | 328.7 ± 10.7 | 241 ± 31 | 0.73 |
| 1-2 | 0.95 | 6101 ± 196 | 3507 ± 356 | 261.4 ± 8.5 | 202 ± 30 | 0.77 |
| 2-3 | 1.27 | 8085 ± 260 | 2987 ± 310 | 203.6 ± 6.7 | 169 ± 26 | 0.83 |
| 3-5 | 1.18 | 2255 ± 73 | 1422 ± 91 | 101.2 ± 3.4 | 131 ± 22 | 1.29 |
| 5-10 | 1.60 | 385 ± 13 | 320 ± 45 | 48.1 ± 1.7 | 97 ± 20 | 2.03 |
| 10-15 | 1.58 | 78 ± 3 | - | 17.3 ± 0.7 | 72 ± 17 | 4.15 |
| 15-20 | 1.68 | 24 ± 0.9 | - | 11.2 ± 0.4 | 72 ± 17 | 6.43 |
| 20-25 | 1.64 | 46 ± 2 | 168 ± 33 | 9.1 ± 0.4 | 72 ± 17 | 7.86 |
| 25-40 | 1.84 | 20 ± 0.8 | 210 ± 50 | 5.4 ± 0.2 | 58 ± 14 | 10.75 |

Table B - 20: Woronewo 4

| Depth [cm] | Dry density [g/cm ³] | Specific activity Bq kg ⁻¹ | | deposition densities kBq m ⁻² | | ¹³⁴ Cs/ ¹³⁷ Cs |
|------------|----------------------------------|---------------------------------------|--------------|------------------------------------------|----------|--------------------------------------|
| | | Cs-137 | Cs-134 | Cs-137 | Cs-134 | |
| humus/soil | 0.44 | 21424 ± 688 | 11442 ± 640 | 795.2 ± 26 | 505 ± 37 | 0.64 |
| 0-1 | 0.76 | 54226 ± 1741 | 29160 ± 1347 | 746.7 ± 24 | 482 ± 36 | 0.65 |
| 1-2 | 0.67 | 29110 ± 935 | 15531 ± 802 | 337.0 ± 11 | 282 ± 27 | 0.84 |
| 2-3 | 0.85 | 6992 ± 225 | 4745 ± 420 | 143.0 ± 5 | 189 ± 22 | 1.32 |
| 3-5 | 1.00 | 1634 ± 53 | 1200 ± 73 | 83.2 ± 2.8 | 152 ± 19 | 1.83 |
| 5-10 | 1.36 | 426 ± 14 | 627 ± 57 | 50.5 ± 1.7 | 130 ± 17 | 2.58 |
| 10-15 | 1.58 | 58 ± 2 | 281 ± 42 | 21.6 ± 0.8 | 92 ± 14 | 4.25 |
| 15-20 | 1.54 | 36 ± 1.3 | 745 ± 110 | 17.0 ± 0.6 | 72 ± 11 | 4.21 |
| 20-25 | 1.63 | 30 ± 1.1 | 266 ± 41 | 14.2 ± 0.5 | 20 ± 3 | 1.38 |
| 25-40 | 1.81 | 43 ± 1.5 | - | 11.8 ± 0.4 | - | - |

Table B - 21: Woronewo 5

| Depth [cm] | Dry density [g/cm ³] | Specific activity Bq kg ⁻¹ | | deposition densities kBq m ⁻² | | ¹³⁴ Cs/ ¹³⁷ Cs |
|------------|----------------------------------|---------------------------------------|------------|------------------------------------------|----------|--------------------------------------|
| | | Cs-137 | Cs-134 | Cs-137 | Cs-134 | |
| humus/soil | 0.33 | 47425 ± 1523 | 3005 ± 202 | 559.8 ± 18 | 194 ± 40 | 0.35 |
| 0-1 | 0.48 | 31429 ± 1009 | 3998 ± 260 | 268.5 ± 9 | 176 ± 38 | 0.66 |
| 1-2 | 1.02 | 3910 ± 126 | 994 ± 138 | 118.0 ± 4 | 157 ± 37 | 1.33 |
| 2-3 | 1.05 | 1859 ± 60 | 529 ± 46 | 78.2 ± 3 | 147 ± 36 | 1.88 |
| 3-5 | 1.35 | 933 ± 30 | 884 ± 88 | 58.7 ± 2 | 141 ± 35 | 241 |
| 5-10 | 1.37 | 252 ± 8 | 309 ± 75 | 33.4 ± 1 | 117 ± 33 | 3.51 |
| 10-15 | 1.48 | 94 ± 3 | 188 ± 61 | 16.2 ± 2 | 96 ± 28 | 5.93 |
| 15-20 | 1.57 | 53 ± 2 | 208 ± 60 | 9.3 ± 4 | 82 ± 23 | 8.89 |
| 20-25 | 1.70 | 25 ± 1.1 | 181 ± 65 | 5.1 ± 5 | 66 ± 19 | 12.98 |
| 25-40 | 1.74 | 11 ± 0.7 | 194 ± 53 | 2.9 ± 7 | 51 ± 14 | 17.34 |

Table B - 22: Woronewo 6

| Depth [cm] | Dry density [g/cm ³] | Specific activity Bq kg ⁻¹ | | deposition densities kBq m ⁻² | | ¹³⁴ Cs/ ¹³⁷ Cs |
|------------|----------------------------------|---------------------------------------|------------|------------------------------------------|----------|--------------------------------------|
| | | Cs-137 | Cs-134 | Cs-137 | Cs-134 | |
| humus/soil | 0.94 | 10511 ± 338 | 6030 ± 315 | 539.6 ± 17.5 | 292 ± 25 | 0.54 |
| 0-1 | 0.98 | 5610 ± 180 | 2620 ± 308 | 491.9 ± 15.9 | 264 ± 23 | 0.54 |
| 1-2 | 1.09 | 5244 ± 168 | 2408 ± 127 | 437.0 ± 14.2 | 239 ± 20 | 0.55 |
| 2-3 | 1.08 | 4839 ± 156 | 2311 ± 123 | 379.7 ± 12.3 | 212 ± 19 | 0.56 |
| 3-5 | 1.39 | 5804 ± 186 | 3474 ± 155 | 327.5 ± 10.6 | 187 ± 17 | 0.57 |
| 5-10 | 1.55 | 1799 ± 58 | 708 ± 55 | 166.2 ± 5.5 | 91 ± 14 | 0.55 |
| 10-15 | 1.56 | 228 ± 7 | 116 ± 26 | 26.5 ± 1 | 36 ± 9 | 1.35 |
| 15-20 | 1.65 | 74 ± 2.5 | 164 ± 41 | 8.7 ± 0.6 | 27 ± 7 | 3.06 |
| 20-25 | 1.74 | 19 ± 0.9 | 151 ± 39 | 2.7 ± 0.7 | 13 ± 3 | 4.95 |
| 25-40 | 1.86 | 4 ± 0.3 | | 1.0 ± 1 | | |

Table B - 23: Woronewo 7

| Depth [cm] | Dry density [g/cm ³] | Specific activity Bq kg ⁻¹ | | deposition densities kBq m ⁻² | | ¹³⁴ Cs/ ¹³⁷ Cs |
|------------|----------------------------------|---------------------------------------|-----------|------------------------------------------|----------|--------------------------------------|
| | | Cs-137 | Cs-134 | Cs-137 | Cs-134 | |
| humus/soil | 1.54 | 726 ± 24 | 962 ± 107 | 267.3 ± 8.7 | 231 ± 30 | 0.87 |
| 0-1 | 1.41 | 838 ± 27 | 500 ± 91 | 261.3 ± 8.5 | 224 ± 29 | 0.86 |
| 1-2 | 1.67 | 573 ± 19 | 480 ± 144 | 249.5 ± 8.1 | 217 ± 28 | 0.87 |
| 2-3 | 1.81 | 191 ± 6 | 164 ± 50 | 239.9 ± 7.8 | 209 ± 26 | 0.87 |
| 3-5 | 1.85 | 230 ± 8 | 362 ± 62 | 236.5 ± 7.7 | 206 ± 25 | 0.87 |
| 5-10 | 1.73 | 640 ± 21 | 441 ± 60 | 227.9 ± 7.4 | 193 ± 23 | 0.85 |
| 10-15 | 1.73 | 1087 ± 35 | 1134 ± 85 | 172.7 ± 5.7 | 156 ± 18 | 0.91 |
| 15-20 | 1.86 | 621 ± 20 | 639 ± 69 | 78.9 ± 2.6 | 62 ± 11 | 0.78 |
| 20-25 | 2.02 | 205 ± 7 | 38 ± 45 | 21.0 ± 0.8 | 4 ± 4 | 0.18 |
| 25-40 | 2.11 | 0.7 ± 0.3 | - | 0.2 ± 0.1 | - | - |

Table B - 24: Baraschewka1

| Depth [cm] | Dry density [g/cm ³] | Specific activity Bq kg ⁻¹ | | deposition densities k Bq m ⁻² | |
|------------|----------------------------------|---------------------------------------|--------|-------------------------------------------|--------|
| | | Cs-137 | Cs-134 | Cs-137 | Cs-134 |
| humus/soil | 0.23 | 145 ± 5.9 | - | 2.9 ± 0.2 | - |
| 0-1 | 0.63 | 84 ± 3.2 | - | 2.7 ± 0.2 | - |
| 1-2 | 0.84 | 67 ± 2.5 | - | 2.1 ± 0.2 | - |
| 2-3 | 1.02 | 51 ± 1.9 | - | 1.6 ± 0.1 | - |
| 3-5 | 1.10 | 25 ± 1.1 | - | 1.1 ± 0.1 | - |
| 5-10 | 1.18 | 5 ± 0.8 | - | 0.6 ± 0.1 | - |
| 10-15 | 1.24 | 1.7 ± 0.5 | - | 0.2 ± 0.1 | - |
| 15-20 | 1.25 | 1.8 ± 0.4 | - | 0.1 ± 0.02 | - |
| 20-25 | 1.48 | - | - | - | - |
| 25-40 | 1.81 | - | - | - | - |

Table B - 25: Oserjanka 2

| Depth [cm] | Dry density [g/cm ³] | Specific activity Bq kg ⁻¹ | | deposition densities k Bq m ⁻² | |
|------------|----------------------------------|---------------------------------------|--------|-------------------------------------------|--------|
| | | Cs-137 | Cs-134 | Cs-137 | Cs-134 |
| humus/soil | 1.09 | 24.8 ± 1.3 | - | 1.8 ± 0.2 | - |
| 0-1 | 1.23 | 45.7 ± 2 | - | 1.7 ± 0.2 | - |
| 1-2 | 1.01 | - | - | 1.4 ± 0.2 | - |
| 2-3 | 1.25 | 23.9 ± 0.9 | - | 1.4 ± 0.2 | - |
| 3-5 | 1.36 | 13.4 ± 0.6 | - | 1.2 ± 0.2 | - |
| 5-10 | 1.36 | 7.1 ± 0.4 | - | 0.9 ± 0.2 | - |
| 10-15 | 1.52 | 3.2 ± 0.4 | - | 0.4 ± 0.2 | - |
| 15-20 | 1.44 | 0.8 ± 0.3 | - | 0.2 ± 0.1 | - |
| 20-25 | 1.40 | - | - | 0.2 ± 0.1 | - |
| 25-40 | 1.39 | 0.6 ± 0.5 | - | 0.2 ± 0.1 | - |

Table B - 26: Oserjanka 3

| Depth [cm] | Dry density [g/cm ³] | Specific activity Bq kg ⁻¹ | | deposition densities k Bq m ⁻² | |
|------------|----------------------------------|---------------------------------------|--------|-------------------------------------------|--------|
| | | Cs-137 | Cs-134 | Cs-137 | Cs-134 |
| humus/soil | 0.60 | 14.3 ± 0.8 | - | 6.4 ± 0.4 | - |
| 0-1 | 1.02 | 7.5 ± 0.5 | - | 6.4 ± 0.4 | - |
| 1-2 | 1.09 | - | - | 6.3 ± 0.4 | - |
| 2-3 | 1.19 | 4.0 ± 0.4 | - | 6.3 ± 0.4 | - |
| 3-5 | 1.13 | 5.8 ± 0.4 | - | 6.3 ± 0.4 | - |
| 5-10 | 0.96 | 4.9 ± 0.4 | - | 6.2 ± 0.4 | - |
| 10-15 | 0.94 | 5.1 ± 0.5 | - | 5.8 ± 0.4 | - |
| 15-20 | 0.92 | 7.8 ± 0.5 | - | 5.5 ± 0.4 | - |
| 20-25 | 0.94 | 5.6 ± 0.4 | - | 4.9 ± 0.3 | - |
| 25-40 | 0.53 | 17.9 ± 1.1 | - | 4.5 ± 0.3 | - |

Table B - 27: Dawidowka 1

| Depth [cm] | Dry density [g/cm ³] | Specific activity Bq kg ⁻¹ | | deposition densities k Bq m ⁻² | |
|------------|----------------------------------|---------------------------------------|--------|-------------------------------------------|--------|
| | | Cs-137 | Cs-134 | Cs-137 | Cs-134 |
| humus/soil | 0.23 | 74 ± 2.9 | - | 5.2 ± 0.3 | - |
| 0-1 | 0.63 | 64 ± 2.4 | - | 5.0 ± 0.3 | - |
| 1-2 | 0.84 | 60 ± 2.3 | - | 4.3 ± 0.3 | - |
| 2-3 | 1.02 | 50 ± 2.0 | - | 3.6 ± 0.3 | - |
| 3-5 | 1.10 | 30 ± 1.4 | - | 3.1 ± 0.2 | - |
| 5-10 | 1.18 | 17 ± 0.9 | - | 2.3 ± 0.2 | - |
| 10-15 | 1.24 | 8 ± 0.8 | - | 1.3 ± 0.1 | - |
| 15-20 | 1.25 | 4 ± 0.7 | - | 0.7 ± 0.1 | - |
| 20-25 | 1.48 | 7 ± 0.7 | - | 0.5 ± 0.1 | - |
| 25-40 | 1.81 | - | - | - | - |

Table B - 28: Lewkow 1

| Depth [cm] | Dry density [g/cm ³] | Specific activity Bq kg ⁻¹ | | deposition densities k Bq m ⁻² | |
|------------|----------------------------------|---------------------------------------|--------|-------------------------------------------|--------|
| | | Cs-137 | Cs-134 | Cs-137 | Cs-134 |
| humus/soil | 0.63 | 62.4 ± 2.8 | - | 5.1 ± 0.3 | - |
| 0-1 | 0.76 | 68.0 ± 2.5 | - | 4.9 ± 0.3 | - |
| 1-2 | 0.91 | 87.2 ± 3.2 | - | 4.4 ± 0.2 | - |
| 2-3 | 1.00 | 68.3 ± 2.6 | - | 3.6 ± 0.2 | - |
| 3-5 | 0.99 | 41.5 ± 1.7 | - | 2.9 ± 0.2 | - |
| 5-10 | 1.12 | 7.2 ± 0.5 | - | 2.1 ± 0.2 | - |
| 10-15 | 1.05 | 18.0 ± 0.9 | - | 1.7 ± 0.1 | - |
| 15-20 | 1.21 | 8.6 ± 0.6 | - | 0.8 ± 0.1 | - |
| 20-25 | 1.24 | 4.2 ± 0.7 | - | 0.3 ± 0.04 | - |
| 25-40 | 1.33 | - | - | - | - |

Table B - 29: Lewkow 2

| Depth [cm] | Dry density [g/cm ³] | Specific activity Bq kg ⁻¹ | | deposition densities k Bq m ⁻² | |
|------------|----------------------------------|---------------------------------------|--------|-------------------------------------------|--------|
| | | Cs-137 | Cs-134 | Cs-137 | Cs-134 |
| humus/soil | 1.08 | 23.53 ± 0.9 | - | 2.6 ± 0.1 | - |
| 0-1 | 1.29 | 27.92 ± 1.1 | - | 2.4 ± 0.1 | - |
| 1-2 | 1.25 | 28.73 ± 1.1 | - | 2.4 ± 0.1 | - |
| 2-3 | 1.29 | - | - | 2.0 ± 0.1 | - |
| 3-5 | 1.42 | - | - | 2.0 ± 0.1 | - |
| 5-10 | 1.15 | 20.83 ± 0.8 | - | 2.0 ± 0.1 | - |
| 10-15 | 1.50 | - | - | 0.8 ± 0.1 | - |
| 15-20 | 1.47 | 5.79 ± 0.4 | - | 0.8 ± 0.1 | - |
| 20-25 | 1.49 | 5.05 ± 0.4 | - | 0.4 ± 0.03 | - |
| 25-40 | 1.70 | - | - | - | - |

Concentration of natural radionuclides in depth profile and surface soil samples from Lower Saxony, North Germany.

Table B - 30: Activity concentration (Bq kg⁻¹) of ²³⁸U, ²²⁶Ra, ²¹⁰Pb, ²³⁵U, ⁴⁰K, ²²⁸Ra, ²²⁸Th, and ²³²Th in soil profile samples collected from Klein Lobke, (field) in Hanover, North Germany.

| Depth [cm] | Dry density [g/cm ³] | U-238 [Bq/kg] | Ra-226 [Bq/kg] | Pb-210 [Bq/kg] | U-235 [Bq/kg] | K-40 [Bq/kg] | Ra-228 [Bq/kg] | Th-228 [Bq/kg] | Th-232 [Bq/kg] |
|------------|----------------------------------|---------------|----------------|----------------|---------------|--------------|----------------|----------------|----------------|
| 0-15 | 1.28 | 28.1 ± 8 | 20.8 ± 2 | 32.5 ± 1.4 | 1.3 ± 0.39 | 462 ± 15 | 25.4 ± 0.27 | 24.2 ± 1.4 | 24.3 ± 1.1 |
| 15-30 | 1.25 | 20.7 ± 1 | 20.6 ± 1 | 34.5 ± 1.5 | 0.95 ± 0.1 | 451 ± 15 | 24.2 ± 1.76 | 23.1 ± 3.2 | 23.7 ± 0.5 |
| 30-40 | 1.18 | 16.9 ± 3 | 18.8 ± 1 | 32.4 ± 1.4 | 0.78 ± 0.1 | 421 ± 14 | 22.8 ± 2.34 | 20.8 ± 3 | 22.3 ± 1.3 |
| 40-50 | 1.25 | 15.5 ± 6 | 19.9 ± 1 | 30.1 ± 1.4 | 0.7 ± 0.29 | 442 ± 15 | 24.9 ± 1.13 | 22.8 ± 2.4 | 24.7 ± 1.8 |
| 50-70 | 1.48 | 18.0 ± 4 | 16.9 ± 1 | 21.9 ± 1.1 | 0.83 ± 0.2 | 461 ± 15 | 22.9 ± 0.83 | 20.3 ± 2.6 | 21.7 ± 1.3 |
| 70-90 | 1.27 | 14.6 ± 1 | 13.4 ± 1 | 16.2 ± 0.9 | 0.67 ± 0.1 | 414 ± 14 | 20.1 ± 0.95 | 18.2 ± 2 | 19.3 ± 1 |
| 90-105 | 1.36 | 20.6 ± 4 | 22.5 ± 1 | 26.0 ± 1.2 | 0.95 ± 0.2 | 528 ± 18 | 28.5 ± 1.29 | 26.1 ± 2.3 | 27.8 ± 1.4 |
| 105-130 | 1.24 | 15.5 ± 1 | 16.2 ± 1 | 22.3 ± 1.1 | 0.7 ± 0.04 | 443 ± 15 | 19.7 ± 2.09 | 18.2 ± 1.6 | 19.6 ± 1.4 |
| 130-150 | 1.27 | 18.9 ± 3 | 20.7 ± 1 | 30.7 ± 1.4 | 0.9 ± 0.2 | 502 ± 17 | 26.1 ± 1.93 | 22.9 ± 3.6 | 25.6 ± 2.6 |
| 150-200 | 1.29 | 24.4 ± 6 | 25.0 ± 1 | 27.4 ± 1.3 | 1.12 ± 0.3 | 502 ± 17 | 29.6 ± 3.08 | 27.8 ± 1.3 | 28.8 ± 0.8 |
| 200-250 | 1.35 | 22.8 ± 9 | 19.4 ± 1 | 31.4 ± 1.4 | 1.1 ± 0.44 | 474 ± 16 | 22.0 ± 1.15 | 19.8 ± 2.6 | 21.3 ± 1.3 |

Table B - 31: Activity concentration (Bq kg⁻¹) of ²³⁸U, ²²⁶Ra, ²¹⁰Pb, ²³⁵U, ⁴⁰K, ²²⁸Ra, ²²⁸Th, and ²³²Th in soil profile samples collected from Vestrup (meadow), North Germany.

| Depth [cm] | Dry density [g/cm ³] | U-238 [Bq/kg] | Ra-226 [Bq/kg] | Pb-210 [Bq/kg] | U-235 [Bq/kg] | K-40 [Bq/kg] | Ra-228 [Bq/kg] | Th-228 [Bq/kg] | Th-232 [Bq/kg] |
|------------|----------------------------------|---------------|----------------|----------------|---------------|--------------|----------------|----------------|----------------|
| 0-15 | 1.18 | 11 ± 3.2 | 8.9 ± 0.73 | 26 ± 1.2 | 0.50 ± 0.15 | 139 ± 5 | 9 ± 1 | 8.50 ± 1.9 | 8.4 ± 1 |
| 15-27 | 1.24 | 14 ± 9.4 | 8.7 ± 0.59 | - | 0.65 ± 0.43 | 145 ± 5 | 9 ± 0.4 | 8.17 ± 1.9 | 8.5 ± 0.6 |
| 27-36 | 1.41 | 17 ± 4.6 | 7.4 ± 0.55 | 14 ± 0.8 | 0.77 ± 0.21 | 248 ± 8 | 9 ± 1 | 8.94 ± 0.6 | 8.8 ± 0.2 |
| 36-50 | 1.48 | 12 ± 0.9 | 11.3 ± 0.6 | 8 ± 0.6 | 0.54 ± 0.04 | 376 ± 12 | 14 ± 1 | 13.6 ± 1.2 | 13.6 ± 0.3 |
| 50-75 | 1.49 | 10 ± 3.1 | 10 ± 0.55 | 15 ± 0.9 | 0.47 ± 0.14 | 382 ± 13 | 13 ± 1 | 12.9 ± 1.1 | 13 ± 0.4 |
| 75-100 | 1.40 | 14 ± 0.6 | 15 ± 0.87 | 17 ± 0.9 | 0.66 ± 0.03 | 433 ± 14 | 22 ± 1 | 23.3 ± 4 | 22 ± 1.5 |

Table B - 32: Activity concentration (Bq kg⁻¹) of ²³⁸U, ²²⁶Ra, ²¹⁰Pb, ²³⁵U, ⁴⁰K, ²²⁸Ra, ²²⁸Th, and ²³²Th in soil profile samples collected from Barum (field), North Germany.

| Depth (cm) | Dry density [g/cm ³] | U-238 [Bq/kg] | Ra-226 [Bq/kg] | Pb-210 [Bq/kg] | U-235 [Bq/kg] | K-40 [Bq/kg] | Ra-228 [Bq/kg] | Th-228 [Bq/kg] | Th-232 [Bq/kg] |
|------------|----------------------------------|---------------|----------------|----------------|---------------|--------------|----------------|----------------|----------------|
| 0-20 | 1.230 | 24 ± 4 | 21 ± 1.5 | 25 ± 1.2 | 1.11 ± 0.2 | 315 ± 11 | 23.4 ± 1.28 | 21 ± 3.5 | 23 ± 3 |
| 20-37 | 1.195 | 17 ± 10 | 21 ± 1.2 | 18 ± 1 | 0.79 ± 0.48 | 424 ± 14 | 24.2 ± 1.51 | 22 ± 2 | 23 ± 2 |
| 37-57 | 1.268 | 23 ± 5 | 2 ± 1.3 | 33 ± 1.5 | 1.07 ± 0.25 | 472 ± 16 | 25.4 ± 1.33 | 22 ± 2 | 21 ± 2 |
| 57-73 | 1.275 | 23 ± 3 | 23 ± 1.6 | 31 ± 1.4 | 1.05 ± 0.13 | 497 ± 17 | 26.8 ± 2.59 | 24 ± 2.1 | 25 ± 2 |
| 73-88 | 1.217 | 27 ± 7 | 21 ± 1.02 | 31 ± 1.4 | 1.23 ± 0.34 | 492 ± 16 | 28.0 ± 2.09 | 26 ± 2.1 | 27 ± 2 |
| 88-120 | 1.233 | 26 ± 11 | 21 ± 1.1 | 32 ± 1.4 | 1.20 ± 0.51 | 494 ± 17 | 28.6 ± 1.23 | 24 ± 2.4 | 26 ± 3 |
| 120-133 | 1.295 | 31 ± 13 | 23 ± 1.4 | 27 ± 1.4 | 1.44 ± 0.6 | 474 ± 16 | 29.2 ± 1.52 | 26 ± 2.9 | 28 ± 2 |
| 133-143 | 1.501 | 13 ± 1 | 13 ± 0.8 | 16 ± 0.9 | 0.60 ± 0.05 | 304 ± 10 | 18.3 ± 0.55 | 12 ± 7.2 | 15 ± 5 |
| 143-160 | 1.675 | 12 ± 10 | 11 ± 3.3 | 9 ± 0.6 | 0.58 ± 0.48 | 247 ± 8 | 16.7 ± 0.75 | 14 ± 1.7 | 15 ± 2 |

Table B - 33: Activity concentration (Bq kg⁻¹) of ²³⁸U, ²²⁶Ra, ²¹⁰Pb, ²³⁵U, ⁴⁰K, ²²⁸Ra, ²²⁸Th, and ²³²Th in soil profile samples collected from Badenstedt (field), North Germany.

| Depth (cm) | Dry density [g/cm ³] | U-238 [Bq/kg] | Ra-226 [Bq/kg] | Pb-210 [Bq/kg] | U-235 [Bq/kg] | K-40 [Bq/kg] | Ra-228 [Bq/kg] | Th-228 [Bq/kg] | Th-232 [Bq/kg] |
|------------|----------------------------------|---------------|----------------|----------------|---------------|--------------|----------------|----------------|----------------|
| 0-15 | 1.182 | 25 ± 0.5 | 26 ± 2 | 39.6 ± 1.7 | 1.15 ± 0.02 | 496 ± 17 | 32 ± 2 | 31 ± 4 | 32 ± 3 |
| 15-30 | 1.147 | 25 ± 3 | 25 ± 1 | 38.2 ± 1.6 | 1.13 ± 0.13 | 495 ± 16 | 31 ± 2 | 28 ± 3 | 29 ± 2 |
| 30-40 | 1.258 | 29 ± 6 | 25 ± 1 | 33.7 ± 1.5 | 1.35 ± 0.3 | 527 ± 18 | 32 ± 2 | 29 ± 3 | 30 ± 2 |
| 40-50 | 1.208 | 25 ± 3 | 25 ± 2 | 34.4 ± 1.5 | 1.14 ± 0.12 | 508 ± 17 | 32 ± 2 | 30 ± 3 | 31 ± 3 |
| 50-75 | 1.200 | 31 ± 6 | 27 ± 2 | 31.7 ± 1.4 | 1.41 ± 0.26 | 499 ± 17 | 34 ± 3 | 31 ± 4 | 33 ± 3 |
| 75-100 | 1.199 | 26 ± 2 | 25 ± 1 | 30.5 ± 2.2 | 1.18 ± 0.1 | 524 ± 18 | 36 ± 2 | 29 ± 4 | 32 ± 5 |
| 100-150 | 1.188 | 28 ± 5 | 27 ± 1 | 33.1 ± 1.5 | 1.30 ± 0.21 | 518 ± 17 | 33 ± 2 | 30 ± 4 | 32 ± 4 |
| 150-200 | 1.313 | 31 ± 9 | 28 ± 2 | 28.7 ± 1.3 | 1.42 ± 0.43 | 536 ± 18 | 31 ± 3 | 29 ± 4 | 30 ± 3 |

Table B - 34: Activity concentration (Bq kg⁻¹) of ²³⁸U, ²²⁶Ra, ²¹⁰Pb, ²³⁵U, ⁴⁰K, ²²⁸Ra, ²²⁸Th, and ²³²Th in soil profile samples collected from Neßmerpolder (meadow), North Germany.

| Depth (cm) | Dry density [g/cm ³] | U-238 [Bq/kg] | Ra-226 [Bq/kg] | Pb-210 [Bq/kg] | U-235 [Bq/kg] | K-40 [Bq/kg] | Ra-228 [Bq/kg] | Th-228 [Bq/kg] | Th-232 [Bq/kg] |
|------------|----------------------------------|---------------|----------------|----------------|---------------|--------------|----------------|----------------|----------------|
| 0-1 | 1.00 | 27.2 ± 3.2 | 21.5 ± 1 | 68.9 ± 7.6 | 1.3 ± 0.15 | 385 ± 13 | 26.8 ± 1.1 | 24.5 ± 1.3 | 25.7 ± 1.2 |
| 1-2 | 0.98 | 29.4 ± 3.1 | 22.1 ± 1 | 71.7 ± 7.6 | 1.4 ± 0.14 | 391 ± 13 | 24.8 ± 1 | 24.1 ± 1.3 | 24.4 ± 1.2 |
| 2-3 | 1.05 | 28.8 ± 3 | 22.2 ± 1 | 67.9 ± 7.6 | 1.3 ± 0.14 | 395 ± 14 | 27.8 ± 1.1 | 24.8 ± 1.4 | 26.3 ± 1.3 |
| 3-5 | 1.04 | 34.0 ± 3.5 | 24.7 ± 1 | 70.2 ± 7.8 | 1.6 ± 0.16 | 401 ± 14 | 27.7 ± 1.1 | 25.5 ± 1.3 | 26.6 ± 1.2 |
| 5-10 | 1.11 | 26.8 ± 2.8 | 25.0 ± 1 | 59.4 ± 6.8 | 1.2 ± 0.13 | 402 ± 14 | 27.8 ± 1.1 | 24.7 ± 1.3 | 26.3 ± 1.2 |
| 10-15 | 1.15 | 24.3 ± 2.8 | 25.8 ± 1 | 31.0 ± 4.6 | 1.1 ± 0.13 | 419 ± 14 | 29.1 ± 1.1 | 26.7 ± 1.3 | 27.9 ± 1.3 |
| 15-20 | 1.16 | 29.2 ± 3 | 22.6 ± 1 | 19.5 ± 4.4 | 1.3 ± 0.14 | 420 ± 14 | 29.3 ± 1.1 | 28.0 ± 1.4 | 28.6 ± 1.3 |
| 20-25 | 1.23 | 19.9 ± 2.5 | 23.8 ± 1 | 26.8 ± 4.1 | 0.9 ± 0.12 | 428 ± 15 | 27.1 ± 1 | 26.0 ± 1.3 | 26.6 ± 1.2 |
| 25-30 | 1.29 | 20.2 ± 2.8 | 24.1 ± 2 | 18.9 ± 4.6 | 0.9 ± 0.13 | 274 ± 10 | 27.3 ± 1 | 25.2 ± 1.3 | 26.3 ± 1.2 |

Lippe (North Rhine-Westphalia), Germany.

Table B - 35: Activity concentration of ²³⁸U, ²²⁶Ra, ²¹⁰Pb, ²³⁵U, ⁴⁰K, ²²⁸Ra, ²²⁸Th and ²³²Th (in Bq kg⁻¹) in soil collected from (Bp3-30) Lippe, North Rhine-Westphalia, Germany.

| Depth (cm) | Dry density [g/cm ³] | U-238 [Bq/kg] | Ra-226 [Bq/kg] | Pb-210 [Bq/kg] | U-235 [Bq/kg] | K-40 [Bq/kg] | Ra-228 [Bq/kg] | Th-228 [Bq/kg] | Th-232 [Bq/kg] |
|------------|----------------------------------|---------------|----------------|----------------|---------------|--------------|----------------|----------------|----------------|
| 0-2 | 0.91 | - | 304 ± 8 | 175 ± 29 | 1.0 | 377 ± 138 | 89 ± 4 | 75 ± 5 | 82 ± 5 |
| 2-4 | 0.95 | - | 306 ± 5 | 166 ± 27 | 0.6 | 383 ± 158 | 76 ± 3 | 69 ± 3 | 73 ± 3 |
| 4-6 | 0.98 | 57 | 317 ± 16 | 172 ± 27 | 1.8 | 382 ± 175 | 73 ± 7 | 78 ± 7 | 76 ± 7 |
| 6-10 | 1.00 | - | 320 ± 6 | 179 ± 29 | 1.0 | 366 ± 193 | 62 ± 2 | 63 ± 4 | 62 ± 3 |
| 10-15 | 0.98 | 36 | 258 ± 13 | 199 ± 29 | 1.0 | 375 ± 195 | 42 ± 4 | 43 ± 4 | 42 ± 4 |
| 15-20 | 0.94 | 33 | 219 ± 11 | 189 ± 27 | 1.1 | 388 ± 200 | 33 ± 4 | 33 ± 3 | 33 ± 3 |
| 20-30 | 0.92 | - | 216 ± 3 | 198 ± 26 | 1.3 | 374 ± 217 | 29 ± 1 | 22 ± 3 | 26 ± 2 |

Natural radionuclides in depth profiles from Ukraine.Table B - 36: Activity concentration of ^{238}U , ^{226}Ra , ^{210}Pb , ^{235}U , ^{40}K , ^{228}Ra , ^{228}Th and ^{232}Th (in Bq kg^{-1}) in soil collected from Nosdrischtsche II, Ukraine.

| Depth (cm) | Dry density [g/cm^3] | U-238 [Bq/kg] | Ra-226 [Bq/kg] | Pb-210 [Bq/kg] | U-235 [Bq/kg] | K-40 [Bq/kg] | Ra-228 [Bq/kg] | Th-228 [Bq/kg] | Th-232 [Bq/kg] |
|------------|---------------------------------|---------------|----------------|----------------|-----------------|--------------|----------------|----------------|----------------|
| humus soil | 1.10 | 3.0 ± 7.9 | 5 ± 2 | 197 ± 27 | 0.14 ± 0.4 | 155 ± 7 | 6 ± 2 | 4.3 ± 1 | 5 ± 2 |
| 0-1 | 1.18 | - | 6 ± 4 | 101 ± 33 | - | 322 ± 14 | 15 ± 2 | 11.6 ± 3 | 13 ± 3 |
| 1-2 | 1.63 | - | 5 ± 2 | 54 ± 17 | - | 267 ± 11 | 11 ± 1 | 7.2 ± 2 | 9 ± 2 |
| 2-3 | 1.46 | - | 6 ± 2 | - | - | 128 ± 6 | 8 ± 3 | 8.5 ± 2 | 8 ± 2 |
| 3-5 | 1.77 | - | 8 ± 2 | - | - | 194 ± 8 | 6 ± 1 | 4.9 ± 1 | 5 ± 1 |
| 5-10 | 1.78 | - | - | -- | - | 186 ± 8 | - | 5.9 ± 2 | 7 ± 2 |
| 10-15 | 1.84 | 8.8 ± 8.6 | 3 ± 1 | 9 ± 9 | 0.40 ± 0.4 | 200 ± 8 | - | 5.1 ± 2 | 5 ± 2 |
| 15-20 | 1.84 | 0.5 ± 3.2 | 7 ± 1 | 18 ± 6 | 0.02 ± 0.15 | 191 ± 7 | 8 ± 2 | 7.9 ± 1 | 8 ± 1 |
| 20-25 | 1.91 | 3.8 ± 2.3 | 8 ± 1 | 15 ± 4 | 0.18 ± 0.11 | 200 ± 8 | 8 ± 1 | 8.3 ± 1 | 8 ± 1 |
| 25-40 | 1.90 | 6.5 ± 2.2 | 8 ± 1 | 15 ± 4 | 0.30 ± 0.1 | 162 ± 7 | 6 ± 1 | 5.8 ± 0.4 | 6 ± 1 |

Table B - 37: Activity concentration of ^{238}U , ^{226}Ra , ^{210}Pb , ^{235}U , ^{40}K , ^{228}Ra , ^{228}Th , and ^{232}Th (in Bq kg^{-1}) in soil collected from Chirstinovka River shore, Ukraine.

| Depth (cm) | Dry density [g/cm^3] | U-238 [Bq/kg] | Ra-226 [Bq/kg] | Pb-210 [Bq/kg] | U-235 [Bq/kg] | K-40 [Bq/kg] | Ra-228 [Bq/kg] | Th-228 [Bq/kg] | Th-232 [Bq/kg] |
|------------|---------------------------------|---------------|----------------|----------------|----------------|--------------|----------------|----------------|----------------|
| humus soil | 0.66 | | 25 ± 5 | 116 ± 34 | - | 506 ± 21 | 34 ± 4 | 30 ± 5 | 35 ± 4 |
| 0-1 | 1.07 | 7 ± 33 | 31 ± 6 | - | 0.30 ± 1.5 | 471 ± 18 | 33 ± 2 | 30 ± 5 | 34 ± 4 |
| 1-2 | 1.21 | 34 ± 33 | 32 ± 6 | 14 ± 55 | 1.58 ± 1.5 | 462 ± 17 | 28 ± 2 | 27 ± 5 | 28 ± 4 |
| 2-3 | - | - | - | - | - | - | - | - | - |
| 3-5 | 1.38 | 34 ± 6 | 30 ± 2 | 30 ± 2 | 1.56 ± 0.3 | 573 ± 21 | 30 ± 2 | 34 ± 7 | 30 ± 2 |
| 5-10 | 1.45 | 17 ± 8 | 35 ± 3 | 32 ± 9 | 0.80 ± 0.4 | 596 ± 22 | 39 ± 3 | 41 ± 2 | 40 ± 3 |
| 10-15 | 1.41 | 16 ± 7 | 31 ± 3 | 45 ± 8 | 0.75 ± 0.3 | 559 ± 21 | 42 ± 3 | 38 ± 5 | 40 ± 4 |
| 15-20 | 1.52 | 21 ± 5 | 25 ± 2 | 23 ± 6 | 0.96 ± 0.2 | 518 ± 19 | 30 ± 3 | 21 ± 4 | 26 ± 3 |
| 20-25 | 1.47 | 10 ± 5 | 29 ± 2 | 22 ± 5 | 0.48 ± 0.2 | 503 ± 19 | 32 ± 3 | 30 ± 3 | 31 ± 3 |
| 25-40 | 1.57 | 20 ± 5 | 27 ± 2 | 26 ± 5 | 0.93 ± 0.2 | 556 ± 20 | 36 ± 3 | 35 ± 4 | 36 ± 3 |

Table B - 38: Activity concentration of ^{238}U , ^{226}Ra , ^{210}Pb , ^{235}U , ^{40}K , ^{228}Ra , ^{228}Th and ^{232}Th (in Bq kg^{-1}) in soil collected from Chirstinovka meadow, Ukraine.

| Depth (cm) | Dry density [g/cm^3] | U-238 [Bq/kg] | Ra-226 [Bq/kg] | Pb-210 [Bq/kg] | U-235 [Bq/kg] | K-40 [Bq/kg] | Ra-228 [Bq/kg] | Th-228 [Bq/kg] | Th-232 [Bq/kg] |
|------------|---------------------------------|---------------|----------------|----------------|---------------|--------------|----------------|----------------|----------------|
| humus soil | 1.41 | 4 ± 7 | 18 ± 2 | 24 ± 9 | 0.2 ± 0.3 | 236 ± 10 | 18 ± 3 | 13.3 ± 1 | 16 ± 2 |
| 0-1 | 1.32 | 2 ± 9 | 19 ± 2 | 40 ± 16 | 0.1 ± 0.4 | 237 ± 10 | 19 ± 3 | 13.8 ± 3 | 16 ± 3 |
| 1-2 | 1.43 | 27 ± 7 | 20 ± 2 | 33 ± 8 | 1.2 ± 0.3 | 267 ± 11 | 24 ± 3 | 20.6 ± 4 | 21 ± 4 |
| 2-3 | 1.41 | - | 18 ± 2 | 23 ± 8 | - | 256 ± 11 | 22 ± 3 | 20.0 ± 3 | 21 ± 3 |
| 3-5 | 1.40 | 14 ± 8 | 17 ± 2 | 6 ± 8 | 0.6 ± 0.4 | 264 ± 11 | 21 ± 3 | 20.4 ± 4 | 21 ± 3 |
| 5-10 | 1.47 | 20 ± 7 | 20 ± 2 | 19 ± 8 | 0.9 ± 0.3 | 251 ± 10 | 21 ± 3 | 18.4 ± 3 | 20 ± 3 |
| 10-15 | 1.44 | 15 ± 7 | 20 ± 2 | 44 ± 8 | 0.7 ± 0.3 | 261 ± 11 | 22 ± 3 | 15.9 ± 1 | 19 ± 2 |
| 15-20 | 1.57 | 6 ± 7 | 19 ± 2 | 38 ± 8 | 0.3 ± 0.3 | 246 ± 10 | 25 ± 3 | 22.0 ± 3 | 19 ± 3 |
| 20-25 | 1.47 | 16 ± 7 | 18 ± 2 | 12 ± 7 | 0.8 ± 0.3 | 241 ± 10 | 20 ± 3 | 14.7 ± 3 | 17 ± 3 |
| 25-40 | 1.74 | 16 ± 4 | 15 ± 1 | 10 ± 4 | 0.7 ± 0.2 | 261 ± 10 | 15 ± 2 | 14.0 ± 2 | 14 ± 2 |

Table B - 39: Activity concentration of ^{238}U , ^{226}Ra , ^{210}Pb , ^{235}U , ^{40}K , ^{228}Ra , ^{228}Th and ^{232}Th (in Bq kg^{-1}) in soil collected from Nove Scharnow 3, Ukraine.

| Depth (cm) | Dry density [g/cm^3] | U-238 [Bq/kg] | Ra-226 [Bq/kg] | Pb-210 [Bq/kg] | U-235 [Bq/kg] | K-40 [Bq/kg] | Ra-228 [Bq/kg] | Th-228 [Bq/kg] | Th-232 [Bq/kg] |
|------------|---------------------------------|---------------|----------------|----------------|---------------|--------------|----------------|----------------|----------------|
| humus soil | 1.49 | | 22 ± 3 | 33 ± 18 | - | 303 ± 12 | 22 ± 10 | 12 ± 4 | 20 ± 9 |
| 0-1 | 1.49 | 7.5 ± 15 | 22 ± 4 | 57 ± 19 | 0.34 ± 0.7 | 344 ± 13 | 18 ± 2 | 13 ± 3 | 14 ± 3 |
| 1-2 | 1.54 | 2.2 ± 13 | 22 ± 3 | 20 ± 15 | 0.10 ± 0.6 | 330 ± 12 | 22 ± 5 | 21 ± 4 | 22 ± 4 |
| 2-3 | 1.55 | - | 19 ± 4 | 10 ± 15 | - | 335 ± 13 | 19 ± 2 | 15 ± 3 | 17 ± 2 |
| 3-5 | 1.81 | - | 13 ± 2 | - | - | 310 ± 12 | 17 ± 5 | 14 ± 3 | 16 ± 4 |
| 5-10 | 1.64 | 9.2 ± 14 | 15 ± 3 | 40 ± 6 | 0.42 ± 0.6 | 308 ± 12 | 21 ± 2 | 20 ± 4 | 20 ± 3 |
| 10-15 | 1.68 | - | 14 ± 2 | 11 ± 9 | - | 294 ± 11 | 20 ± 2 | 14 ± 3 | 16 ± 3 |
| 15-20 | 1.89 | 12.1 ± 4 | 14 ± 1 | 19 ± 6 | 0.56 ± 0.2 | 321 ± 12 | 17 ± 3 | 14 ± 1 | 16 ± 2 |
| 20-25 | 1.76 | 2.9 ± 3 | 14 ± 1 | 30 ± 6 | 0.13 ± 0.1 | 310 ± 12 | 18 ± 3 | 19 ± 3 | 19 ± 3 |
| 25-40 | 1.42 | 5.7 ± 7 | 18 ± 3 | 37 ± 13 | 0.26 ± 0.3 | 308 ± 15 | 24 ± 5 | 21 ± 1 | 23 ± 5 |

Table B - 40: Activity concentration of ^{238}U , ^{226}Ra , ^{210}Pb , ^{235}U , ^{40}K , ^{228}Ra , ^{228}Th and ^{232}Th (in Bq kg^{-1}) in soil collected from Tschigiri 1, Ukraine.

| Depth (cm) | Dry density [g/cm^3] | U-238 [Bq/kg] | Ra-226 [Bq/kg] | Pb-210 [Bq/kg] | U-235 [Bq/kg] | K-40 [Bq/kg] | Ra-228 [Bq/kg] | Th-228 [Bq/kg] | Th-232 [Bq/kg] |
|------------|---------------------------------|---------------|----------------|----------------|---------------|--------------|----------------|----------------|----------------|
| humus soil | 0.36 | - | 10 ± 9 | 438 ± 56 | - | 446 ± 24 | 40 ± 8 | 25 ± 9 | 32 ± 8 |
| 0-1 | 0.60 | 24.4 ± 13 | 17 ± 4 | 137 ± 22 | 1.12 ± 0.6 | 145 ± 8 | 20 ± 3 | 19 ± 2 | 17 ± 3 |
| 1-2 | 0.96 | 17.7 ± 6 | 22 ± 2 | 48 ± 10 | 0.82 ± 0.3 | 199 ± 9 | 17 ± 3 | 19 ± 2 | 18 ± 2 |
| 2-3 | 1.32 | 29.2 ± 5 | 26 ± 2 | 51 ± 9 | 1.35 ± 0.2 | 330 ± 13 | 20 ± 2 | 21 ± 1 | 20 ± 2 |
| 3-5 | 1.44 | 31.6 ± 4 | 27 ± 1 | 51 ± 7 | 1.45 ± 0.2 | 349 ± 13 | 21 ± 2 | 23 ± 1 | 22 ± 2 |
| 5-10 | 1.49 | 34.6 ± 4 | 25 ± 1 | 52 ± 7 | 1.59 ± 0.2 | 355 ± 14 | 23 ± 2 | 19 ± 1 | 22 ± 2 |
| 10-15 | 1.54 | 35.3 ± 4 | 27 ± 1 | 46 ± 6 | 1.63 ± 0.2 | 359 ± 14 | 21 ± 2 | 21 ± 1 | 21 ± 2 |
| 15-20 | 1.55 | 23.9 ± 4 | 28 ± 1 | 52 ± 6 | 1.10 ± 0.2 | 357 ± 13 | 22 ± 2 | 21 ± 1 | 22 ± 2 |
| 20-25 | 1.58 | 29.7 ± 4 | 30 ± 1 | 41 ± 5 | 1.37 ± 0.2 | 362 ± 13 | 22 ± 2 | 21 ± 1 | 22 ± 1 |
| 25-40 | 1.61 | 31.7 ± 4 | 31 ± 1 | 42 ± 5 | 1.46 ± 0.2 | 421 ± 15 | 25 ± 2 | 24 ± 1 | 25 ± 2 |

Table B - 41: Activity concentration of ^{238}U , ^{226}Ra , ^{210}Pb , ^{235}U , ^{40}K , ^{228}Ra , ^{228}Th , and ^{232}Th (in Bq kg^{-1}) in soil collected from Tschigiri 3, Ukraine.

| Depth (cm) | Dry density [g/cm^3] | U-238 [Bq/kg] | Ra-226 [Bq/kg] | Pb-210 [Bq/kg] | U-235 [Bq/kg] | K-40 [Bq/kg] | Ra-228 [Bq/kg] | Th-228 [Bq/kg] | Th-232 [Bq/kg] |
|------------|---------------------------------|---------------|----------------|----------------|---------------|--------------|----------------|----------------|----------------|
| humus soil | 0.77 | - | 13 ± 2 | 30 ± 12 | - | 334 ± 16 | 9 ± 1 | - | - |
| 0-1 | 1.04 | 16.1 ± 8 | 24 ± 3 | 101 ± 18 | 0.74 ± 0.4 | 121 ± 8 | 10 ± 4 | 22 ± 2 | 14 ± 3 |
| 1-2 | 1.34 | - | 16 ± 2 | 49 ± 10 | - | 142 ± 6 | - | 16 ± 2 | 16 ± 2 |
| 2-3 | 1.40 | - | 16 ± 2 | 21 ± 7 | - | 190 ± 8 | - | 20 ± 1 | 20 ± 1 |
| 3-5 | 1.32 | 21.0 ± 4 | 16 ± 2 | 24 ± 6 | 0.97 ± 0.2 | 233 ± 10 | 21 ± 2 | 21 ± 2 | 21 ± 2 |
| 5-10 | 1.51 | 3.2 ± 1 | 19 ± 1 | 5 ± 1 | 0.15 ± 0.1 | 278 ± 12 | 22 ± 2 | 22 ± 1 | 22 ± 1 |
| 10-15 | 1.45 | 8.6 ± 1 | 21 ± 1 | 6 ± 1 | 0.40 ± 0.1 | 235 ± 11 | 26 ± 2 | 21 ± 1 | 23 ± 1 |
| 15-20 | 1.50 | 3.7 ± 1 | 20 ± 1 | 3 ± 1 | 0.17 ± 0.1 | 259 ± 10 | 20 ± 1 | 20 ± 1 | 20 ± 1 |
| 20-25 | 1.73 | 18.8 ± 3 | 25 ± 1 | 80 ± 14 | 0.87 ± 0.1 | 336 ± 13 | 23 ± 1 | 24 ± 1 | 24 ± 1 |
| 25-40 | 1.84 | 11.2 ± 2 | - | - | 0.52 ± 0.1 | 661 ± 24 | - | 30 ± 1 | - |

Table B - 42: Activity concentration of ^{238}U , ^{226}Ra , ^{210}Pb , ^{235}U , ^{40}K , ^{228}Ra , ^{228}Th , and ^{232}Th (in Bq kg^{-1}) in soil collected from Tschigiri Zwintor 1, Ukraine.

| Depth (cm) | Dry density [g/cm^3] | U-238 [Bq/kg] | Ra-226 [Bq/kg] | Pb-210 [Bq/kg] | U-235 [Bq/kg] | K-40 [Bq/kg] | Ra-228 [Bq/kg] | Th-228 [Bq/kg] | Th-232 [Bq/kg] |
|------------|---------------------------------|---------------|----------------|----------------|---------------|--------------|----------------|----------------|----------------|
| humus soil | 0.39 | - | 42 ± 18 | - | - | 414 ± 26 | 22 ± 4 | 12 ± 7 | 17 ± 5 |
| 0-1 | 0.76 | 5.6 ± 10 | 16 ± 4 | 95 ± 17 | 0.26 ± 0.5 | 295 ± 12 | 16 ± 5 | 13 ± 2 | 15 ± 4 |
| 1-2 | 1.28 | 19.9 ± 6 | 12 ± 2 | 89 ± 15 | 0.92 ± 0.3 | 281 ± 11 | 14 ± 1 | 15 ± 1 | 13 ± 2 |
| 2-3 | 1.48 | 21.6 ± 4 | 18 ± 1 | 41 ± 7 | 0.99 ± 0.2 | 337 ± 13 | 16 ± 2 | 16 ± 1 | 16 ± 1 |
| 3-5 | 1.51 | 13.6 ± 4 | 23 ± 1 | 49 ± 8 | 0.63 ± 0.2 | 439 ± 16 | 22 ± 2 | 20 ± 1 | 21 ± 2 |
| 5-10 | 0.00 | 14.5 ± 5 | 20 ± 1 | 59 ± 9 | 0.67 ± 0.2 | 198 ± 8 | 21 ± 2 | 23 ± 1 | 22 ± 1 |
| 10-15 | 1.66 | 19.3 ± 3 | 18 ± 1 | 35 ± 5 | 0.89 ± 0.1 | 429 ± 16 | 19 ± 2 | 18 ± 2 | 18 ± 3 |
| 15-20 | 1.61 | 16.1 ± 3 | 18 ± 1 | 31 ± 5 | 0.74 ± 0.1 | 371 ± 14 | 22 ± 2 | 16 ± 2 | 19 ± 2 |
| 20-25 | 1.61 | 20.4 ± 3 | 18 ± 1 | 34 ± 5 | 0.94 ± 0.1 | 337 ± 13 | 17 ± 2 | 19 ± 2 | 18 ± 2 |
| 25-40 | 1.96 | 14.2 ± 3 | 20 ± 1 | 27 ± 4 | 0.65 ± 0.1 | 457 ± 17 | 21 ± 2 | 19 ± 2 | 20 ± 2 |

Table B - 43: Activity concentration of ^{238}U , ^{226}Ra , ^{210}Pb , ^{235}U , ^{40}K , ^{228}Ra , ^{228}Th , and ^{232}Th (in Bq kg^{-1}) in soil collected from Woronewo 1, Ukraine.

| Depth (cm) | Dry density [g/cm^3] | U-238 [Bq/kg] | Ra-226 [Bq/kg] | Pb-210 [Bq/kg] | U-235 [Bq/kg] | K-40 [Bq/kg] | Ra-228 u [Bq/kg] | Th-228 ±u [Bq/kg] | Th-232 ±u [Bq/kg] |
|------------|---------------------------------|---------------|----------------|----------------|---------------|--------------|------------------|-------------------|-------------------|
| humus soil | 0.70 | 13.0 ± 8 | 14 ± 3 | 74 ± 14 | 0.60 ± 0.4 | 390 ± 16 | 19 ± 4 | 18 ± 2 | 19 ± 3 |
| 0-1 | 1.18 | 15.2 ± 8 | 15 ± 2 | 79 ± 16 | 0.70 ± 0.4 | 407 ± 16 | - | 19 ± 2 | 19 ± 2 |
| 1-2 | 1.01 | 10.3 ± 8 | 12 ± 3 | 68 ± 15 | 0.47 ± 0.3 | 387 ± 15 | 19 ± 3 | 15 ± 2 | 17 ± 2 |
| 2-3 | 1.08 | 18.1 ± 9 | 24 ± 3 | 70 ± 17 | 0.83 ± 0.4 | 412 ± 16 | 18 ± 4 | 15 ± 2 | 17 ± 3 |
| 3-5 | 1.41 | 6.1 ± 7 | 22 ± 2 | 42 ± 14 | 0.28 ± 0.3 | 439 ± 16 | 17 ± 3 | 16 ± 2 | 16 ± 2 |
| 5-10 | 1.62 | 15.9 ± 5 | 20 ± 1 | 35 ± 8 | 0.73 ± 0.2 | 436 ± 16 | 20 ± 2 | 19 ± 1 | 20 ± 1 |
| 10-15 | 1.66 | 26.9 ± 4 | 20 ± 1 | 31 ± 5 | 1.24 ± 0.2 | 429 ± 16 | 22 ± 2 | 19 ± 1 | 20 ± 1 |
| 15-20 | 1.70 | 21.1 ± 3 | 23 ± 1 | 26 ± 5 | 0.97 ± 0.2 | 405 ± 15 | 21 ± 1 | 21 ± 1 | 21 ± 1 |
| 20-25 | 1.74 | 20.5 ± 3 | 21 ± 1 | 37 ± 6 | 0.94 ± 0.1 | 434 ± 16 | 21 ± 1 | 21 ± 1 | 21 ± 1 |
| 25-40 | 1.79 | 21.5 ± 3 | 20 ± 1 | 20 ± 5 | 0.99 ± 0.1 | 424 ± 15 | 21 ± 2 | 18 ± 1 | 19 ± 1 |

Table B - 44: Activity concentration of ^{238}U , ^{226}Ra , ^{210}Pb , ^{235}U , ^{40}K , ^{228}Ra , ^{228}Th , and ^{232}Th (in Bq kg^{-1}) in soil collected from Woronewo 2, Ukraine.

| Depth (cm) | Dry density [g/cm^3] | U-238 [Bq/kg] | Ra-226 [Bq/kg] | Pb-210 [Bq/kg] | U-235 [Bq/kg] | K-40 [Bq/kg] | Ra-228 [Bq/kg] | Th-228 [Bq/kg] | Th-232 [Bq/kg] |
|------------|---------------------------------|---------------|----------------|----------------|---------------|--------------|----------------|----------------|----------------|
| humus soil | 0.89 | 5.7 ± 3 | 3 ± 1 | 48 ± 7 | 0.26 ± 0.1 | 100 ± 4 | 2 ± 1 | 3 ± 1 | 3 ± 1 |
| 0-1 | 1.28 | 25.4 ± 7 | 18 ± 2 | 9 ± 15 | 1.17 ± 0.3 | 198 ± 9 | 18 ± 5 | 17 ± 2 | 17 ± 3 |
| 1-2 | 1.42 | 5.5 ± 1 | 18 ± 1 | 6 ± 1 | 0.26 ± 0.1 | 232 ± 10 | 20 ± 2 | 20 ± 2 | 20 ± 2 |
| 2-3 | 1.42 | 6.7 ± 1 | 17 ± 1 | 5 ± 1 | 0.31 ± 0.1 | 186 ± 9 | 24 ± 3 | 22 ± 2 | 21 ± 2 |
| 3-5 | 1.55 | 4.7 ± 1 | 15 ± 1 | 4 ± 1 | 0.21 ± 0.1 | 224 ± 10 | 19 ± 2 | 18 ± 1 | 19 ± 1 |
| 5-10 | 1.64 | 5.4 ± 1 | 17 ± 1 | 4 ± 1 | 0.25 ± 0.1 | 239 ± 10 | 20 ± 1 | 19 ± 1 | 19 ± 1 |
| 10-15 | 1.74 | 16.6 ± 2 | 19 ± 1 | 121 ± 14 | 0.77 ± 0.1 | 212 ± 9 | 25 ± 2 | 25 ± 1 | 25 ± 1 |
| 15-20 | 1.77 | 19.9 ± 2 | 19 ± 1 | 109 ± 12 | 0.92 ± 0.1 | 436 ± 17 | 27 ± 2 | 22 ± 1 | 25 ± 2 |
| 20-25 | 1.83 | 19.9 ± 2 | 17 ± 1 | 99 ± 13 | 0.92 ± 0.1 | 383 ± 15 | 25 ± 2 | 23 ± 1 | 24 ± 1 |
| 25-40 | 1.88 | 14.3 ± 2 | 20 ± 1 | 100 ± 13 | 0.66 ± 0.1 | 295 ± 12 | 27 ± 2 | 25 ± 1 | 26 ± 2 |

Table B - 45: Activity concentration of ^{238}U , ^{226}Ra , ^{210}Pb , ^{235}U , ^{40}K , ^{228}Ra , ^{228}Th , and ^{232}Th (in Bq kg^{-1}) in soil collected from Woronewo 3, Ukraine.

| Depth (cm) | Dry density [g/cm^3] | U-238 [Bq/kg] | Ra-226 [Bq/kg] | Pb-210 [Bq/kg] | U-235 [Bq/kg] | K-40 [Bq/kg] | Ra-228 [Bq/kg] | Th-228 [Bq/kg] | Th-232 [Bq/kg] |
|------------|---------------------------------|---------------|----------------|----------------|---------------|--------------|----------------|----------------|----------------|
| humus soil | 0.57 | 43.3 ± 16 | 32 ± 5 | 189 ± 23 | 2.00 ± 0.7 | 288 ± 20 | 49 ± 17 | 44 ± 5 | 46 ± 9 |
| 0-1 | 0.91 | 26.2 ± 8 | 20 ± 3 | 159 ± 19 | 1.21 ± 0.4 | 114 ± 6 | 12 ± 1 | 22 ± 2 | 18 ± 2 |
| 1-2 | 0.95 | 19.2 ± 8 | 23 ± 3 | 129 ± 17 | 0.89 ± 0.4 | 160 ± 8 | 24 ± 4 | 26 ± 2 | 25 ± 3 |
| 2-3 | 1.27 | - | 14 ± 5 | 582 ± 79 | - | 564 ± 31 | 33 ± 5 | 44 ± 5 | 40 ± 5 |
| 3-5 | 1.18 | 25.9 ± 5 | 21 ± 2 | 66 ± 10 | 1.19 ± 0.2 | 190 ± 9 | 21 ± 4 | 21 ± 1 | 21 ± 3 |
| 5-10 | 1.60 | 6.2 ± 1 | 18 ± 1 | 5 ± 1 | 0.29 ± 0.1 | 237 ± 10 | 20 ± 2 | 19 ± 1 | 19 ± 2 |
| 10-15 | 1.58 | 6.3 ± 1 | 19 ± 1 | 4 ± 0.5 | 0.29 ± 0.1 | 298 ± 12 | 22 ± 2 | 20 ± 1 | 21 ± 1 |
| 15-20 | 1.68 | 4.8 ± 1 | 17 ± 1 | 3 ± 0.3 | 0.22 ± 0.1 | 134 ± 7 | 16 ± 2 | 18 ± 1 | 17 ± 1 |
| 20-25 | 1.64 | 5.9 ± 1 | 18 ± 1 | 4 ± 0.4 | 0.27 ± 0.1 | 133 ± 7 | 20 ± 2 | 19 ± 1 | 20 ± 1 |
| 25-40 | 1.84 | 17.3 ± 2 | 19 ± 1 | 101 ± 14 | 0.80 ± 0.1 | 382 ± 15 | 24 ± 2 | 22 ± 1 | 23 ± 1 |

Table B - 46: Activity concentration of ^{238}U , ^{226}Ra , ^{210}Pb , ^{235}U , ^{40}K , ^{228}Ra , ^{228}Th , and ^{232}Th (in Bq kg^{-1}) in soil collected from Woronewo 4, Ukraine.

| Depth (cm) | Dry density [g/cm^3] | U-238 [Bq/kg] | Ra-226 [Bq/kg] | Pb-210 [Bq/kg] | U-235 [Bq/kg] | K-40 [Bq/kg] | Ra-228 [Bq/kg] | Th-228 [Bq/kg] | Th-232 [Bq/kg] |
|------------|---------------------------------|---------------|----------------|----------------|---------------|--------------|----------------|----------------|----------------|
| humus soil | 0.38 | 3.2 ± 6 | - | 125 ± 13 | 0.15 ± 0.3 | 120 ± 7 | - | - | - |
| 0-1 | 0.76 | - | 10 ± 20 | 1044 ± 66 | - | 264 ± 11 | 16 ± 1 | - | - |
| 1-2 | 0.67 | 8.6 ± 9 | 4 ± 2 | 105 ± 16 | 0.40 ± 0.4 | 307 ± 12 | 16 ± 2 | 8 ± 2 | 12 ± 2 |
| 2-3 | - | 10.2 ± 8 | 16 ± 2 | 133 ± 18 | 0.47 ± 0.4 | 379 ± 15 | 20 ± 2 | 15 ± 2 | 17 ± 2 |
| 3-5 | 1.00 | 15.2 ± 5 | 15 ± 1 | 66 ± 11 | 0.70 ± 0.2 | 302 ± 12 | 16 ± 2 | 12 ± 1 | 14 ± 1 |
| 5-10 | 1.36 | 30.6 ± 5 | 23 ± 2 | 55 ± 8 | 1.41 ± 0.2 | 423 ± 16 | 21 ± 2 | 19 ± 1 | 20 ± 2 |
| 10-15 | 1.58 | 17.0 ± 3 | 19 ± 35 | 28 ± 5 | 0.78 ± 0.1 | 411 ± 15 | 70 ± 11 | 18 ± 2 | 19 ± 2 |
| 15-20 | 1.54 | 20.8 ± 3 | 19 ± 1 | 22 ± 5 | 0.96 ± 0.1 | 405 ± 15 | 20 ± 1 | 19 ± 1 | 19 ± 1 |
| 20-25 | 1.63 | 18.7 ± 3 | 19 ± 1 | 17 ± 5 | 0.86 ± 0.1 | 417 ± 15 | 19 ± 2 | 17 ± 1 | 18 ± 1 |
| 25-40 | 1.81 | 12.8 ± 3 | 17 ± 1 | 27 ± 5 | 0.59 ± 0.1 | 365 ± 13 | 16 ± 1 | 16 ± 1 | 16 ± 1 |

Table B - 47: Activity concentration of ^{238}U , ^{226}Ra , ^{210}Pb , ^{235}U , ^{40}K , ^{228}Ra , ^{228}Th , and ^{232}Th (in Bq kg^{-1}) in soil collected from Woronewo 5, Ukraine.

| Depth (cm) | Dry density [g/cm^3] | U-238 [Bq/kg] | Ra-226 [Bq/kg] | Pb-210 [Bq/kg] | U-235 [Bq/kg] | K-40 [Bq/kg] | Ra-228 [Bq/kg] | Th-228 [Bq/kg] | Th-232 [Bq/kg] |
|------------|---------------------------------|---------------|----------------|----------------|---------------|--------------|----------------|----------------|----------------|
| humus soil | 0.34 | - | - | 434 ± 91 | - | 193 ± 14 | - | - | - |
| 0-1 | 0.48 | - | 18 ± 5 | 288 ± 56 | - | 188 ± 10 | 11 ± 3 | 6 ± 4 | 8 ± 4 |
| 1-2 | 1.02 | - | 21 ± 2 | 106 ± 15 | - | 306 ± 13 | 22 ± 3 | 16 ± 2 | 21 ± 3 |
| 2-3 | 1.05 | 17.1 ± 8 | 23 ± 2 | 51 ± 13 | 0.79 ± 0.4 | 332 ± 14 | 20 ± 3 | 21 ± 2 | 20 ± 3 |
| 3-5 | 1.35 | 6.1 ± 6 | 27 ± 2 | 49 ± 8 | 0.28 ± 0.3 | 361 ± 14 | 26 ± 3 | 24 ± 2 | 25 ± 2 |
| 5-10 | 1.37 | 22.9 ± 5 | 24 ± 2 | 22 ± 6 | 1.06 ± 0.2 | 373 ± 15 | 25 ± 2 | 24 ± 1 | 24 ± 2 |
| 10-15 | 1.48 | 6.0 ± 5 | 25 ± 2 | 23 ± 5 | 0.28 ± 0.2 | 370 ± 14 | 29 ± 2 | 24 ± 1 | 27 ± 2 |
| 15-20 | 1.57 | 13.7 ± 5 | 23 ± 2 | 28 ± 5 | 0.63 ± 0.2 | 394 ± 15 | 27 ± 2 | 22 ± 1 | 27 ± 2 |
| 20-25 | 1.70 | 7.1 ± 4 | 22 ± 1 | 22 ± 5 | 0.33 ± 0.2 | 376 ± 14 | 21 ± 2 | 22 ± 1 | 21 ± 2 |
| 25-40 | 1.74 | 14.3 ± 4 | 22 ± 2 | 23 ± 6 | 0.66 ± 0.2 | 412 ± 15 | 25 ± 2 | 24 ± 1 | 25 ± 2 |

Table B - 48: Activity concentration of ^{238}U , ^{226}Ra , ^{210}Pb , ^{235}U , ^{40}K , ^{228}Ra , ^{228}Th , and ^{232}Th (in Bq kg^{-1}) in soil collected from Woronewo 6, Ukraine.

| Depth (cm) | Dry density [g/cm^3] | U-238 [Bq/kg] | Ra-226 [Bq/kg] | Pb-210 [Bq/kg] | U-235 [Bq/kg] | K-40 [Bq/kg] | Ra-228 [Bq/kg] | Th-228 [Bq/kg] | Th-232 [Bq/kg] |
|------------|---------------------------------|---------------|----------------|----------------|---------------|--------------|----------------|----------------|----------------|
| humus soil | 0.91 | - | 29 ± 3 | 58 ± 13 | - | 584.0 ± 26 | - | 35 ± 3 | 30 ± 3 |
| 0-1 | 0.98 | - | 15 ± 2 | - | - | 215 ± 10 | 19 ± 6 | 13 ± 2 | 13 ± 2 |
| 1-2 | 1.09 | - | 7 ± 1 | 40 ± 13 | - | 198 ± 8 | 7 ± 1 | 10 ± 1 | 12 ± 2 |
| 2-3 | 1.08 | 39.9 ± 4 | 37 ± 2 | 59 ± 7 | 1.84 ± 0.2 | 447 ± 17 | 31 ± 2 | 29 ± 1 | 30 ± 2 |
| 3-5 | 1.39 | 5.3 ± 2 | 15 ± 2 | 5 ± 1 | 0.24 ± 0.1 | 125 ± 7 | 9 ± 3 | 17 ± 2 | 13 ± 2 |
| 5-10 | 1.55 | 3.3 ± 1 | 16 ± 1 | 6 ± 1 | 0.15 ± 0.05 | 424 ± 16 | 13 ± 2 | 15 ± 1 | 14 ± 1 |
| 10-15 | 1.56 | 5.3 ± 1 | 17 ± 1 | 5 ± 0.5 | 0.24 ± 0.03 | 159 ± 7 | 18 ± 1 | 16 ± 1 | 17 ± 1 |
| 15-20 | 1.65 | 5.4 ± 1 | 16 ± 1 | 4 ± 0.5 | 0.25 ± 0.03 | 77 ± 5 | 21 ± 1 | 16 ± 1 | 18 ± 1 |
| 20-25 | 1.74 | 17.6 ± 3 | 19 ± 1 | 102 ± 14 | 0.81 ± 0.1 | 417 ± 16 | 21 ± 2 | 22 ± 1 | 22 ± 1 |
| 25-40 | 1.86 | 17.7 ± 2 | 19 ± 1 | 108 ± 14 | 0.82 ± 0.1 | 435 ± 17 | 25 ± 2 | 21 ± 1 | 21 ± 1 |

Table B - 49: Activity concentration of ^{238}U , ^{226}Ra , ^{210}Pb , ^{235}U , ^{40}K , ^{228}Ra , ^{228}Th , and ^{232}Th (in Bq kg^{-1}) in soil collected from Woronewo 7, Ukraine.

| Depth (cm) | Dry density [g/cm^3] | U-238 [Bq/kg] | Ra-226 [Bq/kg] | Pb-210 [Bq/kg] | U-235 [Bq/kg] | K-40 [Bq/kg] | Ra-228 [Bq/kg] | Th-228 [Bq/kg] | Th-232 [Bq/kg] |
|------------|---------------------------------|---------------|----------------|----------------|---------------|--------------|----------------|----------------|----------------|
| humus soil | 1.31 | 11.9 ± 7 | 21 ± 2 | 50 ± 9 | 0.55 ± 0.3 | 392 ± 15 | 28 ± 3 | 26 ± 4 | 27 ± 3 |
| 0-1 | 1.41 | 18.5 ± 7 | 26 ± 2 | 15 ± 7 | 0.85 ± 0.3 | 400 ± 16 | 27 ± 3 | 25 ± 4 | 26 ± 4 |
| 1-2 | 1.67 | 9.6 ± 4 | 31 ± 3 | 18 ± 6 | 0.44 ± 0.2 | 352 ± 13 | 21 ± 2 | 19 ± 2 | 20 ± 2 |
| 2-3 | 1.81 | 5.0 ± 3 | 19 ± 1 | 16 ± 5 | 0.23 ± 0.1 | 343 ± 13 | 21 ± 2 | 20 ± 2 | 20 ± 2 |
| 3-5 | 1.85 | 11.4 ± 4 | 18 ± 1 | 26 ± 6 | 0.52 ± 0.2 | 342 ± 13 | 19 ± 2 | 19 ± 3 | 19 ± 2 |
| 5-10 | 1.73 | 9.0 ± 4 | 18 ± 2 | 19 ± 6 | 0.41 ± 0.2 | 348 ± 13 | 23 ± 2 | 20 ± 1 | 22 ± 2 |
| 10-15 | 1.73 | 14.4 ± 5 | 26 ± 3 | 29 ± 9 | 0.67 ± 0.2 | 327 ± 13 | 18 ± 2 | 20 ± 3 | 23 ± 3 |
| 15-20 | 1.86 | 14.5 ± 4 | 16 ± 1 | 16 ± 7 | 0.67 ± 0.2 | 313 ± 12 | 19 ± 2 | 18 ± 3 | 18 ± 3 |
| 20-25 | 2.02 | 5.4 ± 3 | 14 ± 1 | 15 ± 5 | 0.25 ± 0.1 | 276 ± 10 | 14 ± 2 | 14 ± 1 | 16 ± 2 |
| 25-40 | 2.11 | 1.7 ± 2 | 11 ± 1 | 5 ± 4 | 0.08 ± 0.1 | 232 ± 9 | 12 ± 1 | 13 ± 1 | 12 ± 1 |

Table B - 50: Activity concentration of ^{238}U , ^{226}Ra , ^{210}Pb , ^{235}U , ^{40}K , ^{228}Ra , ^{228}Th , and ^{232}Th (in Bq kg^{-1}) in soil collected from Baraschewka 1, Ukraine.

| Depth (cm) | Dry density [g/cm^3] | U-238 [Bq/kg] | Ra-226 [Bq/kg] | Pb-210 [Bq/kg] | U-235 [Bq/kg] | K-40 [Bq/kg] | Ra-228 [Bq/kg] | Th-228 [Bq/kg] | Th-232 [Bq/kg] |
|------------|---------------------------------|---------------|----------------|----------------|---------------|--------------|----------------|----------------|----------------|
| humus soil | 0.23 | - | 21 ± 4 | 257 ± 32 | - | 195 ± 18 | 16 ± 7 | 11 ± 3 | 13 ± 4 |
| 0-1 | 0.63 | 9.5 ± 8 | 11 ± 2 | - | 0.44 ± 0.4 | 104 ± 8 | 12 ± 3 | 7 ± 1 | 9 ± 2 |
| 1-2 | 0.84 | 14.2 ± 5 | 13 ± 2 | 110 ± 13 | 0.66 ± 0.3 | 94 ± 7 | 12 ± 3 | 10 ± 1 | 11 ± 2 |
| 2-3 | 1.02 | 5.6 ± 5 | 15 ± 1 | 94 ± 12 | 0.26 ± 0.2 | 96 ± 6 | 10 ± 1 | 10 ± 1 | 13 ± 2 |
| 3-5 | 1.10 | 2.7 ± 4 | 11 ± 2 | 72 ± 9 | 0.13 ± 0.2 | 84 ± 6 | 13 ± 2 | 9 ± 1 | 11 ± 2 |
| 5-10 | 1.18 | - | 13 ± 1 | 23 ± 6 | - | 91 ± 7 | 10 ± 2 | 12 ± 1 | 11 ± 2 |
| 10-15 | 1.24 | 3.3 ± 4 | 11 ± 1 | 19 ± 5 | 0.15 ± 0.2 | 76 ± 5 | 10 ± 2 | 8 ± 1 | 9 ± 2 |
| 15-20 | 1.25 | 3.3 ± 4 | 12 ± 1 | 16 ± 5 | 0.15 ± 0.2 | 56 ± 4 | 11 ± 2 | 8 ± 1 | 10 ± 1 |
| 20-25 | 1.48 | 0.6 ± 5 | 7 ± 1 | 1 ± 5 | 0.03 ± 0.2 | 78 ± 5 | 8 ± 2 | 7 ± 1 | 8 ± 1 |
| 25-40 | 1.81 | - | 7 ± 1 | 10 ± 4 | - | 68 ± 5 | 6 ± 2 | 7 ± 1 | 9 ± 1 |

Table B - 51: Activity concentration of ^{238}U , ^{226}Ra , ^{210}Pb , ^{235}U , ^{40}K , ^{228}Ra , ^{228}Th , and ^{232}Th (in Bq kg^{-1}) in soil collected from Oserjaka 2, Ukraine.

| Depth (cm) | Dry density [g/cm^3] | U-238 [Bq/kg] | Ra-226 [Bq/kg] | Pb-210 [Bq/kg] | U-235 [Bq/kg] | K-40 [Bq/kg] | Ra-228 [Bq/kg] | Th-228 [Bq/kg] | Th-232 [Bq/kg] |
|------------|---------------------------------|---------------|----------------|----------------|---------------|--------------|----------------|----------------|----------------|
| humus soil | 1.00 | 36 ± 4 | 21 ± 1 | 53 ± 5 | 1.7 ± 0.2 | 298 ± 15 | 23 ± 2 | 24 ± 1 | 24 ± 2 |
| 0-1 | 1.23 | 39 ± 4 | 29 ± 2 | 112 ± 9 | 1.8 ± 0.2 | 462 ± 23 | 41 ± 3 | 34 ± 2 | 39 ± 3 |
| 1-2 | 1.01 | 62 ± 4 | 26 ± 1 | 65 ± 6 | 2.8 ± 0.2 | 506 ± 20 | 33 ± 2 | 29 ± 1 | 32 ± 2 |
| 2-3 | 1.25 | 34 ± 3 | 17 ± 1 | 68 ± 6 | 1.6 ± 0.1 | 198 ± 8 | 20 ± 1 | 22 ± 1 | 21 ± 1 |
| 3-5 | 1.36 | 32 ± 3 | 16 ± 1 | 12 ± 2 | 1.5 ± 0.1 | 214 ± 8 | 19 ± 1 | 22 ± 1 | 21 ± 1 |
| 5-10 | 1.36 | 31 ± 3 | 18 ± 1 | 33 ± 4 | 1.4 ± 0.1 | 190 ± 8 | 24 ± 1 | 25 ± 1 | 25 ± 1 |
| 10-15 | 1.52 | 42 ± 4 | 23 ± 1 | 31 ± 5 | 1.9 ± 0.2 | 221 ± 9 | 25 ± 2 | 26 ± 1 | 26 ± 1 |
| 15-20 | 1.44 | 43 ± 4 | 28 ± 1 | 53 ± 6 | 2.0 ± 0.2 | 238 ± 10 | 39 ± 2 | 37 ± 2 | 37 ± 2 |
| 20-25 | 1.40 | 20 ± 2 | 23 ± 1 | 23 ± 2 | 0.9 ± 0.1 | 443 ± 17 | 30 ± 2 | 29 ± 1 | 30 ± 2 |
| 25-40 | 1.39 | 47 ± 4 | 26 ± 1 | 36 ± 5 | 2.2 ± 0.2 | 368 ± 18 | 27 ± 2 | 29 ± 1 | 28 ± 2 |

Table B - 52: Activity concentration of ^{238}U , ^{226}Ra , ^{210}Pb , ^{235}U , ^{40}K , ^{228}Ra , ^{228}Th , and ^{232}Th (in Bq kg^{-1}) in soil collected from Oserjanka 3, Ukraine.

| Depth (cm) | Dry density [g/cm^3] | U-238 [Bq/kg] | Ra-226 [Bq/kg] | Pb-210 [Bq/kg] | U-235 [Bq/kg] | K-40 [Bq/kg] | Ra-228 [Bq/kg] | Th-228 [Bq/kg] | Th-232 [Bq/kg] |
|------------|---------------------------------|---------------|----------------|----------------|---------------|--------------|----------------|----------------|----------------|
| humus soil | 0.72 | 38 ± 4 | 19 ± 1 | 101 ± 8 | 1.8 ± 0.2 | 378 ± 15 | 21 ± 2 | 18 ± 1 | 20 ± 2 |
| 0-1 | 1.02 | 59 ± 5 | 21 ± 1 | 52 ± 8 | 2.7 ± 0.2 | 455 ± 17 | 28 ± 2 | 23 ± 1 | 26 ± 2 |
| 1-2 | 1.09 | 47 ± 5 | 21 ± 1 | 91 ± 10 | 2.2 ± 0.2 | 340 ± 14 | 28 ± 2 | 27 ± 3 | 28 ± 3 |
| 2-3 | 1.19 | 62 ± 5 | 22 ± 1 | 54 ± 7 | 2.9 ± 0.2 | 497 ± 19 | 29 ± 2 | 24 ± 1 | 27 ± 2 |
| 3-5 | 1.13 | 43 ± 4 | 20 ± 1 | 47 ± 8 | 2.0 ± 0.2 | 356 ± 13 | 26 ± 2 | 22 ± 1 | 24 ± 1 |
| 5-10 | 0.96 | 61 ± 4 | 19 ± 1 | 57 ± 9 | 2.8 ± 0.2 | 330 ± 13 | 19 ± 2 | 22 ± 1 | 20 ± 2 |
| 10-15 | 0.94 | 55 ± 4 | 17 ± 1 | 37 ± 6 | 2.6 ± 0.2 | 378 ± 15 | 25 ± 2 | 22 ± 3 | 24 ± 2 |
| 15-20 | 0.92 | 63 ± 5 | 21 ± 1 | 61 ± 10 | 2.9 ± 0.2 | 157 ± 7 | 30 ± 2 | 22 ± 1 | 26 ± 2 |
| 20-25 | 0.94 | 58 ± 4 | 23 ± 1 | 71 ± 8 | 2.7 ± 0.2 | 362 ± 14 | 22 ± 2 | 23 ± 2 | 22 ± 2 |
| 25-40 | 0.53 | 63 ± 8 | 43 ± 2 | 68 ± 8 | 2.9 ± 0.4 | 567 ± 24 | 66 ± 5 | 54 ± 3 | 61 ± 4 |

Table B - 53: Activity concentration of ^{238}U , ^{226}Ra , ^{210}Pb , ^{235}U , ^{40}K , ^{228}Ra , ^{228}Th , and ^{232}Th (in Bq kg^{-1}) in soil collected from Dawidowka 1, Ukraine.

| Depth (cm) | Dry density [g/cm^3] | U-238 [Bq/kg] | Ra-226 [Bq/kg] | Pb-210 [Bq/kg] | U-235 [Bq/kg] | K-40 [Bq/kg] | Ra-228 [Bq/kg] | Th-228 [Bq/kg] | Th-232 [Bq/kg] |
|------------|---------------------------------|---------------|----------------|----------------|---------------|--------------|----------------|----------------|----------------|
| humus soil | 0.7 | 35 ± 9 | 43 ± 3 | 195 ± 17 | 1.6 ± 0.4 | 357 ± 17 | 42 ± 4 | 44 ± 2 | 47 ± 4 |
| 0-1 | 1.1 | 26 ± 7 | 43 ± 3 | 103 ± 12 | 1.2 ± 0.3 | 277 ± 12 | 34 ± 3 | 36 ± 4 | 35 ± 4 |
| 1-2 | 1.1 | 50 ± 7 | 40 ± 4 | 135 ± 14 | 2.3 ± 0.3 | 370 ± 16 | 40 ± 4 | 41 ± 4 | 42 ± 5 |
| 2-3 | 1.1 | 45 ± 7 | 40 ± 4 | 109 ± 13 | 2.1 ± 0.3 | 351 ± 15 | 42 ± 5 | 38 ± 4 | 40 ± 5 |
| 3-5 | 1.3 | 19 ± 6 | 31 ± 4 | 69 ± 10 | 0.9 ± 0.3 | 279 ± 12 | 30 ± 4 | 31 ± 5 | 32 ± 4 |
| 5-10 | 1.2 | 28 ± 5 | 30 ± 2 | 28 ± 5 | 1.3 ± 0.2 | 260 ± 11 | 29 ± 3 | 28 ± 4 | 28 ± 4 |
| 10-15 | 1.4 | 38 ± 6 | 32 ± 4 | 43 ± 6 | 1.8 ± 0.3 | 306 ± 12 | 33 ± 4 | 32 ± 4 | 32 ± 4 |
| 15-20 | 1.2 | 17 ± 4 | 36 ± 2 | 24 ± 5 | 0.8 ± 0.2 | 289 ± 12 | 35 ± 4 | 32 ± 4 | 33 ± 4 |
| 20-25 | 1.4 | 37 ± 7 | 50 ± 3 | 73 ± 10 | 1.7 ± 0.3 | 428 ± 17 | 51 ± 3 | 48 ± 6 | 50 ± 5 |
| 25-40 | 1.1 | 39 ± 8 | 50 ± 6 | 55 ± 11 | 1.8 ± 0.4 | 356 ± 17 | 50 ± 7 | 49 ± 5 | 49 ± 6 |

Table B - 54: Activity concentration of ^{238}U , ^{226}Ra , ^{210}Pb , ^{235}U , ^{40}K , ^{228}Ra , ^{228}Th , and ^{232}Th (in Bq kg^{-1}) in soil collected from Lewkow 1, Ukraine.

| Depth (cm) | Dry density [g/cm^3] | U-238 [Bq/kg] | Ra-226 [Bq/kg] | Pb-210 [Bq/kg] | U-235 [Bq/kg] | K-40 [Bq/kg] | Ra-228 [Bq/kg] | Th-228 [Bq/kg] | Th-232 [Bq/kg] |
|------------|---------------------------------|---------------|----------------|----------------|---------------|--------------|----------------|----------------|----------------|
| 0-1 | 0.8 | 113 ± 6 | 48 ± 2 | 109 ± 9 | 5.2 ± 0.3 | - | 17 ± 2 | 20 ± 1 | 19 ± 2 |
| 1-2 | 0.9 | 140 ± 8 | 78 ± 3 | 184 ± 15 | 6.4 ± 0.3 | 256 ± 14 | 24 ± 3 | 28 ± 2 | 26 ± 2 |
| 2-3 | 1.0 | 140 ± 7 | 83 ± 3 | 171 ± 13 | 6.5 ± 0.3 | 264 ± 14 | 32 ± 3 | 30 ± 2 | 31 ± 2 |
| 3-5 | 1.0 | 130 ± 7 | 84 ± 3 | 146 ± 12 | 6.0 ± 0.3 | 300 ± 14 | 41 ± 3 | 31 ± 1 | 36 ± 2 |
| 5-10 | 1.1 | 228 ± 11 | 86 ± 3 | 181 ± 14 | 10.5 ± 0.5 | 275 ± 14 | 26 ± 2 | 25 ± 1 | 26 ± 2 |
| 10-15 | 1.0 | 30 ± 4 | - | 11 ± 5 | 1.4 ± 0.2 | 153 ± 8 | - | 17 ± 1 | - |
| 15-20 | 1.2 | 69 ± 5 | 44 ± 2 | 69 ± 5 | 3.2 ± 0.2 | 228 ± 11 | - | 18 ± 1 | 20 ± 1 |
| 20-25 | 1.2 | 51 ± 4 | 71 ± 3 | 39 ± 7 | 2.4 ± 0.2 | 292 ± 14 | 38 ± 3 | 35 ± 2 | 37 ± 2 |
| 25-40 | 1.3 | 38 ± 4 | 49 ± 2 | 18 ± 6 | 1.8 ± 0.2 | 279 ± 12 | 24 ± 2 | 33 ± 1 | 30 ± 2 |

Table B - 55: Activity concentration of ^{238}U , ^{226}Ra , ^{210}Pb , ^{235}U , ^{40}K , ^{228}Ra , ^{228}Th , and ^{232}Th (in Bq kg^{-1}) in soil collected from Lewkow 2, Ukraine.

| Depth (cm) | Dry density [g/cm^3] | U-238 [Bq/kg] | Ra-226 [Bq/kg] | Pb-210 [Bq/kg] | U-235 [Bq/kg] | K-40 [Bq/kg] | Ra-228 [Bq/kg] | Th-228 [Bq/kg] | Th-232 [Bq/kg] |
|------------|---------------------------------|---------------|----------------|----------------|---------------|--------------|----------------|----------------|----------------|
| humus soil | 1.1 | 27 ± 4 | 27 ± 1 | 98 ± 8 | 1.3 ± 0.2 | 276 ± 11 | 19 ± 1 | 16 ± 1 | 18 ± 1 |
| 0-1 | - | 35 ± 4 | 32 ± 2 | 98 ± 9 | 1.6 ± 0.2 | 322 ± 12 | 21 ± 2 | 18 ± 1 | 19 ± 1 |
| 1-2 | 1.2 | - | - | - | - | 323 ± 12 | - | - | - |
| 2-3 | 1.3 | 31 ± 4 | 29 ± 1 | 90 ± 8 | 1.4 ± 0.2 | - | 25 ± 2 | 18 ± 1 | 21 ± 1 |
| 3-5 | - | - | - | - | - | - | - | - | - |
| 5-10 | 1.2 | 35 ± 4 | 31 ± 1 | 66 ± 8 | 1.6 ± 0.2 | 245 ± 9 | 20 ± 2 | 19 ± 1 | 19 ± 1 |
| 10-15 | - | - | - | - | - | - | - | - | - |
| 15-20 | 1.5 | 33 ± 4 | 42 ± 2 | 63 ± 7 | 1.5 ± 0.2 | 388 ± 15 | 26 ± 2 | 25 ± 1 | 25 ± 1 |
| 20-25 | 1.5 | 36 ± 4 | 33 ± 2 | 60 ± 8 | 1.7 ± 0.2 | 406 ± 15 | 24 ± 2 | 22 ± 2 | 23 ± 2 |
| 25-40 | - | - | - | - | - | - | - | - | - |

Elemental correlation in soil samples from Lower Saxony, North Germany.

Table B - 56: Vestrup

| Depth (cm) | Dry density [g/cm^3] | $^{238}\text{U}/^{40}\text{K}$ | $^{232}\text{Th}/^{40}\text{K}$ | $^{232}\text{Th}/^{238}\text{U}$ | $^{210}\text{Pb}/^{226}\text{Ra}$ | $^{226}\text{Ra}/^{238}\text{U}$ |
|------------|---------------------------------|--------------------------------|---------------------------------|----------------------------------|-----------------------------------|----------------------------------|
| 0-15 | 1.18 | 0.08 | 0.06 | 0.77 | 2.95 | 0.82 |
| 15-27 | 1.24 | 0.10 | 0.06 | 0.60 | - | 0.62 |
| 27-36 | 1.41 | 0.07 | 0.05 | 0.53 | 1.94 | 0.44 |
| 36-50 | 1.48 | 0.03 | 0.04 | 1.15 | 0.74 | 0.96 |
| 50-75 | 1.49 | 0.03 | 0.06 | 1.30 | 1.44 | 1.04 |
| 75-100 | 1.40 | 0.03 | 0.05 | 1.56 | 1.15 | 1.03 |

Table B - 57: Eilenrede

| Depth (cm) | Dry density [g/cm ³] | ²³⁸ U/ ⁴⁰ K | ²³² Th/ ⁴⁰ K | ²³² Th/ ²³⁸ U | ²¹⁰ Pb/ ²²⁶ Ra | ²²⁶ Ra/ ²³⁸ U |
|------------|----------------------------------|-----------------------------------|------------------------------------|-------------------------------------|--------------------------------------|-------------------------------------|
| 0-10 | 1.133 | 0.07 | 0.06 | 0.80 | 3.08 | 0.65 |
| 10-20 | 1.286 | 0.08 | 0.05 | 0.69 | 1.41 | 0.56 |
| 20-30 | 1.334 | 0.08 | 0.05 | 0.64 | 1.14 | 0.57 |
| 30-40 | 1.407 | 0.06 | 0.05 | 0.79 | 1.59 | 0.67 |
| 40-50 | 1.349 | 0.04 | 0.05 | 1.12 | 1.34 | 0.92 |
| 50-70 | 1.373 | 0.03 | 0.08 | 1.71 | 1.24 | 1.50 |
| 70-100 | 1.356 | 0.06 | 0.03 | 1.03 | 1.32 | 0.88 |
| 100-120 | 1.536 | 0.03 | 0.08 | 1.21 | 1.61 | 1.02 |

Table B - 58: Barum

| Depth (cm) | Dry density [g/cm ³] | ²³⁸ U/ ⁴⁰ K | ²³² Th/ ⁴⁰ K | ²³² Th/ ²³⁸ U | ²¹⁰ Pb/ ²²⁶ Ra | ²²⁶ Ra/ ²³⁸ U |
|------------|----------------------------------|-----------------------------------|------------------------------------|-------------------------------------|--------------------------------------|-------------------------------------|
| 0-20 | 1.230 | 0.08 | 0.07 | 0.94 | 1.20 | 0.86 |
| 20-37 | 1.195 | 0.04 | 0.05 | 1.33 | 0.84 | 1.22 |
| 37-57 | 1.268 | 0.05 | 0.05 | 0.91 | 1.47 | 0.95 |
| 57-73 | 1.275 | 0.05 | 0.05 | 1.12 | 1.36 | 1.01 |
| 73-88 | 1.217 | 0.05 | 0.05 | 1.01 | 1.50 | 0.78 |
| 88-120 | 1.233 | 0.05 | 0.06 | 1.01 | 1.51 | 0.80 |
| 120-133 | 1.295 | 0.07 | 0.03 | 0.88 | 1.17 | 0.74 |
| 133-143 | 1.501 | 0.04 | 0.05 | 1.19 | 1.17 | 1.03 |
| 143-160 | 1.675 | 0.05 | 0.03 | 1.22 | 0.79 | 0.86 |

Table B - 59: Badenstedt

| Depth (cm) | Dry density [g/cm ³] | ²³⁸ U/ ⁴⁰ K | ²³² Th/ ⁴⁰ K | ²³² Th/ ²³⁸ U | ²¹⁰ Pb/ ²²⁶ Ra | ²²⁶ Ra/ ²³⁸ U |
|------------|----------------------------------|-----------------------------------|------------------------------------|-------------------------------------|--------------------------------------|-------------------------------------|
| 0-15 | 1.182 | 0.05 | 0.06 | 1.27 | 1.52 | 1.04 |
| 15-30 | 1.147 | 0.05 | 0.06 | 1.19 | 1.51 | 1.03 |
| 30-40 | 1.258 | 0.06 | 0.06 | 1.03 | 1.32 | 0.86 |
| 40-50 | 1.208 | 0.05 | 0.06 | 1.26 | 1.36 | 1.02 |
| 50-75 | 1.200 | 0.06 | 0.06 | 1.06 | 1.19 | 0.87 |
| 75-100 | 1.199 | 0.05 | 0.06 | 1.24 | 1.20 | 0.99 |
| 100-150 | 1.188 | 0.05 | 0.06 | 1.12 | 1.25 | 0.94 |
| 150-200 | 1.313 | 0.06 | - | 0.98 | 1.01 | 0.92 |
| 200-250 | - | - | - | - | - | - |

Table B - 60: Neßmerpolder

| Depth (cm) | Dry density [g/cm ³] | ²³⁸ U/ ⁴⁰ K | ²³² Th/ ⁴⁰ K | ²³² Th/ ²³⁸ U | ²¹⁰ Pb/ ²²⁶ Ra | ²²⁶ Ra/ ²³⁸ U |
|------------|----------------------------------|-----------------------------------|------------------------------------|-------------------------------------|--------------------------------------|-------------------------------------|
| 0-1 | 1.00 | 0.07 | 0.07 | 0.94 | 3.21 | 0.79 |
| 1-2 | 0.98 | 0.08 | 0.06 | 0.83 | 3.25 | 0.75 |
| 2-3 | 1.05 | 0.07 | 0.07 | 0.91 | 3.07 | 0.77 |
| 3-5 | 1.04 | 0.08 | 0.07 | 0.78 | 2.84 | 0.73 |
| 5-10 | 1.11 | 0.07 | 0.07 | 0.98 | 2.38 | 0.93 |
| 10-15 | 1.15 | 0.06 | 0.07 | 1.15 | 1.20 | 1.06 |
| 15-20 | 1.16 | 0.07 | 0.07 | 0.98 | 0.86 | 0.77 |
| 20-25 | 1.23 | 0.05 | 0.06 | 1.33 | 1.13 | 1.19 |
| 25-30 | 1.29 | 0.07 | 0.10 | 1.30 | 0.78 | 1.19 |

Lippe, NRW, Gemany,

Table B - 61: Bp 3-30, Lippe

| Depth cm | Dry density [g/cm ³] | ²³⁸ U/ ⁴⁰ K | ²³² Th/ ⁴⁰ K | ²³² Th/ ²³⁸ U | ²¹⁰ Pb/ ²²⁶ Ra | ²²⁶ Ra/ ²³⁸ U |
|----------|----------------------------------|-----------------------------------|------------------------------------|-------------------------------------|--------------------------------------|-------------------------------------|
| 0-2 | 0.91 | - | 0.22 | - | 0.58 | - |
| 2-4 | 0.95 | - | 0.19 | - | 0.54 | - |
| 4-6 | 0.98 | 0.148 | 0.198 | 1.341 | 0.542 | 5.615 |
| 6-10 | 1.00 | - | 0.169 | - | 0.560 | - |
| 10-15 | 0.98 | 0.095 | 0.112 | 1.188 | 0.773 | 7.259 |
| 15-20 | 0.94 | 0.084 | 0.085 | 1.016 | 0.859 | 6.731 |
| 20-30 | 0.92 | - | 0.069 | - | 0.918 | - |

Depth profiles from Ukraine

Table B - 62: Nosdrischtsche II

| Depth [cm] | Dry density [g/cm ³] | ²³⁸ U/ ⁴⁰ K | ²³² Th/ ⁴⁰ K | ²³² Th/ ²³⁸ U | ²¹⁰ Pb/ ²²⁶ Ra | ²²⁶ Ra/ ²³⁸ U |
|------------|----------------------------------|-----------------------------------|------------------------------------|-------------------------------------|--------------------------------------|-------------------------------------|
| humus soil | 1.10 | 0.02 | 0.03 | 1.74 | 39.87 | 1.64 |
| 0-1 | 1.18 | - | 0.04 | - | 16.65 | - |
| 1-2 | 1.63 | - | 0.03 | - | 11.18 | - |
| 2-3 | 1.46 | - | 0.06 | - | 0.01 | - |
| 3-5 | 1.77 | - | 0.03 | - | 0.01 | - |
| 5-10 | 1.78 | - | 0.04 | - | - | - |
| 15-10 | 1.84 | 0.04 | 0.03 | 0.58 | 3.29 | 0.30 |
| 15-20 | 1.84 | 0.01 | 0.04 | 17.15 | 2.50 | 15.71 |
| 20-25 | 1.91 | 0.02 | 0.04 | 2.11 | 1.93 | 2.06 |
| 25-40 | 1.90 | 0.04 | 0.04 | 0.95 | 1.92 | 1.19 |

Table B - 63: Chirstinovka shore

| Depth [cm] | Dry density [g/cm ³] | ²³⁸ U/ ⁴⁰ K | ²³² Th/ ⁴⁰ K | ²³² Th/ ²³⁸ U | ²¹⁰ Pb/ ²²⁶ Ra | ²²⁶ Ra/ ²³⁸ U |
|------------|----------------------------------|-----------------------------------|------------------------------------|-------------------------------------|--------------------------------------|-------------------------------------|
| humus soil | 0.66 | | 0.07 | - | 4.59 | - |
| 0-1 | 1.07 | 0.01 | 0.07 | 5.22 | 0.00 | 4.78 |
| 1-2 | 1.21 | 0.07 | 0.06 | 0.81 | 0.43 | 0.93 |
| 2-3 | - | - | - | - | - | - |
| 3-5 | 1.38 | 0.06 | 0.05 | 0.88 | 1.00 | 0.88 |
| 5-10 | 1.45 | 0.03 | 0.07 | 2.31 | 0.89 | 2.04 |
| 15--10 | 1.41 | 0.03 | 0.07 | 2.46 | 1.47 | 1.88 |
| 15-20 | 1.52 | 0.04 | 0.05 | 1.22 | 0.93 | 1.19 |
| 20-25 | 1.47 | 0.02 | 0.06 | 2.98 | 0.75 | 2.75 |
| 25-40 | 1.57 | 0.04 | 0.07 | 1.79 | 0.95 | 1.36 |

Table B - 64: Nove Scharnow 3

| Depth [cm] | Dry density [g/cm ³] | ²³⁸ U/ ⁴⁰ K | ²³² Th/ ⁴⁰ K | ²³² Th/ ²³⁸ U | ²¹⁰ Pb/ ²²⁶ Ra | ²²⁶ Ra/ ²³⁸ U |
|------------|----------------------------------|-----------------------------------|------------------------------------|-------------------------------------|--------------------------------------|-------------------------------------|
| humus soil | 1.49 | - | 0.07 | - | 1.46 | - |
| 0-1 | 1.49 | 0.02 | 0.04 | 1.90 | 2.54 | 3.00 |
| 1-2 | 1.54 | 0.01 | 0.07 | 9.99 | 0.91 | 10.19 |
| 2-3 | 1.55 | - | 0.05 | - | 0.52 | - |
| 3-5 | 1.81 | - | 0.05 | - | 0.00 | - |
| 5-10 | 1.64 | 0.03 | 0.07 | 2.23 | 2.58 | 1.69 |
| 15--10 | 1.68 | - | 0.06 | - | 0.77 | - |
| 15-20 | 1.89 | 0.04 | 0.05 | 1.33 | 1.34 | 1.16 |
| 20-25 | 1.76 | 0.01 | 0.06 | 6.44 | 2.09 | 4.92 |
| 25-40 | 1.42 | 0.02 | 0.07 | 4.07 | 2.08 | 3.14 |

Table B - 65: Tschigiri 1

| Depth [cm] | Dry density [g/cm ³] | ²³⁸ U/ ⁴⁰ K | ²³² Th/ ⁴⁰ K | ²³² Th/ ²³⁸ U | ²¹⁰ Pb/ ²²⁶ Ra | ²²⁶ Ra/ ²³⁸ U |
|------------|----------------------------------|-----------------------------------|------------------------------------|-------------------------------------|--------------------------------------|-------------------------------------|
| humus soil | 0.36 | - | 0.07 | - | 42.30 | - |
| 0-1 | 0.60 | 0.17 | 0.12 | 0.70 | 8.05 | 0.70 |
| 1-2 | 0.96 | 0.09 | 0.09 | 1.02 | 2.16 | 1.26 |
| 2-3 | 1.32 | 0.09 | 0.06 | 0.69 | 1.94 | 0.90 |
| 3-5 | 1.44 | 0.09 | 0.06 | 0.69 | 1.90 | 0.85 |
| 5-10 | 1.49 | 0.10 | 0.06 | 0.64 | 2.04 | 0.73 |
| 15--10 | 1.54 | 0.10 | 0.06 | 0.59 | 1.67 | 0.77 |
| 15-20 | 1.55 | 0.07 | 0.06 | 0.91 | 1.84 | 1.19 |
| 20-25 | 1.58 | 0.08 | 0.06 | 0.74 | 1.39 | 1.00 |
| 25-40 | 1.61 | 0.08 | 0.06 | 0.78 | 1.37 | 0.97 |

Table B - 66: Tschigiri 3

| Depth [cm] | Dry density [g/cm ³] | ²³⁸ U/ ⁴⁰ K | ²³² Th/ ⁴⁰ K | ²³² Th/ ²³⁸ U | ²¹⁰ Pb/ ²²⁶ Ra | ²²⁶ Ra/ ²³⁸ U |
|------------|----------------------------------|-----------------------------------|------------------------------------|-------------------------------------|--------------------------------------|-------------------------------------|
| humus soil | 0.77 | - | - | - | 2.23 | - |
| 0-1 | 1.04 | 0.13 | 0.11 | 0.85 | 4.21 | 1.50 |
| 1-2 | 1.34 | - | 0.12 | - | 3.02 | - |
| 2-3 | 1.40 | - | 0.11 | - | 1.36 | - |
| 3-5 | 1.32 | 0.09 | 0.09 | 1.00 | 1.50 | 0.77 |
| 5-10 | 1.51 | 0.01 | 0.08 | 6.78 | 0.27 | 5.88 |
| 15--10 | 1.45 | 0.04 | 0.10 | 2.73 | 0.30 | 2.49 |
| 15-20 | 1.50 | 0.01 | 0.08 | 5.26 | 0.16 | 5.44 |
| 20-25 | 1.73 | 0.06 | 0.07 | 1.29 | 3.21 | 1.33 |
| 25-40 | 1.84 | 0.02 | - | - | - | - |

Table B - 67: Tschigiri Zwintor 1

| Depth [cm] | Dry density [g/cm ³] | ²³⁸ U/ ⁴⁰ K | ²³² Th/ ⁴⁰ K | ²³² Th/ ²³⁸ U | ²¹⁰ Pb/ ²²⁶ Ra | ²²⁶ Ra/ ²³⁸ U |
|------------|----------------------------------|-----------------------------------|------------------------------------|-------------------------------------|--------------------------------------|-------------------------------------|
| humus soil | 0.39 | - | 0.04 | - | - | - |
| 0-1 | 0.76 | 0.02 | 0.05 | 2.72 | 5.91 | 2.86 |
| 1-2 | 1.28 | 0.07 | 0.05 | 0.67 | 7.44 | 0.60 |
| 2-3 | 1.48 | 0.06 | 0.05 | 0.74 | 2.30 | 0.83 |
| 3-5 | 1.51 | 0.03 | 0.05 | 1.56 | 2.08 | 1.72 |
| 5-10 | 0.00 | 0.07 | 0.11 | 1.55 | 2.99 | 1.35 |
| 15--10 | 1.66 | 0.05 | 0.04 | 0.95 | 1.95 | 0.94 |
| 15-20 | 1.61 | 0.04 | 0.05 | 1.20 | 1.66 | 1.15 |
| 20-25 | 1.61 | 0.06 | 0.05 | 0.87 | 1.87 | 0.90 |
| 25-40 | 1.96 | 0.03 | 0.04 | 1.44 | 1.31 | 1.44 |

Table B - 68: Woronewo 1

| Depth [cm] | Dry density [g/cm ³] | ²³⁸ U/ ⁴⁰ K | ²³² Th/ ⁴⁰ K | ²³² Th/ ²³⁸ U | ²¹⁰ Pb/ ²²⁶ Ra | ²²⁶ Ra/ ²³⁸ U |
|------------|----------------------------------|-----------------------------------|------------------------------------|-------------------------------------|--------------------------------------|-------------------------------------|
| humus soil | 0.70 | 0.03 | 0.05 | 1.42 | 5.42 | 1.05 |
| 0-1 | 1.18 | 0.04 | 0.05 | 1.25 | 5.39 | 0.97 |
| 1-2 | 1.01 | 0.03 | 0.04 | 1.65 | 5.47 | 1.21 |
| 2-3 | 1.08 | 0.04 | 0.04 | 0.93 | 2.90 | 1.34 |
| 3-5 | 1.41 | 0.01 | 0.04 | 2.69 | 1.97 | 3.54 |
| 5-10 | 1.62 | 0.04 | 0.04 | 1.23 | 1.71 | 1.28 |
| 15--10 | 1.66 | 0.06 | 0.05 | 0.76 | 1.54 | 0.74 |
| 15-20 | 1.70 | 0.05 | 0.05 | 1.00 | 1.13 | 1.10 |
| 20-25 | 1.74 | 0.05 | 0.05 | 1.01 | 1.77 | 1.01 |
| 25-40 | 1.79 | 0.05 | 0.05 | 0.90 | 1.00 | 0.91 |

Table B - 69: Woronewe 2

| Depth [cm] | Dry density [g/cm ³] | ²³⁸ U/ ⁴⁰ K | ²³² Th/ ⁴⁰ K | ²³² Th/ ²³⁸ U | ²¹⁰ Pb/ ²²⁶ Ra | ²²⁶ Ra/ ²³⁸ U |
|------------|----------------------------------|-----------------------------------|------------------------------------|-------------------------------------|--------------------------------------|-------------------------------------|
| humus soil | 0.89 | 0.06 | 0.03 | 0.50 | 15.78 | 0.53 |
| 0-1 | 1.28 | 0.13 | 0.09 | 0.68 | 0.52 | 0.71 |
| 1-2 | 1.42 | 0.02 | 0.09 | 3.58 | 0.36 | 3.22 |
| 2-3 | 1.42 | 0.04 | 0.11 | 3.16 | 0.30 | 2.55 |
| 3-5 | 1.55 | 0.02 | 0.08 | 4.03 | 0.27 | 3.31 |
| 5-10 | 1.64 | 0.02 | 0.08 | 3.54 | 0.25 | 3.07 |
| 15--10 | 1.74 | 0.08 | 0.12 | 1.49 | 6.28 | 1.16 |
| 15-20 | 1.77 | 0.05 | 0.06 | 1.25 | 5.71 | 0.96 |
| 20-25 | 1.83 | 0.05 | 0.06 | 1.18 | 5.84 | 0.85 |
| 25-40 | 1.88 | 0.05 | 0.09 | 1.82 | 4.99 | 1.40 |

Table B - 70: Woronewo3

| Depth [cm] | Density [g/cm ³] | ²³⁸ U/ ⁴⁰ K | ²³² Th/ ⁴⁰ K | ²³² Th/ ²³⁸ U | ²¹⁰ Pb/ ²²⁶ Ra | ²²⁶ Ra/ ²³⁸ U |
|------------|------------------------------|-----------------------------------|------------------------------------|-------------------------------------|--------------------------------------|-------------------------------------|
| humus soil | 0.57 | 0.15 | 0.16 | 1.06 | 5.99 | 0.73 |
| 0-1 | 0.91 | 0.23 | 0.16 | 0.70 | 7.98 | 0.76 |
| 1-2 | 0.95 | 0.12 | 0.15 | 1.28 | 5.67 | 1.18 |
| 2-3 | 1.27 | - | 0.07 | - | 40.68 | - |
| 3-5 | 1.18 | 0.14 | 0.11 | 0.82 | 3.10 | 0.82 |
| 5-10 | 1.60 | 0.03 | 0.08 | 3.13 | 0.30 | 2.90 |
| 15--10 | 1.58 | 0.02 | 0.07 | 3.26 | 0.19 | 2.96 |
| 15-20 | 1.68 | 0.04 | 0.13 | 3.51 | 0.19 | 3.65 |
| 20-25 | 1.64 | 0.04 | 0.15 | 3.33 | 0.22 | 3.13 |
| 25-40 | 1.84 | 0.05 | 0.06 | 1.35 | 5.25 | 1.12 |

Table B - 71: Woronewo 4

| Depth [cm] | Dry density [g/cm ³] | ²³⁸ U/ ⁴⁰ K | ²³² Th/ ⁴⁰ K | ²³² Th/ ²³⁸ U | ²¹⁰ Pb/ ²²⁶ Ra | ²²⁶ Ra/ ²³⁸ U |
|------------|----------------------------------|-----------------------------------|------------------------------------|-------------------------------------|--------------------------------------|-------------------------------------|
| humus soil | 0.38 | - | - | - | - | - |
| 0-1 | 0.76 | - | - | - | 102.00 | - |
| 1-2 | 0.67 | 0.03 | 0.04 | 1.40 | 26.03 | 0.47 |
| 2-3 | 0.98 | 0.03 | 0.05 | 1.71 | 8.37 | 1.55 |
| 3-5 | 1.00 | 0.05 | 0.05 | 0.95 | 4.52 | 0.96 |
| 5-10 | 1.36 | 0.07 | 0.05 | 0.66 | 2.37 | 0.76 |
| 15--10 | 1.58 | 0.04 | 0.05 | 1.11 | 1.46 | 1.12 |
| 15-20 | 1.54 | 0.05 | 0.05 | 0.92 | 1.18 | 0.90 |
| 20-25 | 1.63 | 0.04 | 0.04 | 0.98 | 0.94 | 0.99 |
| 25-40 | 1.81 | 0.04 | 0.04 | 1.26 | 1.64 | 1.31 |

Table B - 72: Woronewo 5

| Depth [cm] | Dry density [g/cm ³] | ²³⁸ U/ ⁴⁰ K | ²³² Th/ ⁴⁰ K | ²³² Th/ ²³⁸ U | ²¹⁰ Pb/ ²²⁶ Ra | ²²⁶ Ra/ ²³⁸ U |
|------------|----------------------------------|-----------------------------------|------------------------------------|-------------------------------------|--------------------------------------|-------------------------------------|
| humus soil | 0.34 | - | - | - | - | - |
| 0-1 | 0.48 | - | 0.04 | - | 15.84 | - |
| 1-2 | 1.02 | - | 0.07 | - | 5.17 | - |
| 2-3 | 1.05 | 0.05 | 0.06 | 1.20 | 2.23 | 1.33 |
| 3-5 | 1.35 | 0.02 | 0.07 | 4.07 | 1.84 | 4.36 |
| 5-10 | 1.37 | 0.06 | 0.06 | 1.05 | 0.91 | 1.04 |
| 15--10 | 1.48 | 0.02 | 0.07 | 4.52 | 0.93 | 4.18 |
| 15-20 | 1.57 | 0.03 | 0.07 | 1.96 | 1.18 | 1.71 |
| 20-25 | 1.70 | 0.02 | 0.06 | 3.01 | 1.00 | 3.12 |
| 25-40 | 1.74 | 0.03 | 0.06 | 1.74 | 1.03 | 1.54 |

Table B - 73: Woronewo 6

| Depth [cm] | Dry density [g/cm ³] | ²³⁸ U/ ⁴⁰ K | ²³² Th/ ⁴⁰ K | ²³² Th/ ²³⁸ U | ²¹⁰ Pb/ ²²⁶ Ra | ²²⁶ Ra/ ²³⁸ U |
|------------|----------------------------------|-----------------------------------|------------------------------------|-------------------------------------|--------------------------------------|-------------------------------------|
| humus soil | 0.91 | - | 0.05 | - | 1.98 | - |
| 0-1 | 0.98 | - | 0.06 | - | 0.00 | - |
| 1-2 | 1.09 | - | 0.06 | - | 5.84 | - |
| 2-3 | 1.08 | 0.09 | 0.07 | 0.75 | 1.57 | 0.94 |
| 3-5 | 1.39 | 0.04 | 0.11 | 2.52 | 0.36 | 2.79 |
| 5-10 | 1.55 | 0.01 | 0.03 | 4.31 | 0.36 | 4.79 |
| 15--10 | 1.56 | 0.03 | 0.11 | 3.31 | 0.27 | 3.25 |
| 15-20 | 1.65 | 0.07 | 0.23 | 3.33 | 0.23 | 3.01 |
| 20-25 | 1.74 | 0.04 | 0.05 | 1.24 | 5.43 | 1.07 |
| 25-40 | 1.86 | 0.04 | 0.05 | 1.19 | 5.78 | 1.05 |

Table B - 74: Woronewo 7

| Depth [cm] | Dry density [g/cm ³] | ²³⁸ U/ ⁴⁰ K | ²³² Th/ ⁴⁰ K | ²³² Th/ ²³⁸ U | ²¹⁰ Pb/ ²²⁶ Ra | ²²⁶ Ra/ ²³⁸ U |
|------------|----------------------------------|-----------------------------------|------------------------------------|-------------------------------------|--------------------------------------|-------------------------------------|
| humus soil | 1.31 | 0.03 | 0.07 | 2.26 | 2.40 | 1.75 |
| 0-1 | 1.41 | 0.05 | 0.06 | 1.40 | 0.60 | 1.38 |
| 1-2 | 1.67 | 0.03 | 0.06 | 2.08 | 0.57 | 3.26 |
| 2-3 | 1.81 | 0.01 | 0.06 | 4.02 | 0.84 | 3.75 |
| 3-5 | 1.85 | 0.03 | 0.06 | 1.70 | 1.43 | 1.60 |
| 5-10 | 1.73 | 0.03 | 0.06 | 2.40 | 1.05 | 2.04 |
| 15--10 | 1.73 | 0.04 | 0.07 | 1.57 | 1.11 | 1.79 |
| 15-20 | 1.86 | 0.05 | 0.06 | 1.28 | 1.00 | 1.11 |
| 20-25 | 2.02 | 0.02 | 0.06 | 2.91 | 1.05 | 2.58 |
| 25-40 | 2.11 | 0.01 | 0.05 | 7.55 | 0.43 | 6.95 |

Table B - 75: Baraschewka 1

| Depth [cm] | Dry density [g/cm ³] | ²³⁸ U/ ⁴⁰ K | ²³² Th/ ⁴⁰ K | ²³² Th/ ²³⁸ U | ²¹⁰ Pb/ ²²⁶ Ra | ²²⁶ Ra/ ²³⁸ U |
|------------|----------------------------------|-----------------------------------|------------------------------------|-------------------------------------|--------------------------------------|-------------------------------------|
| humus soil | 0.23 | 0.00 | 0.06 | - | 12.23 | - |
| 0-1 | 0.63 | 0.09 | 0.09 | 0.98 | 0.00 | 1.18 |
| 1-2 | 0.84 | 0.15 | 0.11 | 0.75 | 8.56 | 0.91 |
| 2-3 | 1.02 | 0.06 | 0.14 | 2.33 | 6.32 | 2.64 |
| 3-5 | 1.10 | 0.03 | 0.13 | 4.06 | 6.39 | 4.17 |
| 5-10 | 1.18 | 0.00 | 0.12 | - | 1.79 | - |
| 15-10 | 1.24 | 0.04 | 0.12 | 2.73 | 1.67 | 3.40 |
| 15-20 | 1.25 | 0.06 | 0.17 | 2.91 | 1.38 | 3.51 |
| 20-25 | 1.48 | 0.01 | 0.10 | 13.18 | 0.08 | 11.81 |
| 25-40 | 1.81 | 0.01 | 0.13 | - | 1.42 | - |

Table B - 76: Oserjanka 2

| Depth [cm] | Dry density [g/cm ³] | ²³⁸ U/ ⁴⁰ K | ²³² Th/ ⁴⁰ K | ²³² Th/ ²³⁸ U | ²¹⁰ Pb/ ²²⁶ Ra | ²²⁶ Ra/ ²³⁸ U |
|------------|----------------------------------|-----------------------------------|------------------------------------|-------------------------------------|--------------------------------------|-------------------------------------|
| humus soil | 1.00 | 0.12 | 0.08 | 0.65 | 2.50 | 0.59 |
| 0-1 | 1.23 | 0.09 | 0.08 | 1.00 | 3.82 | 0.75 |
| 1-2 | 1.01 | 0.12 | 0.06 | 0.51 | 2.55 | 0.41 |
| 2-3 | 1.25 | 0.17 | 0.11 | 0.62 | 3.88 | 0.51 |
| 3-5 | 1.36 | 0.15 | 0.10 | 0.67 | 0.77 | 0.50 |
| 5-10 | 1.36 | 0.16 | 0.13 | 0.80 | 1.81 | 0.58 |
| 15-10 | 1.52 | 0.19 | 0.12 | 0.60 | 1.36 | 0.53 |
| 15-20 | 1.44 | 0.18 | 0.16 | 0.86 | 1.89 | 0.65 |
| 20-25 | 1.40 | 0.04 | 0.07 | 1.50 | 0.98 | 1.19 |
| 25-40 | 1.39 | 0.13 | 0.08 | 0.60 | 1.38 | 0.55 |

Table B - 77: Oserjanka 3

| Depth [cm] | Dry density [g/cm ³] | ²³⁸ U/ ⁴⁰ K | ²³² Th/ ⁴⁰ K | ²³² Th/ ²³⁸ U | ²¹⁰ Pb/ ²²⁶ Ra | ²²⁶ Ra/ ²³⁸ U |
|------------|----------------------------------|-----------------------------------|------------------------------------|-------------------------------------|--------------------------------------|-------------------------------------|
| humus soil | 0.72 | 0.10 | 0.05 | 0.51 | 5.35 | 0.49 |
| 0-1 | 1.02 | 0.13 | 0.06 | 0.44 | 2.47 | 0.36 |
| 1-2 | 1.09 | 0.14 | 0.08 | 0.59 | 4.35 | 0.44 |
| 2-3 | 1.19 | 0.13 | 0.05 | 0.44 | 2.47 | 0.35 |
| 3-5 | 1.13 | 0.12 | 0.07 | 0.56 | 2.43 | 0.45 |
| 5-10 | 0.96 | 0.19 | 0.06 | 0.33 | 2.94 | 0.32 |
| 15-10 | 0.94 | 0.15 | 0.06 | 0.43 | 2.12 | 0.31 |
| 15-20 | 0.92 | 0.40 | 0.17 | 0.42 | 2.95 | 0.33 |
| 20-25 | 0.94 | 0.16 | 0.06 | 0.38 | 3.09 | 0.39 |
| 25-40 | 0.53 | 0.11 | 0.11 | 0.97 | 1.58 | 0.68 |

Table B - 78: Dawidowka 1

| Depth [cm] | Dry density [g/cm ³] | ²³⁸ U/ ⁴⁰ K | ²³² Th/ ⁴⁰ K | ²³² Th/ ²³⁸ U | ²¹⁰ Pb/ ²²⁶ Ra | ²²⁶ Ra/ ²³⁸ U |
|------------|----------------------------------|-----------------------------------|------------------------------------|-------------------------------------|--------------------------------------|-------------------------------------|
| humus soil | 0.7 | 0.10 | 0.13 | 1.34 | 4.52 | 1.23 |
| 0-1 | 1.1 | 0.09 | 0.13 | 1.38 | 2.38 | 1.69 |
| 1-2 | 1.1 | 0.13 | 0.11 | 0.84 | 3.34 | 0.81 |
| 2-3 | 1.1 | 0.13 | 0.11 | 0.87 | 2.72 | 0.88 |
| 3-5 | 1.3 | 0.07 | 0.12 | 1.71 | 2.25 | 1.62 |
| 5-10 | 1.2 | 0.11 | 0.11 | 1.02 | 0.92 | 1.09 |
| 10--15 | 1.4 | 0.12 | 0.10 | 0.83 | 1.32 | 0.85 |
| 15-20 | 1.2 | 0.06 | 0.11 | 1.96 | 0.65 | 2.15 |
| 20-25 | 1.4 | 0.09 | 0.12 | 1.36 | 1.45 | 1.36 |
| 25-40 | 1.1 | 0.11 | 0.14 | 1.28 | 1.10 | 1.29 |

Table B - 79: Lewkow 1

| Depth [cm] | Dry density [g/cm ³] | ²³⁸ U/ ⁴⁰ K | ²³² Th/ ⁴⁰ K | ²³² Th/ ²³⁸ U | ²¹⁰ Pb/ ²²⁶ Ra | ²²⁶ Ra/ ²³⁸ U |
|------------|----------------------------------|-----------------------------------|------------------------------------|-------------------------------------|--------------------------------------|-------------------------------------|
| 0-1 | 0.8 | - | - | 0.16 | 2.29 | 0.42 |
| 1-2 | 0.9 | 0.55 | 0.10 | 0.19 | 2.36 | 0.56 |
| 2-3 | 1.0 | 0.53 | 0.12 | 0.22 | 2.05 | 0.59 |
| 3-5 | 1.0 | 0.43 | 0.12 | 0.27 | 1.75 | 0.64 |
| 5-10 | 1.1 | 0.83 | 0.09 | 0.11 | 2.11 | 0.38 |
| 15--10 | 1.0 | 0.20 | - | - | - | - |
| 15-20 | 1.2 | 0.30 | 0.09 | 0.29 | 1.56 | 0.64 |
| 20-25 | 1.2 | 0.18 | 0.13 | 0.72 | 0.56 | 1.38 |
| 25-40 | 1.3 | 0.14 | 0.11 | 0.78 | 0.37 | 1.28 |

Table B - 80: Lewkow 2

| Depth [cm] | Dry density [g/cm ³] | ²³⁸ U/ ⁴⁰ K | ²³² Th/ ⁴⁰ K | ²³² Th/ ²³⁸ U | ²¹⁰ Pb/ ²²⁶ Ra | ²²⁶ Ra/ ²³⁸ U |
|------------|----------------------------------|-----------------------------------|------------------------------------|-------------------------------------|--------------------------------------|-------------------------------------|
| humus soil | 1.1 | 0.10 | 0.06 | 0.65 | 3.60 | 1.01 |
| 0-1 | - | 0.11 | 0.06 | 0.56 | 3.07 | 0.91 |
| 1-2 | 1.2 | - | - | - | - | - |
| 2-3 | 1.3 | - | - | 0.69 | 3.07 | 0.95 |
| 3-5 | - | - | - | - | - | - |
| 5-10 | 1.2 | 0.14 | 0.08 | 0.55 | 2.14 | 0.87 |
| 15--10 | - | - | - | - | - | - |
| 15-20 | 1.5 | 0.09 | 0.07 | 0.76 | 1.50 | 1.26 |
| 20-25 | 1.5 | 0.09 | 0.06 | 0.63 | 1.83 | 0.90 |
| 25-40 | - | - | - | - | - | - |

7 References

- Alb99 A. Albrecht "Radiocesium and ^{210}Pb in sediments, soils and surface waters of a high alpine catchment: A mass balance approach relevant to radionuclide migration and storage" *Aquat. sci.* 61, 1- 22, (1999).
- And01 I. Andersson, H. Lönsjö and Klas Rosén "Long-term studies on transfer of ^{137}Cs from soil to vegetation and to grazing lambs in a mountain area in Northern Sweden, *Journal of Environmental Radioactivity*, 52, 45-66, (2001).
- Ant95 D. Antonopoulos, M., Clouvas, A., Hiladakis, S. "radiocesium distribution in undisturbed soil: measurements and diffusion-advection model" *Health physics*, 69, 949-953, (1995).
- Arn89 O. Arnalds, Cutshall Norman H., Nielsen Gerald A. "Cesium-137 in Montana Soils" *Health physics*, 57, 6, 955-958, (1989).
- Asl03 M. A. A. Aslani, Sule Aytas, Sema Akyil, Günseli Yaprak, Gungor Yener and Meral Eral "Activity concentration of caesium-137 in agricultural soils" *Journal of Environmental Radioactivity*, 65, 131-145, (2003).
- Bel98 D. Beltz, *Spaltprodukte in der Umgebung von Tschernobyl und die Strahlenexposition der dortigen Bevölkerung*, Diplomarbeit Zentrum für Strahlenschutz und Radioökologie (ZSR), Hannover Universität, Juli 1998.
- Bla95 R. Blagoeva, and L. Zikovskiy "Geographic and vertical distribution of Cs-137 in soils in Canada" 27, 269-174, (1995).
- Bon93 G. C. Bonazzola, R. Ropol, and Facchinelli, A., "Profiles and downward migration of ^{134}Cs and ^{106}Ru deposited on Italian soils after the Chernobyl accident" *Health physics*, 64, 479-484, (1993).
- Bot00 W. Botsch "Untersuchungen zur Strahlenexposition von Einwohnern kontaminierter Ortschaften der nördlichen Ukraine" Doktorarbeit Zentrum für Strahlenschutz und Radioökologie (ZSR), Hannover Universität, 2000.
- Bra02 M. Brai, S. Basile, S. Bellia, S. Hauser, P. Puccio, S. Rizzo, A. Bartolotta and A. Licciardello Applied "Environmental radioactivity at Stromboli (Aeolian Islands)" *Radiation and Isotopes*, 57, 99-107, (2002).
- Bra92 M. Brai, Bellia S., Liberto R., Dongarra G., Hauser S., Parello F., Puccio P., Rizzo S, "Environmental Gamma Radiation Measurements on the Island of Pantelleria" *Health physics*, 63, 3, 356-359, (1992).
- BfS99 Bundesamt für Strahlenschutz (BfS) *Berechnungsgrundlagen zur Ermittlung der Strahlenexposition infolge bergbaulicher Umweltradioaktivität (Berechnungsgrundlage Bergbau)*, (Stand 30.07.1999).

- Can02 “*Considerations for Environmental Gamma Spectroscopy Systems*” available at <http://www.canberra.com/literature/972.asp> (2002).
- Car03 P. Carbol, D. Solatie, N. Erdmann, T. Nylén and M. Betti “*Deposition and distribution of Chernobyl fallout fission products and actinides in a Russian soil profile*” *Journal of Environmental Radioactivity*, 68, 27- 46, (2003).
- Che93 W. Chelmiki, J. W. Mietelski, P. Macharki and J. Swiechowicz “*Natural factors of ¹³⁷Cs redistribution in soil*” report No. 1615/D, Institute of nuclear physics, Krakow, Poland, 1993.
- Chi97 A. Chieco, *The procedures manual of the environmental measurements laboratory*, HASL-300 volume I, 28th Edition February, U.S. Department of Energy New York, (1997).
- Chi99 Y. Chih, Chiu, Shu-Yin Lai, Yu-Ming Lin. and Hsien-Chueh Chiang “*Distribution of the radionuclide ¹³⁷Cs in soils of a wet mountainous forest in Taiwan*” *Applied Radiation and Isotope*, 50, 1097-1130, (1999).
- Cho95 G. R. Choppin, R. Rydberg and J. O. Liljenzin “*Radiochemistry and nuclear chemistry*” 2nd edition of *Nuclear Chemistry Theory and applications*, New York, Pergmon Press. (1995).
- Cop00 D. Copplestone, M. S. Johnson, S. R. Jones “*Radionuclide Behaviour and Transport in a Coniferous Woodland Ecosystem: The Distribution of Radionuclides in Soil and Leaf Litter*” *Water, Air, & Soil Pollution*, 122, 389- 404, (2000).
- Cop01 D. Copplestone, M. S. Johnson and S. R. Jones “*Behaviour and transport of radionuclides in soil and vegetation of a sand dune ecosystem*” *Journal of Environmental Radioactivity*, 55, 93-108, (2001).
- Cur68 L. A. Currie, “*Limits for qualitative detection and quantitative determination. Applications of radiochemistry*” *Anal. Chem.* 40, 586, (1968).
- Daz01 M. J. Daza, B. Quintana, M. Garcia-Talavera, F. Fernandez “*Efficiency calibration of a HPGe detector in the [46.54 - 2000] keV energy range for the measurement of environmental samples*” *nuclear instruments and methods in physics research A* 470, 520-532, (2001).
- Deb88 K. Debertin und R. G. Helmer, *Gamma- and X-Ray Spectrometry with Semiconductor Detectors*, Elsevier Science Publishers, (1988).
- Dia02 K. Dias da Cunha, J. L. Lipsztein, A. M. Azeredo, D. Melo, L. M. Q. C. Julião. F. F. Lamego, M. Santos, C. V. Barros Leite “*Study of Worker's Exposure to Thorium. Uranium and Niobium Mineral Dust*” *Water, Air, & Soil Pollution*, 137, 45-61, (2002).
- Die72 W. S. Diethorn and W. L. Stockho “*The dose to man from atmospheric krypton-85*” *Health physics*, 23: 653-662 (1972).

- Dil75 L.T. Dillman, and F. C. von der Lage, *Radionuclide decay schemes and Nuclear Parameters for use in Radiation Dose Estimation*, NM/MIRD Pamphlet No. 10, Society of Nuclear Medicine, (September 1975).
- Dix84 D. W. Dixon “*Hazard assessment of work with ores containing elevated levels of natural radioactivity*” NRPB-R143 National Radiological Protection Board, (1984).
- Dow02 M. Dowdall and John O’Dea “ *$^{226}\text{Ra}/^{238}\text{U}$ disequilibrium in an upland organic soil exhibiting elevated natural radioactivity*” *Journal of Environmental Radioactivity*, 59, 91-104, (2002).
- Dow03 M. Dowdall, S. Gerland, and B. Lind “*Gamma-emitting natural and anthropogenic radionuclides in the terrestrial environment of Kongsfjord, Svalbard*” *The Science of the Total Environment*, 305, 229-240, (2003).
- Dub03 G. Dubois, and P. Bossew “*Chernobyl ^{137}Cs deposition in Austria: analysis of the spatial correlation of the deposition levels*” *Journal of Environmental Radioactivity*, 65, 29-45, (2003).
- Ead98 L. J. Eades, J. G. Farmer, A. B. MacKenzie, A. Kirika and A. E. Bailey-Watts “*High-resolution Profile of Radiocaesium Deposition in Loch Lomond Sediments*” *Journal of Environmental Radioactivity*, 39, 107-115, (1998).
- Eis97 M. Eisenbud, and T. Geseel “*Environmental Radioactivity from Natural, Industrial, and Military Sources*” fourth edition, Academic press (1997).
- Em97 U. S. department of energy, office of environmental management available at <http://www.em.doe.gov/define/techs/chap3a.html> (1997).
- Erl86 B. Erlandsson, Isaksson M. “*Relation between the air activity and the deposition of Chernobyl debris*” *Environment International* 14,165-1(1988).
- Esp02 M. Esposito, P. Polić, P. Bartolomei, V. Benzi, M. Martellini, O. Cvetković, V. Damjanov, M. Simić, Z. Žunić, B. Živančević et al. “*Survey of natural and anthropogenic radioactivity in environmental samples from Yugoslavia*” *Journal of Environmental Radioactivity*, 61, 271-282, (2002).
- Faa00 A. Faanhof “*The measurement of natural radioactivity and the impact on humans*” *Czech. J. Phys.* 50, (2000).
- Fir96 R. B. Firestone and V. S. Shirley “*Table of isotopes*” eight edition volum II: A = 151-272, (1996)
- Flu02 M. Flues, V. Moraes and B. P. Mazzilli “*The influence of a coal-fired power plant operation on radionuclide concentrations in soil*” *Journal of Environmental Radioactivity*, 63, 285-294, (2002).
- For00 S. Forsberg, K. Rosén, V. Fernandez and H. Juhan “*Migration of ^{137}Cs and ^{90}Sr in undisturbed soil profiles under controlled and close-to-real conditions*” *Journal of Environmental Radioactivity*, 50, 235-252, (2000).

- Fre66 L. Fredriksson, R. J. Garner and R. S. Russell “*Caesium-137, in Radioactivity and Human Diet* (R. S. Russell, ed.), P. 317-352, Pergamon Press. (1966).
- Gar95 F. García-Oliva, R. Martínez Lugo and J. M. Maass “*Soil ^{137}Cs Activity in a Tropical Deciduous Ecosystem Under Pasture Conversion in Mexico*” *Journal of Environmental Radioactivity*, 26. 1, 37-49, (1995).
- God98 J. M. Godoy, L. A. Schuch, D. J. R. Nordemann, V. R. G. Reis, M. Ramalho. J. C. Recio, R. R. A. Brito and M. A. Olech “ *^{137}Cs , $^{226,228}\text{Ra}$, ^{210}Pb and ^{40}K concentrations in Antarctic soil, sediment and selected moss and lichen samples*” *Journal of Environmental Radioactivity*, 41, 33-45, (1998).
- Gol95 N. Golchert, and R. Kolzow “*1995 ANL-E Site Environmental Report*” available at http://www.anl.gov/ESH/anleser/1995/chapter7/7_1.html (1995).
- Gra85 P. W. Gray, A. Ahmed “*Linear classes of Ge(Li) detector efficiency functions*” *Nuclear Instruments and Methods in Physics Research A237*, 577-589, (1985).
- Gre90 D. J. Greeman, and A. W. Rose, “*Form and behaviour of radium, uranium and thorium in central Pennsylvania soils derived from Dolomite*” *Geophysical Research Letters*, 17/6, 833–836, (1990).
- Gun96 V. Gunten, H. R., Surbeck, H., and Rossler, E. “*Uranium series disequilibrium and high thorium and radium enrichments in Karst formations*” *Environmental Science and Technology*, 30, 1268–1274, (1996).
- Guo99 J. Guogang, Corrado Testa, Donatella Desideri. Francesca Guerra, Maria A. Meli, Carla Roselli, and Maria E. Belli “*Soil concentration, vertical distribution and inventory of plutonium, ^{241}Am , ^{90}Sr and ^{137}Cs in the Marche region of central Italy*” *Health physics*, 77, 1, 52-61, (1999).
- Gus69 P. F. Gustafson, and J. E. Miller, “*The significance of ^{137}Cs in man and his diet*” *Health physics* 16: 167-183, (1969).
- Ham03 I. Al Hamarneh, A. Wreikat, and K. Toukan “*Radioactivity concentrations of ^{40}K , ^{134}Cs , ^{137}Cs , ^{90}Sr , ^{241}Am , ^{238}Pu and $^{239+240}\text{Pu}$ radionuclides in Jordanian soil samples*” *Journal of Environmental Radioactivity*, 67, 53-67, (2003).
- IAE89 International Atomic Energy Agency, Vienna, “*Measurement of radionuclides in food and the environment*” A Guide book, technical report series No. 295, (1989).
- IAE91 International Atomic Energy Agency (Hrsg), “*The international Chernobyl Project, Surface Contamination Maps*” IAEA, Wien (1991).
- ICR94 International commission on radiation units and measurments “*Gamma-ray spectrometry in the environment*” ICRU Report 53, (1994).
- ICR90 International Commission on Radiological Protection “*Recommendations of the international commission on radiological protection*” ICRP publication 60, (1990).

- ICR96 International Commission on Radiological Protection “*Age-dependent doses to members of the public from intake of radionuclides: part 5 compilations of ingestion and inhalation dose coefficients*” ICRP publication 72, annual of the ICRP 26(1), pergamon press, Oxford, (1996).
- IPC83 *IPCS International Programme on Chemical Safety Environmental Health Criteria 25 Selected Radionuclides*, (1983).
- Isa97 M. Isaksson “*Methods of Measuring Radioactivity in the Environment*” Ph.D., Thesis, Department of nuclear physics, university of Lund, Sweden, (1997).
- Isa97 M. Isaksson and B. Erlandsson “*Investigation of the Distribution of ¹³⁷Cs from Fallout in the Soils of the City of Lund and the Province of Skåne in Sweden*” Journal of Environmental Radioactivity, 38, 1, 105-131(1997).
- ISO93 International Standards Organization, ISO international vocabulary of basic and general terms in metrology, International Organization for Standardization, Geneva, (1993).
- ISO95 ISO Guide to the Expression of Uncertainty in Measurement, ISO International Organization for Standardization, Geneva 1993 correct reprint (1995).
- ISO99 International Standards Organization, 1999 “general requirements for the competence of testing and calibration laboratories (ISO/IEC 17025:1999), European Committee for Standardization, Brussels, (1999).
- Iva92 M. Ivanovich and R.S. Harmon “*Uranium-Series Disequilibrium: Applications to earth Marine and Environmental Sciences*, Oxford: Clarendon Press, 2th Edit, (1992).
- Jon93 D. Jong, E. Acton, D. F., and Kozak, L. M. “*Naturally occurring gamma-emitting isotopes, radon release and properties of parent materials of Saskatchewan Soils*” Canadian Journal of Soil Science, 74, 47–53, (1993).
- Kar02 D. Karamanis, V. Lacoste, S. Andriamonje, G. Barreau and M. Petit “*Experimental and simulated efficiency of a HPGe detector with point-like and extended sources*” nuclear instruments and methods in physics research A 487, 477-487,(2002).
- Kat84 R. L. Kathren “*Radioactivity in the Environment Sources, Distribution, and Surveillance*” Harwood Academic Publishers, New York (1984).
- Kem96 J. Kemski, R. Klingel, and A. Siehl “*Die terrestrische Strahlung durch natürlich radioaktive Elemente in Gesteinen und Böden*“ In A. Siehl, Editor, *Umweltradioaktivität*, Ernst und Sohn Verlag (1996).
- Kno00 G. F. Knoll “*Radiation detection and measurement*” John Wiley, & Sons, New York, (2000).

- Kor01 M. Korun “*Propagation of uncertainties in sample properties to the uncertainty of the counting efficiency in gamma-ray spectrometry*“ Applied Radiation and Isotopes 55, 685-691, (2001).
- Kor98 E. Korobova, Ermakov A, Linnik V., “*¹³⁷Cs and ⁹⁰Sr mobility in soils and transfer in soil-plant systems in the Novozybkov district affected by the Chernobyl accident*” Appl Geochem 13(7): 803-814, (1998).
- Kva86 J. Kvasincka, “*Radiation data input for the design of dry or semidry U tailings deposal*” Health physics 51, 392-336, (1986).
- LaB96 J. LaB recque, Rosales PA, *The migration of ¹³⁷Cs in Venezuelan soils*” J Trace Microprobe Tech. 14(1): 213-221, (1996).
- Lai99 K. K. Lai, S. J. Hu, S. Minato, K. Kodaira, K. S. Tan, *Terrestrial gamma ray dose rates of Brunei Darussalam*” Appl. Radiation Isotopes, 50, 599, (1999).
- Lan86 D. Landeen, Mitchell RM. “*Radionuclide uptake by trees at a RAD waste pond in Washington State*” Health Phys 50(6): 769-774, (1986).
- Lay93 D. W. Layton “*Metabolically consistent breathing rates for use in dose assessments*” Health physics, 64, 1, (1993).
- Led77 C. M. Lederer et al. “*Table of isotopes*” seventh Edition, Wiley, New York, (1977).
- Lei02 R. Z. Leifer, E. M. Jacob, S. F. Marschke and D. M. Pranita “*Atmospheric aerosol measurements of ²³⁸U and ²³²Th at Fernald, Ohio, and implications on inhalation dose calculations*” Health physics 83, 6, 892-900, (2002).
- Maj90 S. K. Majumdar, R. F. Schmalz and Easton, P. “*Environmental radon : occurrence, control, and health hazards*” Pennsylvania Academy of Science, (1990).
- Man99 I. C. Mantazul, M. N. Alam and S. K. S. Hazari “*Distribution of radionuclides in the river sediments and coastal soils of Chittagong, Bangladesh and evaluation of the radiation hazard*” Applied Radiation and Isotopes, 51, 747-755, (1999).
- Mas94 H. Masaharu, Yamamoto Masayoshi. Kawamura Hisao. Shinohara Kunihiko, Shibata Yoshisada. Kozlenko Mikhail T., Takatsuji Toshihiro. Yamashita Shunichi. Namba Hiroyuki. Yokoyama Naokata. Izumi Motomori. Fujimura Kingo, Danilyuk Valery V., Nagataki Shigenobu, Kuramoto Atsushi, Okajima Shunzo, Kiikuni Kenzo, Shigematsu Itsuzo “*Fallout Radioactivity in Soil and Food Samples in the Ukraine: Measurements of Iodine, Plutonium, Cesium, and Strontium Isotopes*“ Health physics, 97, 2, 469-476, (1994).
- McA92 I.R. McAulay and D. Marsh “*²²⁶Ra Concentrations in Soil in the Republic of Ireland*” Radiat. Prot. Dosim. 45(1-4), 265-267, (1992).
- Meg88 K. Megumi, T. Oka, M. Doi, S. Rimura, T. Tsujimoto, T. Ishiyama, and K. Katsurayama “*Relationships Between the Concentrations of Natural Radionuclides*

- and the Mineral Composition of the Surface Soil*” Radiat. Prot. Dosim. 24, (1-4), 69-72, (1988).
- Mic00 R. Michel “*Quality assurance of nuclear analytical techniques based on Bayesian characteristic limits*” Journal of Radioanalytical and Nuclear Chemistry, Vol. 245, No. 1, 137-144, (2000).
- Mil90 K. M. Miller, J. L. Kuiper and I. K. Helfer “¹³⁷Cs fallout depth distribution in forest versus field sites: implications for external gamma dose rates” 12, 23-48, (1990).
- Nab00 Y. B. Nabyvanets, Thomas F. Gesell, Min Hua Jen and Wushou P. Chang “*Distribution of ¹³⁷Cs in soil along Ta-han River Valley in Tau-Yuan County in Taiwan*” Journal of Environmental Radioactivity, 54, 391- 400, (2000).
- Naz88 W. W. Nazaroff “*Radon and its decay products in indoor air*” New York, Wiley, 1988
- NCR75 National council on Radiation Protection and Measurements “*Natural background radiation in the United States*” NCRP No. 45, (1975).
- NCR75a National council on Radiation Protection and Measurements, *Krypton-85 in the atmosphere accumulation, biological significance and control technology*, NCRP No. 44 (1975).
- NCR76 National council on Radiation Protection and Measurements “*Environmental radiation measurements*” NCRP Report No. 50, (1976).
- NCR78 National council on Radiation Protection and Measurements, “*A handbook of radioactivity measurements procedures*, NCRP No. 58 (1978).
- NCR85 National council on Radiation Protection and Measurements “*A Handbook of radioactivity measurements procedures*” NCRP, report No.58, (1985).
- NCR87 National council on Radiation Protection and Measurements “*Limitation of exposure to ionizing Radiation*” NCRP No. 116, (1987).
- NCR93 National council on Radiation Protection and Measurements “*Ionizing Radiation Exposure of the population of the United states*” NCRP No. 93, (1993).
- NCR94 National council on Radiation Protection and Measurements “*Dose control at nuclear power plants*” NCRP No. 120, (1994).
- NCR99 National council on Radiation Protection and Measurements “*Recommended screening limits for contaminated surface soil and review of factors relevant to site-specific studies*, NCRP No. 129, (1999).
- NIS98 “*Essentials of expressing measurement uncertainty*” available at <http://physics.nist.gov/cuu/Uncertainty/index.html> (1998).

- Nou03 A. Noura, E. H. Sayouty, and M. Benmansour "Use of ^{137}Cs technique for soil erosion study in the agricultural region of Casablanca in Morocco" Journal of Environmental Radioactivity, 68, 11-26, (2003).
- OCR02 The Office of Civilian Radioactive Waste Management (OCRWM), 2002 "Chart of the Isotopes in the U-238, U-235, and Th-232 Decay Series" available at http://www.ocrwm.doe.gov/pm/program_docs/curriculum/unit_2_toc/unit_2_toc.htm
- Ortec *Germanium detector- user's manual*
- Owe96 P. Owens, Walling DE, He Q. "The behaviour of bomb-derived caesium-137 fallout in concentrations of fallout following the Chernobyl reactor accident" Sci Total Environ 84:283-289, (1996).
- Pap88 C. Papastefanou, Manolopoulou, m. & Charalambous, S., "Cesium-137 in soils from Chernobyl fallout" Health physics, 55, 985-987, (1988).
- Pap89 C. Papastefanou, Manolopoulou M, Ioannidou A, et al. "Time-dependent radioactive catchment soils" J Environ Radioact 32(3): 169-191, (1989).
- Pat94 N. J. Pattenden and W. A. McKay "Studies of artificial radioactivity in the coastal environment of northern Scotland: A review" Journal of Environmental Radioactivity, 24, 1-51, (1994).
- Peh77 R. H. Peh, "Germanium gamma-ray detectors" Phys. Today, 30, No. 11, 50, (1977).
- Qui94 L.S. Quindos, Fernandez P. L., Soto J., Rodenas C., Gomez J."Natural Radioactivity in Spanish Soils" Health physics, 66, 2, 194-200, (1994).
- Rau79 T. W. Raudorf, Tranmell. R. C., and Darken. L. S. "N-type high purity germanium coaxial detectors" IEEE Trans. Nuclear Sci. NS 26, 297, (1979).
- Ros96 K. Rosen, A. Eriksson, and E. Haak "Transfer of radiocaesium in sensitive agricultural environments after the Chernobyl fallout in Sweden. I. County of Gävleborg" Sci. Total Environ., 182, 117-133 (1996).
- Rus00 M. Ruse, Peart M. *Intrasite sampling of Hong Kong soils contaminated by Cs-137* Chemosphere 41: 45-51, (2000).
- Ryb02 L. Rybach, D. Bachler, B. Bucher, G. Schwarz c "Radiation doses of Swiss population from external sources" Journal of Environmental Radioactivity, 62, 277-286, (2002).
- Sam97 B. E. Sample, M. S. Aplin, R. A. Efroymsen, G. W. Suter and C. J. E. Welsh "Methods and tools for estimation of the exposure of terrestrial wildlife to contaminants" ORNL/TM-13391 environmental sciences division, publication No. 4650, (1997).
- San02 E. E. Santos, D. C. Lauria, E. C. S. Amaral, E. R. Rochedo "Daily ingestion of ^{232}Th , ^{238}U , ^{226}Ra , ^{228}Ra and ^{210}Pb in vegetables by inhabitants of Rio de Janeiro City " Journal of Environmental Radioactivity, 62 75-86, (2002).

- San94 J. D. Sanoit “*Silica Spiked with Mixed γ -Ray Standards for use as Environmental Reference Material*“ Radiochemical acta, 65, 249-257, (1994).
- Sch02 P. Schuller, G. Voigt, J. Handl, A. Ellies and L. Oliva “*Global weapons fallout ^{137}Cs in soils and transfer to vegetation in south-central Chile*” Journal of Environmental Radioactivity, 62, 181-193, (2002).
- Sch98 U. K. Schkade, D. Arnold, M. Hartmann and M. Naumann “*Bestimmung der spezifischen Aktivität natürlicher Radionuklide in Umweltproben*“ 5. vergleichsanalyse, Boden 1998, ST2-27/1998, (November 1998).
- Sch98 U. Schötzig and H. Schrader “*Halbwertszeiten und Photonen-Emission wahrscheinlichkeiten von häufig vewendeten Radionukliden*“ 5, erweitere Auflage Physikalisch Technische Bundesanstalt (PTB), Braunschweig, september (1998).
- Sch98 W. Schimmack, H. Steindl, K. Bunzl “*Variability of water content and of depth profiles of global fallout ^{137}Cs in grassland soils and the resulting external gamm-dose rates*” Radiat. Environ. Biophys. 37: 27-33, (1998).
- Sch89 J. Schmidt, Ergenzinger E., W. Kolb “*Migration and distribution of radionuclides in soils after the Chernobyl accident*” Edt. By W. Feldt, Proceeding of the XVth Regional Congress of IRPA Visby, Gotland, Sweden, 10-14 septamber, (1989).
- Sie96 A. Siehl, *Grundlagen und geowissenschaftliche Aspekte der natürlichen Radioaktivität*, Ernst und Sohn Verlag (1996).
- Sim89 S. E. Simopoulos ”*Soil sampling and ^{137}Cs analysis of the Chernobyl fallout in Greece*” Appl. Radiation and isotopes, 40, 607-613, (1989).
- Sto99 J. M. Stone, R. D. Whicker, S. A. Ibrahim, F. W. Whicker, ”*spatial variations in natural background radiation: Absorbed dose rates in air in Colorado*” Health Phys., 76 516, (1999).
- Tak98 C. Takenaka, Onda Y, Hamajima Y., “*Distribution of cesium-137 in Japanese forest soils: Correlation with the contents of organic carbon*” Sci Total Environ 222:193-199, (1998).
- Tam60 T. Tamura and D.G. Jacobs “*Structural Implications in Caesium Sorption*” Health physics 2: 391-398, (1960).
- Tay65 S. R. Taylot “*Abundance of chemical elements in the continental curst: a new table*” Geochi. Cosmochim. Acta 29: 1273-1285 (1965).
- Tho03 M.C. Thorne “*Background radiation: natural and man-made*“ J. Radiol. Prot. 23 29-42, (2003).
- Tra83 B. L. Tracy, Prantl F. A., Quinn J. M. “*Transfer of ^{226}Ra . ^{210}Pb and Uranium from Soil to Garden Produce: Assessment of Risk*“ Health physics, 44, 5, 469-476, (1983).

- Tyk95 R. Tykov, and J. Sabol “*Low-level environmental radioactivity Sources and Evaluation*” Technomic Publishing Company, Inc., Lancaster, Pennsylvania (1995).
- UNS00 United Nations Scientific Committee on the Effects of Atomic Radiation, Report to the General Assembly, United Nations, New York UNSCEAR (2000).
- UNS01 United Nations Scientific Committee on the Effects of Atomic Radiation, Report to the General Assembly, United Nations, New York UNSCEAR (2001).
- UNS77 United Nations Scientific Committee on the Effects of Atomic Radiation, Report to the General Assembly, United Nations, New York UNSCEAR (1977).
- UNS82 United Nations Scientific Committee on the Effects of Atomic Radiation, Report to the General Assembly, United Nations, New York UNSCEAR (1982).
- UNS88 United Nations Scientific Committee on the Effects of Atomic Radiation, Report to the General Assembly, United Nations, New York UNSCEAR (1988).
- UNS93 United Nations Scientific Committee on the Effects of Atomic Radiation, Report to the General Assembly, United Nations, New York UNSCEAR (1993).
- Val00 V. Valkovic “*Radioactivity in the environment*” Elsevier science, (2000).
- Vah02 J.-W. Vahlbruch, R. Sachse, S. Harb, D. Jakob, R. Michel, W.-U. Müller, J. Schabronath, D. Düputell, *Untersuchungen zur Strahlenexposition durch natürliche Radionuklide aus dem Steinkohlebergbau in der Vorflut*, in : R. Michel, M. Täschner, A. Bayer (Hrsg.) Praxis des Strahlenschutzes: - Messen, Modellieren, Dokumentieren -, Tagungsband der 34. Jahrestagung des Fachverbandes für Strahlenschutz e.V., Kloster Seeon, 21. - 25. April 2002, TÜV-Verlag, Köln, 227 – 234, (2002).
- Van99 A. J. VandenBygaart, R. Protz, and D. C. McCabe “*Distribution of natural radionuclides and ¹³⁷Cs in soils of southwestern Ontario*” Canadian Journal of Soil Science, 79, 1, 61-71, (1999).
- Vid01 T. Vidmar, M. Korun, A. Likar, R. Martincic “*A semi-empirical model of the efficiency curve for extended sources in gamma-ray spectrometry*” nuclear instruments and methods in physics research A 470, 533-547, (2001).
- Vid02 T. Vidmar, and A. Likar “*A automated construction of detector models for efficiency interpolation in gamma-ray spectrometry*” applied Radiation and Isotopes 65, 99-103, (2002).
- Vin03 M. M. Vinichuk and Karl J. Johanson “*Accumulation of ¹³⁷Cs by fungal mycelium in forest ecosystems of Ukraine*” Journal of Environmental Radioactivity, 64, 27-43, (2003).
- Waj 93 W. chelmiki, J. W. Mietelski, P. Macharki and J. Swiechowicz “*Natural factors of ¹³⁷Cs redistribution in soil*” report No. 1615/D, Institute of nuclear physics, Krakow, Poland, 1993.

-
- Wil92 A. J. Wilson, Scott L. Max “*Characterization of Radioactive Petroleum Piping Scale With an Evaluation of Subsequent Land Contamination*” *Health physics*, 63, 6, 681-685, (1992).
- Wil92 K. William, Nemeth and Bahman Parsa “*Density correction of gamma-ray detection efficiency in environmental samples*” *Radioactivity & Radiochemistry*, 3, 3, (1992).
- You81 J. A. Young and C. W. Thomas, *Atmospheric radionuclide concentrations measured by the pacific Northwest Laboratory since 1961*, USDOE Report PNL-3826 (Battelle Pacific Northwest Laboratory, Richland, Washington) (1981).
- Zac91 R. Zach and S. C. Sheppard “*Food chain and dose model, CALDOS, for assessing Canada’s nuclear fuel waste management concept*” *Health physics* 60, 5, 643-656, (1991).
- Zan78 K. Zanio “*Semiconductors and semimetals: Cadmium Telluride*” vol. 13, Willardson. R. K. and Beer, A. C., Eds (Academic Press, New York). (1978).